Commission of the European Communities

nuclear science and technology

The geological, geochemical, topographical and hydrogeological characteristics of the Broubster natural analogue site, Caithness

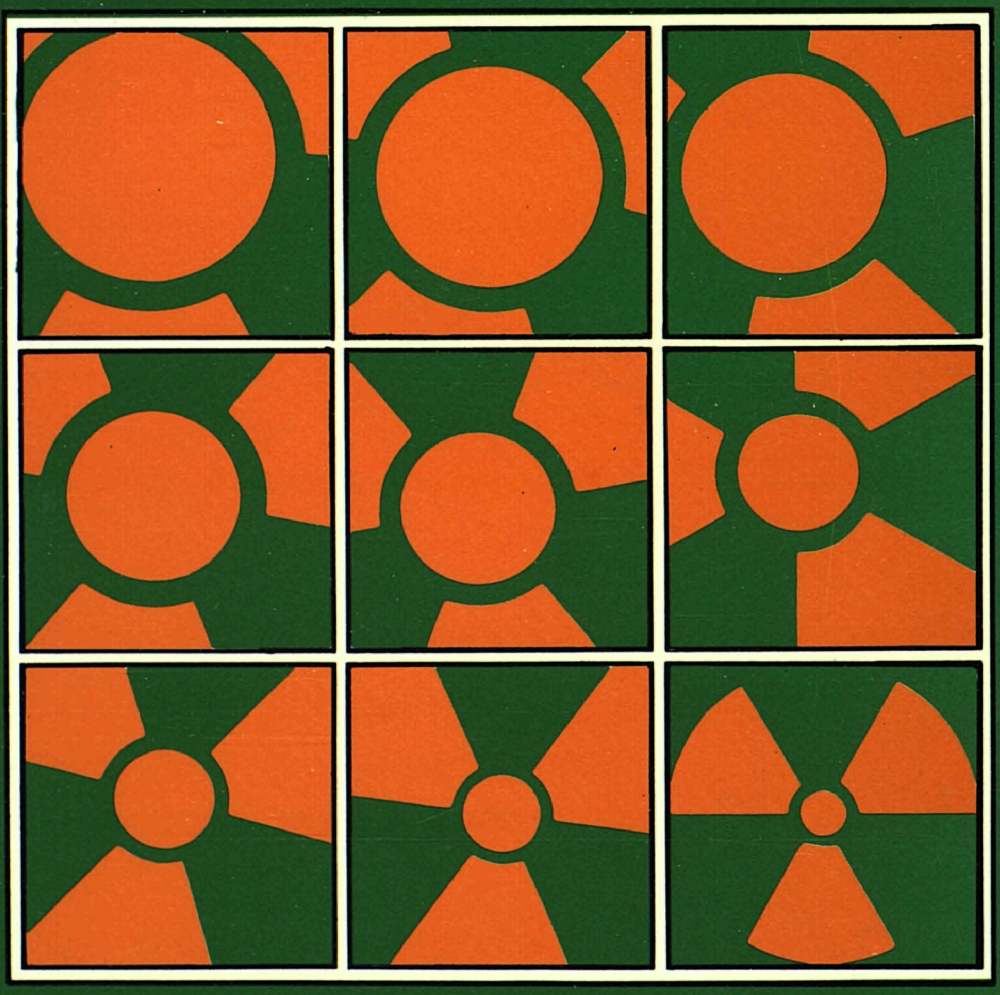

Report

EUR 13275 EN

FIGURE 1.1 THE BROUBSTER NATURAL ANALOGUE SITE

CAITHNESS, SCOTLAND

LEGEND

- Geochemical traverse
- PIT 1 — Soil or geochemical sampling pit
- W8 ● — Piezometer site and number
- [a] [c] W8 [b] [d] — hygeological and topographical data at piezometer or other sites
  - a = depth of piezometer sampling point in metres below ground level
  - b = depth to bedrock in metres below ground level
  - c = elevation of surface above base level in metres
  - d = depth to water surface in metres below ground level
- * — Base level datum point
- Topographic features
- Areas of generally permanent surface standing water
- Areas of generally transient surface standing water (dependent on weather conditions)
- 1.5 / 1.0 / <1.0 — Contours of peat thickness (west side of road only) in metres (at 0.5m intervals)
- Limit of brown earths (west side of road)

Scale

0 10 20 30 40 50m

N

PEAT THICKNESS NO DATA

PEAT THICKNESS NO DATA

PEAT THICKNESS NO DATA

PEAT THICKNESS NO DATA

PEAT THICKNESS NO DATA

WET DITCH

DRY DITCH

DRY DITCH

Road

Drainage Channel - Poorly Defined

Drainage Channel - Well Defined

Limit of Brown Earths

Quarry Edge (Buried)

Mounded Fill

Limit of Brown Earths

Kiln

Sedge Filled Drainage Hollow

Telegraph pole

Fence

Pond

[-0.134m below base level to water surface]

TRAVERSE 1 (1987)

TRAVERSE 2 (1987)

TRAVERSE 3 (1987)

TRAVERSE 4 (1988)

TRAVERSE 5 (1988)

1986 TRAVERSE

LINE 1 (1968)

LINE 2 (1968)

LINE 3 (1968)

[0.20-0.47] [-1.025] E6 [0.118]

[0.06-0.33] [-1.385] E5 [0.105]

[0.22-0.47] [-1.728] E4 [0.58] [+0.05]

[0.16-0.43] [1.34] E7 [0.00]

[0.57-0.84] [-1.350] E3 [0.125]

[0.62-0.89] [-1.258] E10A [0.645]

[0.28-0.55] [-1.258] E10B [0.260]

[0.30-0.57] [-1.018] E2 [0.210]

[1.50] [-0.638] E1 [1.50] [0.365]

[0.71-0.98] [-0.288] E8 [0.730]

[1.09-1.36] [-1.029] E9 [0.860]

[0.23-0.50] [-0.296] W10 [0.59] [0.220]

[0.69-0.96] [+0.164] W1 [1.05] [0.220]

[1.23-1.50] [+0.947] W5 [1.59] [DRY TO 1.5]

[0.81-1.08] [+0.588] W3 [1.17] [DRY TO 1.08]

[1.03-1.30] [+0.70] W2 [1.39] [1.07]

[0.81-1.08] [+0.756] W4 [1.17] [1.075]

[1.63-1.90] [+1.495] W6 [1.99] [1.385]

[1.240-1.510] [+2.160] W7 [1.600] [DRY TO 1.5]

[1.060-1.330] [+4.358] W8 [1.420] [1.160]

[1.340-1.610] [+4.918] W9 [1.700] [0.855]

PIT 1 PIT 2 PIT 3 PIT 4 PIT 5 PIT 6 PIT 7 PIT 8 PIT 9

PIT 6 [0.370]

<0.5 0.5 1.0 1.5 >1.5 >1.0

Commission of the European Communities

nuclear science and technology

The geological, geochemical, topographical and hydrogeological characteristics of the Broubster natural analogue site, Caithness

T. K. Ball, A. E. Milodowski

British Geological Survey
Keyworth
Nottingham NG12 5GG
United Kingdom

Topical report

Work carried out under cost-sharing contract
No FI1W/0073/UK with the European Atomic Energy Community,
in the framework of its third R&D programme on
'Management and storage of radioactive waste', Part A, Task 4
'Geological disposal studies'

Directorate-General
Science, Research and Development

1991

Published by the
COMMISSION OF THE EUROPEAN COMMUNITIES
Directorate-General
Telecommunications, Information Industries and Innovation
L-2920 Luxembourg

Cataloguing data can be found at the end of this publication

Luxembourg: Office for Official Publications of the European Communities, 1991

ISBN 92-826-2358-0 Catalogue number: CD-NA-13275-EN-C

Printed in Belgium

PREFACE

The British Geological Survey (BGS) has been conducting a co-ordinated research programme at the Broubster natural analogue site in Caithness, N Scotland. This work on a natural radioactive geochemical system has been carried out with the aim of improving our confidence in using predictive models of radionuclide migration in the geosphere. It has involved collaboration with the Harwell Laboratory for U/Th series analytical work, and with WS Atkins Engineering Sciences for modelling. The natural analogue work jointly carried out has been supported by the Department of the Environment from July 1986 to March 1989 and by the Commission of the European Communities from July 1988 to September 1989 under the CEC shared-cost action MIRAGE II Project.

This report is one of a series being produced from this effort and it concentrates on the main geological, topographical, hydrogeological and geochemical characteristics of the site. Other reports listed below give more detailed accounts of specific features of the site.

Broubster reports

1. 'Geochemical modelling of the Broubster natural analogue site, Caithness, Scotland' by D. Read of WS Atkins Engineering Sciences. BGS Technical Report WE/88/43 and DOE Report DOE/RW/89.005.
2. 'The development of portable equipment to study physical and chemical phases in natural water' by N. Breward and D. Peachey. BGS Technical Report WE/88/25 and DOE Report DOE/RW/88.102.
3. 'The uranium source-term mineralogy and geochemistry at the Broubster natural analogue site, Caithness' by A.E. Milodowski, I.R. Basham , E.K. Hyslop and J.M. Pearce. BGS Technical Report WE/89/50 and DOE Report DOE/RW/89.073.
4. 'The characterisation of organics from the natural analogue site at Broubster, Caithness, Scotland' by B. Smith, M. Stuart, B. Vickers and D. Peachey. BGS Technical Report WE/89/33.
5. 'Sorption studies of uranium in sediment-groundwater systems from the natural analogue sites of Needle's Eye and Broubster' by J.J.W. Higgo. BGS Technical Report WE/89/40 and DOE Report DOE/RW/89.072.
6. 'Uranium series disequilibrium studies at the Broubster analogue site' by G. Longworth, M. Ivanovich and M.A. Wilkins. 20pp. Harwell Report AERE-R 13609.

EXECUTIVE SUMMARY

Studying a natural geochemical system characterised by movements of radioactive elements may yield data which can be used to test applications of mass transport codes. Codes such as CHEMTARD are employed to predict the distributions of radionuclides migrating from proposed radioactive waste repositories. Equally, it is important to test applications of the CHEMVAL thermodynamic database and equilibrium speciation codes with data acquired from real geological materials in order to create confidence in their use as predictors of the chemical forms of radionuclides. To this end the British Geological survey has been conducting a number of investigations of locations where natural analogues of radionuclide migration can be recognised, with the purpose of describing the processes of movement of uranium (U), thorium (Th) and rare earth elements (REE) in sediments. In this way, data can be compiled to be used in testing the modelling, and inherent ideas of the processes, underpinning the codes. The site of uranium mineralisation at Broubster in Caithness, N Scotland, presents an easily accessible location suitable for such a study with the emphasis on the role of organics in the distribution of the natural radio-elements U and Th. This report compiles new results of the hydrology and geochemistry of the site.

The Broubster site is characterised by surficial deposits of brown earths and peat which play host to the transport and retardation of the U and Th series isotopes and REE, and involve processes that have been present for at least 5000 years over a distance of the order of 100m. The source of the natural radioactivity is a thin mineralised limestone layer exposed to weathering and leaching. Radioactive hydrocarbons are intimately associated with the uraniferous mineralisation. This is one of the few areas studied where a labile form of REE mineralisation exists. Samples of the mineralisation, soils and peat and associated groundwaters have been collected and analysed in the laboratory for their chemical characteristics.

The history of the site is uncertain prior to the glacial deposition of ground moraine. It is likely that the area was planed glacially presenting a relatively flat and fresh surface before the waning phases of the latest glacial period which is thought to have ended some 10-12,000 years ago. There followed a relatively mild climatic episode extending for some 5,000 years BP resulting in an extensive forest cover. This phase ended with the climate apparently cooling, and becoming wetter, with the forest cover being replaced by peat. The main secondary fixing of U following erosion of the limestone was probably initiated at about this time. A major disturbance occurred some 100-200 years ago with the quarrying of the mineralised limestone, and probable liberation of U from both the quarry spoil and freshly exposed limestone, with further fixing in the peats. Further liberation of U has

occurred within the last 20 years as a result of extensive liming of the peaty soils, with a consequent pH increase and remobilisation of the U previously fixed in the soils.

Detailed values of soil pH and Eh were recorded from the discovery of the U anomaly in 1968. In the recent past, soils in the area, have had their geochemical character changed markedly by liming resulting in the increase of soil pH. Eh/pH diagrams provide a key to the interpretation of the data and the net result of the liming appears to have been that a greater proportion of the soils now occupy the same stability fields as the stable and easily soluble bicarbonato uranyl complex.

Soil Eh measurements show significant fluctuations which appear to be related to seasonal effects (e.g. waterlogging). The fluctuations appear to be sufficient that, dependent upon the season, the soil Eh/pH may either fall within the stability field of uraninite and thus U becomes relatively immobile; or may be oxidised to the stability fields of the more mobile bicarbonato complexes.

The ground level falls gently from west to east. The main U anomaly, in a quarried zone, is found in the middle part of the area with dispersion of U and associated elements downslope to the east.

Within the quarry area the water table is close to, or at, the bedrock interface. The overlying fill is thus well-drained and aerated and contains abundant limestone fragments and uraniferous waste material. Under such conditions U minerals in the quarry waste will tend to oxidise to the hexavalent state, the U readily complexes with carbonate and mobility will increase. Percolating rainwater and introduced groundwater therefore carry U down the hydraulic gradient. The flow within the quarry is likely to be strongly affected by irregularities in the quarry floor and channelled drainage is a strong possibility together with surface seepage over bedrock and karstic movement through the limestone. U in groundwater increases greatly down gradient in this area, reflecting the source of U in the quarry area.

The observed surface drainage pattern and the U distribution in waters, in general, shows a good agreement. The groundwater pattern indicates a general flow from west to east across the site. There is a possible bifurcation of the flow in the eastern part of the site with some distribution to the northeast and some to the southeast. This has resulted in U transport, and fixing in peat, along divergent paths.

The studies indicate the possibility of significant groundwater movement along the interface

of the bedrock and boulder clay cover, as the result of the removal, by weathering, of detrital feldspar components and the carbonate cement of both siltstones and sandstones. There is thus a potential for two groundwater systems to develop in the near surface environment, separated from each other by boulder clay: (a) one in which the drainage is essentially through the peat in isolation from bedrock and another (b) in which groundwater evolves by drainage along the weathered bedrock/boulder clay interface in isolation from the peat. However in areas of the site where the boulder clay is absent there is the possibility that the two groundwaters would mix and therefore complicate the U dispersion pattern. The soil/groundwater system may be fed directly from bedrock via shallow karstic flow from the mineralised limestone and siltstones. Therefore in the far east of the site the possibility of multiple U inputs must be considered.

Yttrium (Y) appears to show important similarities in behaviour to U, and dissimilarities to the other REE and Th. The Light REE elements have been proposed as appropriate analogues for the transuranic elements americium (Am) and curium (Cm), and Th for plutonium (Pu). Unfortunately there is little information that Th is appreciably mobile at Broubster. However Th is found in some phosphate minerals in organic soils and weathered bedrock and in association with REE. In the soils it is not clear whether these minerals are of detrital or authigenic origin. In waters Th correlates with the sulphate ion.

Where the actual behaviour of Am and Cm in soils has been studied, there appears to be a marked difference to the behaviour suggested by the analogues in the present investigation. Elsewhere Am and Cm have been found to be dominantly associated with insoluble Mn oxides; at other sites Cm was associated with organic complexing agents. In the present study the REE were found dominantly in minerals of monazite, rhabdophanic and plumbogummite types. In many cases these minerals are of primary detrital origin but in some cases, as for example in weathered bedrock, rhabdophane or plumbogummite is seen as a secondary phase and plumbogummite may also be present as a secondary soil mineral. The nature of the Ce anomaly in the REE distribution patterns, in soils and soil porewaters, confirms that the REEs can be mobilised in solution in this environment.

No discrete U mineral has been identified in the soil. The highest values for U are found in the peats implying that organic complexation is the dominant fixing mechanism.

The soil dispersion anomaly appears to be divided into zones which describe the general behaviour of the elements of interest. Up slope from the mineralisation there appears to be little labile U. There appears to be a small amount of REE mobility with a slight cerium (Ce) negative anomaly in the peats, and a small increase in radioactivity related to sesquioxide

coprecipitation of radium (Ra).

In the region of the main radiometric anomaly the gamma activity is higher than would be expected from the U content, and the REEs show evidence of transport with a positive Ce anomaly indicating movement of the REE away from the area leaving a residual Ce anomaly. This area is characterised by brown earths with neutral to high pH and oxidising conditions.

In the adjoining and mostly waterlogged area to the east, pH values remain high but there is a significant decline in Eh consistent with the waterlogged nature of the ground. The gamma activity is lower than would be expected from U in equilibrium with its daughter products. U is statistically related to Y and the REEs, and is probably fixed by organic matter. Th relates to the heavy mineral detrital fraction of the soils. Some of the variance for the REE is explained by part of the Ce being resident in heavy detrital minerals. Further from the source, in the same area, the nature of the fixing mechanism for the U appears to change. U whilst still being related mostly to Y, lanthanum (La) and neodymium (Nd) shows some evidence for being partially fixed by iron sesquioxides. Th and Ce are mostly found within the heavy mineral detrital suite whilst the other REEs appear to be independent of both sesquioxides and heavy minerals.

The extent of the U dispersion is greater than was suspected at first, and the anomaly is still open to the east. The extent of the REE dispersion, or whether it is co-extensive with the U anomaly is equally uncertain. The nature of seasonal variations in redox potential, and the effect these would have on the solubilities of U and the REE, needs to be characterised further. Different methods of estimating the redox potential need to be assessed. An extension of the piezometer array is required to support studies of the flow regime and to provide samples of groundwater for analyses by BGS and Harwell. In particular accurate phosphate determinations would be useful in determining the mechanisms of REE transport.

CONTENTS

		PAGE NO.
1.	INTRODUCTION	1
2.	SITE GEOLOGY AND SOIL TYPE DISTRIBUTION	3
3.	SOIL GEOCHEMICAL TRAVERSES AND SOIL PITS	8
	3.1 The 1968 data Line 1	8
	3.2 The 1968 data Line 2	9
	3.3 The 1968 data Line 3	9
	3.4 The 1968 Traverse	10
	3.5 Rare earth element distributions 1986 Traverse	11
	3.6 1987 Traverse 1	11
	3.7 1987 Traverse 2	13
	3.8 1987 Traverse 3	13
	3.9 1988 Traverse 4	13
	3.10 1988 Traverse 5	13
	3.11 Soil pit profiles	14
	3.11.1 Pit 2 (1987)	14
	3.11.2 Pit 8 (1988)	18
	3.11.3 Pit 3 (1987)	19
	3.11.4 Pit 9 (1987)	20
	3.11.5 Pit 1 (1987 and 1988)	20
4.	MINERALOGY AND PETROGRAPHY	23
	4.1 General	23
	4.2 Sandstones and siltstones	23
	4.3 Limestone and the mineralised zone	28
	4.4 Soils from PIT 2	29
5.	HYDROGEOLOGY AND HYDROGEOCHEMICAL SAMPLING	33
	5.1 General	33
	5.2 Hydrogeology	33
	5.3 Hydrogeochemical Data	35

6. DISCUSSION 38
6.1 Eh and pH controls 38
6.2 Statistical analysis 42

7. CONCLUSIONS 46

8. ACKNOWLEDGEMENTS 49

9. REFERENCES 50

10. APPENDIX 53

PLATES

1.	View to the west of the site	6
2.	View to the east of the site	6
3.	Photograph of waterlogged ground east of the site	7
4.	Photograph of PIT 2 profile	16
5.	Collection of oriented soil sample.	16
6.	Detail of upper part of PIT 2	17
7.	Fe and Mn mottled zones and root channels	17
8.	Profile through soil PIT 1	22
9.	Details of limestone and cavernous porosity in PIT 1	22
10-15.	Photomicrographs of sandstone and siltstone petrography	26
16-21.	Photomicrographs of sandstone and siltstone petrography	27
22-27.	Photomicrographs of limestones, siltstones and soil petrography	32

TABLES

3.1	Analytical data for 1968 Line 1.
3.2	Analytical data for 1968 Line 2.
3.3	Analytical data for 1968 Line 3.
3.4	Analytical data for 1986 Traverse.
3.5	INA Analytical data for 1986 Traverse.
3.6	Analytical data for 1987 Traverse 1.
3.7	Analytical data for 1987 Traverse 2.
3.8	Analytical data for 1987 Traverse 3.
3.9	Analytical data for 1988 Traverse 4.
3.10	Analytical data for 1988 Traverse 5.
3.11	Selected trace element analytical data for soils from PIT 2.
3.12	Selected trace element analytical data for soils from PIT 8.
3.13	REE and selected trace element data for PIT 3.
3.14	Major and trace element data for soils from PITs 3 and 9.
4.1	Major and trace element data for bedrock samples. Limestones from PIT 1 and sandstones from PIT 9.
5.1	Analytical data for groundwaters.
6.1	a) Partial correlation matrix for 1986 Traverse. b) Results of Factor analysis.

6.2 a) Partial correlation matrix for 1986 peat samples.
b) Results of Factor analysis.
6.3 Partial correlation matrix for surface samples 1987 Traverse 2.
6.4 Partial correlation matrix for deep samples 1987 Traverse 2, and Factor Analysis for the whole traverse.
6.5 Correlation matrix for water samples and summary of the Factor Analysis.

FIGURES

1.1 Map showing surface features of the site. Included are positions of the geochemical traverses, the pits, piezometer sites and hydrogeological data and contours of peat thickness.

1.2 Soil geochemical maps (after Gallagher et al., 1971)

3.1.1 - 3.1.9 Geochemical soil profiles for Broubster 1968 Line 1.

3.2.1 - 3.2.9 Geochemical soil profiles for Broubster 1968 Line 2.

3.3.1 - 3.3.9 Geochemical soil profiles for Broubster 1968 Line 3.

3.4.1 - 3.4.14 Geochemical soil profiles for Broubster 1986 Traverse.

3.5.1 - 3.5.2 Chondrite normalised REE profiles for selected samples Broubster 1986 Traverse.

3.6.1 - 3.6.19 Geochemical soil profiles for Broubster 1987 Traverse 1.

3.7.1 - 3.7.20 Geochemical soil profiles for Broubster 1987 Traverse 2.

3.8.1 - 3.8.20 Geochemical soil profiles for Broubster 1987 Traverse 3.

3.9.1 - 3.9.2 Distribution profiles for y spectrometric photopeak intensities and U in soil values for Broubster 1987 Traverse 4.

3.10.1 - 3.10.2 Distribution profiles for y spectrometric photopeak intensities and U in soil values for Broubster 1987 Traverse 5.

3.11.1 Descriptive section for PIT 2.

3.11.2 - 3.11.7 Geochemical profiles for soils in PIT 2.

3.11.8 - 3.11.13 Geochemical profiles for porewaters in PIT 8.

3.11.14 Chondrite normalised REE distribution profiles for soils in PIT 8 and bedrock samples.

3.11.15 Variation of pH and HCO_3 in squeezed porewaters from PIT 8.

3.11.16 Descriptive section for PIT 3.

3.11.17 Chondrite normalised REE distribution profiles for soils in PIT 3.

3.11.18 Descriptive section for PIT 1.

5.1 (a) Construction details of the Casagrande poezometers.
(b) Perspex flow-through cell for Eh and pH determinations on water.

5.2. Contoured groundwater surface and probable flow patterns.

5.3. Geological and hydrogeological cross-section (W9-E4).

5.4. Conceptual model of groundwater and uranium movements.

6.1. Aqueous equilibrium diagram for the $U - O_2 - H_2O - CO_2$ system at 25°C and 1 Atmosphere pressure. CO_2 concentration of 10^{-3} moles and total ionic strength of 10^{-4} moles.

6.2. Aqueous equilibrium diagram for the $U - O_2 - H_2O - CO_2$ system at 25°C and 1 Atmosphere pressure, CO_2 concentration of 10^{-3} moles and total ionic strength of 10^{-5} moles. The diagram compares the data for the westernmost Traverses for September 1968 (open circles) and June 1987 (closed circles). Surface organic soils.

6.3. Aqueous equilibrium diagram for the $U - O_2 - H_2O - CO_2$ system at 25°C and 1 Atmosphere pressure, CO_2 concentration of 10^{-3} moles and total ionic strength of 10^{-5} moles. The diagram compares the data for the westernmost Traverses for September 1968 (open circles) and June 1987 (closed circles). Clays and gleyed soils.

6.4. Aqueous equilibrium diagram for the $U - O_2 - H_2O - CO_2$ system at 25°C and 1 Atmosphere pressure, CO_2 concentration of 10^{-3} moles and total ionic strength of 10^{-5} moles. The diagram compares the data for the Traverses over the middle part of the anomaly, for September 1968 (open circles) and June 1987 (closed circles). Surface soils.

6.5. Aqueous equilibrium diagram for the $U - O_2 - H_2O - CO_2$ system at 25°C and 1 Atmosphere pressure, CO_2 concentration of 10^{-3} moles and total ionic strength of 10^{-5} moles. The diagram compares the data for the Traverses over the middle part of the anomaly, for September 1968 (open circles) and June 1987 (closed circles). Deep soils.

6.6. Aqueous equilibrium diagram for the $U - O_2 - H_2O - CO_2$ system at 25°C and 1 Atmosphere pressure, CO_2 concentration of 10^{-3}moles and total ionic strength of 10^{-5} moles. The diagram compares the data for the easternmost traverse for September 1968 (open circles) and June 1987 (closed circles). Surface soils.

6.7. Aqueous equilibrium diagram for the $U - O_2 - H_2O - CO_2$ system at 25°C and 1 Atmosphere pressure, CO_2 concentration of 10^{-3} moles and total ionic strength of 10^{-5} moles. The diagram compares the data for the easternmost traverse, for September 1968 (open circles) and June 1987 (closed circles). Deep soils.

6.8. Aqueous equilibrium diagram for the $U - O_2 - H_2O - CO_2$ system at 25°C and 1 Atmosphere pressure, CO_2 concentration of 10^{-3} moles and total ionic strength of 10^{-3} moles. The data points are for the 1986 Traverse.

6.9 Eh/pH diagram showing the stability felds for the Eu species. Field I denotes the field occupied by Brown Earths, Field II by Peats and Clays and Field III by heavily gleyed soils and clays.

6.10 Eh/pH diagram showing the stability fields for the Ce species. Field I denotes the field occupied by Brown Earths, Field II by Peats and Clays and Field IIA by heavily gleyed soils and clays. Field III is the field of the groundwater.

6.11 Eh/pH diagram showing the stability fields for the Mo species. Fields as in previous figures.

6.12 Eh/pH diagram showing the stability fields for the Pb species. Fields as in § previous figures.

6.13 Eh/pH diagram showing the stability fields for the Cu species. Fields as in previous figures.

6.14 The approximate positions of the oxidation reaction potentials for the $Fe^{2+} \rightarrow Fe^{3+}$ and $Mn^{2+} \rightarrow Mn^{3+}$ are recorded in relation to the fields occupied by the soils.

6.15 Solubility relationships for Al, Fe and Si in soils environments where gibbsite, haematite and quartz are present. Al=Fe represents conditions of equal Al and Fe solubilities. $Al=10^{-6}M$ and $Fe=10^{-6}M$ are solubility levels below which quartz is more soluble than Al and Fe phases (from Norton, 1973). Position shows the location of the six-fold junction in the presence of organic complexants. (Manley et al. 1987).

6.16 Factor loading plot for the 1986 Traverse.

6.17 Factor loading plot for 1987 Traverse 2

1. INTRODUCTION

The Broubster anomaly (NGR ND021624) was detected by car-borne radiometric survey in 1968, during an investigation by B.G.S. to evaluate the uranium mineral potential of the U.K. The site is located inland of the north coast of Caithness, about 7 miles southwest of Thurso. The site lies on the watershed between a small tributary valley of the Ardvarasdal Burn to the north and the Forss Water to the east. The western side of the site rises moderately steeply to a maximum elevation of about 110m from about 90m OD. On the eastern side the ground slopes gently to the northeast, east and southeast. A minor road connects the abandoned village of Broubster, in the south, to the hamlet of Shebster, in the north, and conveniently bisects the site into different geochemical and geological environments.

A surface radiometric survey was undertaken in 1968, followed by a preliminary soil geochemical survey which measured amongst other parameters; pH, Eh, surface gamma activity, U, Cu, Pb, Zn, Mo and Mn, along three traverses (Figure 1.1)

A more widespread survey which included closer spaced soil sampling, pitting and shallow drilling was subsequently undertaken and the results of this later phase were published in 1971(Gallagher et al.). Unfortunately soil pH and Eh measurements were not taken and the analytical data restricted to elements expected in the mineralised structure vide U, Cu, Pb, and Zn (Figure 1.2).

In order to assess the viability of the site for the study of dipersion around natural analogues of nuclear waste repositories the site was revisited in 1986, during which another series of samples along a traverse east of the road was collected (Figure 1.1). A pit was dug to investigate the soil profile in more detail and a more comprehensive range of elements was determined than in previous investigations.

During 1987 three traverses were occupied approximating to the position of the 1968 traverses and three pits were dug to investigate soil profiles and to collect large samples for more detailed analysis. During June 1988 a further programme of work was carried out involving detailed topographical surveying of the site, the digging of pits to study the soil profiles, emplacement of piezometers and geochemical speciation studies on the ground and surface waters. The opportunity was also taken to collect two further traverses of soil samples, with accompanying radiometric data, further east as an orientation exercise to determine the extent of U dispersion and disequilibrium in this direction.

Examination of data from these studies showed that within the soils, there was considerable secular disequilibrium in the decay series of U-238. Generally surface radiometric measurements do not accord with high values of U in surface soils, the U concentrations being usually displaced to the south (down slope, locally) of the radiometric highs (e.g. Figure 1.2), and apparently following the surface drainage features (Figure 1.1).

Revisiting the site in 1986 showed that although the land use had remained constant (rough pasture) there had been significant changes in certain aspects of surface vegetation in the meantime. Notably in the area to the west of the road there was poor growth of heather where previously heather growth had been normal. Liming of the pasture was therefore suspected and confirmed in 1987 by referring to the farmer Mr. Gunn. Liming results in an increase in pH and in the displacement of heather by grasses. There are also significant changes in the geochemistry of soils in relation to the stability fields of uranium species.

The 1968 data thus provides an useful base against which the later measurements may be compared and thus helps to explain some puzzling aspects of the geochemistry of dispersion around this mineral occurrence.

2. SITE GEOLOGY AND SOIL TYPE DISTRIBUTION

The uranium source mineralisation was defined by Gallagher et al. (1971) as being largely confined to a fracture bound structure within a narrow limestone bed. The structure was described as having a northeasterly trend. The limestone was fractured and veined and the veins reported to contain calcite and dolomite gangue with smaller amounts of sphalerite, galena and uraniferous hydrocarbon. The host rocks are mudstones, siltstones sandstones and limestones of the Lybster subgroup of the Lower Caithness Flagstone Group (Middle Old Red Sandstone) which have a regional dip at 5-10^{o} to the northeast (BGS, 1985).

The lithologies and sedimentology of the Caithness Flagstones have been described by Donovan et al. (1974) and Donovan (1975,1980). The rocks comprise sedimentary cycles typically 5-15m thick, which represent lacustrine transgression and regression, sometimes with fluviatile input during the regressive phases. Four facies were recognised by Donovan (1980):

Lithofacies A; grey black carbonate laminite (calcite or dolomite) comprised of 0.5mm triplets of micritic carbonate, organic matter and siliciclastic laminae. These represent the deposits of a thermally stratified lake. Some carbonate laminites which lack terrigenous input are essentially limestones.

Lithofacies B; alternations of grey black carbon-rich shale and coarse grey siltstone (paired units < 7mm) representing the deposits of a shallow, sediment-starved, permanent lake.

Lithofacies C; alternations of dark-grey carbon-rich shale with coarse grey siltstone (paired units < 10mm). The siltstones display current ripples and are lensoid.

Lithofacies D; alternations of green grey shale and siltstone/fine sandstones which were deposited in a transient lacustrine environment. Locally current ripples, wave ripples, desiccation cracks and pseudomorphs after evaporite minerals are observed.

Locally within the Lybster Subgroup, thin sandstones with abundant fish remains are present. These are exposed nearby on the north shore of Loch Calder (BGS,1985). In addition to the U mineralisation at Broubster, U, Pb, Zn and Ba mineralisation has been found at other nearby localities, for example at Westhead (4km northeast), Brawlbin Mains (7km southeast) and Blar Cnoc na Gaoith (1.5km west), (Gallagher, et al., 1971). Fish remains, which locally are common, may be significantly enriched with U and Th (Bowie and Atkin, 1956)

The major surface features, drift geology and topographical data are illustrated in Figures 1.1 and 1.2. To the west of the road, the surface is slightly higher and relatively well-drained with a thin cover of mostly surface (blanket) peat overlying slightly leached boulder clay. There is often a zone of Mn and Fe enrichment underlying the bleached surface layers of the boulder clay which locally may cement the drift to form a hard "pan".

The main radiometric anomaly corresponds closely with a distinct surface depression (Plates 1 and 2) extending northeast to southwest (Figures 1.1 and 1.2). The area of the anomaly is also outlined by an abrupt change in vegetation type marked by a change from coarse grasses with patches of heather, and sedges in the wetter parts, to shorter and lusher grass with daisies and no heather. This corresponds with a change in soil type from wet, acid peat to well-drained, less acid brown earths overlying the depression.

The depression corresponds to a former small-scale limestone quarry which was subsequently backfilled with quarry spoil. Limestone at this locality was burned for lime at the lime kiln marked on Figure 1.1. A similar overgrown mound, close to the road, probably represents an earlier lime kiln, indicating progressive working of the quarry away from the road and up slope. The quarry was indicated on the earliest Geological Survey field slips of the area in 1898. Local enquiries at the North of Scotland Agricultural College, Thurso (Mr MacDonald, pers. comm.) and with local farmers indicate that this site had not been worked for limestone for at least 100 years. Within the depression, immediately below the lime kiln at the top of the site, laminated and radioactive siltstones suboutcrop, with a cover of only one or two cms of organominerallic soil.

It is not known for certain whether the brown earths were originally a feature developed over the suboutcrop of the limestone or are a function of the disturbed ground occasioned by the small scale quarrying operations. The overall pattern of distribution of the brown earths indicates the former although disturbance is severe over the limestone suboutcrop. Further upslope, beyond the remains of the lime kiln, limestone does not appear to have been extracted and the depression becomes less obvious. However a gully can be traced upslope from the old quarry area, which is sometimes waterlogged, and filled with peaty soil to a depth of at least 1.5m. The vegetation is characterised by an abundant and luxuriant sedge growth. The whole is suggestive of surface corrosion of the limestone to produce the gully.

At the lower end of the quarry area, immediately adjacent to the road (PIT 6, Figure 1.1), boulder clay appears to overly the floor of the depression. This area is subject to periodic flooding. Augered depths to bedrock at piezometer sites are given in Figure 1.1.

To the east of the road, drainage is impeded, and the area is covered by peat of variable thickness (ranging 0 to >1.5m). This is mostly underlain by gleyed boulder clay, also of variable thickness. Boulder clay is absent immediately adjacent to the fence in the waterlogged area (PIT 4, Figure 1.1) where peat rests directly on siltstone bedrock. At PIT 8 the boulder clay is about 1.2m thick. This pit was the only site east of the road where a successful penetration of the boulder clay, by augering, was achieved.

Surface channels are observed on the east of the road and the most prominant appears to follow the projected strike of the quarried limestone bed (Figure 1.1). This channel usually contains some water, with a slight surface flow evident even in dry summer conditions. Towards the fence this channel broadens into a wide waterlogged area with permanent near surface or standing water (Plate 3). Beyond the fence the channel is less distinct and extends down slope to the northeast (Figure 1.1). The U anomaly strongly correlates with this surface drainage feature.

The variation in peat thickness in the eastern area of the site has been measured and contoured peat thicknesses are presented in Figure 1.1. Areas of thickest peat cover correspond to heather-clad mounds. Elsewhere the vegetation cover consists of rough tussocky grass, patchy heather, sphagnum, orchids, Potentilla and Equisetum, with cotton grass, sedges butterwort and Equisetum in the wettest patches. The peat is thinnest (<0.5m) in the area of the drainage channel.

Recent anthropogenic disturbance to the site, and adjacent areas, has been noticed. Between the 1986 and 1987 visits a water main trench had been dug to at least 1m depth, and backfilled, along a line parallel to the road and about 3m east of it. Between 1987 and summer 1988 forestry operations (Fountain Forestry) had dug several trial drainage trenches some 100-200m downslope from the eastern limit of the current investigations. In addition, between 1987 and 1988 a small quarry in flagstones, now flooded, was opened adjacent to the road and pond at the southern limit of the site, to provide roadstone for local forestry tracks.

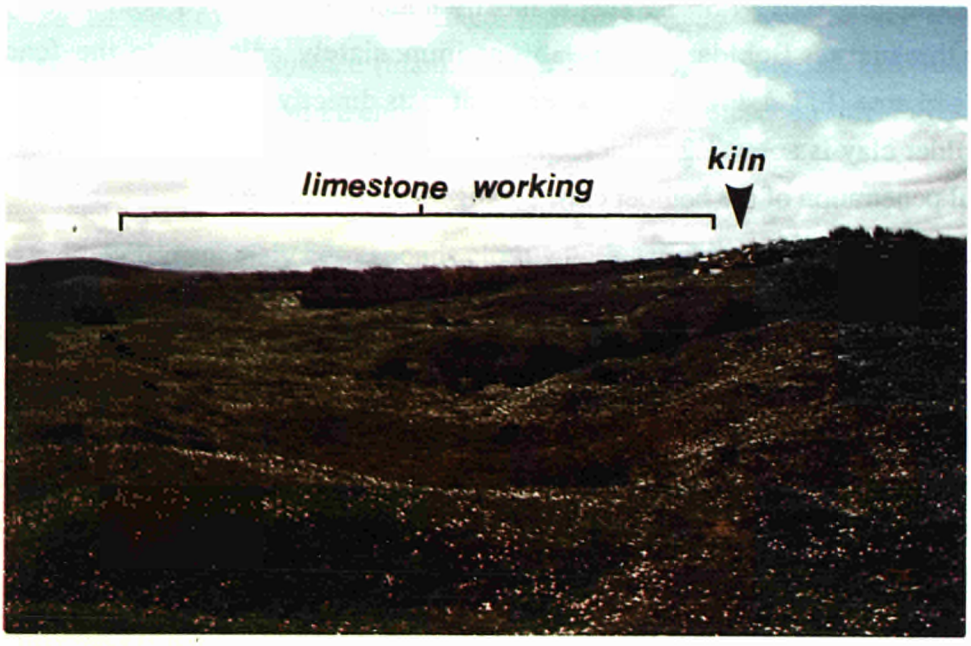

PLATE 1 Photograph of the western side of the site looking southwest from the road to the lime kiln, irregular topography within the depression developed over worked-out limestone area.

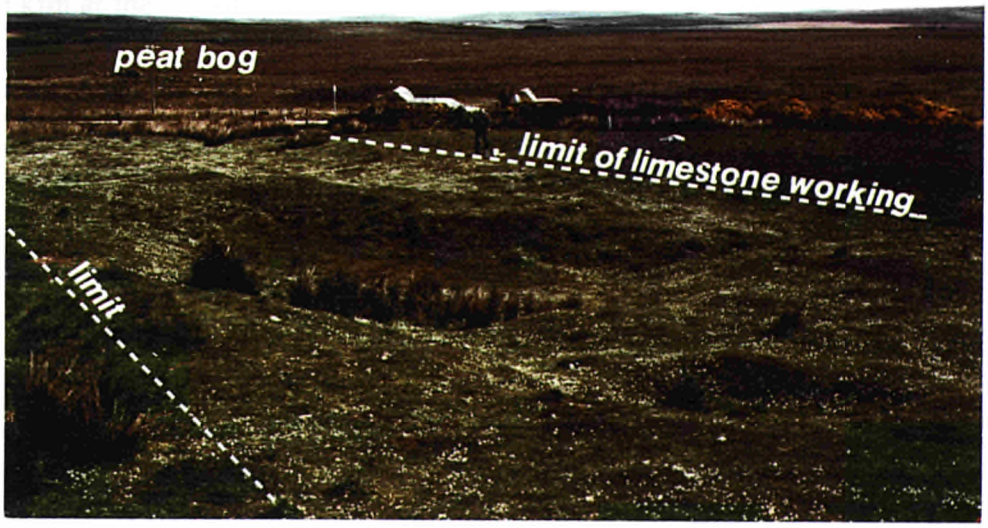

PLATE 2 Photograph showing the view over the site eastwards from the lime kiln. This illustrates the irregular fill within the ancient quarry depression and the variation in vegetation which delineates the brown earths from background blanket peat. The peat-covered area of the eastern side of the road is also evident.

PLATE 3 Photograph of the area around E4 on the east side of the site showing standing surface water resting on peat.

3. SOIL GEOCHEMICAL TRAVERSES AND SOIL PITS

3.1 The 1968 data Line 1

Table 3.1 and Figures 3.1.1 through to 3.1.9 show the data for Line 1. The sample types range from waterlogged peats and organominerallic soils at surface (indicated by the symbol *) to the underlying boulder clay (indicated +). The highest value for γ activity occured at about 50m metres along the traverse. The soils were all moderately acid with the surface peats usually exhibiting lower pH values than the boulder clay. The Eh values for the surface samples were variable with the highest value for the traverse at about 39m and the lowest at about 18m.

The U distribution in the surface soils did not accord with the surface γ radiation values. The highest value was at about 13m, but other peaks occurred at about 30 and 50m. The highest value in the boulder clay sample was at 35m. The surface U value at 13m had an associated small peak in the γ activity profile.

MnO was determined because of its well known scavenging properties in the secondary environment. The near-surface samples showed higher values than in the boulder clay in general. The highest value was in the same position as the peak in the γ profile. It is likely that the MnO had scavenged Ra from solution. Peaks in the Zn and Mo profiles accord with the MnO peak. Cu and Mo also showed similar distributions to U with high values at about 13m.

3.2 The 1968 data Line 2.

Table 3.2 and Figures 3.2.1 through to 3.2.9 give the analytical results for Line 2 which was positioned west of the road and close to Traverse 1 of 1987. The ground was mostly dry with surface drainage near the northern end. The γ activity was generally low with a broad maximum at about 30m. pH values were similarly low rising towards the northern portion, surface values were lower than in the underlying gleys. The Eh values showed moderately oxidising conditions declining slightly towards the northern end of the traverse. The U concentrations were low throughout, the values in the organic rich surface layers being lower than those in the boulder clays. The maximum U concentration was at about 13m. The MnO values reached a maximum in the area of the surface drainage where the pH was high. Cu showed a dissimilar pattern to the other elements peaking near the middle of the traverse. The Pb pattern was erratic with high values in the surface samples distributed unevenly along the traverse. Zn values were similarly erratic, generally with surface samples showing lower

values than the clays. The Mo values were low reaching a minimum where the pH was highest.

3.3 The 1968 data Line 3

Table 3.3 and Figures 3.3.1 through to 3.3.9 exhibit the data for Line 3. This line was through the main radioactive anomaly and the extent of subsurface disturbance was not appreciated at the time. The traverse extended from heather covered peaty ground, underlain by brown earths, bracketing thick brown earths which extended to the surface. The extent of disturbance has since been determined and is about 5m wide, from about 35 to 40m, along the Line. Generally the anomalies centred upon this disturbed zone are wider so that although positional information would be suspect the overall geochemical patterns observed can be useful.

The γ activity peaked at about 35-40m but was seen to rise progressively towards this position. The pH values similarly increased towards the centre of the traverse. As expected the deeper brown earths had higher pH values than the surface peats. Eh measurements for the deeper samples showed lower Eh in those samples with the highest pH.

U values were highest in the disturbed ground but high values were also detected on either side in both surface and deep samples. The MnO pattern was very similar to that of pH. The Cu distribution was erratic but, for the deeper samples, at least, the maximum values were close to the maximum on the U distribution as were the maxima on the Zn and Mo patterns. The Pb distribution follows closely that of pH.

3.4 The 1986 traverse.

X-ray fluorescence spectrometric (XRFS) analytical data for this traverse are itemised in Table 3.4 and illustrations of geochemical profiles for selected elements are shown in Figures 3.4.1 to 3.4.14. The Loss on Ignition (LOI) gives an indication of the peat content of the soils (Figure 3.4.2). At the southern end of the surface profile (0-10cms, *) the minerallic component in the soil was high but the peat content increased rapidly to the north. This was reflected to a greater degree by the profile for the intermediate depth samples (50-80cms, +) where the difference was enhanced. The deepest samples (~100cms, x) were mostly clays although there was very deep peat towards the northern limits of the traverse. The pattern of the LOI and soil types was complementary but antipathetic to that shown by the K_2O profile. The K_2O levels were high where LOI was low, in relation to the clay content. This relationship was also reflected by the surface γ spectrometric data (Figure 3.4.1) for both

total γ and K-40 counts. Although irregular, the U concentration showed a strong affinity to the organic soils (Figure 3.4.3) in contrast to the pattern for Th which showed higher levels in the minerallic soils. For the Rare Earth Elements (REE) Ce and La showed a broadly similar distribution to Th but in strong contrast Y was more abundant in the organic rich soils, generally reflecting the U pattern.

The data for Pb (Figure 3.4.10) reflected the generally immobile nature of this metal, but the Ba distribution showed evidence for a concentration in both mineral rich and organic rich soils.

Unfortunately few Eh/pH data were available for this traverse. The available data are summarised in Table 3.4. pH data were more abundant and the levels range from 5.7 to 6.9 for the surface peats. In the deeper clay rich samples the range was 6.5 to 7.1.

A statistical treatment of the data is given in section 6.2

3.5 Rare earth element distributions 1986 Traverse.

A suite of samples from this traverse was selected for sequential leaching tests. Some REE determinations were made upon untreated material and these provided additional information for this traverse (Table 3.5). The samples selected were in the neighbourhood of the maximum U anomaly and comprise samples from the peats and from the boulder clays. Figure 3.5.1. gives a REE distribution profile for some of the REE in a chondrite normalised (CN, Nakamura, 1974) form for two peat samples. Ce showed evidence of anomalous behaviour with a positive anomaly in the surface sample and a negative anomaly in the deeper peat. The Heavy REEs (HREEs) were more abundant than the Middle REEs (MREEs) and were of similar concentration levels to the Light REEs (LREEs).

The samples from the boulder clays (Figure 3.5.2) showed little variation in absolute concentration, the LREEs>HREEs, and there was evidence for a negative Eu anomaly. The HREEs exhibit mostly a flat distribution pattern. The patterns in the boulder clay are consistent with the bulk of the REE being present in the form of monazite (see Section 4). The peats contain higher concentrations of M and HREE than do the clays.

The anomalous behaviour of Ce helps to explain the apparent absence of strong correlation with the other REE and Y in the traverse (see Section 6).

3.6 1987 Traverse 1

Analytical data for this traverse are in Table 3.6 and Figures 3.6.1 through to 3.6.19. The position was close to but not colinear with Line 2 of the 1968 traverses. The vegetation type was mostly grass with some sedge and small amounts of heather and Potentilla. Common sedge was plentiful in a boggy area extending from 35-40m along the traverse where it was accompanied by Sphagnum.

A small peak in the Total γ, Bi-214 and K-40 photopeaks were observed at about 15m but the K-40 counts were highest near the northern end of the traverse. The surface soils were organo-minerallic over much of the traverse but at 15, 30 and 35m true peats were observed (Figure 3.6.4.)

The pH values increased sharply near the northern end of the traverse where the ground was wetter. The Eh values were lowest where the ground was wet, but generally the organic rich soils exhibit lower values of Eh than the boulder clays.

The U distributions along the traverse are shown in Figure 3.6.5. The values in the surface samples were much lower than those in the deeper clays. There was a peak in the deeper samples at 25m corresponding to high values in the Pb, MnO, REE, Th and Mo profiles indicating the possible suboutcrop of the mineralised structure.

Th was generally higher in the clays than in the surface samples, a feature shown also by U, REE, Zn and Mo. MnO, Zn and pH are high at 35m, in waterlogged surface soil.

The REE profiles in the boulder clays (Figures 3.6.18 and 19) showed a restricted range of values. The highest concentration was at 25m (? close to mineralisation) but the other samples showed a family of curves with a small range, LREE>HREE, and with no evidence of a marked Ce anomaly. The sample at 25m showed slight evidence for a positive Ce anomaly.

Many REEs were not detectable in the surface samples (Figure 3.6.16 and 17) and the values were generally slightly lower than in the clays. The patterns were however similar and are consistent with the bulk of the REE being resident in monazite.

3.7 1987 Traverse 2.

This traverse was in the identical position to Line 1 of 1968, although the sampling points

differ. The analytical data are summarised in Table 3.7 and Figures 3.7.1 to 3.7.20. The soils comprised organic rich surface samples underlain by gleys which were usually dark grey but sometimes mottled. The total gamma profiles for the two years differ considerably. In 1968 there was a marked increase in γ activity (Figure 3.1.1) in the northern section of the traverse which did not appear in the 1987 data (Figure 3.7.1). The specific photopeaks similarly show no evidence of a recognisable pattern. The pH values are low in the peats and gleys in the southern portion of the profile and increased to peak at about 10 and 45m (Figure 3.7.2). These values were very significantly greater than those observed during 1968 (Figure 3.1.2). The Eh values for 1987 (Figure 3.7.3) were generally lower than those observed during 1968 (Figure 3.1.3), presumably a reflection of the wetter conditions during 1987. The U distribution patterns were broadly comparable although the actual values differ considerably, being much higher in the 1987 samples (Figure 3.7.5). Too much attention should not however be given to these figures as the data from the pit profiles indicated that even within the surface soils there was great variation in the concentration of U.

Th increased slightly from S-N (Figure 3.7.6) as reflected by the Tl-208 photopeak intensity, but the pattern was not similar to that of U. K_2O increased towards the northern end of the traverse reflecting the lower LOI values and consistent with the K-40 photopeak activity (Figure 3.7.7).

Cu, Mo and REE mirror the distribution of U in the surface soils. The MnO concentration was particularly high in a number of irregular locations in the surface layers but there was no consistent relationship with other metals. In the deeper gleys a peak at 15m corresponded also to high values in U, Zn, Mo and Y. Minor peaks in the MnO profile at 40m and 50 m corresponded also with peaks in these other distributions.

The few REEs showed distributions in the surface layers which corresponded closely with the distributions displayed by U. Except at these peaks the values in the gleys were slightly higher than those in the surface layers, with the exception of Ce which was generally lower in the surface samples.

REE distribution profiles were presented in Figures 3.7.17 through to 3.7.20. Most of the surface samples showed a well defined negative Ce anomaly and LREE=HREE except for the samples at the northern end of the traverse where the LREE>HREE and there was a barely noticeable Ce anomaly. In the deeper gleys only two samples showed, in a pronounced fashion, the same REE behaviour as the surface samples and these were at 5 and 15m, and to a lesser extent 30, 40 and 50m, corresponding to moderately high MnO (and Zn and U) values.

3.8. 1987 Traverse 3.

The position of this traverse was close to but not identical to Line 3 of 1968. The traverse extended from a peat covered area overlying brown earths at the southern end of the traverse and finished in undisturbed ground at the northern end. The data are summarised in Table 3.8 and Figures 3.8.1 through to 3.8.20.

Compared with the 1968 data the pH values were higher and Eh slightly lower. The γ spectrometric values showed high concentrations for all isotopes in the central portion of the traverse and the patterns reflected the pH values. The U, Th and K_2O values mirrored almost exactly the patterns exhibited by the γ spectrometric data.

MnO, Cu, Mo, Zn, U and to a certain extent Th showed similar distribution patterns.

The REE showed broad increases over the same area. The REE distribution profiles overall showed broad similarities exhibiting a family of curves of almost identical pattern, each with a slight positive Ce anomaly and LREE>HREE. The only exception was at 25m in the deep augured sample where a marked negative Ce anomaly was displayed.

3.9. 1988 Traverse 4

This traverse (along with Traverse 5) was undertaken to test the extent of U dispersion to the east and north-east of the site and to check whether there was evidence for disequilibrium in the U decay series. The data are summarised in Table 3.9 and Figures 3.9.1 and 3.9.2.

There was a broadly similar pattern for the total γ and the counts in the U and Th channel. The U determinations in both surface peats and the underlying boulder clay showed similar distributions but the peaks were considerably displaced from the photopeak maxima.

3.10. 1988 Traverse 5.

The data are summarised in Table 3.10 and Figures 3.10.1 and 3.10.2.

Again there was a reasonable similarity between the gamma spectrometric data for total γ, Bi-214 and Tl-208. The maxima on these graphs corresponded to minima on the U distribution profiles except at the northern extremity where high values are observed for all of these observations.

3.11 Soil pit profiles

3.11.1 PIT 2 (1987)

In order to examine the geochemistry of U and other elements in the peat bog area east of the road in more detail, a large pit (PIT 2, Figure 1.1) was dug. The pit was located in the region of maximum U anomaly from previous work (Figure 1.2). The pit depth of 1.30m was limited by an impenetrable layer of large rocks and boulders, within the underlying boulder clay (Plate 4). By comparison with adjacent PIT 8 the boulder clay is believed to persist to about 1.50m below ground level (bgl). Samples were collected throughout the profile for geochemical analysis in which especial attention was paid to U, Th and the REEs. In addition, a complete section was preserved in the form of undisturbed box samples collected in 10cm intervals from the top of the peat to just below the top of the boulder clay. These were obtained by inserting 10cm by 5cm aluminium soil tins into the cleaned soil face, and then excavating the surrounding soil, leaving the undisturbed material in the box. These samples were collected for microscopic and autoradiographic examination and will be the subject of another report.

The soil profile is described in detail in Figure 3.11.1. Of particular interest were a number of plant roots which were seen to penetrate well into the boulder clay (Plate 6). Some roots were seen to penetrate the entire section of the pit and both dead and living roots were present at depth. Water was seen to seep along the peat/boulder clay interface and the basal 5cm of peat was water saturated. Water also emerged along the sides of living roots and old root channels. Of particular importance were old root channels of Equisetum, a primitive plant with large hollow tough roots which have a stellate cross-section. These appear to remain open and to provide pathways for water transport through the entire section, long after the death of the plant. Concentrations of secondary Fe and Mn sesquioxides are strongly associated with root channels or soil fractures in the boulder clay (Plate 7). Fe and Mn staining around the channels is often zoned with the Mn precipitated as a black stain close to the channel and the Fe present in an ochreous halo around the Mn (Plate 7). Precipitation of secondary Fe and Mn sesquioxides also results in the mottling seen in the upper part of the boulder clay (B/C horizon), but some staining persists in the stonier C/D horizon. Fe staining changes with depth from a yellow ochreous colour in the upper levels to a reddish brown colour at depth.

The top of the boulder clay has a bleached creamy-white E horizon developed in coarse sandy clay. This indicates leaching of Fe and Mn along with other elements from this horizon. In the E and B/C horizon rock fragments are generally relatively small and usually

well-rotted (Plate 7), but with increasing depth they become larger and more competent. Large boulders of local flagstone dominate the C/D horizon and appear to have a preferred orientation with the slabby boulders dipping in a slightly imbricate fashion gently to the east.

The chemical analytical data are summarised in Table 3.11 and Figures 3.11.2 through to 3.11.7. Unfortunately the only available data on the REE were obtained using an Instrumental Neutron Activation Analysis method. The values for Ce may be suspect (see appendix).

Fig 3.11.2 shows chondrite normalised profiles for a small number of the REE at different depths in the peat, whilst Figure 3.11.3. gives the results for the underlying clays. The profiles for the clays are rather typical of well developed sandstone/siltstone mixes with LREE>HREE, and some indication of a small negative Eu anomaly. Monazite has been identified in the boulder clay and the REE distribution patterns are consistent with the bulk of the REE being contained in this mineral.

The patterns for the peats are different. The concentration of the total (T) REE are greater and although LREE>HREE the difference is small.

Both U and Th show a similar distribution pattern (Figure 3.11.4) but Th, consistent with its presence also in a detrital phase is more abundant than U in the clay rich substrate. The main U concentration is at about 25cms depth and corresponds with peaks in the Mo, Ba and As profiles (Figures 3.11.4 - 3.11.7). Br, As and Sb are enriched in the organic rich soils. Fe and Co exhibit similar distribution patterns but Cr is markedly different showing higher values in the detrital soils. Zn shows high but irregular values throughout.

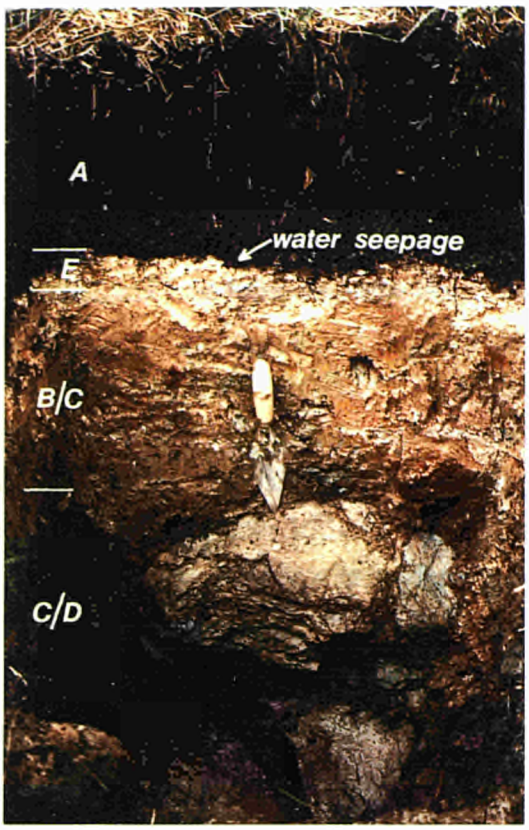

PLATE 4 Photograph of PIT 2 showing brown-black layer of peat overlying boulder clay which becomes increasingly stonier with depth. Leached upper surface of boulder clay (E horizon) indicated. Pit depth limited by the presence of boulders of flagstone.

PLATE 5 Collection of oriented, undisturbed samples for the preparation of petrographic sections of soils (PIT 2).

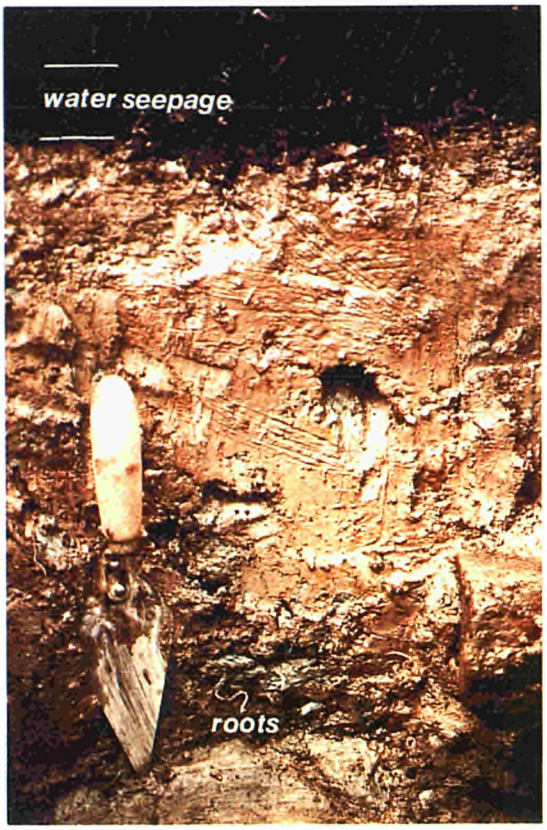

PLATE 6 Detail of soil section in the upper part of the boulder clay in PIT 2 showing seepage of groundwater over the soil-pit face from the contact with the overlying peat and along deep root channels.

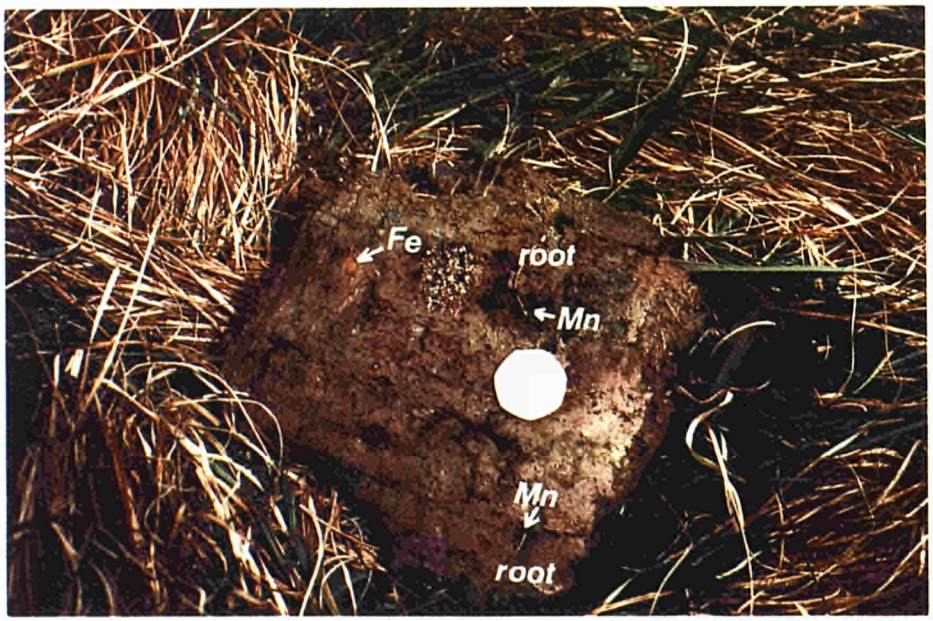

PLATE 7 Detail of Fe and Mn oxide or hydroxide staining and mottling around living and dead root channels in boulder clay, often showing zoning with Mn oxide (black staining) immediately adjacent to root (Mn) surrounded by a halo of Fe sesquioxide (Fe). PIT 2 boulder clay

3.11.2 PIT 8. (1988)

PIT 8 was dug immediately adjacent to the earlier PIT 2, in order to re-examine the earlier geochemical data and to extend sampling for more detailed REE, U, Th determinations, radiocarbon dating of peat and extraction of soil porewaters. The soil profile was identical to PIT 2 (Fig 3.11.1). The pit was dug only to a depth of 55cms, to a large boulder, but penetration to 1.50m bgl was achieved by augering to what is thought to be bedrock. On completing the augering water flowed up the hole and flooded the pit. A large plastic drain pipe was emplaced in the auger hole and sealed by puddling the clay. The water in this piezometer (E1, Figure 1.1) was found to rise close to the top of the boulder clay (36.9cm bgl).

Large samples (1-2kg) for porewater extraction were collected from 2-10cm (upper peat), 10-18cms (middle peat), 22-32cm (basal peat), 32-39cm (leached E horizon), 39-49cm bgl (B/C horizon Boulder Clay). These samples were tightly sealed in polyethylene and placed in tight fitting airtight tubs. Replicate samples were collected for analysis by UKAEA Harwell, and for radiocarbon dating by SURRC, East Kilbride and for whole rock geochemistry.

Tables 3.12 and 5.1, and figures 3.11.8 to 3.11.13, summarise the analytical data for soils and corresponding squeezed porewaters collected from PIT 8. Radiocarbon (C-14) dates for the peats give minimum ages from modern-day, at the top of the peat, to 4630 ± '50 years BP for the basal specimen. This is consistent with the observation of birch and pine boles at the base of the peat which indicate a "Boreal" climate which would have developed during post-Devensian warming, 10000 years BP (West, 1977).

The chondrite normalised REE distribution profiles for the soils are given in Figure 3.11.4. Except for Ce the peats generally have more LREE than the clays and and a substantially greater M and HREE concentration. All samples have a slight negative Eu anomaly and most samples apart from the deepest clay show a high level of Y. The peats exhibit a strong Ce anomaly but in contrast the clays show no evidence for anomalous behaviour of Ce.

The boulder clay and background sandstones display similar REE patterns consistent with most of the REEs being in a monazite host mineral (Henderson, 1984). The REE pattern for the peats shows progressive enrichment from top to bottom, especially for the LREE, with the exception of Ce for which enrichment is only slight. Although the peats show greater TREE than other samples the shape for the profiles for peats, limestones and mineralised limestones are all similar for the M and HREE suggesting that the bulk of the REE in the peat

is limestone derived. The patterns are similar to those observed from apatites (Henderson, 1984).

The REE distribution profiles for the porewaters are given in Figure 3.11.8. In many cases the concentrations were at or below the detection limits. Peat porewaters show a well-marked negative Ce anomaly and a slight positive Eu anomaly. The basal peat sample has the highest pore water trivalent REE content and the most complete (and probably the most reliable) REE distribution pattern which shows a slight enrichment of HREE relative to MREE and LREE. Porewaters from the clays have very low TREE contents and no discernible Ce anomaly.

U, Ca, Ba, HCO_3 and pH are all very high in the waters from the surface sample. The highest U concentration in the solid peat relates to a lower HCO_3 content but moderately higher concentrations of aqueous U and high Fe. The pH and HCO_3 is shown diagrammatically in Figure 3.11.10.

Earlier analysis for Th from PIT 2 had indicated a significant enrichment of Th at the base of the peat. However in PIT 8 no such high values were found, and this was confirmed by both XRF and INAA. The earlier results from PIT 2 (based upon INAA only) are therefore considered suspect.

3.11.3 PIT 3 (1987)

PIT 3 was dug to examine profiles in another area where there were moderate vales of U and high surface radioactivity (Figure 1.1). Three samples were selected for further analysis (Table 3.13) and the soil profile is shown in Figure 3.11.15 . The two peat samples show similar high concentrations of U and S. The near surface sample shows higher levels of Fe_2O_3, MnO, P_2O_5, Ba, Mo, Pb, Y, Zn, Zr and Nb, consistent apart from the last two elements with coprecipitation or scavenging of soluble elements on sesquioxide gels. The deeper peats show especially high levels of CaO, S, Cu, and Sr.

The REE distribution profiles are given in Figure 3.11.16. There is a negative Ce anomaly in the surface peat and a very high Y concentration. The profile in the deep peat shows a slight Ce anomaly and a lower Y content. The profile in the clay is similar to that in the the other boulder clays in the region.

3.11.4 PIT 9 (1987).

A further pit (PIT 9) was dug to the west of the main anomaly and three samples taken representing the basal clay, a Mn/Fe rich zone (pan), and the thin surface organic rich soil. U is generally low (Table 3.14), the highest concentration of only 15 ppm occurring in the deeper sample. There is an indication of a negative Ce anomaly in the surface organic soil. Ba is high throughout but is highest in the pan along with MnO but not Fe_2O_3. There is no indication that the Mn minerals have coprecipitated or scavenged any other elements such as Co, U, or the REE. Sr is however highest in this zone.

3.11.5 PIT 1. (1987 and 1988)

PIT 1 was dug originally to furnish samples for the characterisation of the U source mineralisation (Figure 1.1). It was located within, and close to the edge, of the old quarry workings. The pit was re-exhumed in 1988, further to investigate the mineralisation and to provide samples for BGS and UKAEA, with particular emphasise on obtaining vein hydrocarbons.

Details of the pit are described in Figure 3.11.17 and in Plate 8. A well-drained brown earth soil profile is developed on a highly weathered siltstone overlying a hard, competent finely laminated limestone which in turn rests in a dark grey calcareous siltstone base. Relicts of the original sedimentary fabric can be traced in the gleyed lower horizon of the soil. The upper siltstone layer is well rotted and gleyed towards its upper surface. The base of the limestone is brecciated and mineralised. Water seepage is seen to occur at the base of the limestone and along the backfill/bedrock contact. Small scale karstic development at this level is evident from the presence of cavities (Plate 9) which may extend for more than 25 cms horizontally into the rock face.

At the base of the soil and in the strongly weathered regolith, obvious accumulations of secondary Fe and Mn sesquioxides have occurred. Within this zone irregular bands of black Mn-rich powdery "wad" occur, within irregular patches of red-brown ochreous clay. Further up the profile this strong banding disperses into more mottled-features in which black Mn-rich zones are seen to be surrounded by diffuse Fe-rich ochre. Radiometric observations indicate that the "wad" is significantly more radioactive than the surrounding soils.

The U concentration is generally low for the area, being broadly comparable to the Th levels. MnO is high in the same sample in which the highest Ba level is also noted. Sr is also

slightly high in this sample. Ra often shows a similar behaviour to Ba (and to a lesser extent Sr) and the high radiometric values are ascribed to Ra but not U concentrations in the wad. Ra possibly substitutes for Ba which is commonly present in wads as psilomelane ($Ba,H_2O)_2Mn_5O_{10}$) and is also common in weathered rocks.

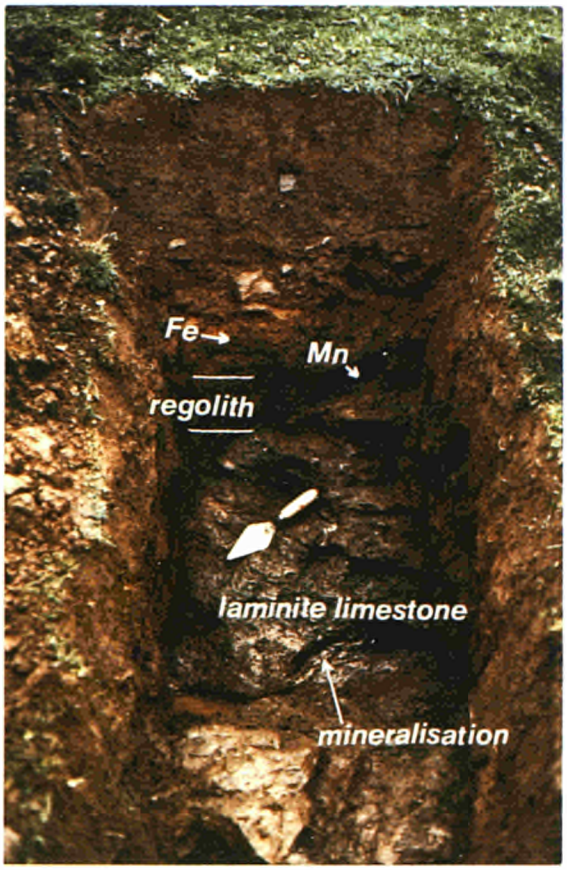

PLATE 8 Photograph of soil section in PIT 1 showing limestone laminite at base of pit. Note zone Mn and Fe accumulation towards base of soil profile and seepage of water at base of pit.

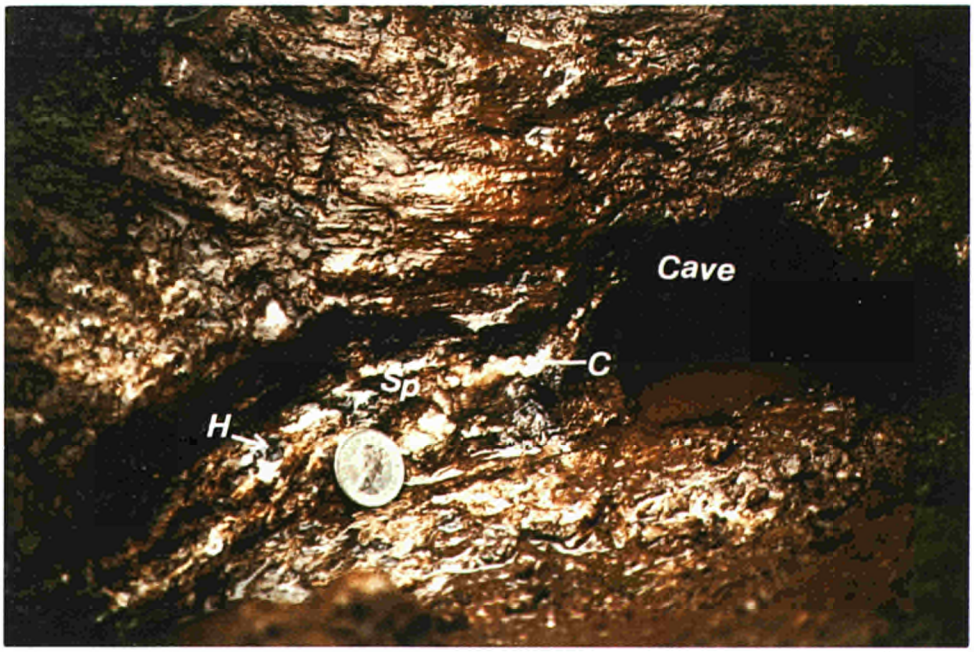

PLATE 9 Detail of irregular pods of calcite veining at the base of the limestone laminite, showing reddish sphalerite (Sp) calcite (C) and hydrocarbon globules (H). Water seeps along backfill bedrock contact and dissolution of the limestone at this level has produced cavernous porosity at the base of the limestone (Cave).

4. MINERALOGY AND PETROGRAPHY

4.1 General

Preliminary mineralogical and petrological studies of the mineralisation, bedrock lithologies,and soils from the peat bog area have been made and are reported here. A more detailed presentation of U source term mineralisation will be presented elsewhere (Milodowski et al, 1989). Limestone, sandstone, siltstones and mineralised rock samples were examined in polished thin sections, by optical microscopy and scanning electron microscopy (SEM) in backscattered electron imagery mode (BSEM) with energy dispersive X-ray microanalysis (EDXA). Whilst capable of giving a semi quantitative chemical analysis of a mineral phase, no indication of the crystalline nature of the sample can be given. The EDXA system cannot determine elements with an Atomic Number less than 11(=Na). Further details of analytical techniques are given in the Appendix.

4.2 Sandstones and Siltstones

Four samples of background silt- and sandstones were collected from a recent quarry by the roadside, and close to the pond (Figure 1.1). At this site boulder clay is absent and peat rests directly upon bedrock. The sandstones are flaggy with shale or siltstone laminae along which the rock splits easily. The rocks are strongly weathered and vary in colour from yellow-buff to rusty brown. Chemical analyses are given in Table 4.1. U ranges 2-7ppm and Th from 1 to 16ppm.

The siltstones and sandstones are arkosic to subarkosic, composed largely of detrital quartz, with subordinate K-feldspar, plagioclase, white mica, chlorite and biotite. In the clay-rich laminae mica is more abundant. Secondary aggregates of fine-grained TiO_2 (anatase) are often abundant and pseudomorph detrital ferromagnesian grains. Accessory detrital minerals include: common zircon, apatite, rutile needles, chromite, a spinel (intermediate between chromite/ spinel/ hercynite/ magnesioferrite) and occasional monazite and xenotime. In the clay-rich laminae the matrix is dominated by fine-grained mica (muscovite-illite) and chlorite or mixed-layer chlorite-smectite.

Sandstone lamellae vary from medium (100-300μm) to very fine (63-100μm) sand with silty or clay partings. The sandstones have a very porous grain supported fabric (Plate 10) with well-developed authigenic grain overgrowth cements of quartz and K-feldspar (e.g.Plate 11), forming a rigid framework. Much of this cementation must have been early diagenetic since less competent grains such as mica show little sign of compaction deformation (Plate 10).

Clay-rich siltstone lamellae have, by contrast, little quartz or feldspar overgrowths and the micas are deformed around competent grains (Plate 12).

Patches of sandstone are tightly cemented with dolomite, ankerite and calcite cements (Plate 13). Within these cemented areas the textures of the carbonate cements are complex. Dolomite appears to be a very early authigenic mineral, always enclosed within other later carbonates. Its grain supporting relationship with other siliclastic grains indicates that it either replaced a detrital precursor or was itself a detrital component (Plates 13 and 14). Alternatively it may represent pellets of reworked penecontemporaneous carbonate sediment ("cornstones"). The dolomite is always enclosed within overgrowths of authigenic ankerite or ferroan dolomite (Plate 14). The ankerite post-dates the formation of the quartz and feldspar overgrowths which it can be seen to corrode and partly replace. Late calcite fills any remaining pore space.

Within the tightly carbonate-cemented rock, pyrite is locally abundant, occurring as finely disseminated octahedra, framboidal aggregates and larger cubiform crystals < 30μm across. Elsewhere it is absent or suspected to have been present where goethite pseudomorphs are seen (Plate 15). Similarly biotite alters to goethite/ haematite, TiO_2 and probable fine illitic clay. Secondary alteration products of biotite are commonly seen along cleavages (Plate 16). Minor secondary LREE rich phosphate (rhabdophane, (Ce, La, Nd) PO_4, H_2O) is also seen along altered biotite cleavages.

Many of the intergranular pores of the sandstone are clearly oversize (Plate 17) a feature characteristic of secondary porosity (Schmidt and McDonald, 1979). This together with the extensive etching of the carbonate cements and to a lesser extent of the detrital feldspar, indicates that much of the porosity in the sandstones and siltstones has resulted from the dissolution of these minerals.

Many pores are lined by spongy fine-grained or amorphous iron sesquioxide (goethite?). Barite is common, occurring both within cement rocks and framework grain dissolution sites (principally K-spar). In the cemented rocks the barite is probably diagenetic. However, barite in the secondary pores may be of later origin, resulting from liberation of Ba from K-spar and its precipitation with SO_4^{2-} produced by pyrite weathering. Rare witherite was also found in the surface sandstone as a late weathering product.

Unweathered Caithness flagstone as seen locally, has little porosity and consequently little intrinsic permeability. These weathered sandstones by contrast have porosities of about 25-30% with large (> 100μm) pore sizes in the sandy laminae. Therefore the weathered

bedrock is likely to represent a relatively permeable pathway for groundwater movement in areas covered by boulder clay.

The sandstones have a geochemistry typical of immature arkoses with an abundance of potassic feldspars (Table 2.1). The sandstones contain moderate amounts of P_2O_5. The U concentration ranges 2-7ppm whilst the Th levels range from <2 to 16 ppm. There is a general trend of increasing U with Th and P_2O_5 which is not reflected in the REE values or in the other elements one would expect in a heavy mineral detrital fraction such as Zr, TiO_2 and Nb. It is likely that there is an U,Th phosphate mineral present in the sandstones but only at low concentrations. Ba is high, shows no correlation with K_2O, and is present as barite. The REE distribution patterns are shown in Figure 3.11.8. The patterns are consistent with the bulk of the REE being present in monazites.

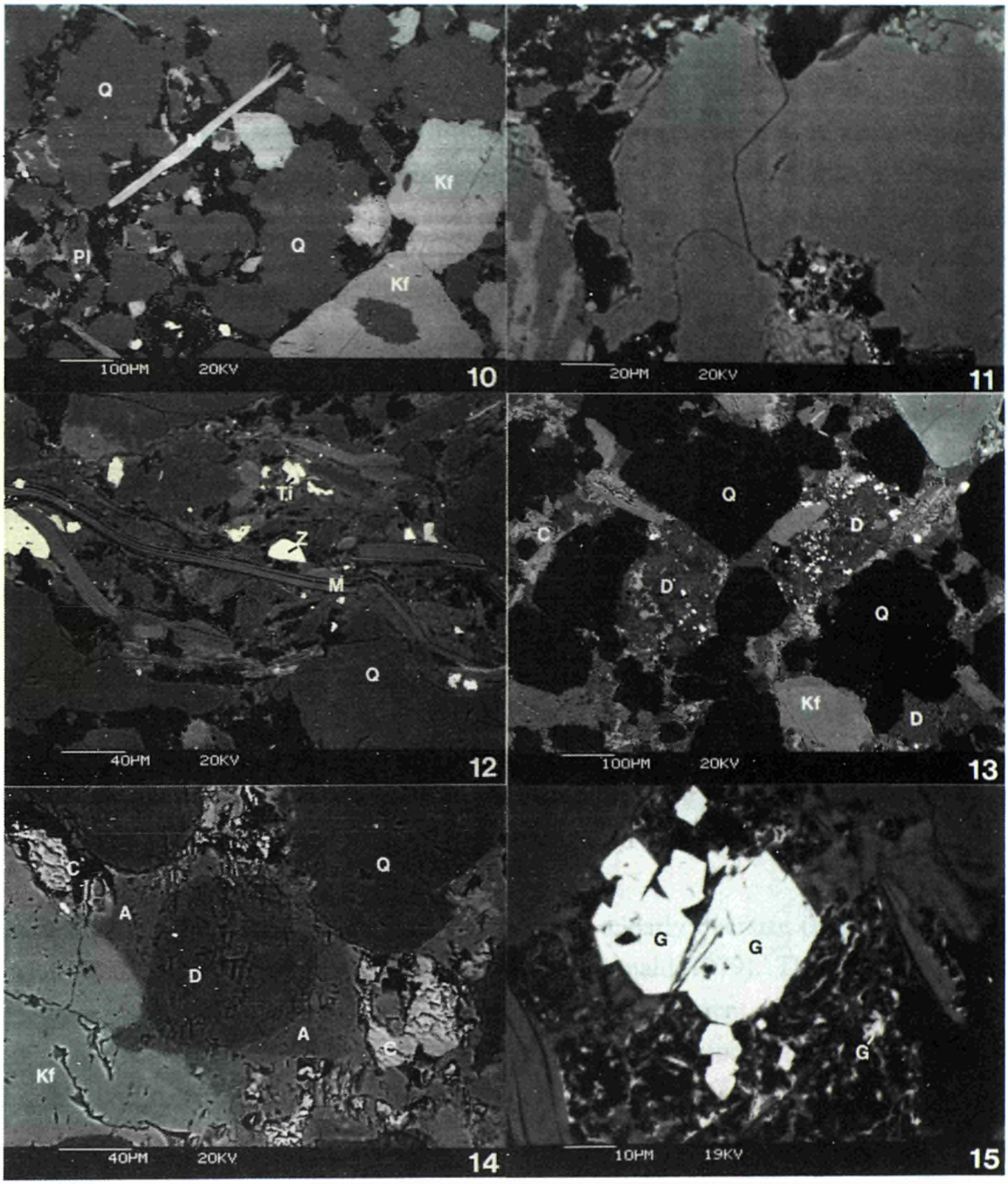

PLATE 10 BSEM photomicrograph showing grain supported detrital fabric of sandstone. Consists of detrital quartz (Q), K-feldspar (KR), muscovite (M) and plagioclase (Pl). Note lack of mica deformation, corroded plagioclase and intergrowth of quartz grains.

PLATE 11 BSEM photomicrograph showing detail of interlocking overgrowths of authigenic quartz forming a rigid grain framework. Flaggy sandstone bedrock.

PLATE 12 BSEM photomicrograph of silty clay Lamellae in flaggy sandstone showing burial-compaction fabric with deformation of detrital muscovite (M) around more competent quartz. Note alignment of detrital micas, parallel to bedding. Detrital zircon (Z) and secondary fine TiO_2 seen in clay matrix.

PLATE 13 BSEM photomicrograph of dolomite (D) cemented sandstone consisting of detrital quartz (Q) and K-feldspar grains. Bright pyrite seen fringing area of "oversized" intergranular dolomite that is obviously a dolomite-replaced former framework-supporting detrital component. Brighter calcite (C) seen as a late replacement of dolomite and as a poikilotopic pore-filling cement.

PLATE 14 BSEM photomicrograph of carbonate-cemented sandstone showing a grain of dolomite (D) in framework supporting relationship to detrital quartz (Q) and K-feldspar (KF) with ankerite (A) overgrowth cement and pore-filling late calcite (C). Note dissolution of calcite.

PLATE 15 BSEM photomicrograph showing goethite (G) pseudomorphs after pyrite crystals in siltstone. Finely dispersed goethite also seen within clay matrix.

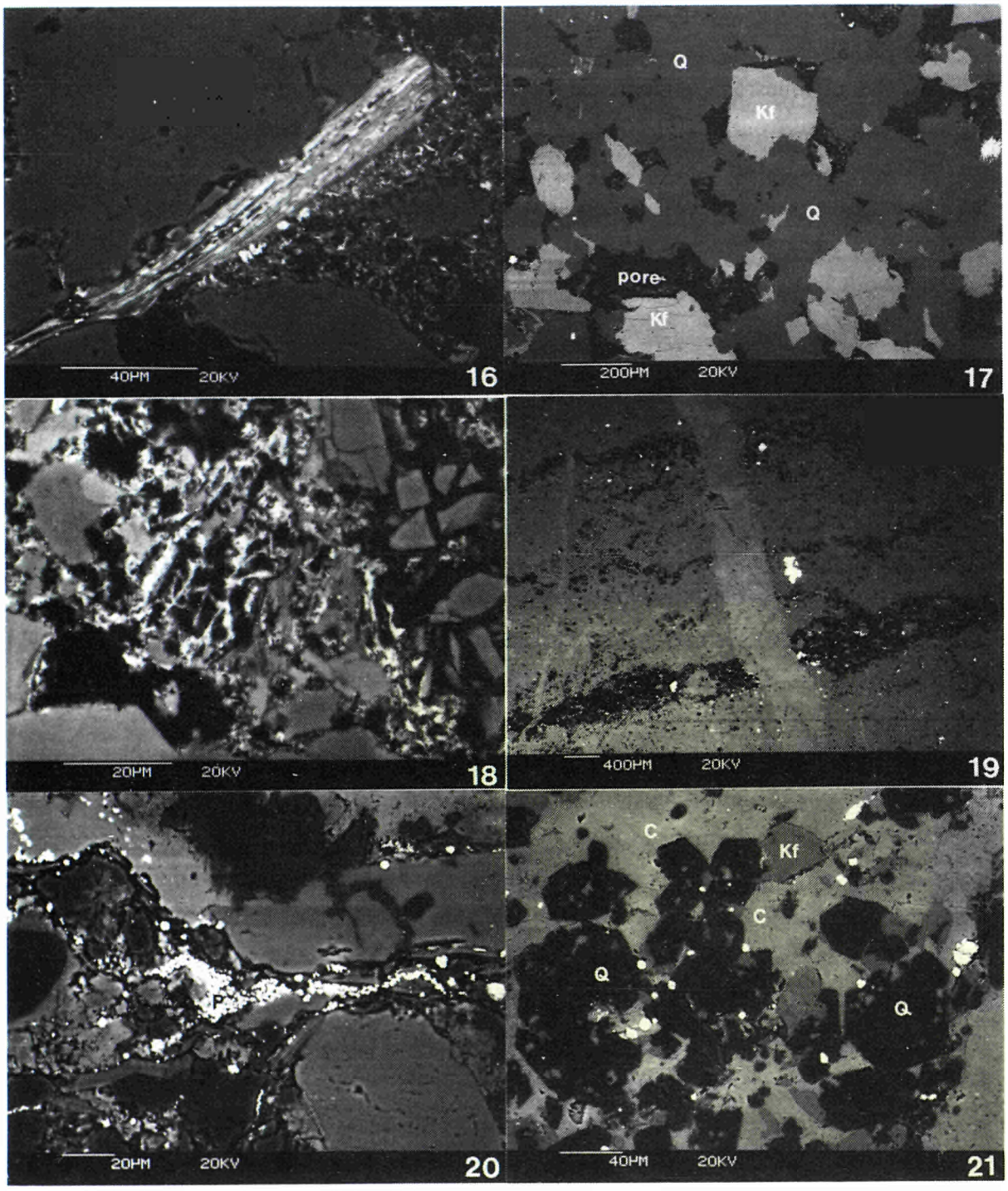

PLATE 16 BSEM photomicrograph of altered detrital biotite within siltstone matrix showing secondary precipitates of bright TiO_2 and ferric oxides along mica cleavage. Note also finely-dispersed goethitic oxide within illite clay matrix.

PLATE 17 BSEM photomicrograph of well-sorted sandstone composed of detrital quartz (Q) and K-feldspar (KF). Note grain-supported fabric rigidly held together by mutually interferring quartz and feldspar authigenic overgrowths. Secondary porosity apparant from presence of oversized pore.

PLATE 18 BSEM photomicrograph showing altered silstone with porosity lined by bright geothite.

PLATE 19 BSEM photomicrograph of finely laminated limestone showing fine laminae of siltstone (dark) interbedded with microsparry calcite (grey) representing recrystallised micrite. Vertical late calcite vein cuts bedding. Bright replacive sulphide minerals are present in wall-rock adjacent to veining.

PLATE 20 BSEM photomicrograph showing silty mudstone lamina within limestone displaying preferential alignment of detrital clay and mica parallel to bedding. Note presence of abundant fine-grained pyrite (P) along this lamina.

PLATE 21 BSEM photomicrograph of well-sorted "clean" siltstone lamina within limestone unit showing extensive euhedral authigenic over-growth of quartz (Q) and K-feldspar (KF) with corrosive replacement by interstitial calcite (C) cement.

4.3 Limestone and the mineralised zone

Six samples of limestone, mineralised limestone and vein carbonate were examined from material collected from PIT 1. Here siltstones rest upon a hard competent finely laminated mudstone which in turn overlies a dark grey laminated siltstone base. The immediately underlying limestone is similar in appearence to the algal rhythmites described by Donovan (1975,1980) and correspond to his lithofacies type "A". The underlying carbonaceous siltstone with fine shaley partings corresponds to type "B" lithofacies. The strata dip at 10-15° N.

The basal 5cm of the limestone is brecciated with irregular lenses of carbonate veining parallel to the bedding. Slickensided surfaces provide evidence for shearing at this level. In addition vertical pods and fine (0.1-0.2mm) carbonate veins are found near the base. Reddish brown sphalerite, pyrite, galena and barite are found in these veins (Plate 9). Hydrocarbon occurs both as black vitreous globules in the calcite or as a brown sticky liquid in vugs. Many of the very fine subvertical fractures contain traces of a dark brown sticky hydrocarbon. Qualitative radiometric observations indicate high levels of activity assciated with the limestone. The bottom siltstone is also significantly radioactive.

The limestone unit is finely laminated comprising alternating thin laminae of microsparrite and coarse calcite cemented siltstone or silty mudstone (Plate 19). These laminae vary in thickness from 0.1 to 0.5mm. In hand speciment the limestone displays thin films or fine laminae of black organic material on bedding surfaces. These organic laminae were not observed in polished thin section, but probably correspond to fine pyritic seams in the clay rich laminae (Plate 20). These organic rich laminae were the sites for slickensided shears in the base of the unit. The clay-free coarse siltstone laminae are calcite-cemented and contain a similar mineral assemblage to the sandstones and siltstones, described previously, except that dolomite and ankerite are notably absent. Detrital quartz and feldspar grains in these laminae are grain-supporting, and exhibit extensive authigenic overgrowths which have produced idiomorphic crystal shapes (Plate 21). The calcite cement post-dates the quartz and feldspar authigenesis and is seen to corrode and replace these detrital grains. The more clay-rich lamellae are pyritic (Plate 20) and generally lack calcite cement. These lamellae also show evidence for burial compaction with the deformation of mica plates around more competent minerals. Many of the siltstone lamellae contain detrital collophane grains (fine grained or amorphous Ca phosphate) which may represent fragments of fish remains. Also present are minor, roughly spherical globules or grains of hydrocarbon or organic matter containing tiny inclusions of U-Ti rich minerals and more rarely Th bearing inclusions (Plate 22).

The intensely veined lower part of the limestone unit displays extensive recrystallisation of the limestone fabric with replacement of the detrital siliciclastic lamellae by calcite (Plate 23). The wall-rock adjacent to the veins may be partly replaced by barite, pyrite and sphalerite with very minor amounts of galena and As/Fe sulphide. In the intensely mineralised limestone, rare inclusions of fine grained (<1μm) gold were identified with the sulphide assemblage and within the calcite veins that replace the siltstones. Stylolitic pressure-solution features are common within the basal part of the limestone and are probably associated with the shear movements that produced the slickensided surfaces.

Two samples of the uraniferous limestone were also analysed (Table 2.1). The limestone has low MgO, and the low abundances of Al_2O_3 and alkalies suggest a small but perceptible clay mineral content. The Pb and Zn levels are moderate and the presence of sphalerite and galena have been recorded. The U and Th values are high with U>Th. The REE concentrations are higher than those in the sandstones, the distribution patterns differ significantly (Figure 3.11.14) and are consistent with an apatite being the main host.

4.4 Soils from PIT 2.

Observations of the mineralogy of the soils east of the road have focused upon the identification of the secondary minerals and possible sites for U, Th and REE. Especial attention has been paid to the PIT 2 materials (Figure 3.11.1).

1. Soil sample PIT 2 at 10cms depth.

Primary minerals include silt size muscovite, chlorite, quartz, albitic plagioclase and K-feldspar all presumably of detrital origin. The feldspars are strongly etched. Mica tends to show some degree of exfoliation. There are possibly some calcite fragments (identified by EDXA). Rootlets and other plant debris show a typical cellular structure. Fe sesquioxides are associated with plant debris as amorphous coatings on cell walls or surrounding peat matrix surfaces. EDXA analyses showed Al, Si, S, K, Ca, Ti and Mn (±Pb, Cr, Ni, Zn and Ba) frequently associated with the Fe oxide phase. Secondary (?) TiO_2 phases are dispersed in the matrix, and are generally very fine grained (<2μm) and often associated with some Fe. Traces of fine grained gold (<1μm) occur in the amorphous Fe oxides and are presumed to be the result of secondary concentration.

Associated with the plant debris are sulphides forming tiny pustules and 1-5μm in diameter (Plate 24). Sulphides also occur as coatings on cellular structures and are often accompanied

by Fe oxides. EDXA spectra indicate the presence of ZnS (?sphalerite). The mode of occurrence is indicative of formation *in situ*

Traces of minute grains of phosphatic minerals are also present, generally disseminated throughout the organic matrix. Many grains are barely resolvable by SEM (<200nm), although others may be as large as 2μm. They range from monazite or rhabdophane like composition to Al-phosphate/REE rich minerals (possibly plumbogummite type, intermediate between crandallite, goyazite and florencite). Th is possibly present in some phosphates but at a level approaching the detection limit for the EDXA (0.5%). It is not clear whether these are clay grade detrital grains or secondary soil minerals. Monazite may well be primary but plumbogummite minerals are known to grow in soils (Brown et al.,1978).

Fe sesquioxides are commonly developed around rootlets and are also quite aluminous suggesting that perhaps a gibbsitic component may be present.

2. Soil sample PIT 2 at 25 cms depth

Generally similar to sample 2. Fe sesquioxides commonly are developed as patches or coatings on rootlets (Plate 25). Traces of gold are more common (although still very rare) and are also found in association with the Fe oxides (Plate 26). Th rich monazites and REE rich Al phosphates are also present and the latter also carry As. Tiny grains of barite may also be present. Traces of secondary Cu, Fe(+Cd) sulphide minerals also occur as tiny grains coating plant cell walls in remnant rootlets.

3. Soil smple PIT 2 at 35 cms depth.

Randomly orientated clay-grade illite or mixed-layer illite-smectite and chlorite along with detrital silt size quartz and feldspar provide the bulk of the sample. Rare flattish rhombs of an Al/S/Ca-rich phase occur. Some EDXA analyses indicate high levels of Ca and S in the clay matrix, presumed to be gypsum (which has been identified by X-ray diffraction in other samples).

Th-rich monazite is present in trace amounts as rare detrital grains.

4. Soil sample PIT 2 at 45cms depth.

A blocky silty clay contains domains of randomly oriented clay size particles and disseminated quartz, feldspar and mica silt. Small grains to pebbles of chloritic rock occur

within which chlorite flakes show some exfoliation. Fe sesquioxide patches are developed around rootlet channels which are often aluminous (possibly due to the presence of discrete gibbsitic component). The matrix is illitic (?) often with well-shaped clay particles (? kaolinite plates). Small (<1μm) REE phosphates (possibly monazite, rhabdophane or plumbogummite) are present in the illitic matrix but owing to the presence of the Al from the clays cannot be identified with certainty. Detrital zircons and monazite, of a silt and fine sand grade, are also seen in trace amounts. Xenotime (containing trace U and abundant HREE) is present but is much less common than the LREE rich monazite. A rare grain of a Th/Si/P phase was also observed as an alteration product of monazite.

Rootlet remains commonly show traces of Cu,Fe sulphides as diffuse grains lining cell walls. These are probably secondary products. Rare fine-grained Cu-rich (hydroxide or carbonate) material is associated with Fe, Mn, and Ni on altered rock fragments

5. Soil sample PIT 2 at 60cms depth.

Very similar to sample 5. Abundant highly altered friable rock clasts which are generally chlorite rich, with illite or illite/smectite developed along fracture surfaces (Plate 27), probably as a secondary product.

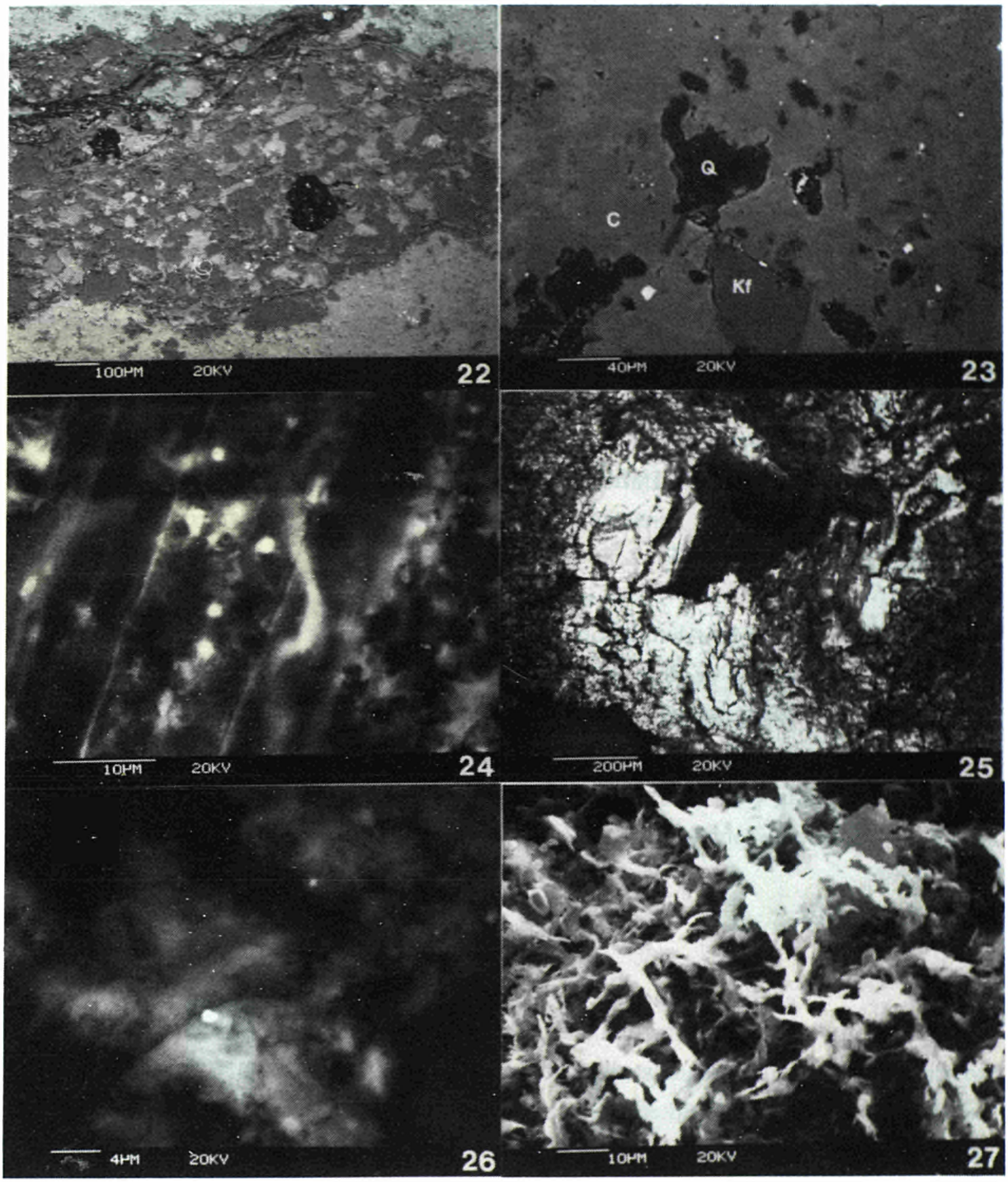

PLATE 22 BSEM photomicrograph of well-compacted siltstone lamina within recrystallised micrite. Spherical globules of dark organic detritus are present and contain bright inclusions of U - Ti mineral. Limestone unit.

PLATE 23 BSEM photomicrograph showing details of extensive replacement of siltstone components in laminated limestone base adjacent to intense veining. Quartz (Q) and K-feldspar (Kf) almost completely replaced by calcite (C) and only preserved as relict gains.

PLATE 24 BSEM photomicrograph of cellular wall of rootlet in peat showing bright grains of secondary sulphide minerals on rootlet walls. PIT 2, 10 cm depth.

PLATE 25 BSEM photomicrograph of probable *equisetum* rootlet showing hollow structure of root in peat matrix. Note zone of bright ferric sesquioxide in peat matrix around root channel. PIT 2, 25 cm depth.

PLATE 26 BSEM photomicrograph showing tiny grains of gold within amorphous ferric sesquioxide in peat matrix. PIT 2, 25 cm depth.

PLATE 27 BSEM photomicrograph showing secondary clay alteration produce along fractured surface of rotted clast in boulder clay. Clay mineral probably illite or mixed-layer illite-smectite. PIT 2, 60 cm depth.

5 HYDROGEOLOGY and HYDROGEOCHEMICAL SAMPLING

5.1 General

Simple hydrogeological measurements were obtained with the use of simple "drive in" standpipe piezometers. The same piezometers were also used for obtaining samples of soil groundwaters for chemical analysis. The piezometers were of a type available commercially ("Casagrande" piezometer, Soil Instruments Ltd.) and constructed in PVC. They are designed for use in shallow hydrogeological investigations of soils and unconsolidated rock. The instrument consists of a porous plastic cylindrical element (60 μm pore size, conductivity $3x10^{-4}ms^{-1}$, low air entry) protected by a 270mm length of perforated PVC casing (19mmID, 26mmOD). This was fitted to a standard black PVC standpipe (19mmID, 26mmOD) using rigid PVC connectors. The tip of the filter was modified by the addition of a solid PVC cone to protect the filter unit and aid the installation. No metal components were used in the piezometer construction and where necessary a standard methyl methacrylate/ dimethyl phthalate based PVC adhesive (TENSOL 70) was used to bond components. The construction of these piezometers is illustrated in Figure 5.1(a).

20 Casagrande type piezometers were installed at the site and emplaced by driving the assembly into a narrow pilot hole augered through the soil. In addition a 60mmID open PVC pipe was installed in an augered hole, through the boulder clay to bedrock, in PIT 8 (E1). All sites were levelled relative to an arbitrary base, their locations being indicated in Figure 1.1. In the western part of the site all piezometers (W1-W10) were installed to bedrock. On the eastern part (E2-E10A) they were driven until the tip reached the hard boulder clay. This represented the limit to which such systems could be installed easily. At site E4 boulder clay is absent and the piezometer rests directly on siltstone bedrock. At site E10 a second piezometer was installed at a higher level in the peat cover (E10B).

Other features of the site relevant to the hydrogeology were also surveyed and levelled. These included positions of ditches, drainage channels, areas of permanent (?) surface water, areas of periodic flooding, and a pond near the southern margin of the site (sometimes referred to elsewhere as the "Chalybeate Pool").

5.2. Hydrogeology

Piezometer water levels were allowed to reach equilibrium before dipping. Depths below ground of the water level at each site, including the pond surface, are given in Figure 1.1. From these data contours of the piezometric surface were constructed and are shown in

Figure 5.2. A geological and hydrogeological cross section, from W9 in the southwest to E4 in the northeast, along the trend of the radiometric anomaly is given in Figure 5.3. In the southwesterly portion the thickness of the peat overlying the boulder clay is estimated on sparse data to be 20-30cm. Similarly the depth to the base of the boulder clay in the eastern area is uncertain, and is extrapolated from the firm data obtained from between W1 and E4.

Hydrogeological data for the western side of the site are more limited than to the east. However, Figure 5.2 shows that there is a relatively good correlation between the topographic features of the site and the piezometric surface. Probable flow paths can be deduced by constructing vectors perpendicular to the contours along the line of maximum gradient (Figures 5.2 and 5.3).

In the southwest area the head gradient is steep (>8.6%) immediately above the lip of the infilled quarry representing a perched water table. Within the quarry area the hydraulic heads are variable but indicate a much lower gradient (about 1.8%). The piezometric surface within the quarry area is only a few centimetres above the bedrock surface. Observations in PIT 1 in 1987 and 1988 showed that water seeped along the interface between bedrock and backfill. Piezometers W3 and W5, close to the face of the old quarry, and W7 were dry indicating that the groundwater table at these points is at or below the bedrock interface. The hydraulic gradients on the west side of the road strongly suggest rapid flow and drainage into, and along the quarry floor. Thus it would appear that the quarry feature represents a regime of much greater permeability than the surrounding area. This is consistent with the nature of the infill which consists of gravel, boulders and sandy brown earth. The quarry probably acts as a channel funnelling groundwater from southwest to north east.

At the lower end of the quarry the water table rises in W1 and comes close to the soil surface. This area is subject to periodic flooding in wet weather. Here a "toe" of boulder clay underlying gravelly backfill is encountered which impedes drainage from the quarry. Flow paths at this end of the quarry are probably deflected by this mound of impermeable clay slightly to the south along the line of brown earth fill. It is uncertain whether this is remnant glacial till or is a spoil heap from the quarry operations.

The effect of the road and drainage ditches cannot be assessed without further measurements. It is probable that the base of the road lies on the boulder clay since the peat cover would have been removed during construction. Thus the road may act as a partial barrier across the site and may consequently raise the water table in the quarry area. However the footings of the road are likely to have been made of permeable rubble to allow drainage. The ditch on the west side of the road is wet but the water level is unknown. However it has been

observed that water drains to the north. To the south of the quarry and on the east side of the road, the ditches were dry. Interestingly Figure 1.2 suggests that some dispersion of Zn and U coincides with the probable drainage pattern along the ditch, parallel to the road, and northwards from the quarry.

On the eastern side of the road the contours of the groundwater table suggest that the flow-paths diverge. Here head measurements indicate gradients to the northeast and southeast across the area of the site. Comparison of the predicted flow patterns (Figure 5.2) compares with the observed pattern of dispersion of U and Zn (Figure 1.2 and present investigations Section 3).

Figure 5.3 illustrates that possible significant flow may occur along the bedrock-boulder clay interface. This is considered likely since observations (Section 4.2) show a considerable amount of the carbonate cement, as well as detrital feldspar, has been removed by weathering from the siltstones and sandstones. Consequently the weathered bedrock probably represents a relatively permeable zone within this shallow hydrogeological system.

At E1 the piezometer rests directly on the bedrock (nature undetermined) and samples the groundwater from this interface. The head measured from the base of the boulder clay is artesian (with respect to the base) or close to the base of the peat, and implies that a positive gradient exists across the boulder clay at this point. Therefore there is a potential for upward movement of water through the boulder clay. At E4 the boulder clay is absent (disappearing between E7 and E4). Consequently the groundwater and surface waters at this point and further east (assuming the boulder clay still to be absent) are likely to be a complex mixture of peat groundwaters draining from upslope (which would have evolved in isolation from the bedrock), and upwelling or "artesian" groundwater flowing along the boulder clay/bedrock interface and through the weathered bedrock which has evolved in isolation from the peat.

5.3 Hydrogeochemical Data

Groundwater samples for geochemical analysis were collected from all piezometer sites with the exception of W3, W5 and W7. Surface water samples were also collected from standing pools or where the water level was close to surface in shallow pits (E4, E5, E6 and E7). Samples were collected for determination of major and trace cations, major anions and Fe^{2+}. At the same time samples were collected for the Harwell Laboratory (Longworth et al., 1989).

Field chemical data obtained at the time included Eh, pH, temperature (T) and some HCO^{3-}.

Eh, pH and T were measured on line as water was pumped from the piezometers, via a peristaltic pump, and a specially constructed perspex cell fitted with the appropriate probes and electrodes (Figure 5.1(b)). It was intended that the Eh would be determined before the groundwater was able to react with atmospheric oxygen.

Samples were vacuum filtered on site through 0.45μm Millipore filters with a coarse glass-fibre prefilter. Aliquots were taken for cation analysis (acidified), trace elements (acidified), sulphide (NaOH added), anions (untreated) and Fe^{2+} (preserved by complexation with 2,2' dipyridyl). All samples were stored in Nalgene high-density polyethylene bottles. During filtration severe problems were encountered due to rapid clogging of filters with a colloidal Fe oxy/hydroxide precipitate which formed rapidly in many samples as they come into contact with air. In order to prevent loss of Fe^{2+} due to oxidation some samples for Fe^{2+} and Fe^{3+} were collected in unfiltered form. These samples were collected directly from the pumping line with a hypodermic syringe which contained a small amount of solid dipyridyl.

Analyses for surface waters and groundwaters are given in Table 5.1. It will be obvious that there are significant differences for pH obtained in the field, from the flow through cell, to those determined in the laboratory. Increases of at least one pH unit, in laboratory measurements, are observed for groundwaters but much less for surface samples. These differences may be accounted for by the loss of volatiles (e.g. organic acids, CO_2) during transport and storage. The outgassing of some samples was apparent during field filtration. The field pH data are therefore likely to be the more reliable.

Detailed discussion of the geochemical modelling of groundwaters is beyond the scope of this report. However a number of relevant points may be made. Background values for groundwaters are typified by samples from W10, PIT 7 and the pond and are 0.2 to 0.6 ppb U. Groundwater flowing into the site along the base of the boulder clay in the gully leading into the quarry (W9), has a slightly higher value (1.8 ppb U), possibly having picked up U from uraniferous bedrock. Groundwater U contents within the old quarry workings increase progressively down gradient from 3.9 ppb at W6, 7.8 ppb at W2 to 22.4 ppb U at W1. The latter site is particularly important as the piezometer samples water from close to the bedrock/boulder clay or gravelly backfill interface. The nearby PIT 6 only sampled near surface waters (20-30cm) on the top of the clay or backfill. The low value of 1.2ppb probably is for water draining into the area from the west and consequently has not passed over U mineralised bedrock.

On the east of the road the highest U values are in surface peats at E10B (13ppb U) decreasing in the basal peats at this locality (8.1 ppb, E10A). High U values in peat

groundwaters at E10A, E10B, E8 (about 8.3ppb U) and E2 (5.4ppb U) correspond with high concentrations of U in surface peats in this area (Figure 1.2). E1 is also in the U-rich peat area, however the sampling point of this piezometer takes water from close to the base of the boulder clay and the value of 1 ppb U is only slightly higher than that of the background samples. The values of U in the peat groundwaters decreases to the north of the drainage channel (E6 2.0 ppb; E5 1.3 ppb U). High U contents in basal peat groundwater (E9 5.0 ppb) are consistent with a significant dispersion of U along flow-paths to the southeast of the quarry source.

Along the main drainage channel flowing from E8 to E4 an interesting distribution of U in peat groundwater is seen. From E8 to E7 U decreases markedly from 8.3 to 2.6 ppb. The U content of the surface water at E7 (PIT 5) is similar to the piezometer samples (2.1ppb U), probably because the peat is very thin at this point. From E7 to E4 the U content increases to 4.0 ppb (similar to surface water at this point). Between E7 and E4 boulder clay disappears and the peat rests directly on bedrock. The bedrock at E4 is directly on strike with the old limestone quarry and it is possible that the mineralised limestone underlies the channel. Consequently the increase in U content seen in the groundwaters at E4 may be caused by mixing of peat groundwaters with upwelling U charged waters from the subjacent bedrock or by direct addition of U from bedrock to the near surface waters.

The features described above are summarised on the conceptual model in Figure 5.4 which illustrates potential sources, sinks and flow paths of U carried in groundwaters. The potential for the the addition of further U to evolved peat groundwaters down-gradient of the present anomaly centred around PIT 2/PIT 8 must be taken into account when modelling the transport of U across the site. This will have important implications for both U-series disequilibrium studies and for the determination of transport mechanisms. Similarly interpretation of the dispersion patterns may have to account for multiple sources.

6. DISCUSSION

6.1 Eh and pH controls.

The concept of, and determination of Eh values in soils, is fraught with difficulties. In particular the measurement of Eh by metal electrodes in peaty soils may be unreliable (Shotyk, 1988). Well drained surface soil solutions usually have an Eh of 0.5 - 0.7V. Confined solutions rapidly lose their dissolved O_2 by soil reactions, usually involving microbial reduction of organic matter, and the oxidation of reduced Fe and Mn (Garrels and Christ, 1965). Typically a waterlogged soil only millimetres away from a free air surface becomes depleted in oxygen. Within one or two days of a soil becoming waterlogged much of the free O_2 is consumed (Garrels and Christ, 1965). It is apparent that the Eh at the Broubster site changes throughout the seasons being least when the ground has become waterlogged. Generally the near-surface peats have lower Eh values than the deeper clays or the very surface peats. There is evidence from both Finland and Denmark for bogs which are relatively oxidising at surface and bottom but reducing in the middle (Shotyk, 1988).

The presence of ferrous iron in all waters tested suggests that at least in these samples the Eh is less than about -240mV at pH5 (-350mV at pH7). The presence of certain key minerals e.g. reduced sulphur species may further help to constrain the Eh fields in general. There is e.g. a marked characteristic smell of mercaptans on removing peat from depth. Some idea of the average Eh value may be obtained also by examination of mineral triple systems. Haematite/gibbsite/quartz has been identified and further helps to constrain the possible ranges of soil Eh/pH (Figure 6.15).

Eh/pH (Pourbaix) diagrams may be used as an aid to explain the relative behaviour of mobile elements in water/solid systems. The particular diagram mostly used is derived from Hostetler and Garrels (1962) and is the aqueous equilibrium diagram of the U-O_2 -H_2O-CO_2 system at 25°C, 1 atm. pressure and with a total CO_2 content of 10^{-3} moles and with a total ionic activity of 10^{-5} moles (Figure 6.2). It accords approximately to the current surface water composition of the area but should be used with caution because of the likely variations in temperature, local variations in composition, and fluctuations in rainfall which would change the Eh values. There are also observed gross variations in the chemical composition of the squeezed waters from the soils. Figure 6.1 is close to the compositions expressed by one such sample (BR08/3, basal peat, PIT 8) and exhibits the stability fields for the same system but with an increased total ionic activity of 10^{-4} moles. As can be seen the stability fields of the stable carbonates and carbonato complexes are larger and extend into lower Eh and pH values. Historical and prehistoric changes in climate and land use, such as

deforestation, would have had profound effects upon the overall Eh/pH balance of the soils. Nonetheless this kind of diagram can provide useful additional insight into the relative mobility of weathering products of rocks and mineral veins.

Figure 6.2 compares the data for the westernmost area (Line 1,1968 and Traverse 1,1987) for two periods, the first in 1968 the second during 1987. The 1987 data for surface soils shows a wider spread of pH values than in 1968, with significantly higher values being observed near drainage gullies. The deeper samples (Figure 6.3) reflect in a similar manner this general increase in soil pH. Eh measurements in 1968 were generally lower reflecting the wetter conditions in autumn 1968 than in the summer of 1987.

Surface samples over the middle part of the anomaly (Line 3,1968 and Traverse 3,1987) show a similar relationship (Figure 6.4). The early work extended further into peat covered areas and this explains some of the low pH values. Deep samples (Figure 6.5) from this traverse show no increase in pH with time, presumably reflecting the adequate pH buffering of the brown earths in this area by limestone fragments. Eh values are again higher for the 1987 samples.

For the traverse east of the road (Line 1, 1968 and Traverse 2, 1987) the surface samples again show a marked increase in pH in the 1987 samples (Figure 6.6) but a significant reduction in the Eh. This is difficult to explain but one possibility is that the absence of rain has allowed the aqueous phase in the waterlogged ground to equilibriate more fully with the euxinic environment of the peat.

The deep augered samples (Figure 6.7) exhibit only a slight increase in pH and again a significantly lower range of Eh values to the extent that many samples fall within or close to, the stability field of uraninite (UO_2) for the system.

The 1968 traverse is located in Figure 1.1. Unfortunately there was no comparable earlier data on Eh or pH. The Eh/pH diagram for this traverse is given in Figure 6.8. Most of the data show the soils to be neutral to mildly alkaline with varying but generally oxidising redox conditions. The most reduced sample occurs in waterlogged peat at the base of a drainage channel.

In nature the REEs usually occur in the trivalent state, with the exception of Eu which can exist also in the bivalent form and Ce which can be quadrivalent. In rocks Eu can occur in both bivalent and trivalent forms. REE minerals often show evidence for Eu depletion because bivalent Eu cannot be incorporated into the trivalent structures of the REE minerals.

Eu^{2+} has similar ionic characteristics to Sr which it may replace in e.g. plagioclase. The sedimentary rocks in the area show a negative Eu anomaly which is also exhibited by the boulder clays and organic soils. Figure 6.9 shows the approximate stability fields of the various Eu species. Any bivalent Eu introduced by breakdown of the parent minerals will therefore be converted into the trivalent form in the soils and pore waters. In this state it will behave like most of the other REE and the weathering products will inherit the Eu anomaly of the bedrock and primary minerals.

Figure 6.10 shows the stability fields of the Ce species. Included is the field occupied by porewater extracted from the soils in PIT 2. The waters show a higher pH than the associated soils and in most cases the soils are in the stability field of the Ce^{3+} ion. The CeO_2 is much more insoluble than the other ions. The REE profiles for the water samples show a strong negative Ce anomaly (Figure 3.11.8) . The corresponding peat samples similarly show a negative anomaly (Figure 3.11.14). All peat samples from the eastern side of the road show strong evidence for a marked negative Ce anomaly, but the brown earths overlying or close to the mineralisation, typically give a positive Ce anomaly. Groundwaters, consistent with the observed values of Eh and pH, will transport Ce-depleted REE. The pattern for MREE and HREE in the distribution profiles for the peats are similar to that for the limestones. The REEs are generally more abundant in the peats than in the underlying boulder clays or any sample of bedrock studied so far. It is concluded that REE are leached from the limestone and brown earths, the residual Ce producing a positive Ce anomaly, and the REEs are deposited in the waterlogged peats in a Ce-depleted form.

Figure 6.11 shows the stability fields for Mo species (Hansuld, 1972). In the Broubster weathering environment the molybdenite (MoS_2) is either stable at low Eh or may become converted into the mobile molybdate or the relatively immobile acid molybdate depending upon the pH conditions. Liming of fields results in the production of molybdate ions which can introduce Mo into the food chain and result in ill health in grazing animals.

Galena is recognised as a primary component in the mineralised structure. In the soils it would tend to be converted to anglesite which is itself immobile (Figure 6.12; Garrels and Christ, 1965). The actual distributions in the soil confirms its lack of mobility with little evidence for dispersion and reconcentration except close to the mineralised structure in Traverse 1.

Figure 6.13 shows the stability fields for Cu species (based on Garrels and Christ 1965). In the more reducing soils the CuS (covellite) is stable but the more oxidising surface soils and

brown earths Cu either forms the relatively mobile Cu^{2+} ion or the hydroxide which is relatively insoluble. Some secondary Cu sulphosalts were found in the peats. Cupriferous peats are not uncommon.

Figure 6.14 shows the approximate oxidation reaction potentials for the ferrous $\rightleftharpoons$ ferric and manganous $\rightleftharpoons$ manganic reactions in solution. Superimposed are the fields for peats and brown earths from the 1968 data. In acid reducing conditions both Fe and Mn tend to be mobile, but to a different extent, becoming fixed when the conditions change to be more oxidising and/or more alkaline. In the normal (original) soil profiles the surface peaty soils were likely to have been much more acid than at present. Mobilisation of Fe and Mn from the surface and reprecipitation at a redox barrier is likely and an Fe/Mn rich horizon has been observed at a depth of 10-50cms, especially west of the road. Under the waterlogged conditions east of the road the peats and subjacent boulder clays are gleyed and consequently Fe can remain in a mobile state. Rootlets penetrating the gleys, especially from *Equisetum* , introduce oxygen and there is a zone of Fe oxide precipitation in and surrounding the root channels. The old root channels provide conduits for oxygenated water to penetrate the gleys. Oxidation at the soil surface results in a thin film of Fe sesquioxides being produced. These oxide/hydroxide gels are important in that they can scavenge mobile elements from solution even though these elements would normally remain mobile. They can also be very fine grained and transport of scavenged elements as colloids could occur. In this area there appears to be fixing of Sr and Ba (and Ra) in Mn pan in the west of the area. There is also evidence for coprecipitation of Zn, Ba, Ra and Zn with sesquioxide gels in the eastern section of the area.

The processes taking place in and around the root channels will have a significant effect on the transport and fixing of U in the peat and drift. Oxygenated waters are likely to enable the more soluble U^{6+} to form and encourage solution. However the Fe and Mn sesquioxides, which would be produced by the same conditions, are very effective scavengers of U.

Figure 6.15 gives the solubility relationships for Al, Fe and Si in soils where gibbsite, haematite and quartz are present in excess (Norton, 1973). Al=Fe represents conditions of equal solubility. $Al=10^{-6M}$ and $Fe=10^{-6M}$ are solubility levels below which quartz is more soluble than Al and Fe phases. The sixfold junction moves to position 2 in the presence of organic complexants which are capable of maintaining Al and Fe in solution up to a limit of 10^2 times greater than of an inorganic control system (Manley et al., 1987). In spite of the difficulties in assigning Eh values to the soils, the measured Eh values fall close to the observed sixfold joins in the diagram.

Gold was also found in trace amounts in both the primary mineralisation (PIT 1) and in the soils in the peaty area east of the road. The gold in the peaty soils is of possible secondary origin and is associated with secondary accumulations of Fe sesquioxides. Similar precipitation of gold has been described previously from surficial deposits where there is a strong association with organic matter and Fe/Mn sesquioxides in the weathering environment (DiLabio et al.,1985). Even the Witwatersrand gold mineralisation is thought to be associated with organic matter and plant remains (Hallbauer, 1975).

6.2 STATISTICAL ANALYSIS

A partial correlation matrix for a comprehensive range of elements in the 1986 Traverse, is given in Table 6.1a, paying particular attention to U, Th and the REE. As can be seen Th correlates well with REE but also with elements which are normally found in resistate minerals such as Zr and Nb. Th correlates to a less, but significant, extent with elements which might be expected to be found in detrital minerals or rock fragments (K,Na,Al,Si in feldspars).

U appears to correlate highly significantly with Y and to a lesser extent with P. The REEs correlate with elements such as Th, Zr and Nb and others which are found in mineral or rock detritus.

Multivariate statistical methods help to clarify the situation somewhat. Table 6.1b summarises the results of a detailed factor analysis (varimax rotation) for the analytical data for the traverse. Factor analysis finds a few weighted averages (factors) of the original variables and provides a summary of the information. A large set of variables may thus be reduced to a small number while retaining as much information as possible. Factor analysis is analogous to a multiple regression analysis but with several dependent variables (which are the original variables), independent variables (the factors) and regression coefficients (the factor loadings). The statistical program used is "SOLO" (BMDP Statistical Software, Inc) and is run on an IBM PC.

The dominant factor (1) contains Si, Al, Ti, Na, K, and negative Ca, loss on ignition (LOI), and sulphur. This sort of relationship might be expected if the soil in the traverse is regarded as being mostly composed of detrital rock fragments containing dominant feldspar, diluted by peat. Gypsum has been identified as a component of peaty ground and would contribute to the Ca and S loading.

Factor 2 is essentially a heavy mineral detrital fraction and typically contains REE, Zr, Nb, Ba, and Th but also rather more puzzlingly Co, and to a lesser extent, Rb and Sr.

Factor 3 is a Fe and Mn sesquioxide factor representing solution, mobilisation and reprecipitation at a redox interface.

Factor 4 is the expected Y, U factor but there is no P loading that might be expected from the correlation matrix.

The final Factor (5) only contains Cs and has not been explained.

The peats for this traverse are treated separately. Because of the strong variation in values dependent upon proximity to source, and the different behaviour of the various elements in this anomalous area, the treatment is confined to this restricted zone. A simplified correlation matrix is given in Table 6.2a. Th again correlates less well with the heavy mineral detrital elements but otherwise shows little covariance with the other elements in the table apart from Na and K. U relates strongly to Y and less to MnO and La. La and Y correlate strongly together, but show only a weak relationship with Ce which appears to be more closely related to K_2O, Rb, Zr and Nb, the "detrital" elements.

The factor analysis of this group of peats (Table 2b) shows a similar relationship to the soils in general, but with a few important differences:

Factor 1 is essentially a peat factor diluted by rock detritus.

Factor 2 is a heavy mineral detrital factor and groups Ce with Zr, Co, Rb, Th, and Nb and to a lesser extent Sr and La.

Factor 3 is an Y, U and to a smaller extent La factor.
Factor 4 is a sesquioxide factor and groups MnO, Fe_2O_3 and Ba.

Figure 6.16 shows a factor loading plot for these data. Factor loadings give an indication of the extent that each variable is associated with a particular factor. A loading of close to 1 indicates a strong positive correlation with that factor. Factor loadings <0.5 are omitted. U and Y load firmly with Factor 3 whilst La is evenly distributed between Factors 2 and 3. The U group show little affinity for the sesquioxides group of elements in Factor 3.

A correlation matrix for the data from 1987 Traverse 2 is presented in Tables 6.3 (for the organic rich waterlogged surface samples) and 6.4 (for the deeper gleyed boulder clay). Similarly to the peat samples from the 1986 traverse the data for Table 6.3 shows a strong correlation between U and Y but also Ba, CaO, S, Mo, and Cu, a moderate correlation with Nd and La and a very poor (and slightly negative) correlation with Ce. Th correlates well only with Zr and V and moderately with the rock detrital elements Si, Na and K. Of the REE, Ce shows the most aberrant behaviour with good relationships with Zr and V and moderate with the "detrital" elements. There is as expected a very poor correlation between Ce and Y but good between Y and the other REE. Generally the relationships are similar to those for the peats from the 1986 Traverse.

Table 6.4 shows a correlation matrix for the boulder clays underlying the organic rich waterlogged soils in the same traverse. U shows a highly significant positive correlation with Cu, CaO, S, Y, Zn, MnO, P_2O_5, Fe_2O_3, Ba, Mo, and a strong negative correlation with SiO_2, Th, V, Zr, Na_2O, K_2O, Ce and Pb. The relationships suggest that the U is located both in phosphates and in sesquioxides and the high values of Ca (Table 3.7) in those samples with high Fe_2O_3, MnO and P_2O_5 suggests a high degree of Eh and pH control.

Th correlates well with the "detrital" elements, including Ce, and negatively with the "chemical precipitates" which include the other REE. Ce correlates in a similar fashion to Th, but La and Nd appear to show little covariance with other elements in this environment suggesting distribution between many host phases. Y in contrast shows an almost identical relationship with U.

A factor analysis of the data for all samples from the traverse is presented in Table 6.4. Factor 1 has a positive loading for probable detrital minerals (Zr, Nb, K_2O etc) and a negative loading of S along with P, Ba and Mo which probably represent a sulphide or sulphate concentration controlled by the Eh/pH conditions.

U is found in Factor 2 along with other elements whose concentration is controlled by the pH e.g. Cu, REE, and Mo.

Factor 3 describes a major element detrital fraction diluted by the LOI (=peat); whilst Factor 4, comprising Pb and Zn, is probably related to mineralisation or alternately, to the opposing pH control to Factor 2.

Factor 5 has a negative factor loading, comprises MgO, CaO, MnO and Fe_2O_3, and is clearly a sesuioxide factor possibly controlled by limestone debris (Ca and Mg).

Factor loading plots are shown in Figure 6.17. As can be seen the REE La and Nd load very strongly onto Factor 2 but U as well as being most strongly represented in Factor 2, along with Y, also shows a significant negative loading with Factors 1 and a positive Factor 5 loading which possibly represent a pH controlled sesquioxide precipitation.

A partial correlation matrix and summary for the factor analysis of the water samples is given in Table 6.5. U correlates well and is found in Factor 1 with Ca, HCO_3, total inorganic carbon (TIC), Ba, Sr, Mn, Mg etc. Its strong loading on Factor 1 in Figure 6.18 and its general geochemical relationship, indicates that dissolution of the mineralised limestone is the most likely source for the U and other cations.

7. CONCLUSIONS

Soils in the area in the recent past have had their geochemical character changed markedly by liming resulting in the increase of soil pH. Eh/pH diagrams provide a key to the interpretation of the data and the net result of the liming appears to have been that a greater proportion of the soils now occupy the same stability fields as the stable and easily soluble bicarbonato uranyl complex.

Soil Eh measurements show significant fluctuations which appear to be related to seasonal effects (e.g. waterlogging). The fluctuations appear to be sufficient that, dependent upon the season, the soil Eh/pH may either fall within the stability field of uraninite and thus U becomes relatively immobile; or may be oxidised to the stability fields of the more mobile bicarbonato complexes.

Within the quarry area the water table is close to or at the bedrock interface. The overlying fill is thus well-drained and aerated and contains abundant limestone fragments and uraniferous waste material. Under such conditions U minerals in the quarry waste will tend to oxidise to the hexavalent state, the U will readily complex with carbonate and mobility will increase. Percolating rainwater and introduced groundwater will therefore carry U down the hydraulic gradient. The flow within the quarry is likely to be strongly affected by irregularities in the quarry floor and channelled drainage is a strong possibility together with surface seepage over bedrock and karstic movement through the limestone. U in groundwater increases greatly down gradient in this area confirming that the major source of U lies in the quarry area.

The observed surface drainage pattern and the U distribution in waters, in general, shows a good agreement. There is a prominent drainage channel flowing to the northeast. However data also indicate possible combined Zn and U dispersion along a drainage ditch flowing to the north alongside the road. This may be of very recent occurrence and post dates the road construction.

The groundwater pattern indicates a general flow from west to east across the site. There is a possible bifurcation of the flow in the eastern part of the site with some distribution to the northeast and some to the southeast. This has resulted in U transport, and fixing in peat, along divergent paths in this area.

The studies indicate the possibility of significant groundwater movement along the interface of the bedrock and boulder clay cover, as the result of the removal, by weathering, of detrital

feldspar components and the carbonate cement of both siltstones and sandstones. There is thus a potential for two groundwater systems to develop in the near surface environment: (a) one in which the drainage is essentially through the peat in isolation from bedrock and another (b) in which groundwater evolves by drainage along the weathered bedrock/boulder clay interface in isolation from the peat. The two systems are isolated from one another by a thin covering of boulder clay. However in areas of the site where the boulder clay is absent there is the possibility that the two groundwaters would mix and therefore complicate the U dispersion pattern. This situation may be present in the eastern area close to E4 and along the drainage channel. In addition it is possible in this area that U may be added to the soil/groundwater system directly from bedrock via shallow karstic flow from the mineralised limestone. Therefore in the far east of the site the possibility of multiple U imputs must be considered and accounted for.

Y appears to show important similarities in behaviour to U, and dissimilarities to the other REE and Th. The LREE elements have been proposed as appropriate analogues for the transuranic elements Am and Cm. (Miller et al.,1982; Airey and Ivanovich,1986). They usually all exist in a trivalent state in near surface weathering conditions, they display similar ionic radii (Nd^{3+}=1.05Å; Am^{3+}=1.05Å; Cm^{3+}=1.06Å) and show similar stability constants for oxides and complexes (Krauskopf, 1986)

Th has been proposed as a natural analogue for the behaviour of Pu (Krauskopf, 1986). Unfortunately there is little information that Th is appreciably mobile at Broubster. However Th is found in some phosphate minerals in organic soils and in association with REE. However it is not clear whether these minerals are of detrital or authigenic origin. In waters there is a relationship with the sulphate ion.

Where the actual behaviour of Am and Cm in soils has been studied there appears to be a marked difference to the behaviour suggested by the analogues in the present investigation. Means et al. (1978) showed that Am and Cm were dominantly associated with insoluble Mn oxides; and Olsen et al. (1986) found that the solubility of Cm increased with acidity and suggested that this was due to the release from organic complexing agents. In the present study the REE were found dominantly in minerals of monazite, rhabdophanic and plumbogummite types. In many cases these minerals are of primary detrital origin but in some cases, as for example in weathered bedrock, rhabdophane or plumbogummite is seen as a secondary phase. Plumbogummite may also be present as a secondary soil mineral (Brown et al., 1978). The nature of the Ce anomaly in the REE distribution patterns, in soils and soil porewaters, confirms that the REEs can be mobilised in solution in this environment.

No discrete U mineral has been identified in the soil. The highest values for U are found in the peats implying that organic complexation is the dominant fixing mechanism.

The soil dispersion anomaly appears to be divided into zones which describe the general behaviour of the elements of interest. Up slope from the mineralisation there appears to be little labile uranium. There appears to be a small amount of REE mobility with a slight Ce negative anomaly in the peats, and a small increase in radioactivity related to sesquioxide coprecipitation.

In the region of the main radiometric anomaly the γ activity is higher than would be expected from the U content, and the REEs show evidence of transport with a positive Ce anomaly indicating movement of the REE away from the area leaving a residual Ce anomaly. This area is characterised by brown earths with neutral to high pH and oxidising conditions.

In the adjoining area to the east of the road pH values remain high but there is a significant decline in Eh consistent with the waterlogged nature of the ground. The γ activity is lower than would be expected from U in equilibrium with its daughter products. U is statistically related to Y and the REEs, but is probably fixed by organic matter. Th relates to the heavy mineral detrital fraction of the soils. Some of the variance for the REE is explained by part of the Ce being resident in heavy detrital minerals.

Farther away from the source, the nature of the fixing mechanism for the U appears to change. In the 1987 Traverse Two, U whilst still being related mostly to Y, La and Nd shows some evidence for being partially fixed by the sesquioxides. Th and Ce are mostly found with the heavy mineral detrital suite whilst the other REEs appear to be independent of both sesquioxides and the heavy mineral detrital suite.

It is uncertain what the history of the site was prior to the glacial deposition of ground moraine. It is likely that the area was planed glacially presenting a relatively flat and fresh surface before the waning phases of the latest glacial period which is thought to have ended some 10-12,000 years ago (West, 1978). There followed a a relatively mild climatic episode extending to some 5,000 years BP resulting in an extensive forest cover. This phase ended with the climate apparently cooling, and becoming wetter, and with the forest cover being replaced by peat. The fixing of U following erosion of the limestone was probably initiated at about this time. A major disturbance occurred some 100-200 years ago with the quarrying of the mineralised limestone, and probable liberation of U from both the quarry spoil and freshly exposed limestone, with further fixing in the peats. Further liberation of U has occurred within the last 20 years as a result of extensive liming of the peaty soils, with a

consequent pH increase and remobilisation of the U previously fixed in the soils.

The extent of the U dispersion is greater than at first suspected, and the anomaly is still open to the east. The extent of the REE dispersion, or whether it is co-extensive with the U anomaly is equally uncertain. The nature of seasonal variations in redox potential, and the effect these would have on the solubilities of U and the REE, needs to be characterised further. Different methods of estimating the redox potential need to be assessed. An extension of the piezometer array is required to support studies of the flow regime and to provide samples of groundwater for analyses by BGS and Harwell. In particular accurate phosphate determinations would be useful in determining the mechanisms of REE transport.

8. ACKNOWLEDGEMENTS

Thanks are due to our colleagues I. Basham, P. Hooker and E. Falck for valuable assistance in the field. In the laboratory: I. Basham and J Pearce helped in the interpretation of the petrographic data, D. Entwisle aided the extraction of porewaters and D.M. Cave the analysis of these. D. Holmes is thanked for advice and discussions for the groundwater measurements.

9. REFERENCES

Airey, P.L. and Ivanovich, M. 1986. Geochemical analogues of high level radioactive waste repositories. Chemical Geology. 55:203-213.

Bowie, S.H.U. and Atkin, D., 1956. An unusually radioactive fossil fish from Thurso, Scotland. Nature. 4056:487-488.

British Geological Survey 1985. Geological Sheet (Scotland) 115(E), Reay (Revised 1985) 1:50,000 series

Brown, G., Newman, A.C.D., Rayner, J.H. and Weir, A.H., 1978. The structures and chemistry of soil clay minerals. In:"The chemistry of soil constituents (Eds: Greenland D.J. and Hayes M.H.B.). 29-178, Wiley and Sons.

DiLabio, R.N.W., Newsome, J.W. and McIvor, D.F. 1985. Gold spheres in surficial sediments. Episodes. 8:39.

Donovan, R.M. 1975. Devonian lacustrine limestones at the margin of the Orcadian Basin, Scotland. Journal of the Geological Society London. 131:489-510

Donovan, R.M. 1980. Lacustrine cycles, fish ecology and stratigraphic zonation in the Middle Devonian of Caithness. Scottish Journal of Geology. 16:35-50.

Donovan, R.M., Foster, R.J. and Westoll, T.S. 1974. A stratigraphical revision of the Old Red Sandstone of North-eastern Caithness. Transactions of the Royal Society of Edinburgh. 69:176-201.

Gallagher, M.J., Michie, U.McL., Smith, R.T. and Haynes, L. 1971. New evidence of uranium and other mineralisation in Scotland. Transactions of the Institute of Mining and Metallurgy (Section B). 80:150-173.

Garrels, R.J. and Christ, C.L. 1965. "Solutions, Minerals and Equilibria". Harper and Row. 450pp

Hallbauer, D.K. 1975. The plant origin of Witwatersrand carbon. Minerals Science and Engineering. 7:111-131.

Hansuld, J.A. 1967. Eh and pH in geochemical prospecting. Geological Survey of Canada Paper 66-54:172-187.

Henderson, P. 1984. "Rare earth element geochemistry". Developments in Geochemistry 2, Elsevier, 510pp.

Hostetler, P.B. and Garrels, D.K. 1962. Transportation and precipitation of uranium and vanadium at low temperatures with special reference to sandstone-type uranium deposits. Economic Geology. 57:137-167.

Krauskopf, K. B.,1986. Thorium and rare-earth metals as analogs for actinide elements. Chemical Geology.55:323-335.

Longworth, G., Ivanovich, M. and Wilkins, M.A. 1989. Uranium series disequilibrium studies at the Broubster analogue site. Harwell report in preparation for DOE. 20pp.

Manley, E.P., Chesworth, W. and Evans, L.J. 1987. The solution chemistry of podsolic soils from the eastern Canadian shield: a thermodynamic interpretation of the mineral phases controlling soluble Al^{3+} and H_4SiO_4. Journal of Soil Science. 38:39-51.

Means, J.L., Crerar, D.A., Borcsik, M.P. and Duguid, J.O., 1978. Adsorption of Co and selected actinides by Mn and Fe oxides in soils and sediments. Geochimica et Cosmochimica Acta 42:1763-1773.

Miller, S.E., Heath, G.R. and Gonzales, R.D. 1982. Effects of temperature on the sorption of lanthanides by montmorillonite. Clays and Clay Minerals 30:111-122.

Milodowski, A.E., Basham, I.R., Hyslop, E.K. and Pearce, J.M. In preparation. The uranium source term mineralogy and geochemistry at the Broubster natural analogue site, Caithness. BGS Technical Report for DOE.

Nakamura, N. 1974. Determination of REE, Ba, Fe, Mg, Na and K in carbonaceous and ordinary chondrites. Geochimical et Cosmochimica Acta. 38:757-775.

Norton, S.A. 1973. Laterite and bauxite formation. Economic Geology. 68:353-361

Ostle, D., Coleman, R.F., and Ball, T.K., 1972. Neutron activation as an aid to the geochemical prospecting for uranium. In: Bowie S.H.U., Davis M. and Ostle D. Uranium Prospecting Handbook. London, Institution of Mining and Metallurgy.

Olsen, C.R., Lowry, P.D., Lee, S.Y,. Larsen, I.L., and Cutshall, N.H., 1986. Geochemical and environmental processes affecting radionuclide migration from a formerly used seepage trench. Geochimica et Cosmochimica Acta 50:593-607.

Schmidt, V. and MacDonald, D.A. 1979. Texture recognition of secondary porosities in sandstones. In "Aspects of Diagenesis" (Eds. Scholle, P. A. and Schluger, P. R.). Society of Economic Paleontologists and Mineralogists, Special Publication No.26. 209-225.

Shotyk, W. 1988 Review of the inorganic geochemistry of peats and peatland waters. Earth Science Reviews. 25:95-176.

West, R.G. 1977. "Pleistocene geology and biology". Second Edition. Longmans. 440pp.

8 APPENDIX

8.1 Sampling procedures and analytical methods.

The samples collected during the 1968 survey were of soils and taken using a screw type auger. Soil samples were double wrapped in polyethylene bags for transmission to the laboratory where they were dried at 150°C. The samples were then mixed and split. One gramme was analysed for U by the delayed neutron method (DNM, Ostle, Coleman and Ball, 1972). Cu,Pb and Zn were determined on other aliquots by leaching with a mixture of hot perchloric acid and nitric acid prior to an Atomic Absorption Spectrometric (AAS) finish. Mo was determined on an ashed sample by a colorimetric method. MnO was determined by X-ray fluorescence spectrometry (XRFS) calibrated by international rock reference samples. Analyses of Eh and pH were made in the field using separate aliquots. Direct determinations were made, using Pt and glass electrodes, where the samples were wet or a slurry with freshly boiled distilled water if the samples were dry. In 1986 samples were collected by a Dutch auger, the soils treated in the same way but the analytical method used for major and trace elements was XRFS. No cross referencing by reanalysis of the earlier samples was possible but separate studies have shown that there is genarally a good to very good relationship between the methods used. Since the AAS method used a partial extraction technique it would be expected that there would a slight bias between the two procedures. In fact the Zn concentration in the same sample by XRFS is usually 30ppm higher than that determined by AAS. Pb usually agrees well except at very high values (not observed in the present study) owing to incomplete solution at high and oxidising levels. Cu generally shows a good correlation even at low values.

The correlation between U by XRFS and DNM is excellent with a product moment correlation coefficient (r) of 0.998 for the range 5-300ppm.

Aliquots of the pit samples were initially analysed by an instrumental neutron activation (INAA) method. Comparison of the XRFS against the INAA method gave poor relationships for the REE. Further determinations of the REE were undertaken by an Inductively Coupled Plasma Mass Spectrometric system at New College (University of London). The agreement with the XRFS determnations were generally excellent, apart from Ce at low levels.

Data for the 1987 soil samples were entirely by XRFS. Whilst during 1988 the preliminary investigations into the dispersal of U to the east were undertaken using DNM.

8.2 Determination of pH.

The determinations of pH in all soils in the present study used a glass electrode calibrated in the field using suitable proprietry buffer solutions. Shotyk (1988) considers the glass electrode to be the most satisfactory to use in peaty soils as it is less subject to the effects of strongly oxidising or reducing substances which affect other methods. In the present study most of the pH determinations were carried out in the field at the time of collection of the soil samples. Where the sample was wet the electrode was simply inserted into the soil and the measurement read off a suitable meter. Where the soil was too dry for this approach a thick slurry was produced by mixing several grammes of the field moist sample with boiled distilled water. Repeat determinations using this procedure on samples which were sufficiently wet showed little or no difference in value. Repeat determinations on samples returned to the laboratory similarly showed little difference in pH values at least two weeks later.

Generally speaking moist peat pH values are considerably lower than extracted water pH values (Shotyk 1988). Similar relationships are observed for the Broubster bog where typically the extracted waters have pH values about one half of an unit above those of the peats.

8.3 Determination of Eh.

The concept of and determination of Eh values in soils is fraught with difficulties. The redox (reduction-oxidation) potential of a soil is determined by immersing an inert electrode (usually Pt) in the soil and determining the potential difference in volts between the Pt and an hydrogen electrode (or for practical purposes, a reference electrode which has been itself calibrated against a H electrode). In the current study a Pt/calomel electrode was used for all measurements of Eh. The wet peats were sufficiently soft that the electrode could be forced into the peat without damaging the surface of the Pt and by agitating the electrode it was possible to exclude much of the oxygen that would normally be introduced along the walls of the electrode. The potential difference was measured with a millivoltmeter and the minimum at each site was recorded.

8.4 Mineralogical Methods

Preliminary mineralogical investigations have been conducted using optical and scanning electron microscopy (SEM). The SEM was a Cambridge Instruments Stereoscan S250 fitted

with a Link Systems 860 energy dispersive X-ray spectrometer equipped with a SiLi detector. Spectrograms were recorded qualitatively to aid mineral identification.

SEM analysis of soil samples was carried out on stub mounted samples. Soil samples were prepared by freeze drying in order to reduce specimen damage by air drying. Liquid nitrogen prefreezing of moist soil blocks was employed prior to the samples being placed in the freeze drying equipment. Sample sizes were limited to 2cms cubes to ensure rapid freezing and prevent ice crystal damage to the soil fabric. The freeze dried soil blocks were slightly impregnated with a solution of "Durofix" dispersed in iso-amyl acetate, and then mounted on aluminium stubs using "LeitC" conducting carbon cement. The top surface was freshly fractured to expose undamaged soil fabric. Specimens were coated with carbon by evaporation under vacuum, prior to SEM observation. Observations were made using backscattered and conventional secondary electron imaging modes. Although the backscattered electron signal is complex owing to the effects of topography and atomic number, it proved very useful in locating dense phases in the organic-rich matrix of the soil, even though the stub samples had large topographic effects.

Sandstone, limestone and mineralised samples were prepared and examined as polished thin sections. The rock samples were impregnated with blue dyed epoxy resin prior to sectioning in order to reveal the porosity. Prior to examination by SEM, the polished thin sections were coated under vacuum with about 250Å of carbon. Backscattered electron imaging enabled minerals with different mean atomic number to be identified since the brightness of the image is proportional to this property.

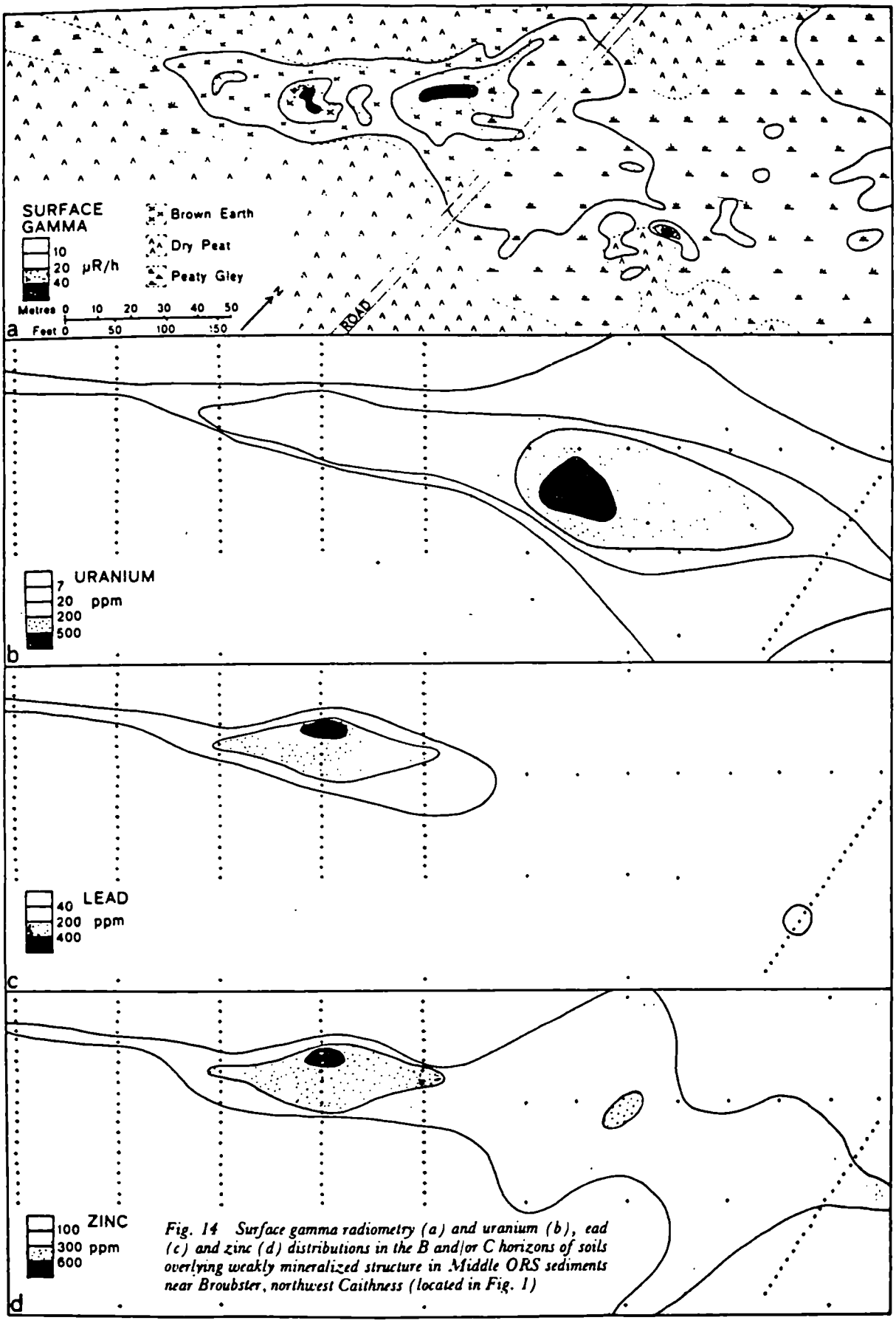

Fig. 14 Surface gamma radiometry (a) and uranium (b), ead (c) and zinc (d) distributions in the B and/or C horizons of soils overlying weakly mineralized structure in Middle ORS sediments near Broubster, northwest Caithness (located in Fig. 1)

FIGURE 1.2

Fig.3.1.1. Broubster 1968 Line 1

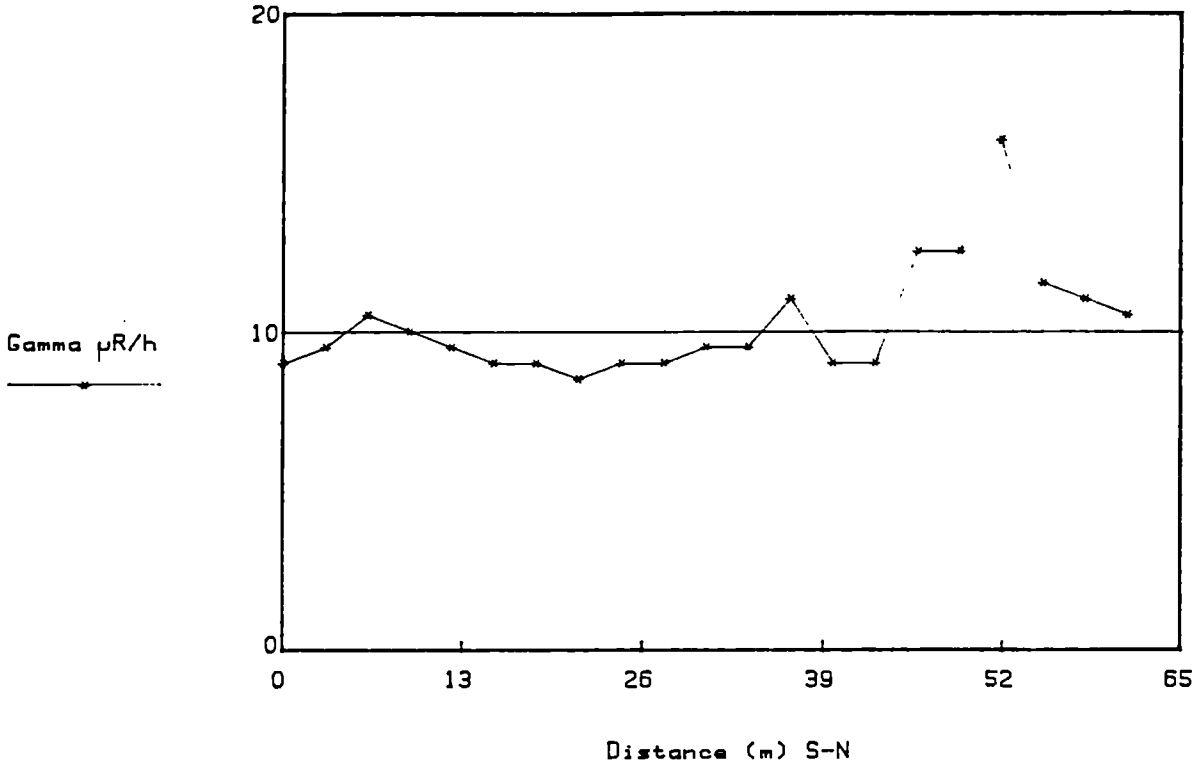

Fig.3.1.2. Broubster 1968 Line 1

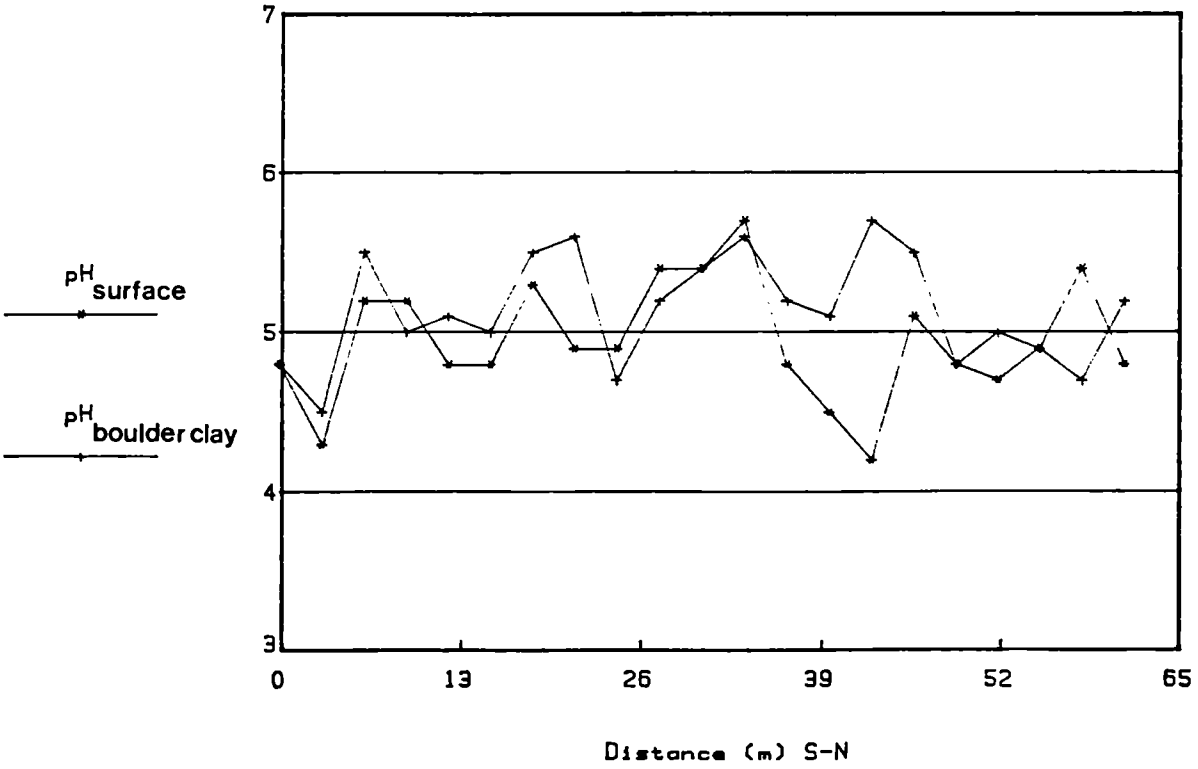

Fig.3.1.3. Broubster 1968 Line 1

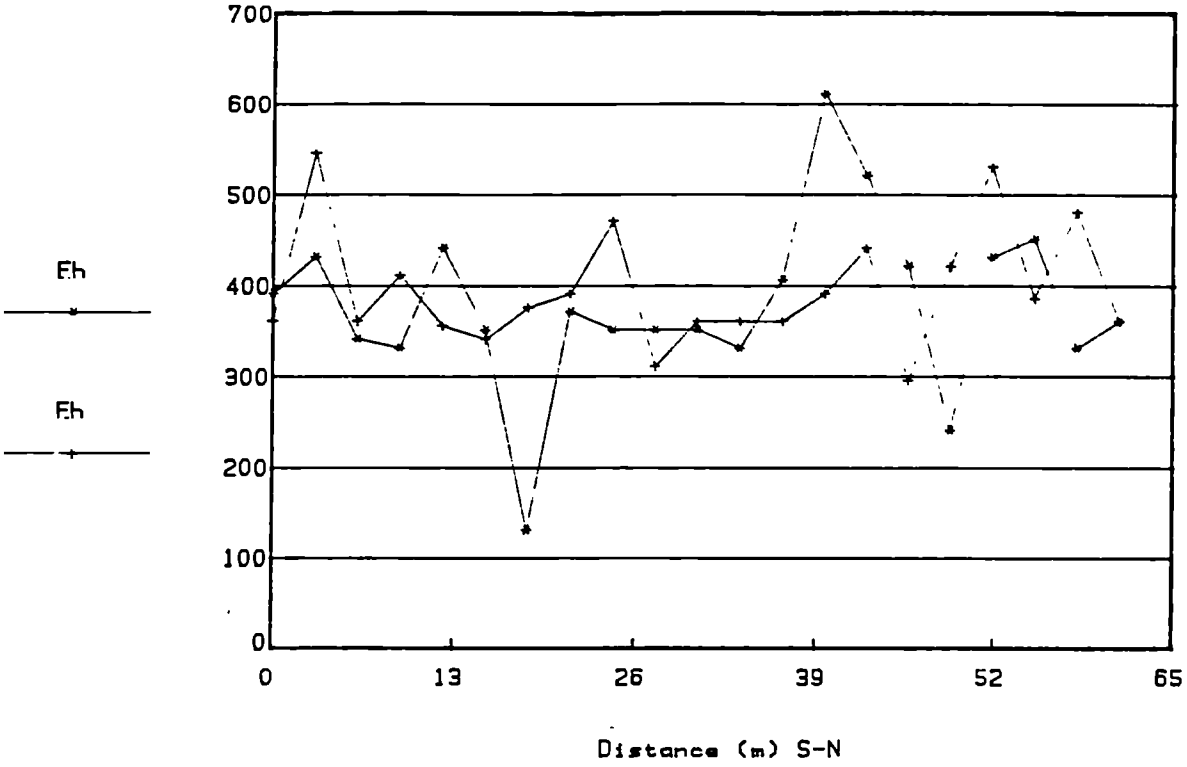

Fig.3.1.4. Broubster 1968 Line 1

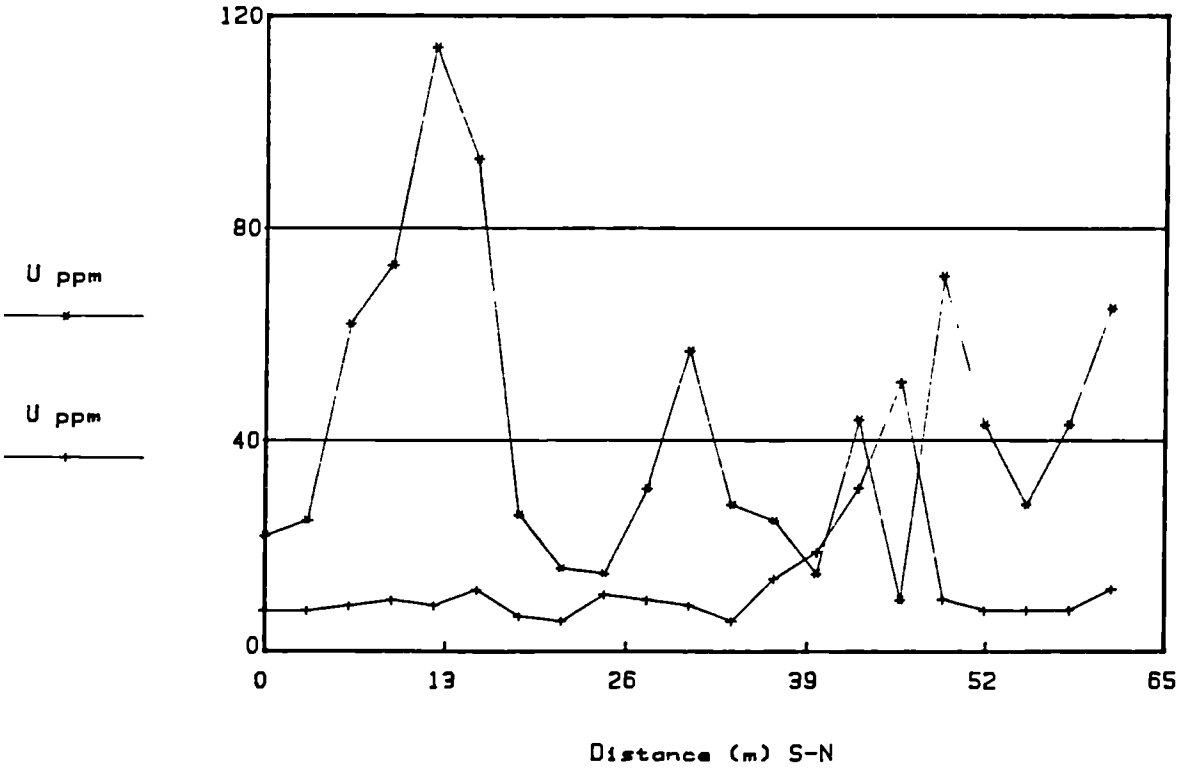

Fig.3.1.5. Broubster 1968 Line 1

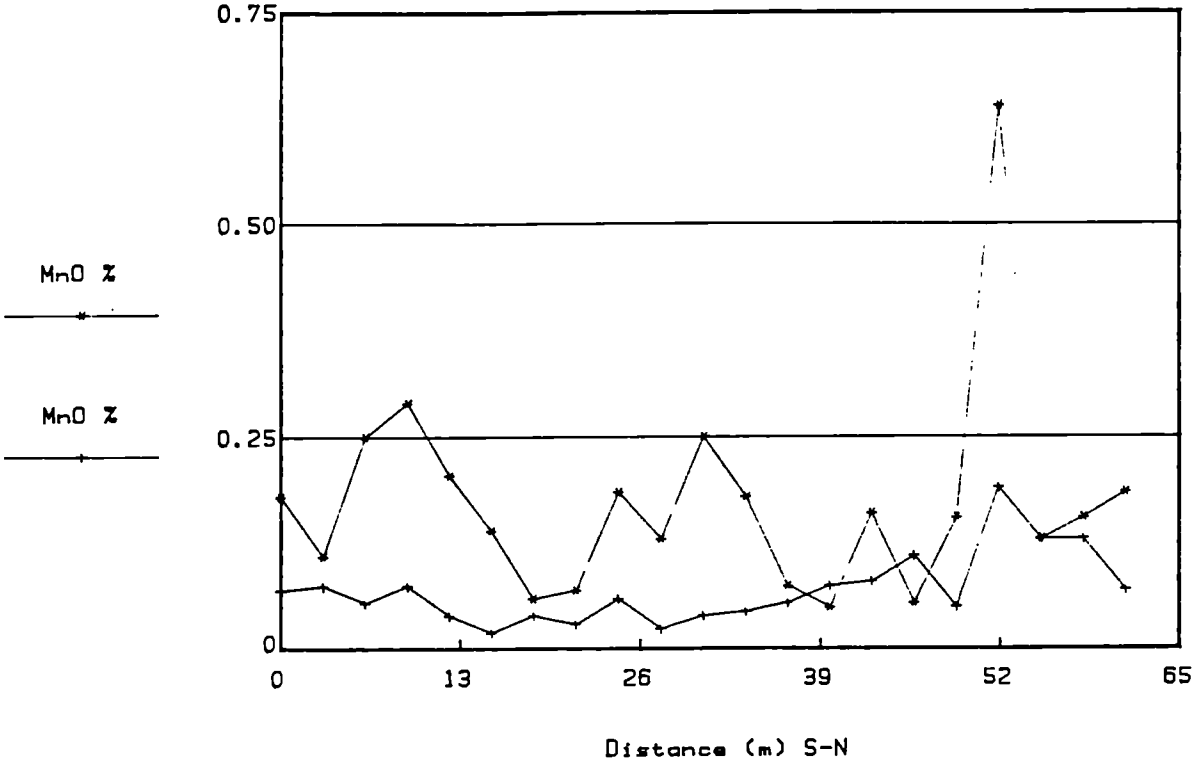

Fig.3.1.6. Broubster 1968 Line 1

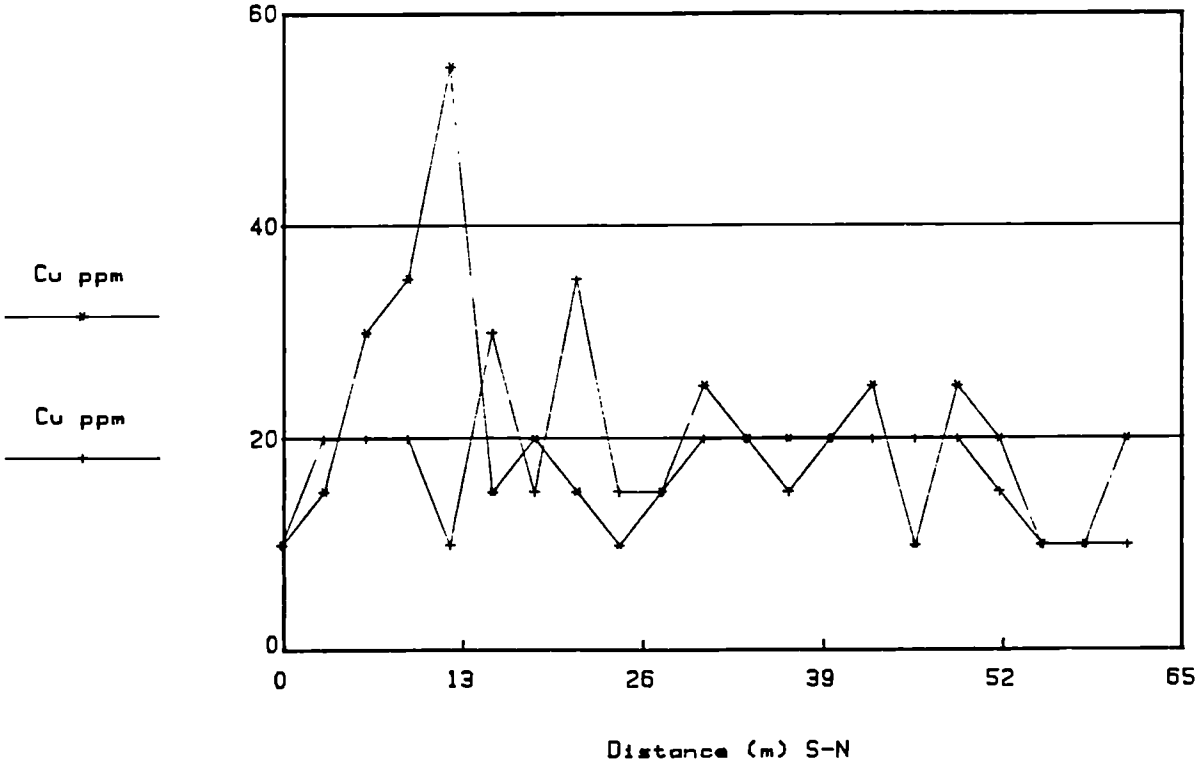

Fig.3.1.7. Broubster 1968 Line 1

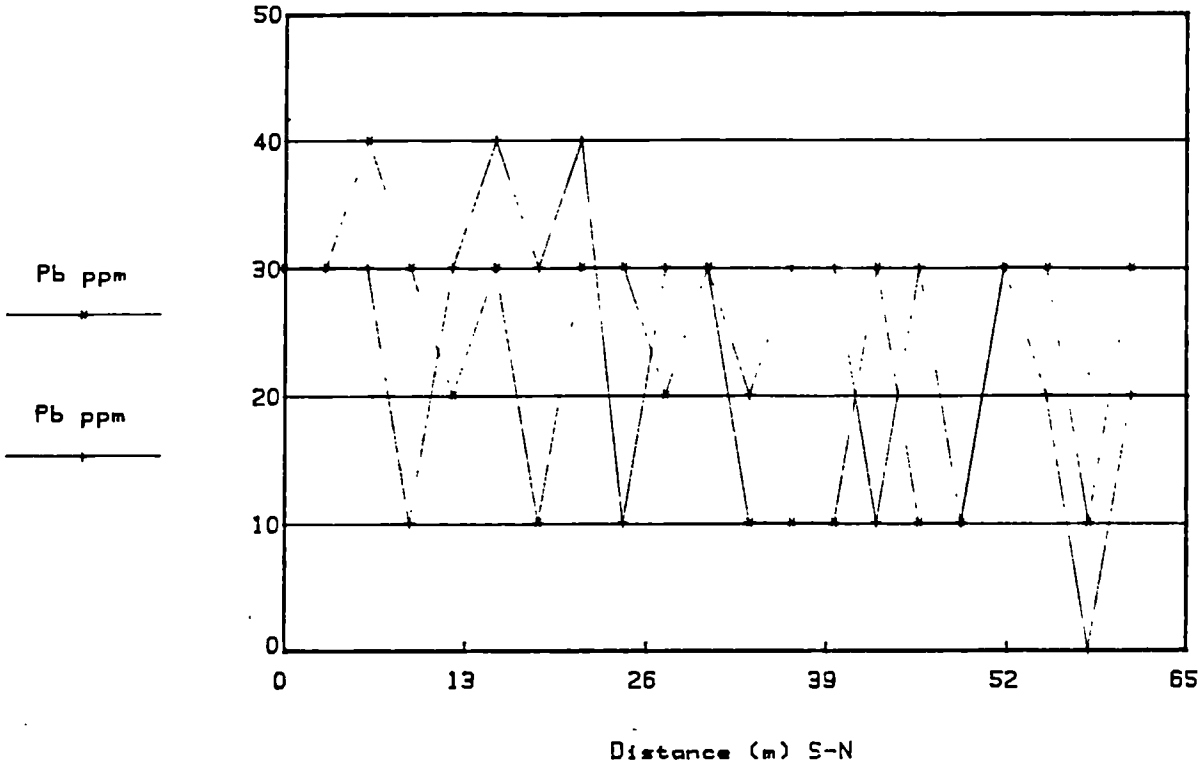

Fig.3.1.8. Broubster 1968 Line 1

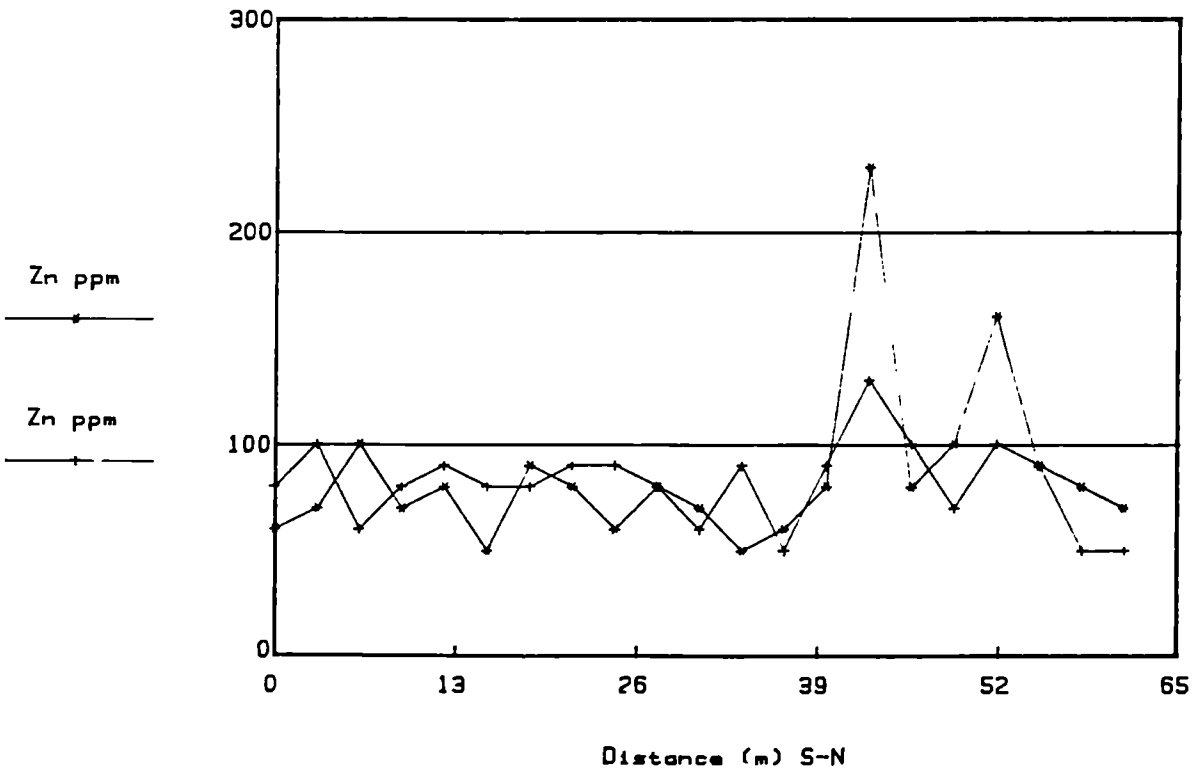

Fig.3.1.9. Broubster 1968 Line 1

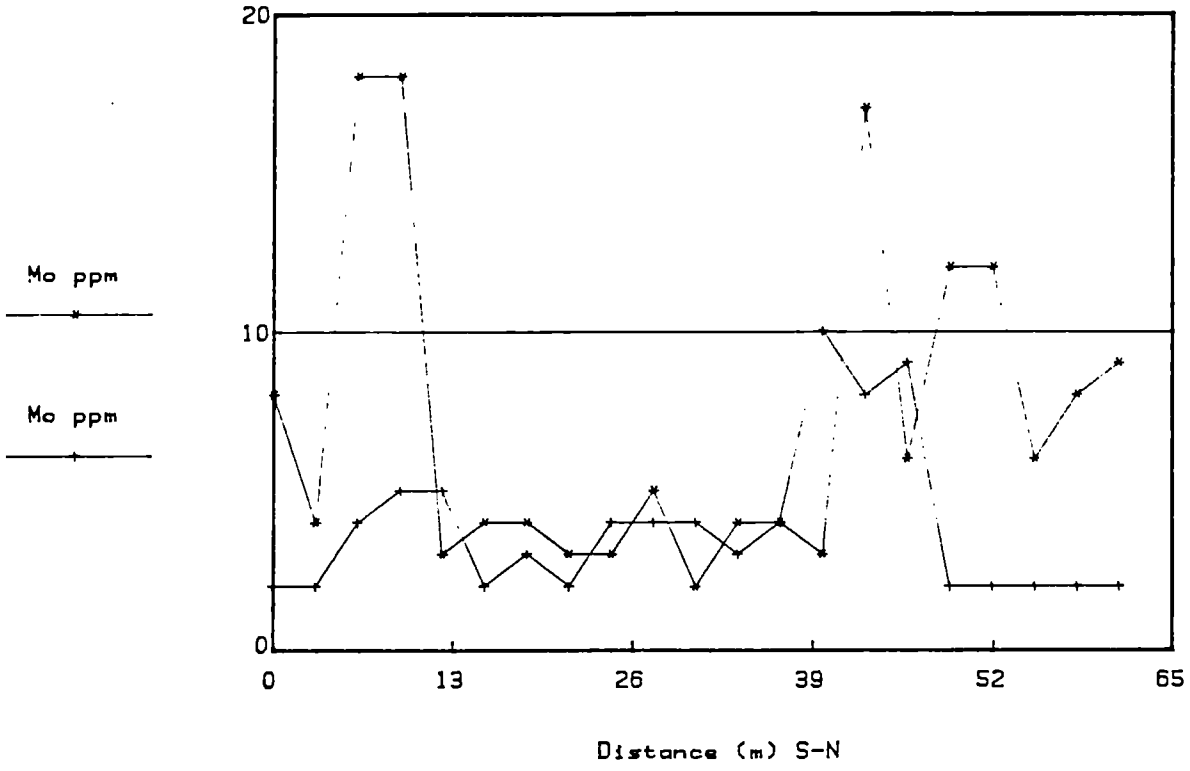

Fig.3.2.1. Broubster 1968 Line 2

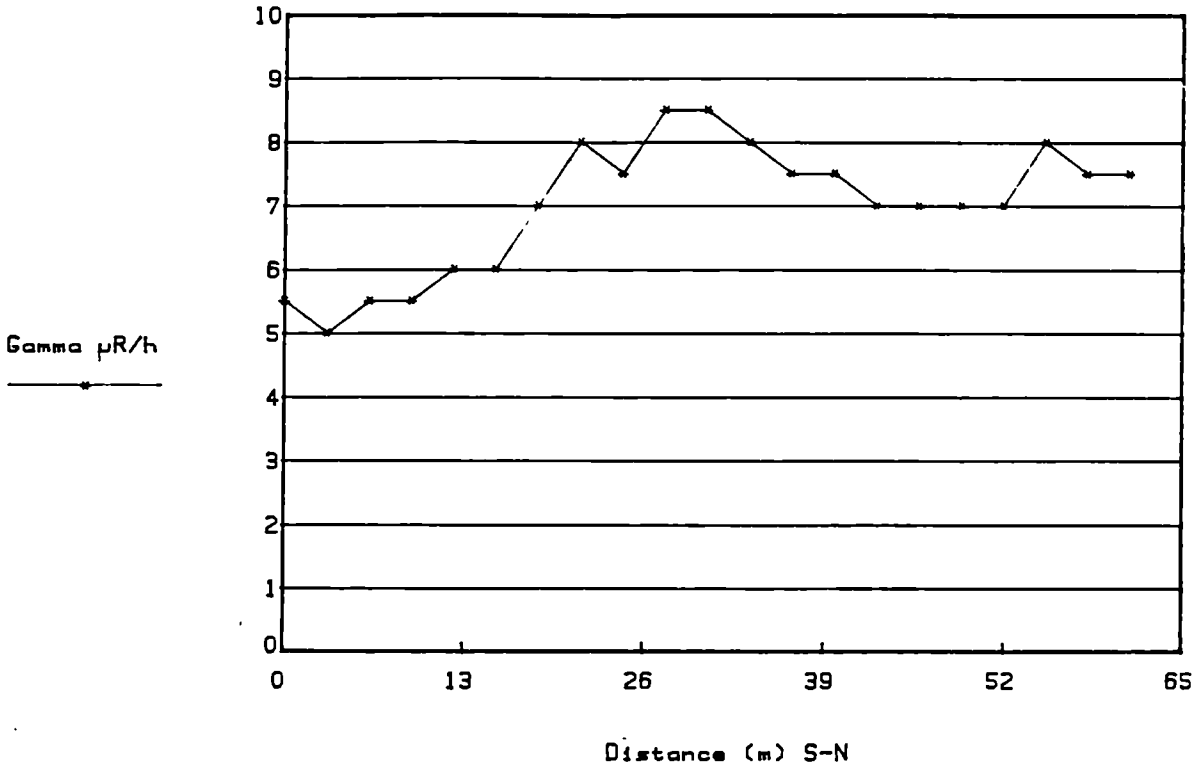

Fig.3.2.2. Broubster 1968 Line 2

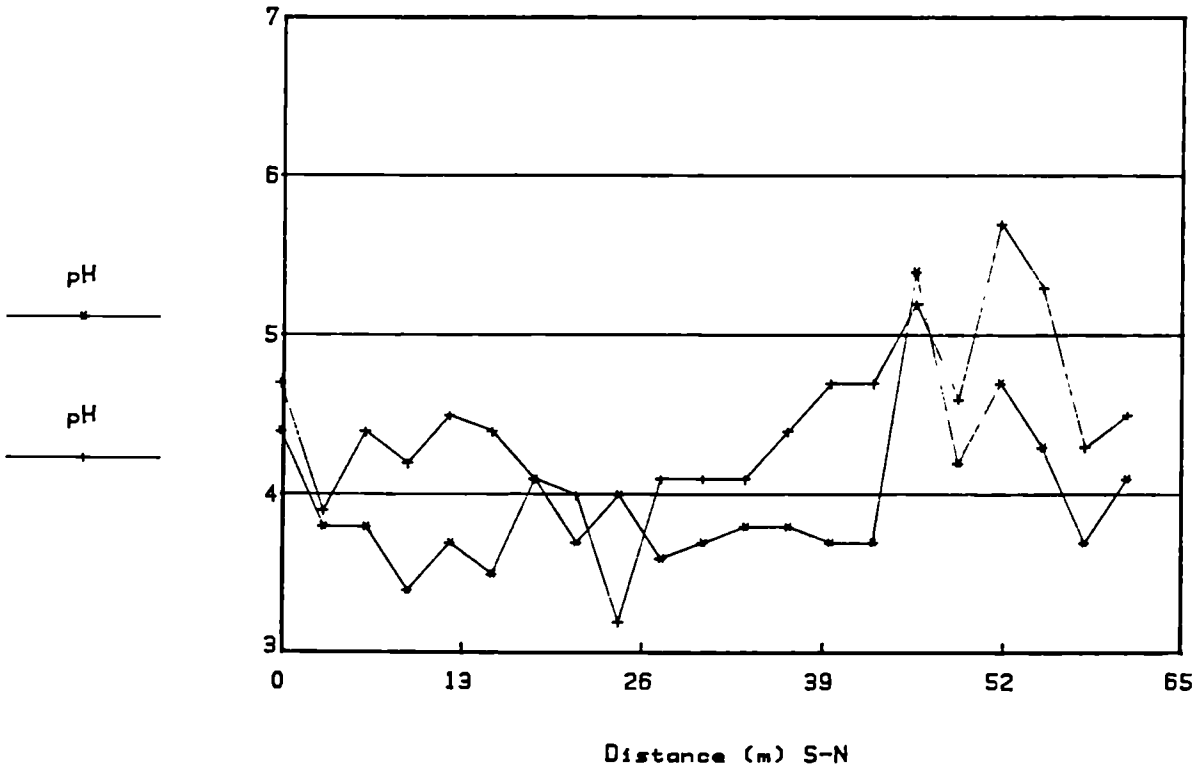

Fig.3.2.3. Broubster 1968 Line 2

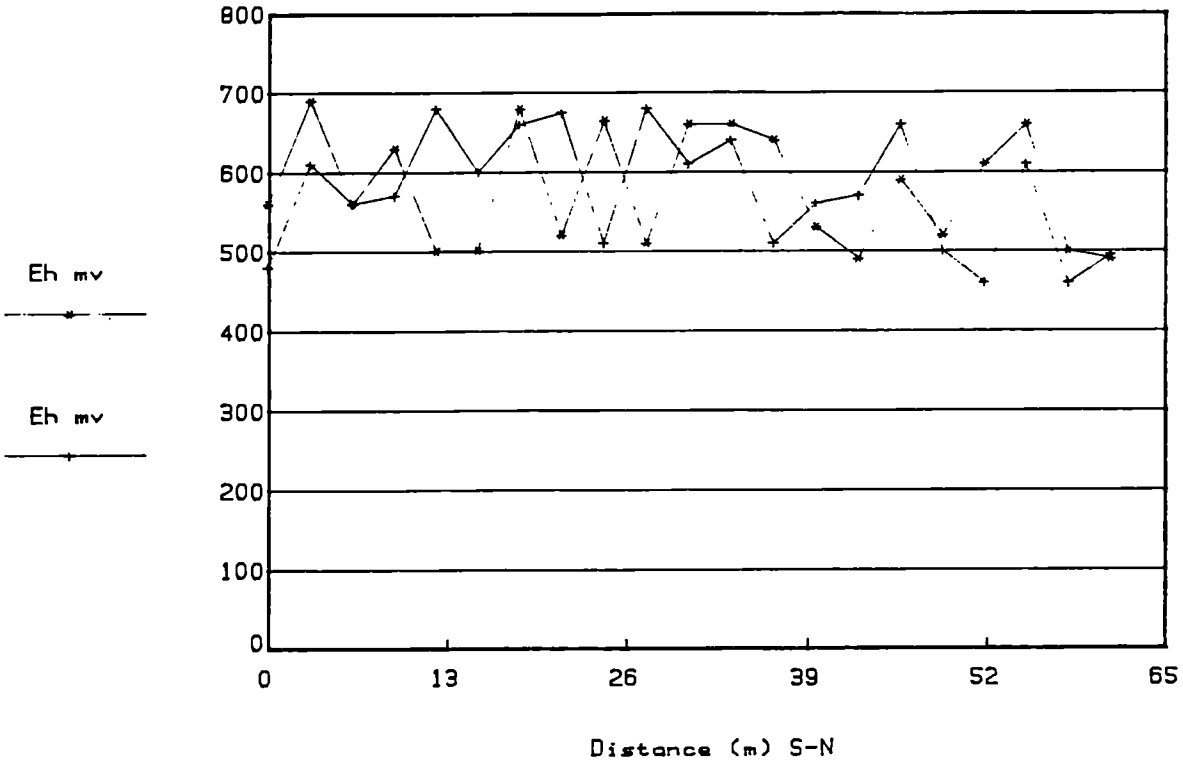

Fig.3.2.4. Broubster 1968 Line 2

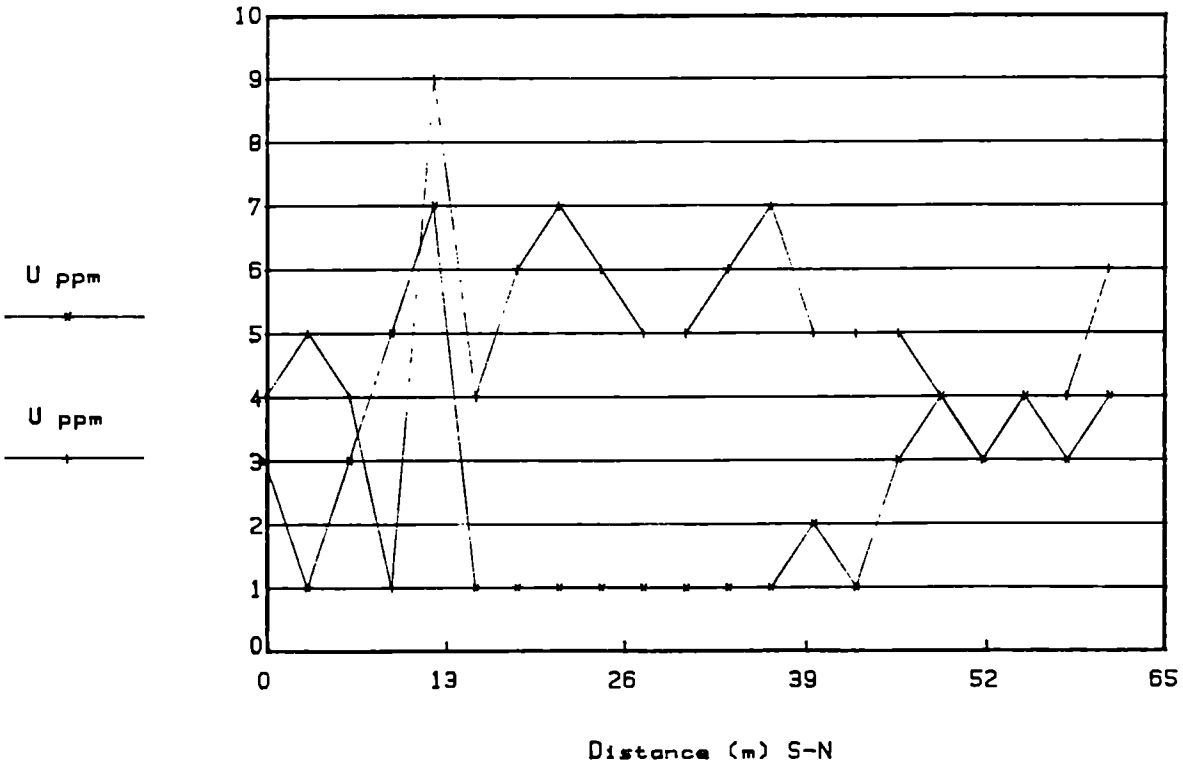

Fig.3.2.5. Broubster 1968 Line 2

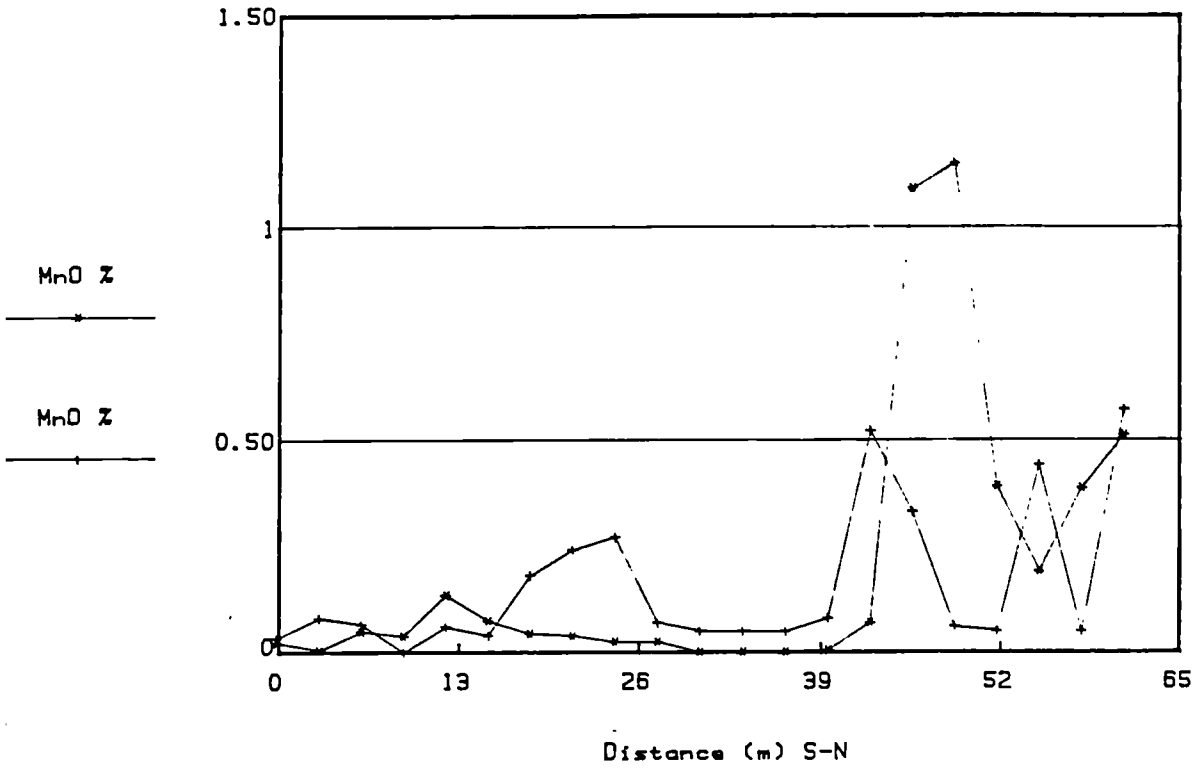

Fig.3.2.6. Broubster 1968 Line 2

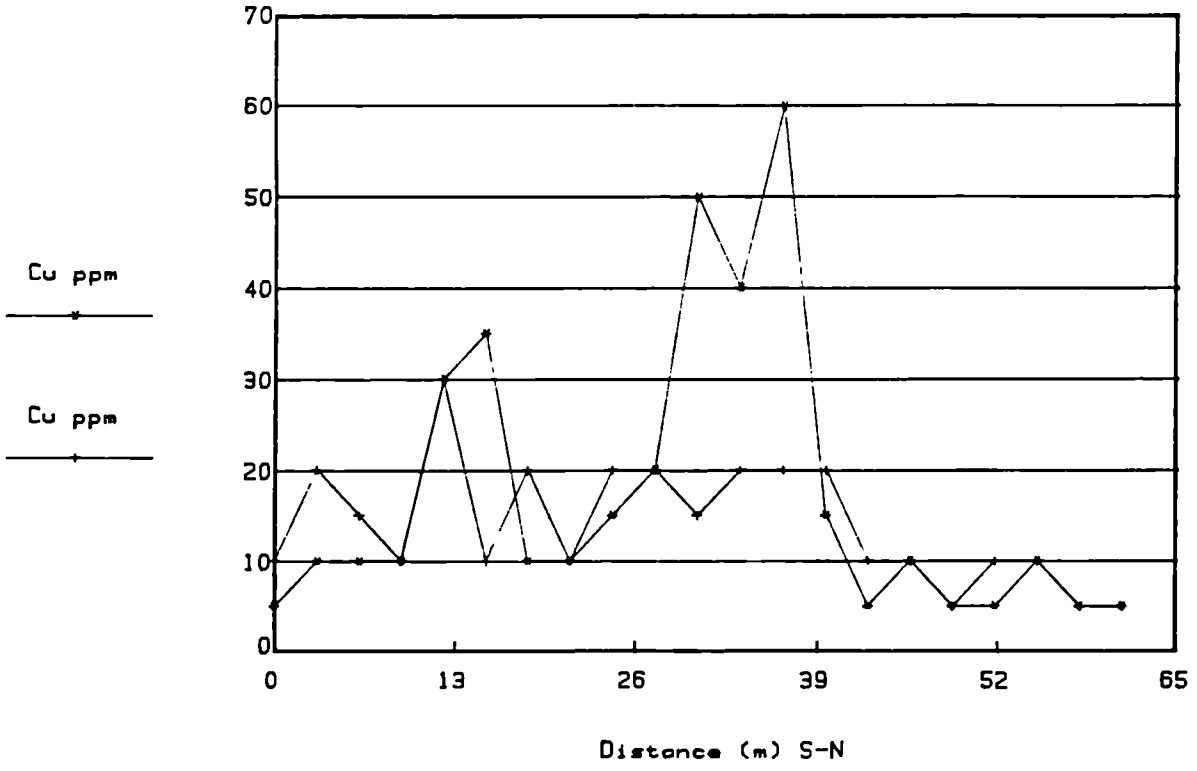

Fig.3.2.7. Broubster 1968 Line 2

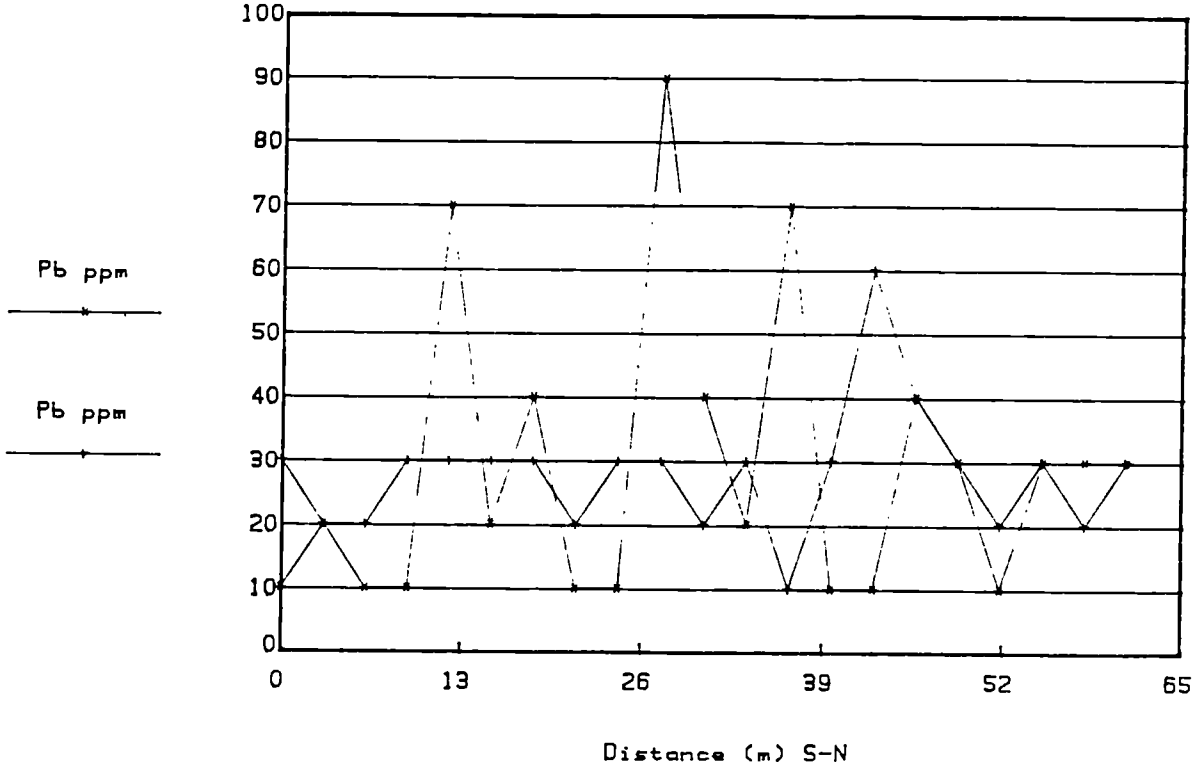

Fig.3.2.8. Broubster 1968 Line 2

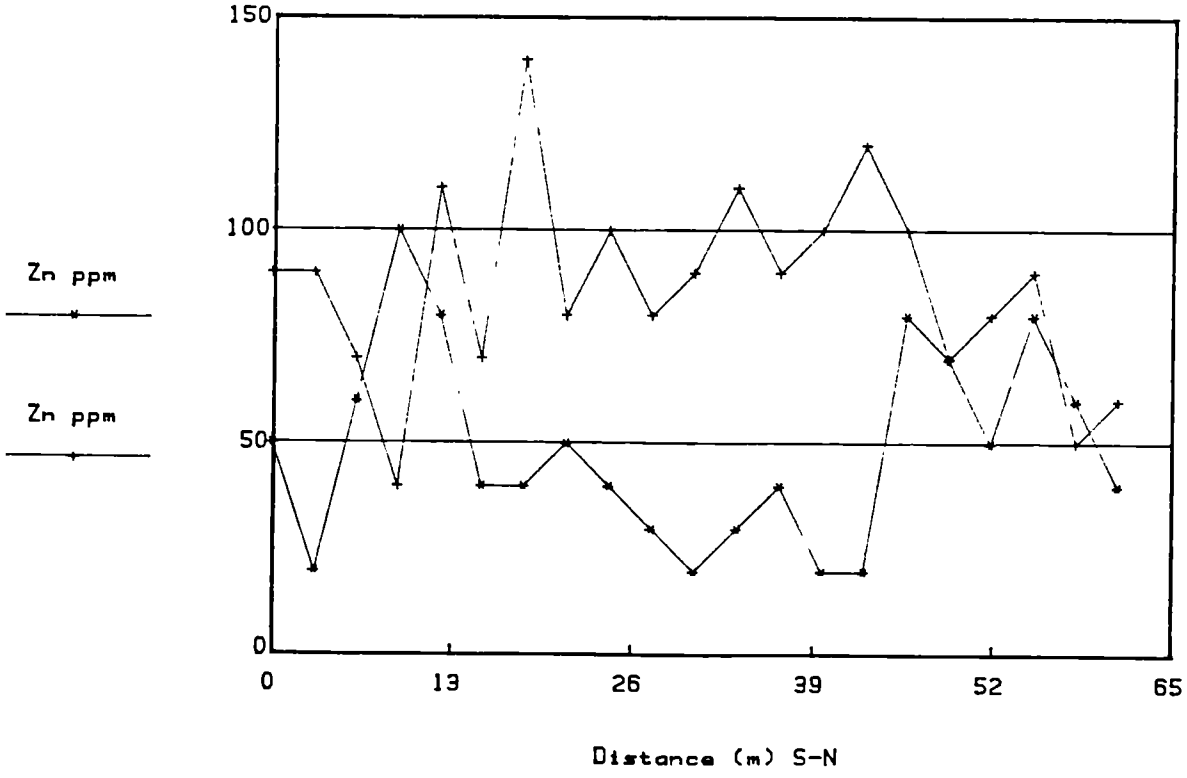

Fig.3.2.9. Broubster 1968 Line 2

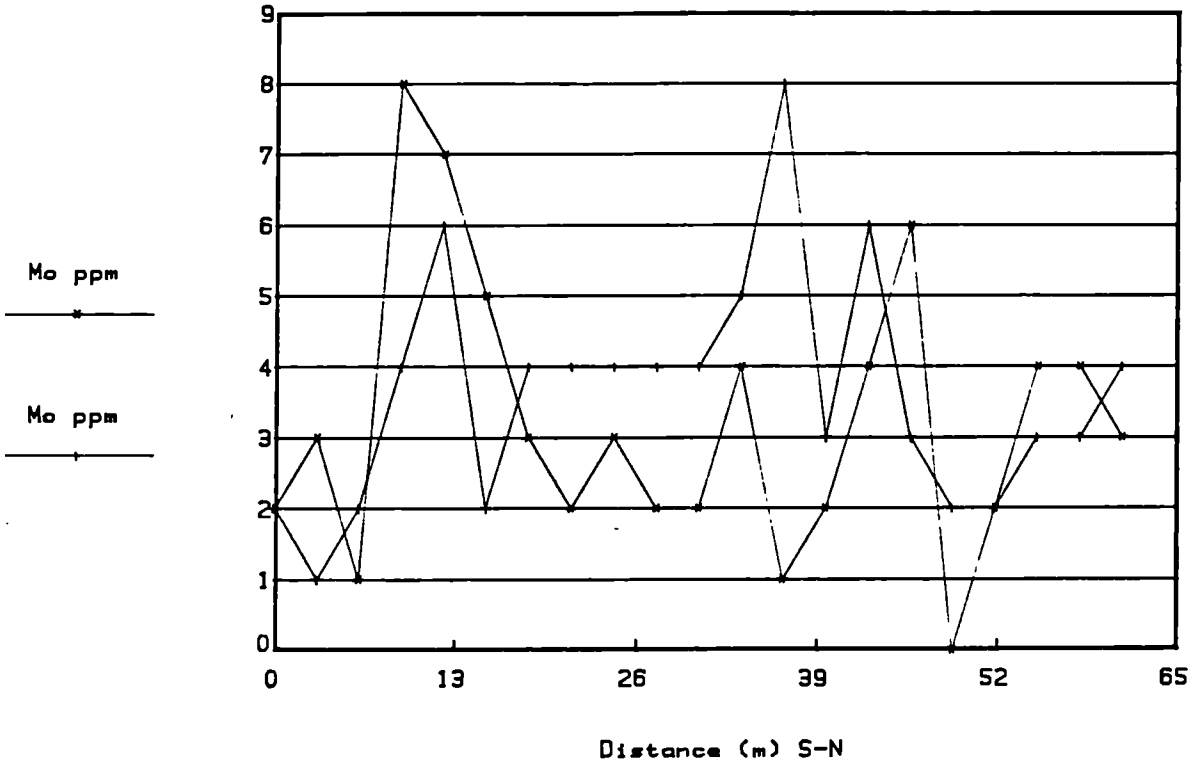

Fig.3.3.1. Broubster 1968 Line 3

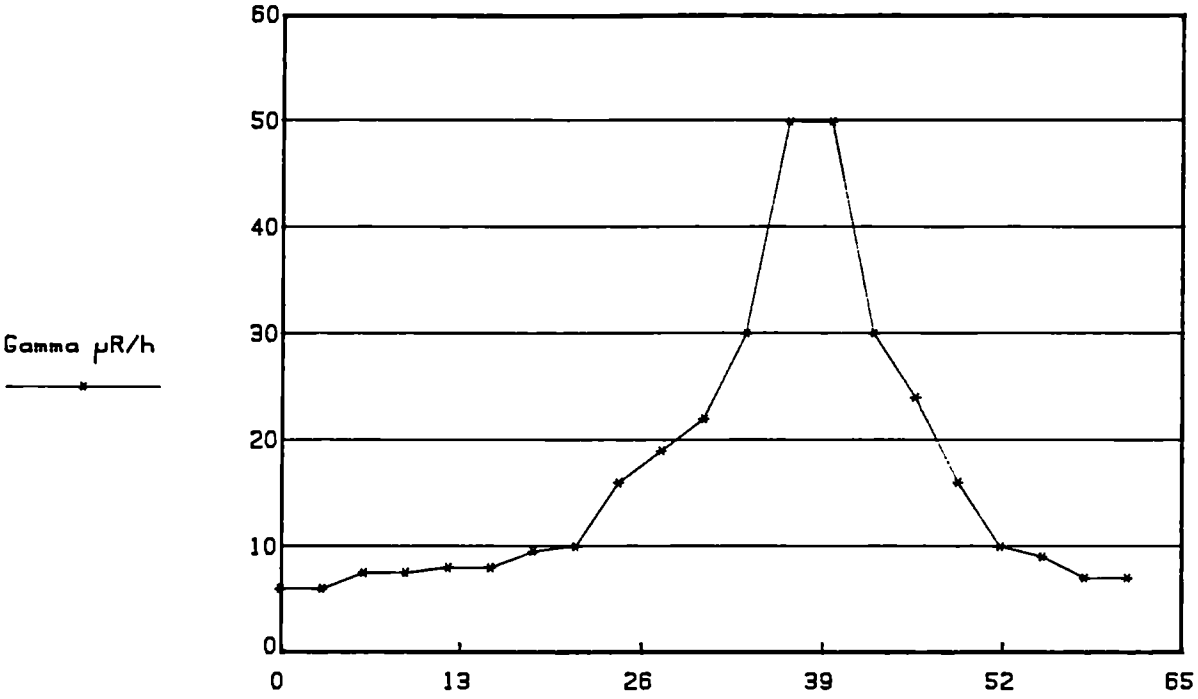

Fig.3.3.2. Broubster 1968 Line 3

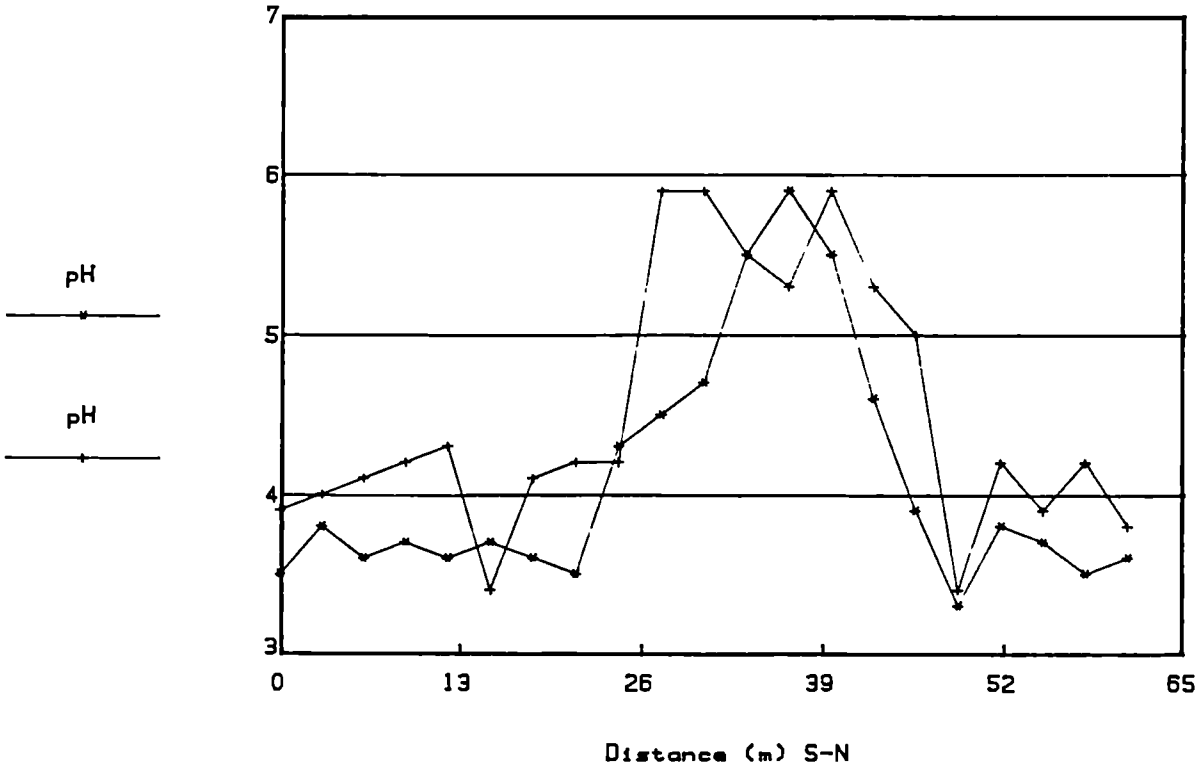

Fig.3.3.3. Broubster 1968 Line 3

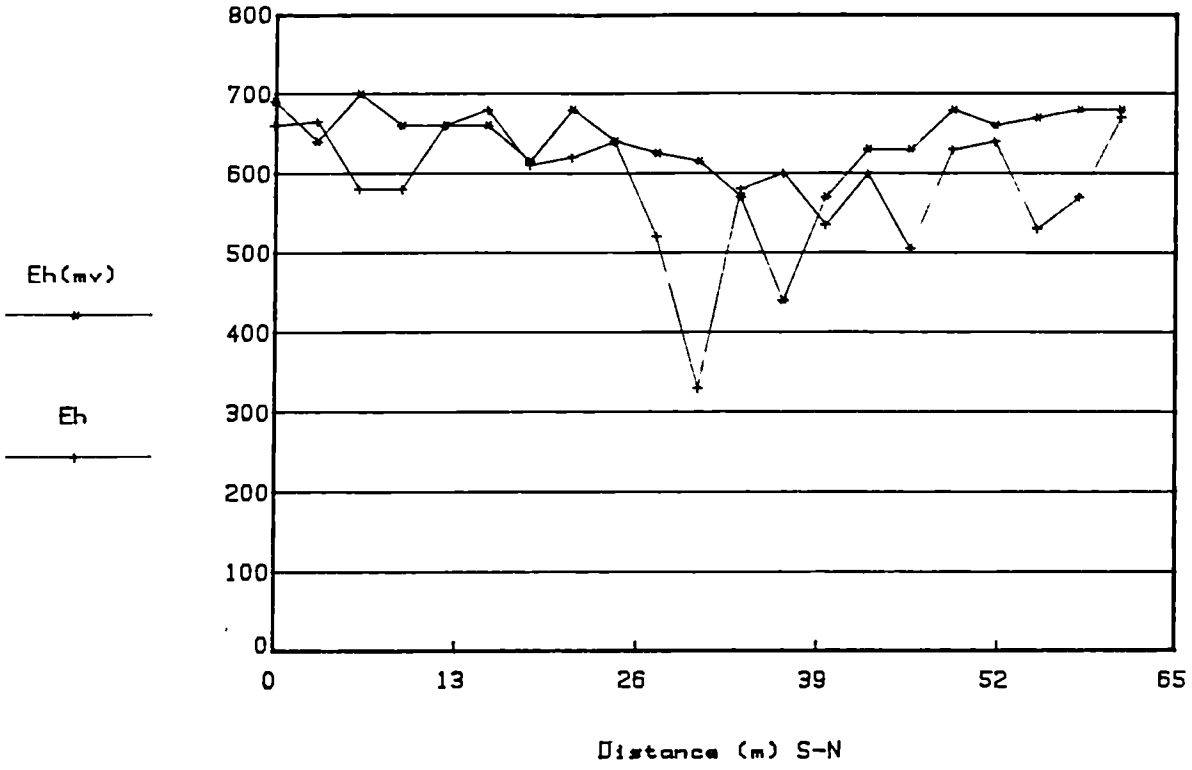

Fig.3.3.4. Broubster 1968 Line 3

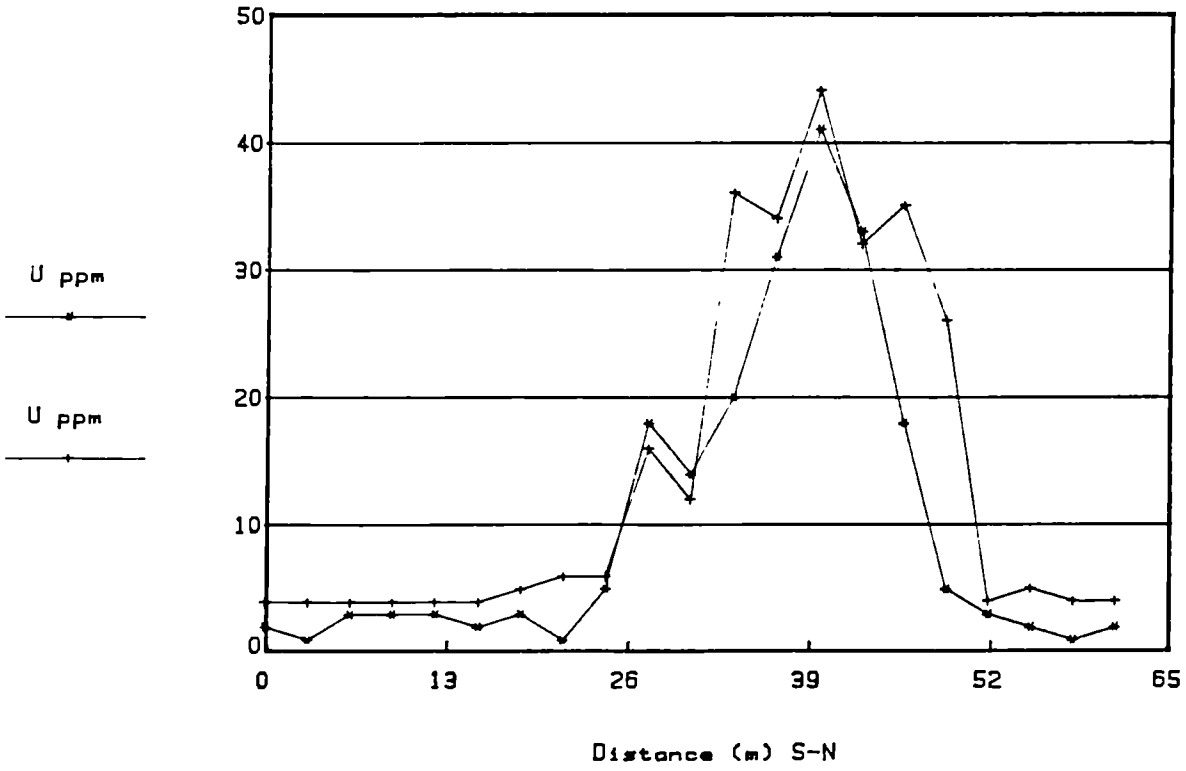

Fig.3.3.5. Broubster 1968 Line 3

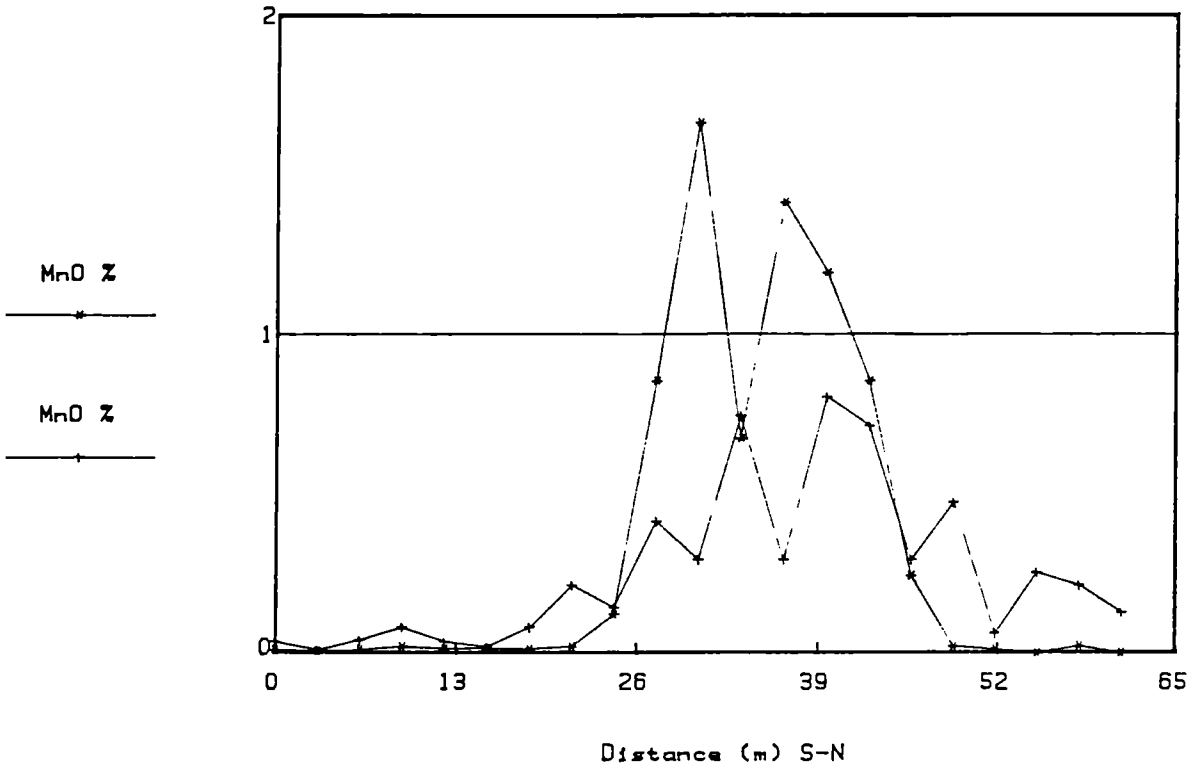

Fig.3.3.6. Broubster 1968 Line 3

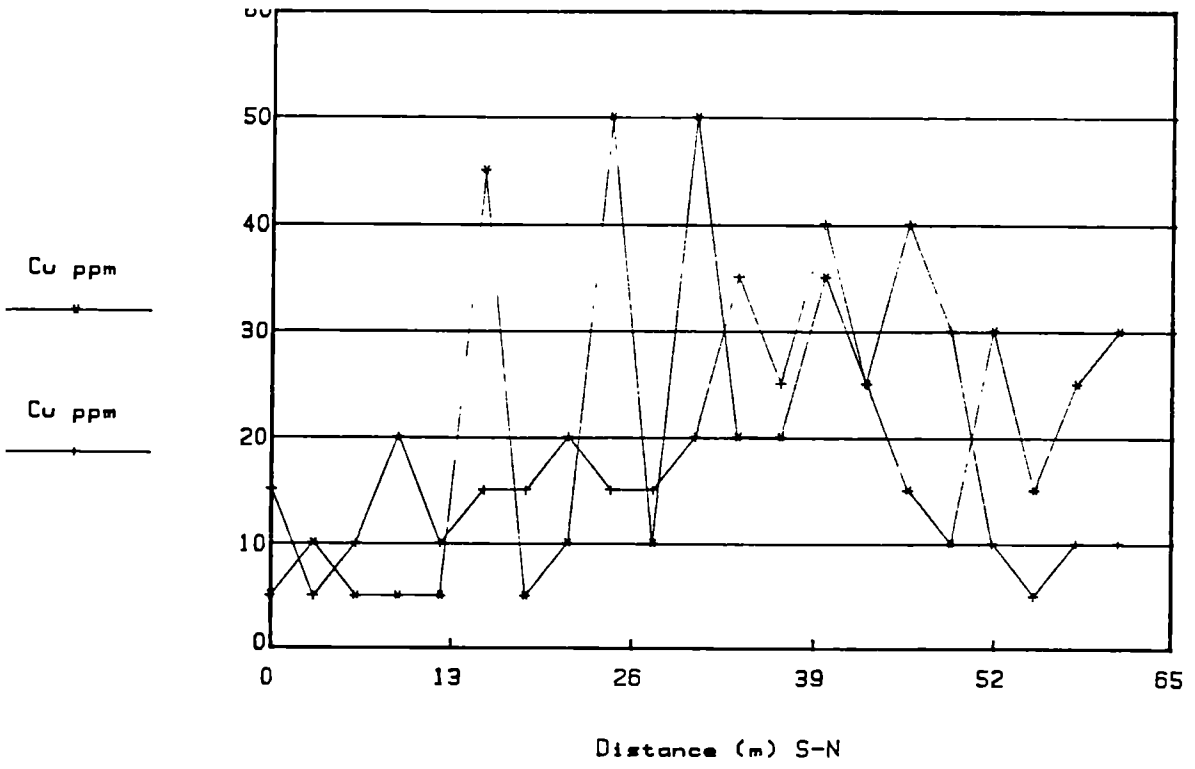

Fig.3.3.7. Broubster 1968 Line 3

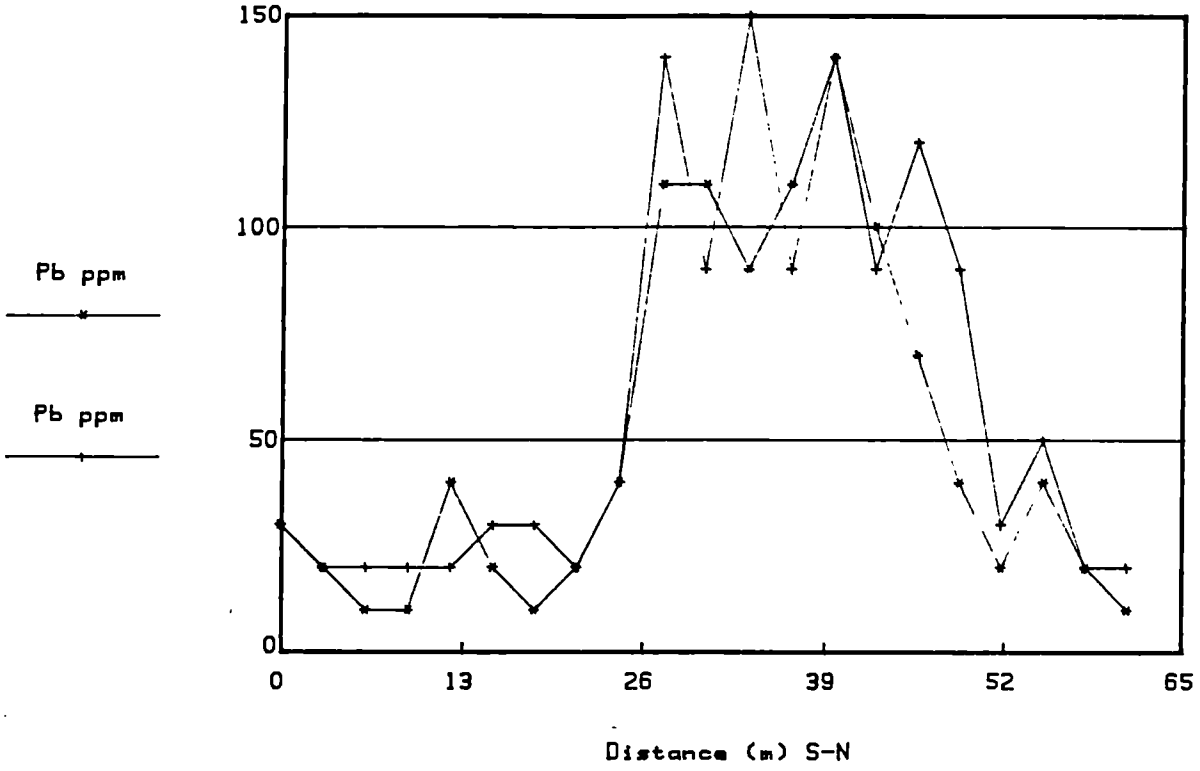

Fig.3.3.8. Broubster 1968 Line 3

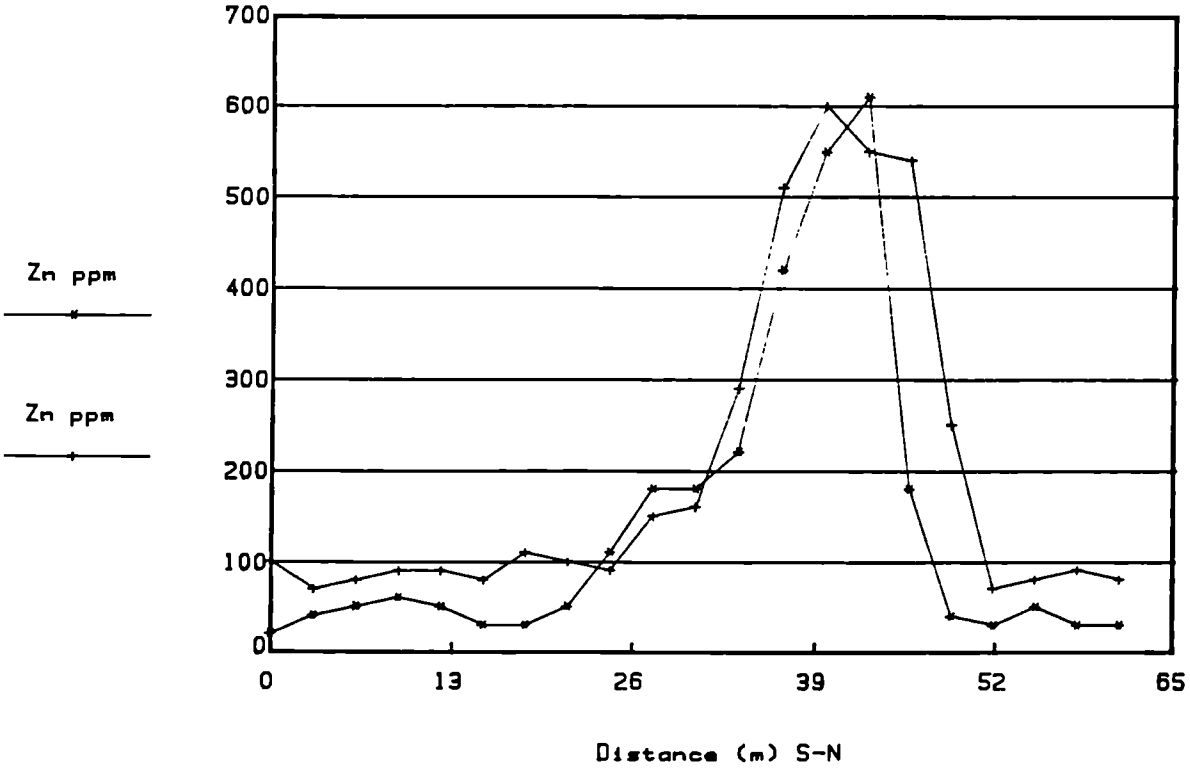

Fig.3.3.9. Broubster 1968 Line 3

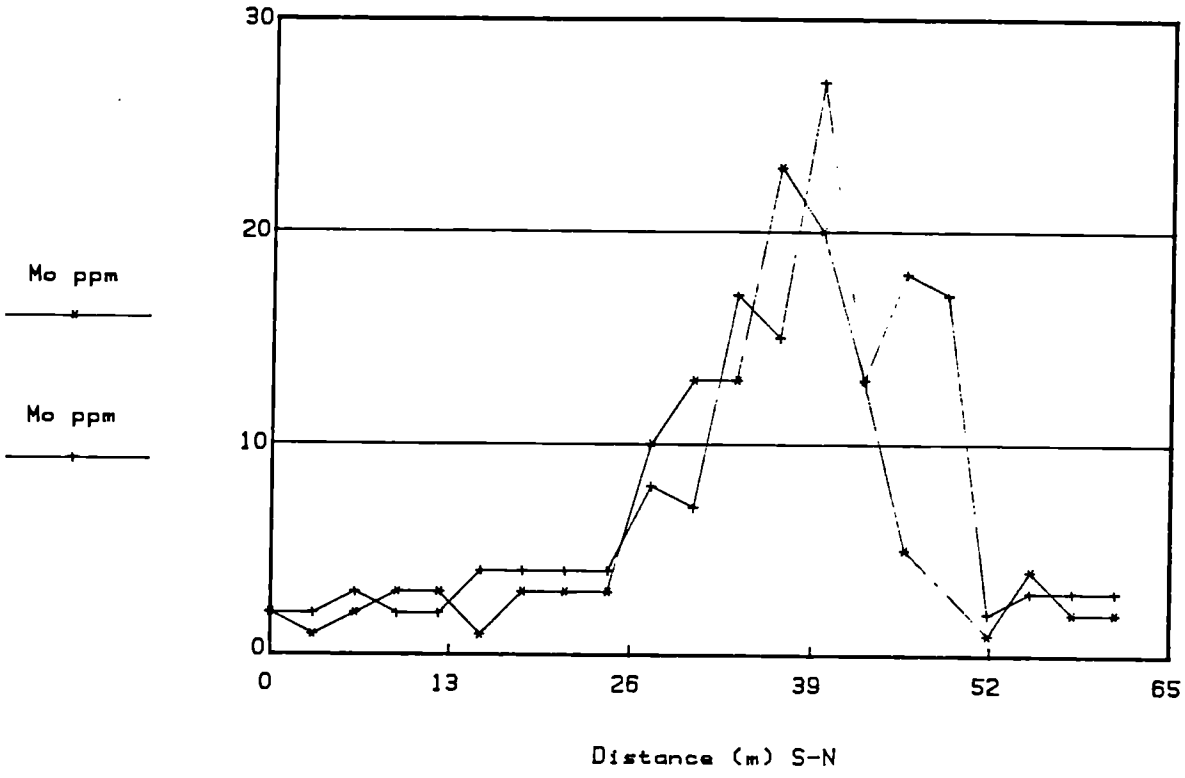

Fig.3.4.1.Broubster 1986 Traverse

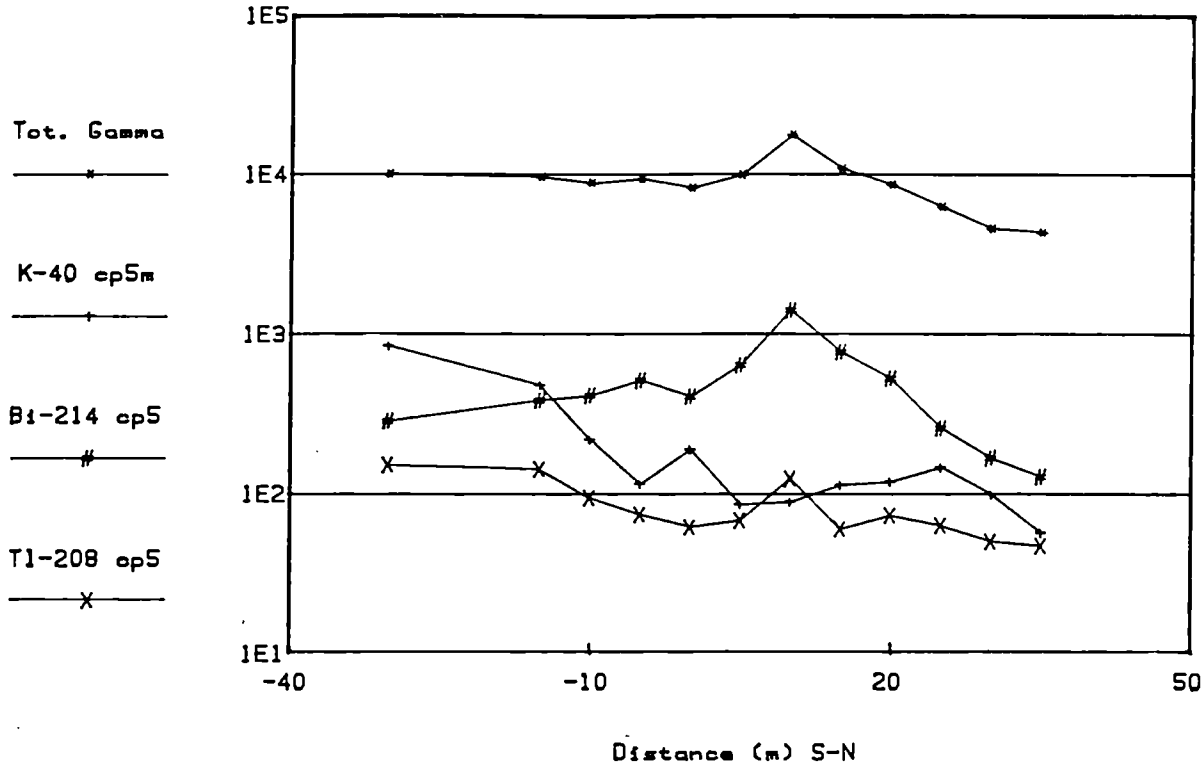

Fig.3.4.2.Broubster 1986 Traverse

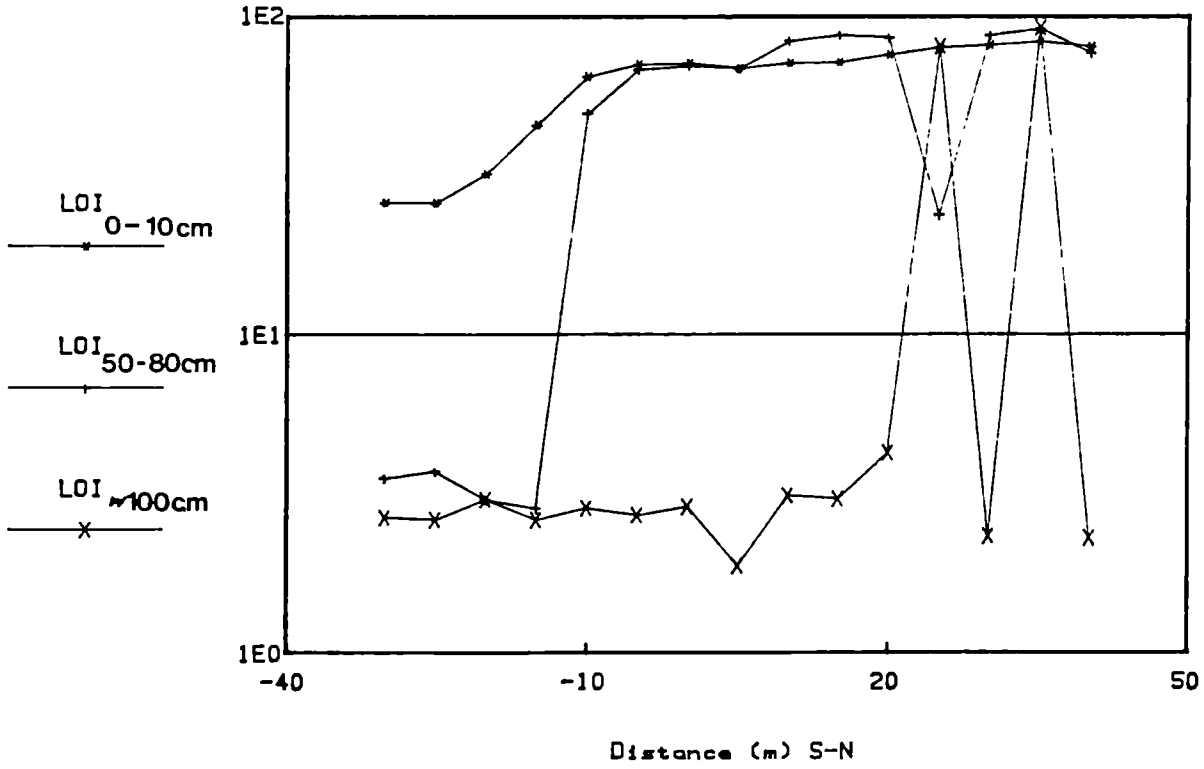

Fig.3.4.3.Broubster 1986 Traverse

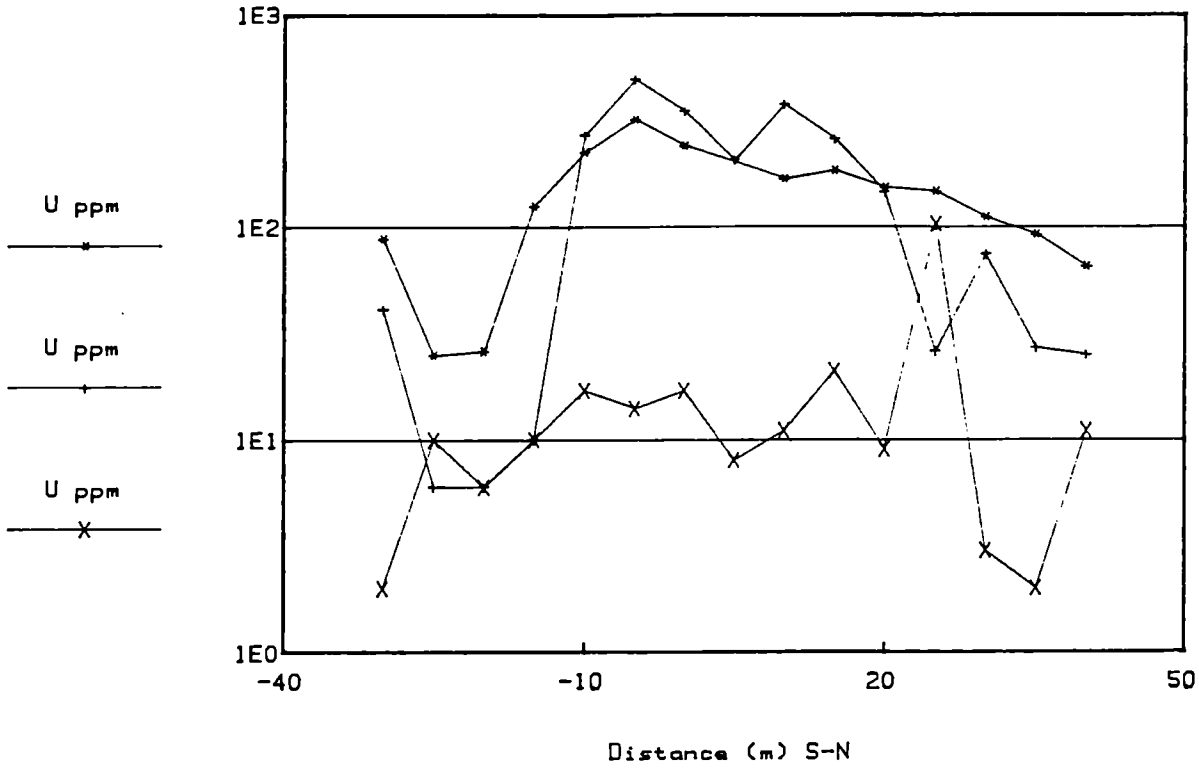

Fig.3.4.4.Broubster 1986 Traverse

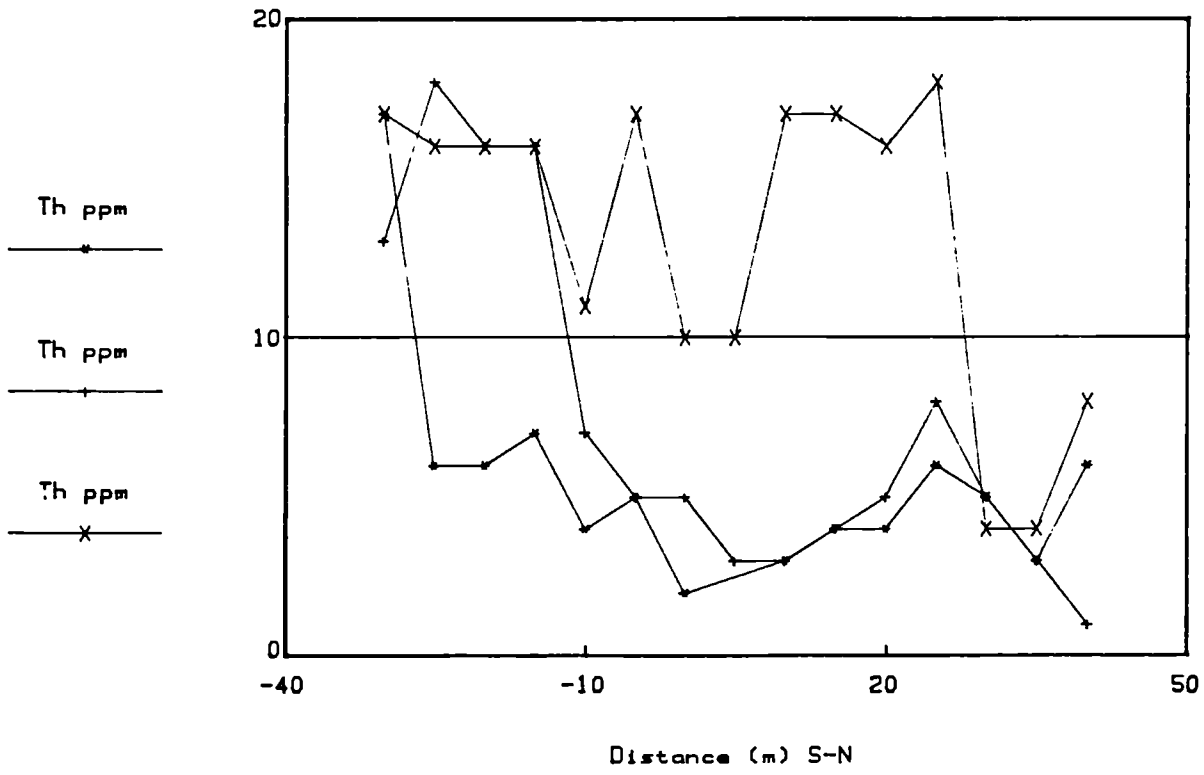

Fig.3.4.5.Broubster 1986 Traverse

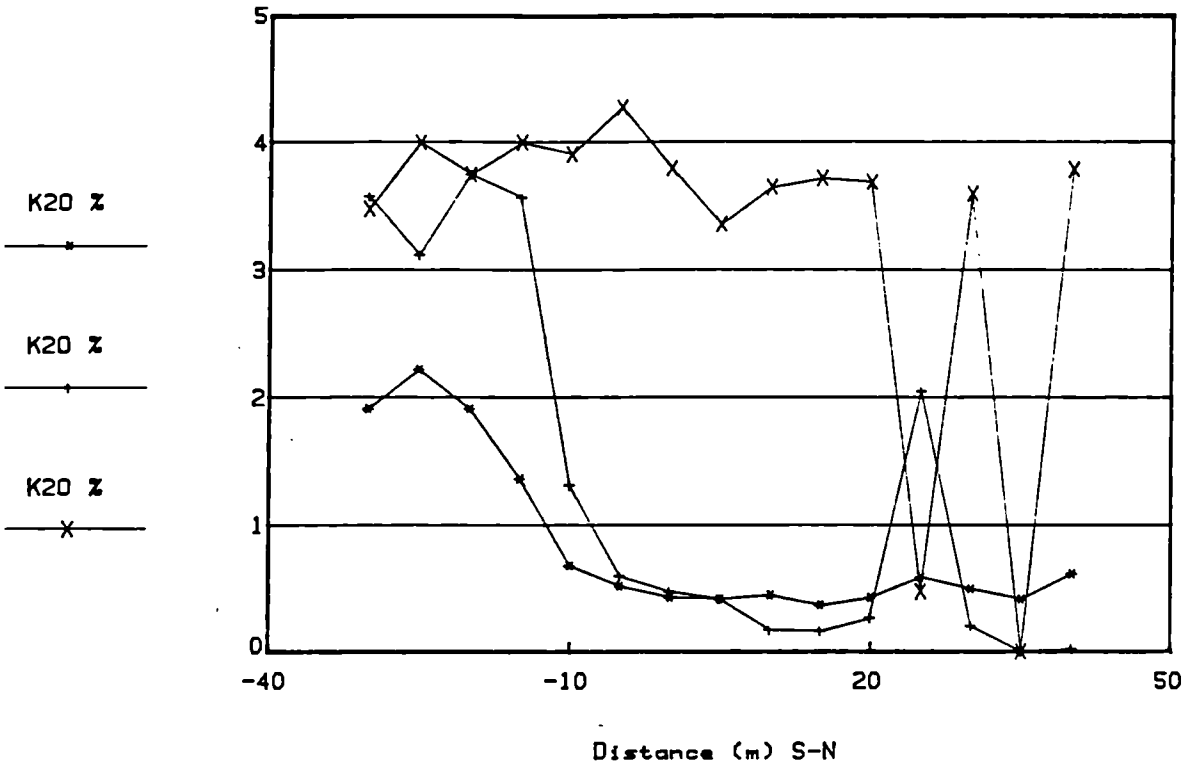

Fig.3.4.6.Broubster 1986 Traverse

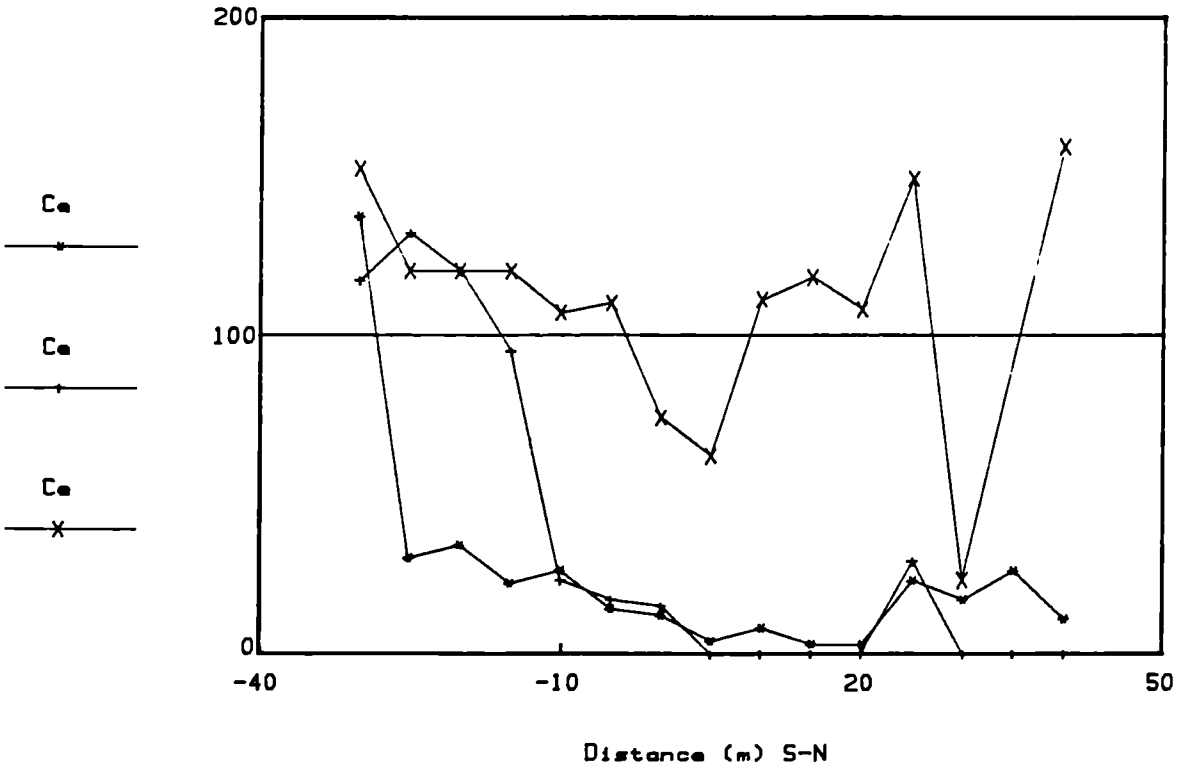

Fig.3.4.7.Broubster 1986 Traverse

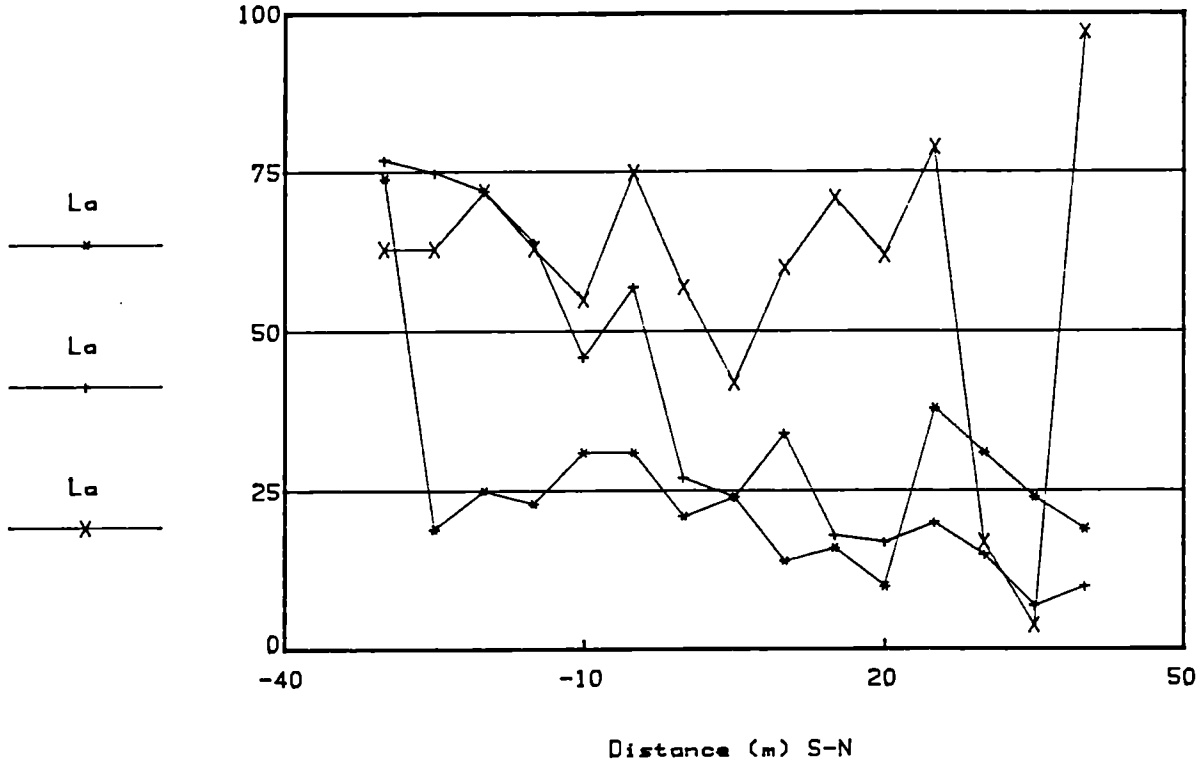

Fig.3.4.8.Broubster 1986 Traverse

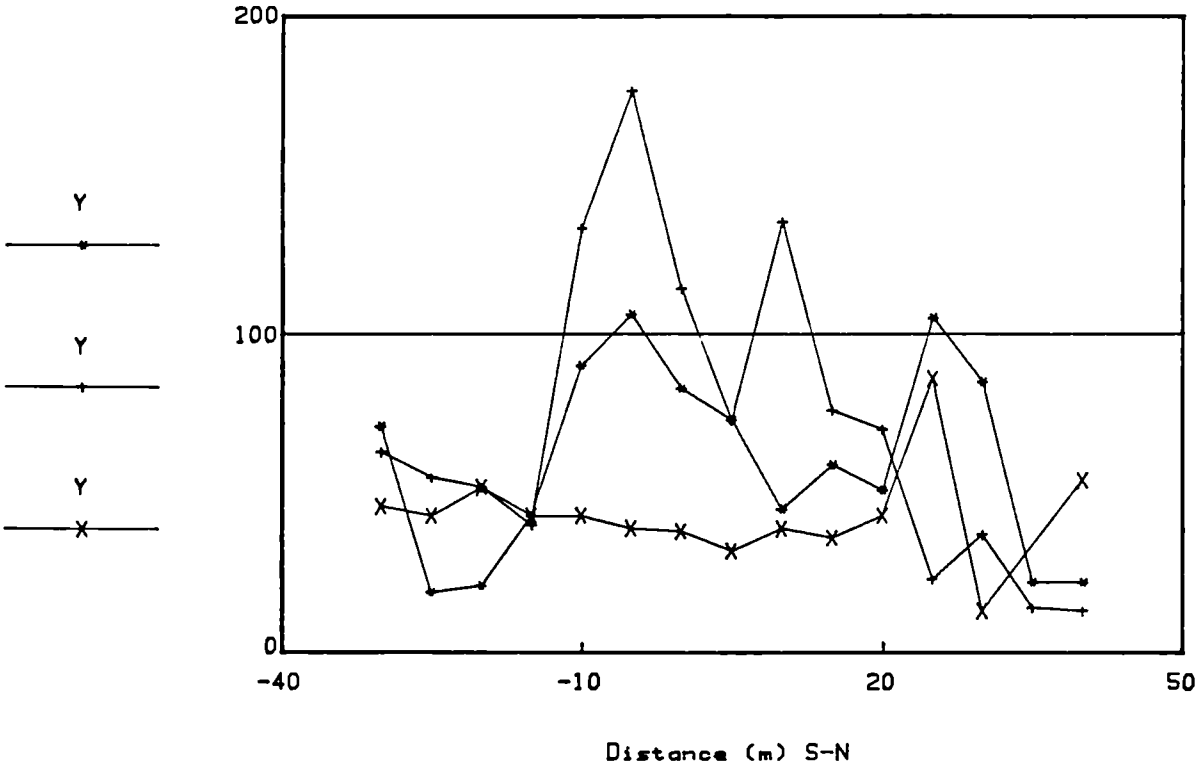

Fig.3.4.9.Broubster 1986 Traverse

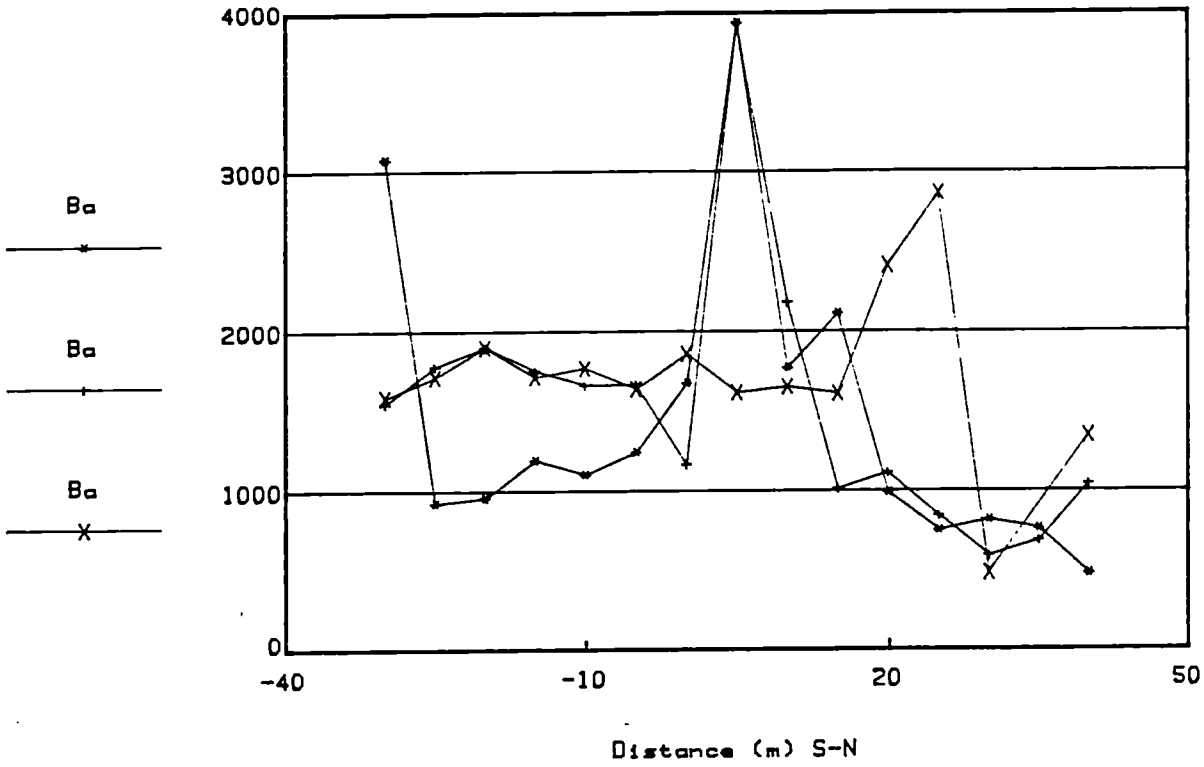

Fig.3.4.10.Broubster 1986 Traverse

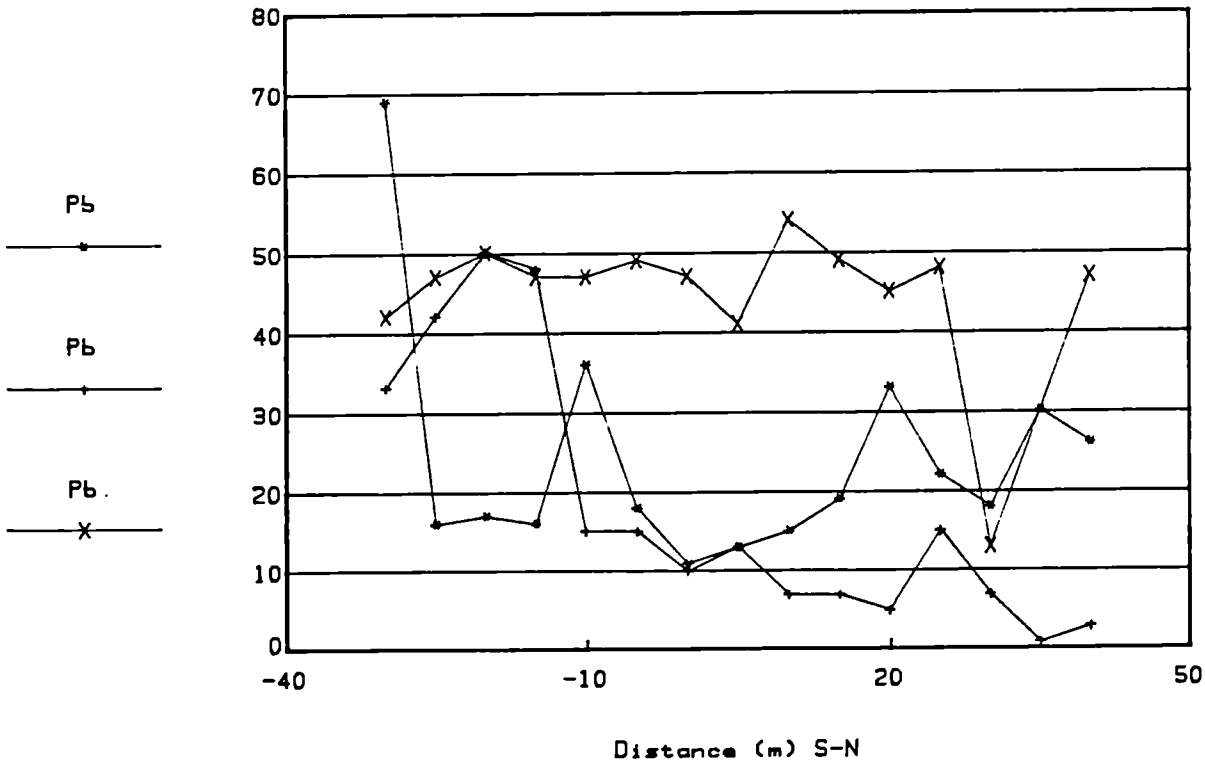

Fig.3.4.11.Broubster 1986 Traverse

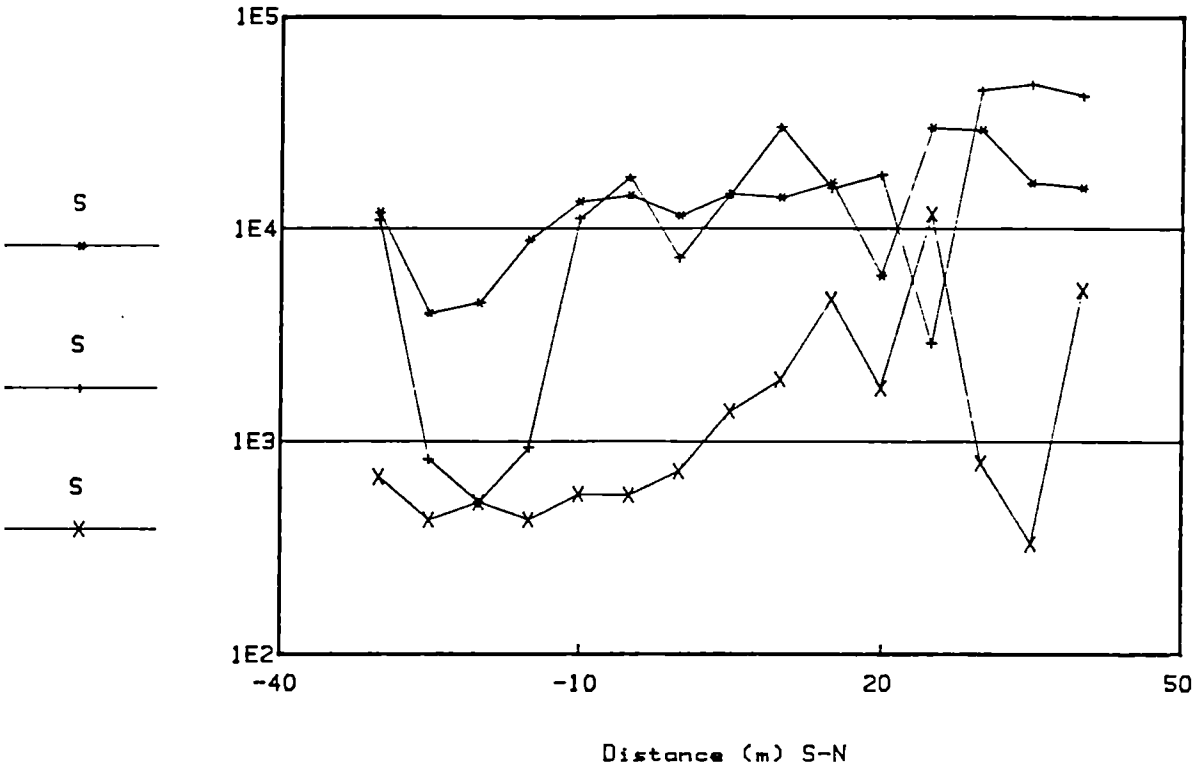

Fig.3.4.12.Broubster 1986 Traverse

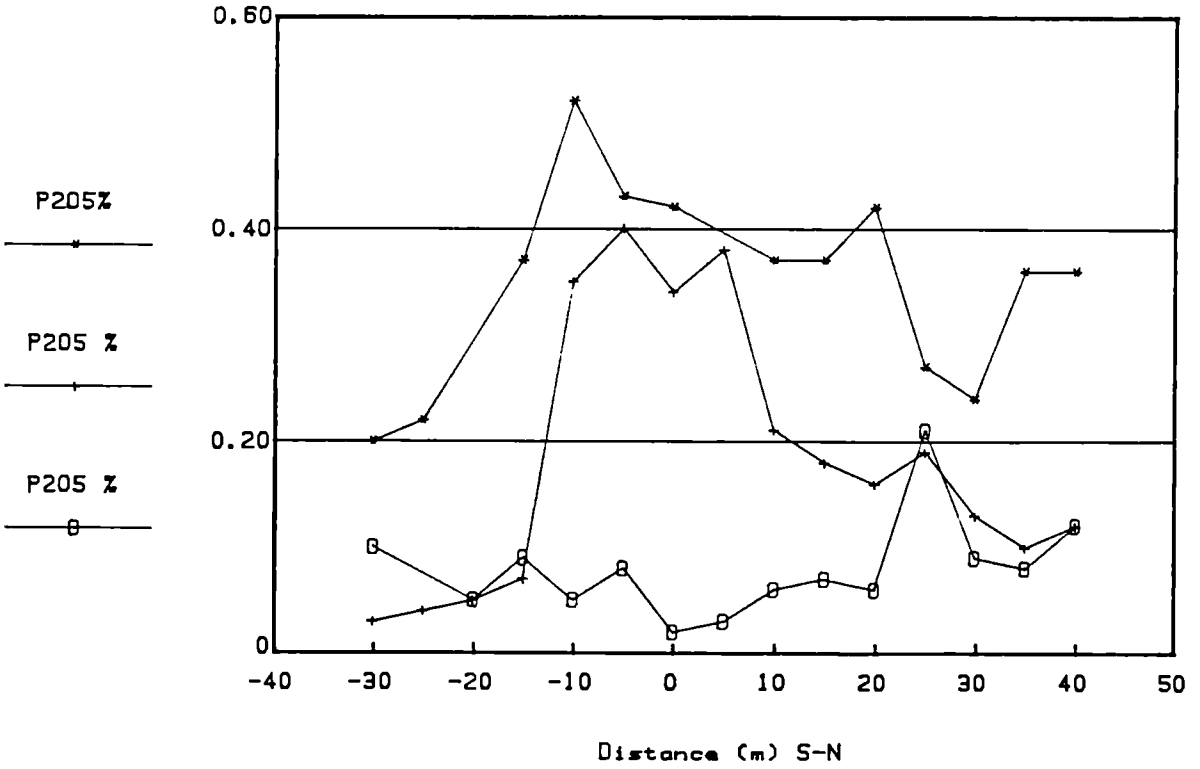

Fig.3.4.13.Broubster 1986 Traverse

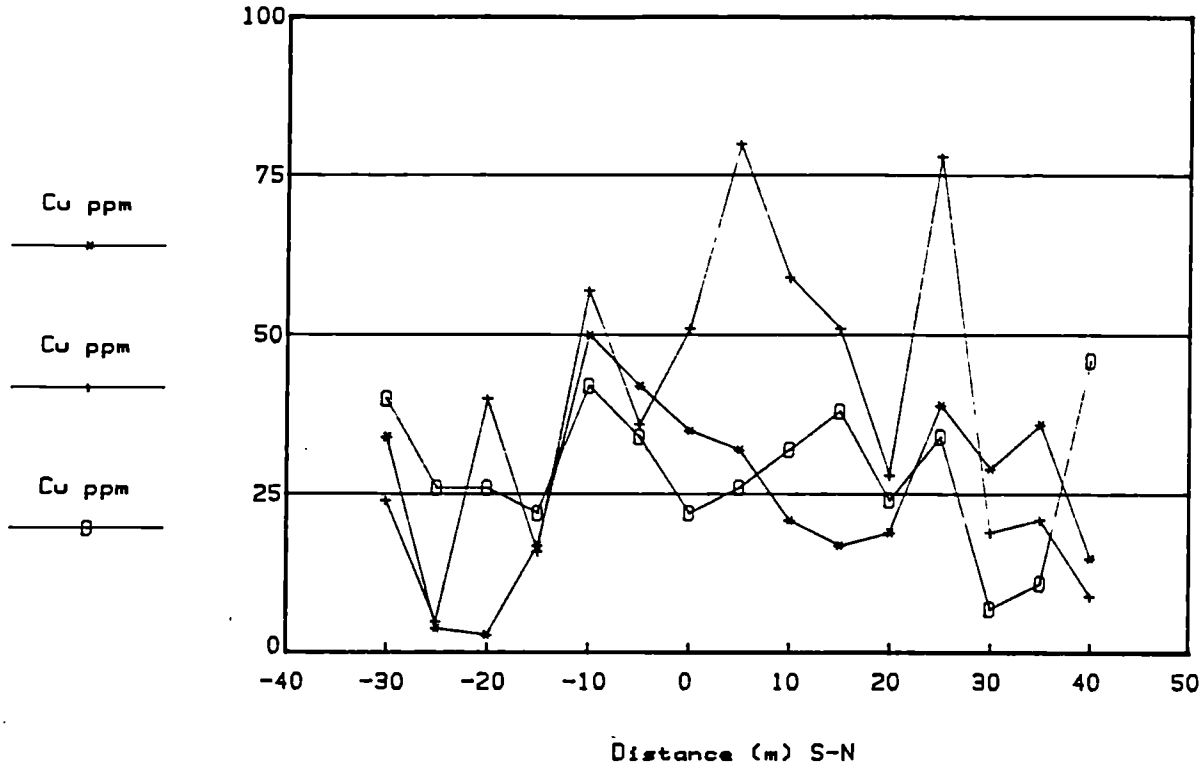

Fig.3.4.14.Broubster 1986 Traverse

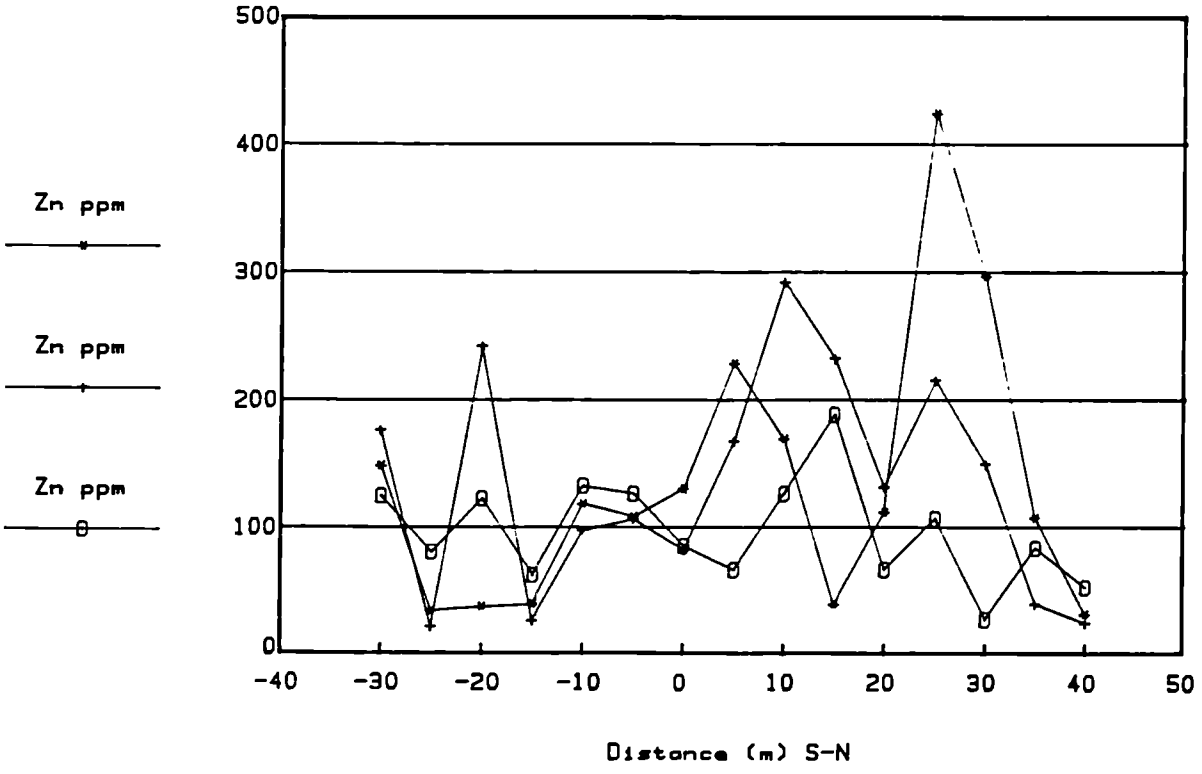

Fig.3.5.1. Broubster 1986 Traverse

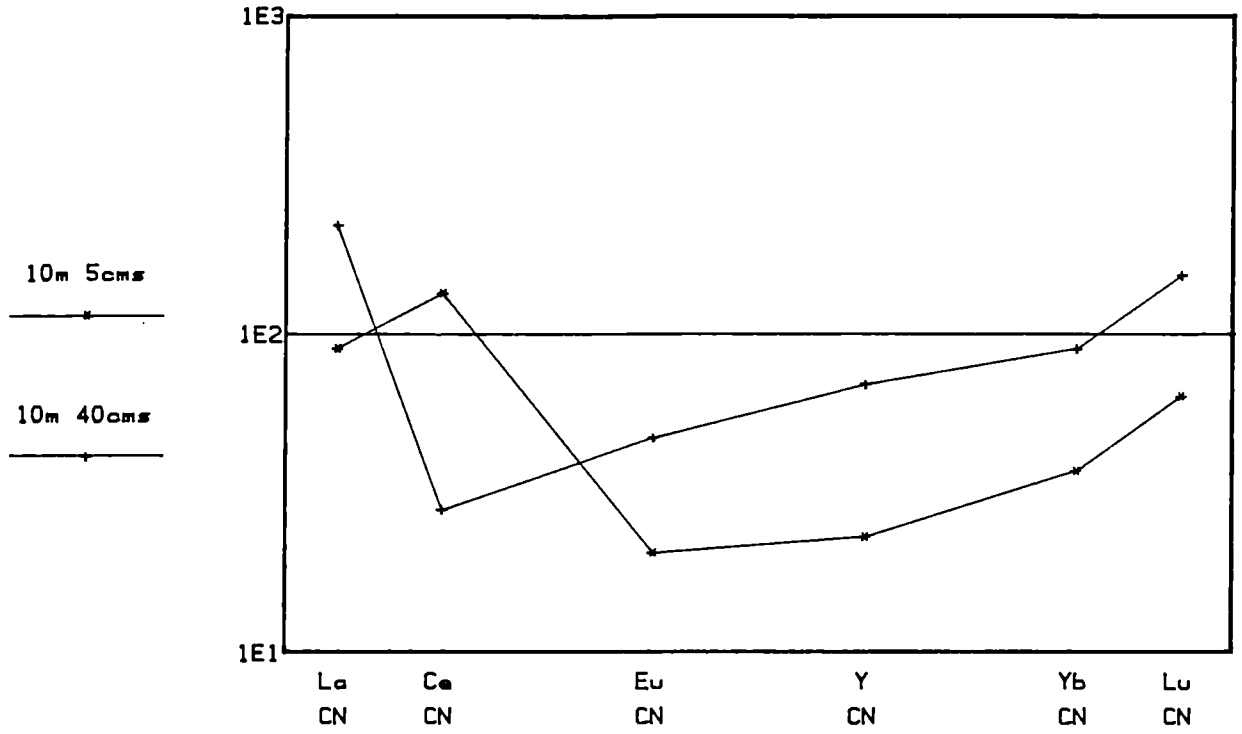

Fig.3.5.2. Broubster 1986 Traverse

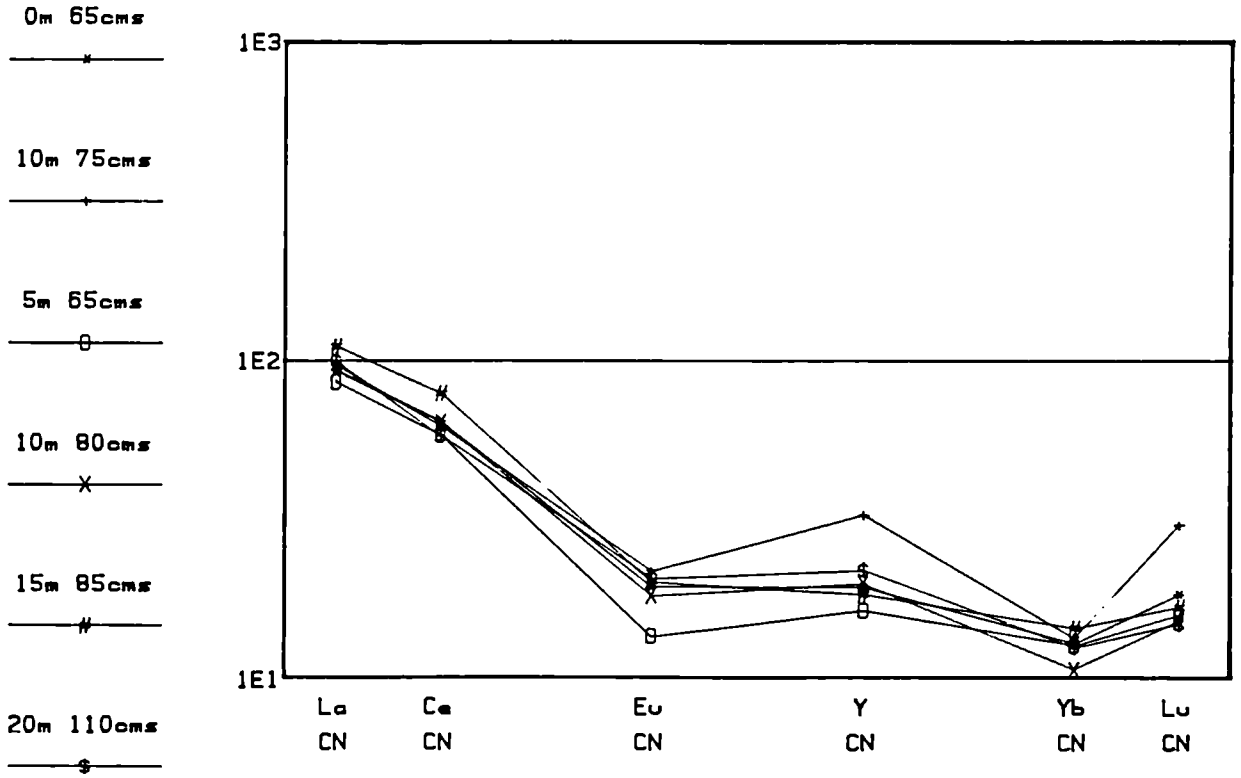

Fig.3.6.1. Broubster 1987 Traverse 1

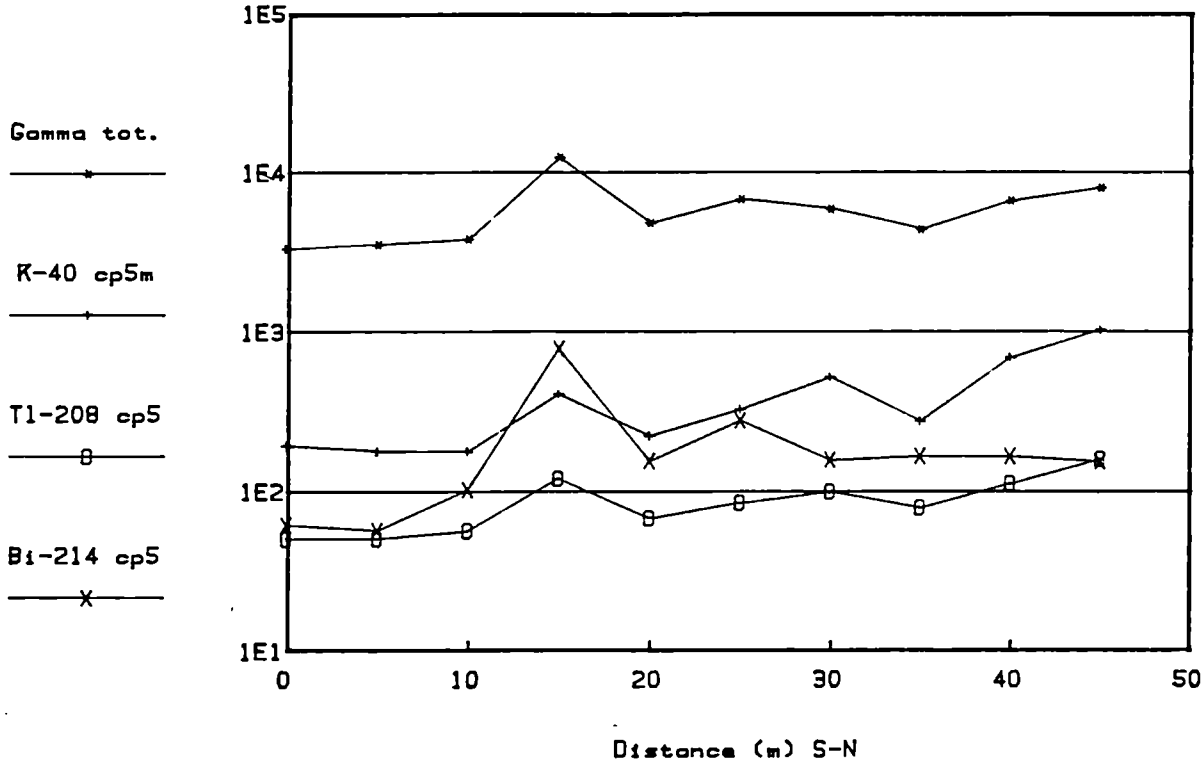

Fig.3.6.2. Broubster 1987 Traverse 1

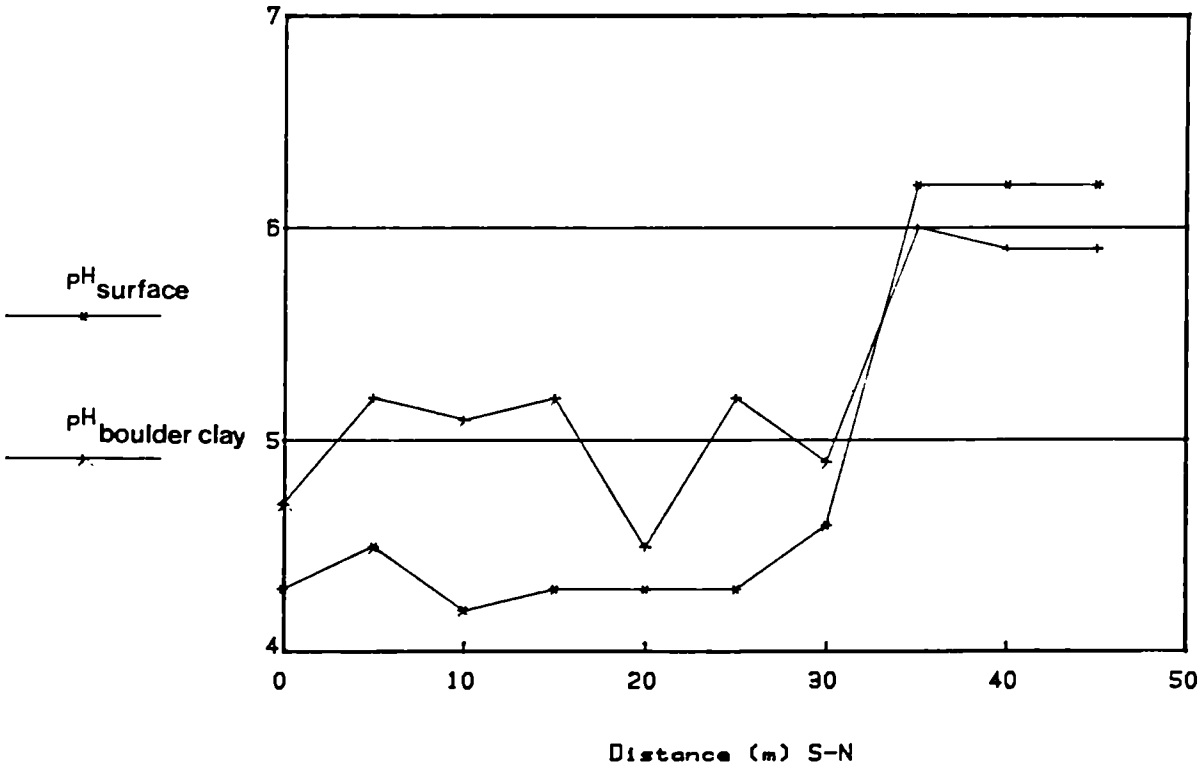

Fig.3.6.3. Broubster 1987 Traverse 1

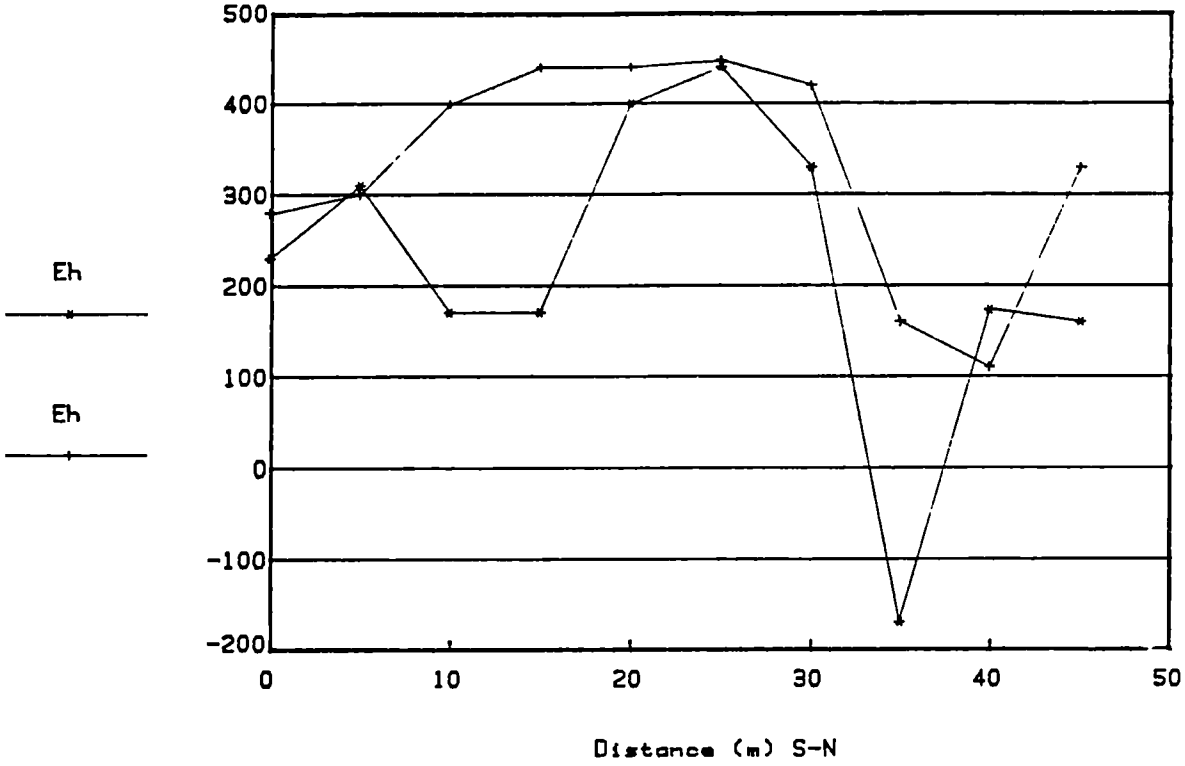

Fig.3.6.4. Broubster 1987 Traverse 1

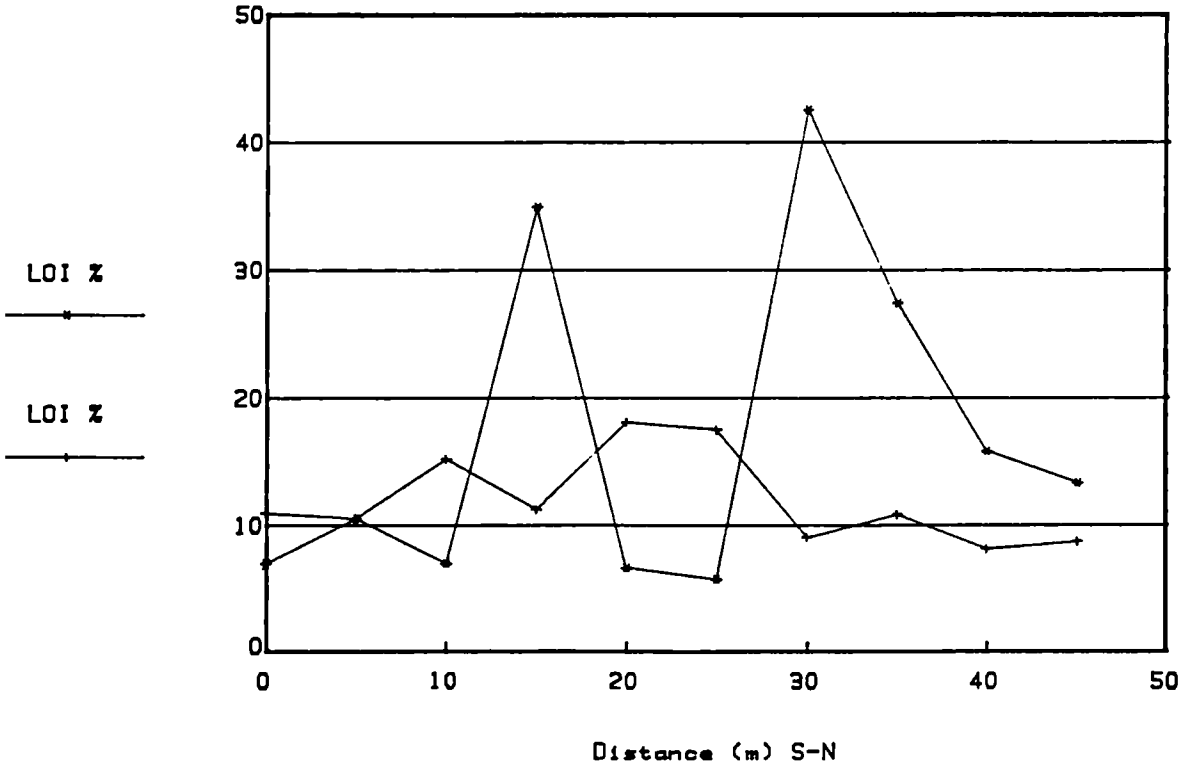

Fig.3.6.5. Broubster 1987 Traverse 1

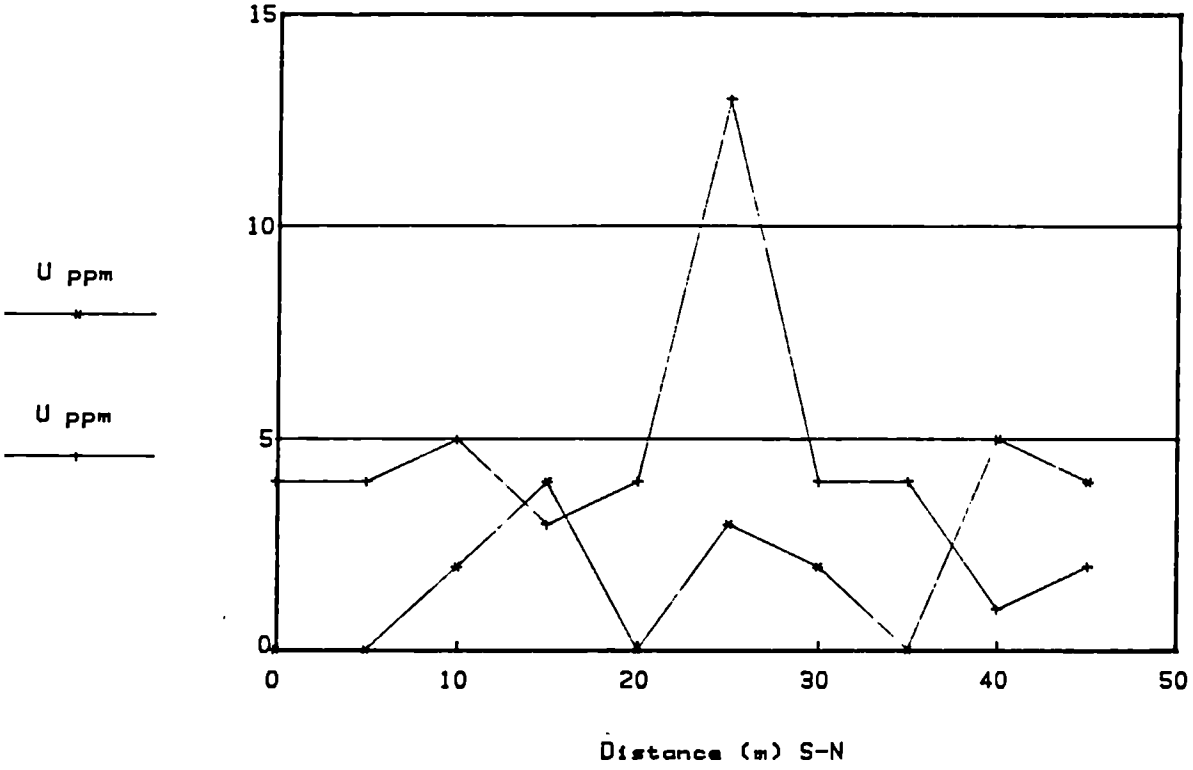

Fig.3.6.6. Broubster 1987 Traverse 1

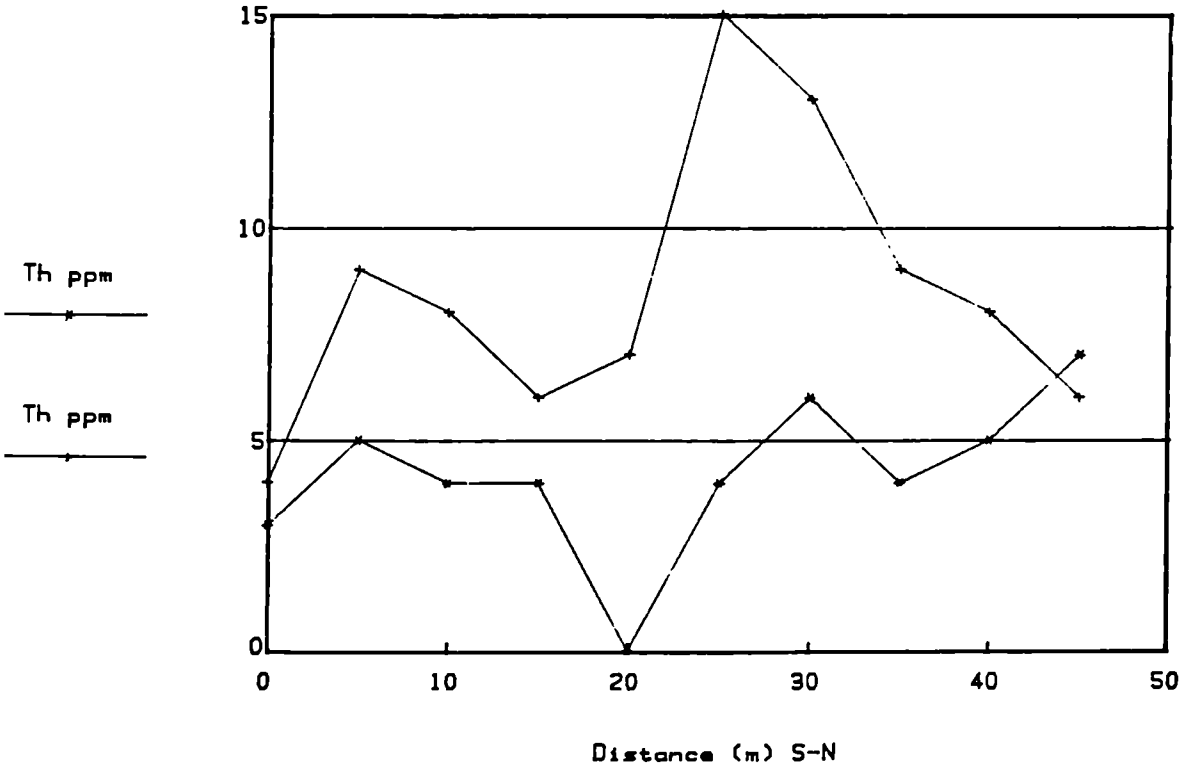

Fig.3.6.7. Broubster 1987 Traverse 1

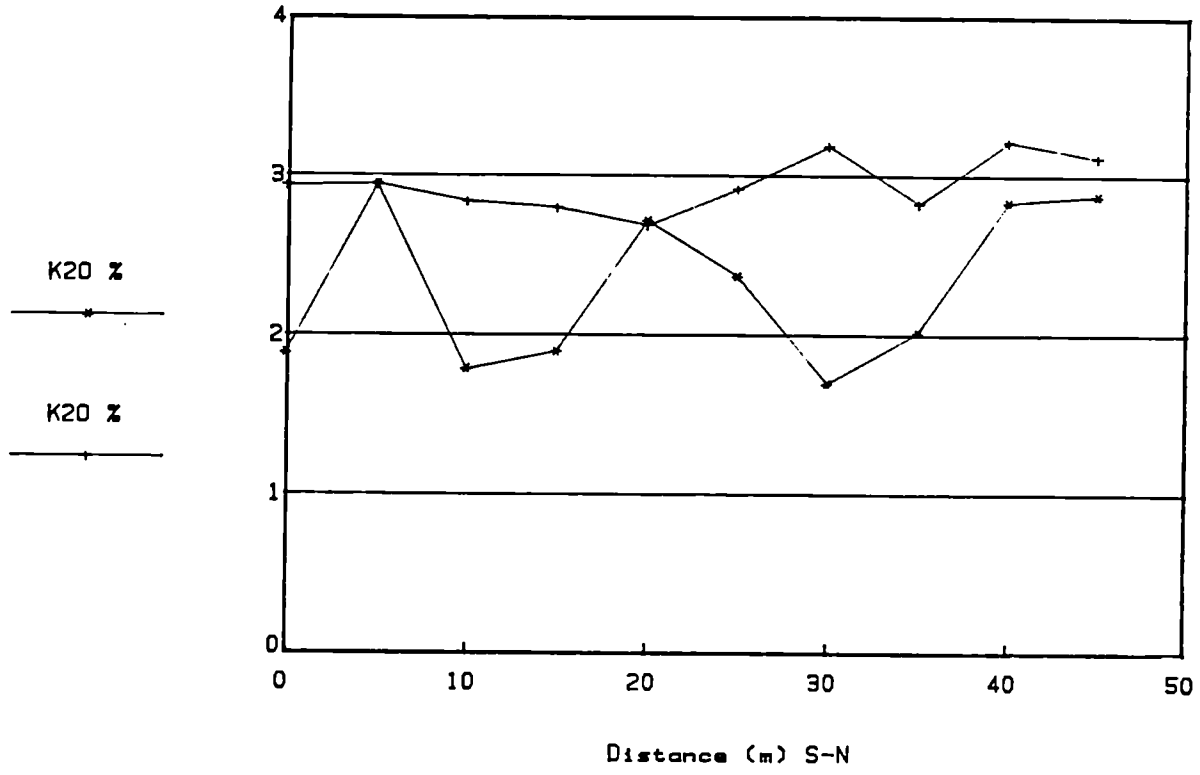

Fig.3.6.8. Broubster 1987 Traverse 1

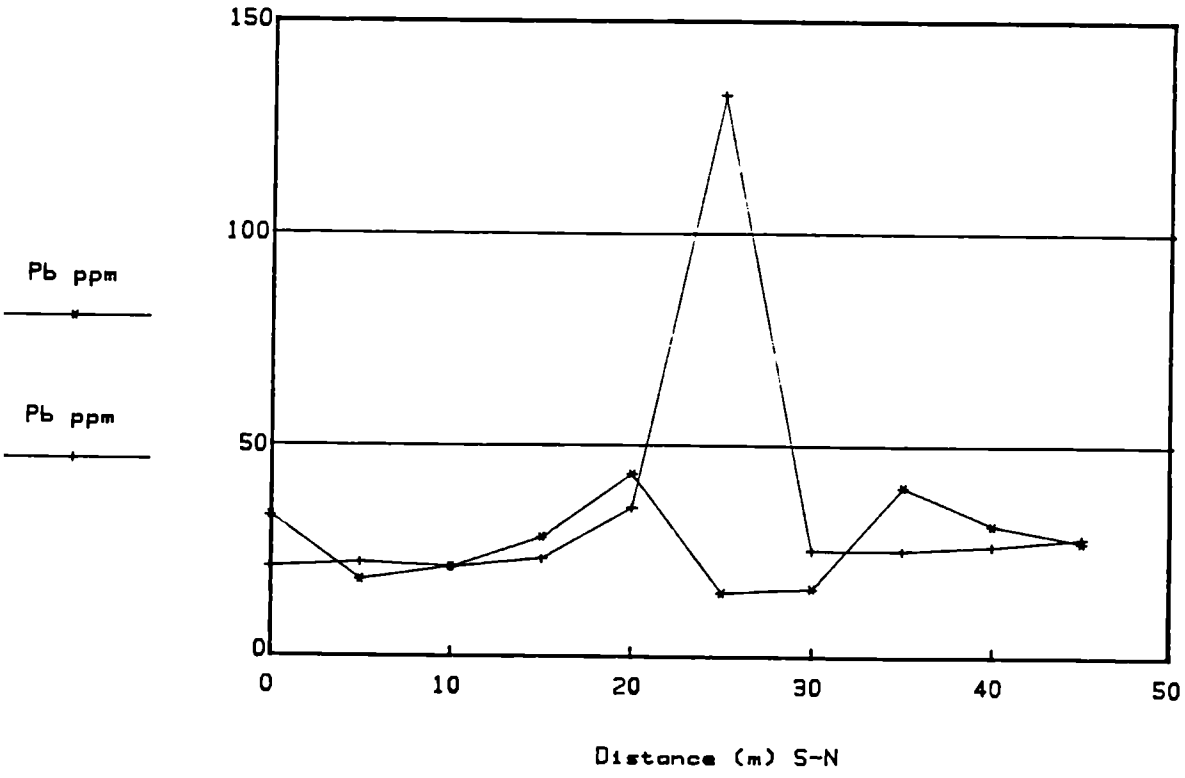

Fig.3.6.9. Broubster 1987 Traverse 1

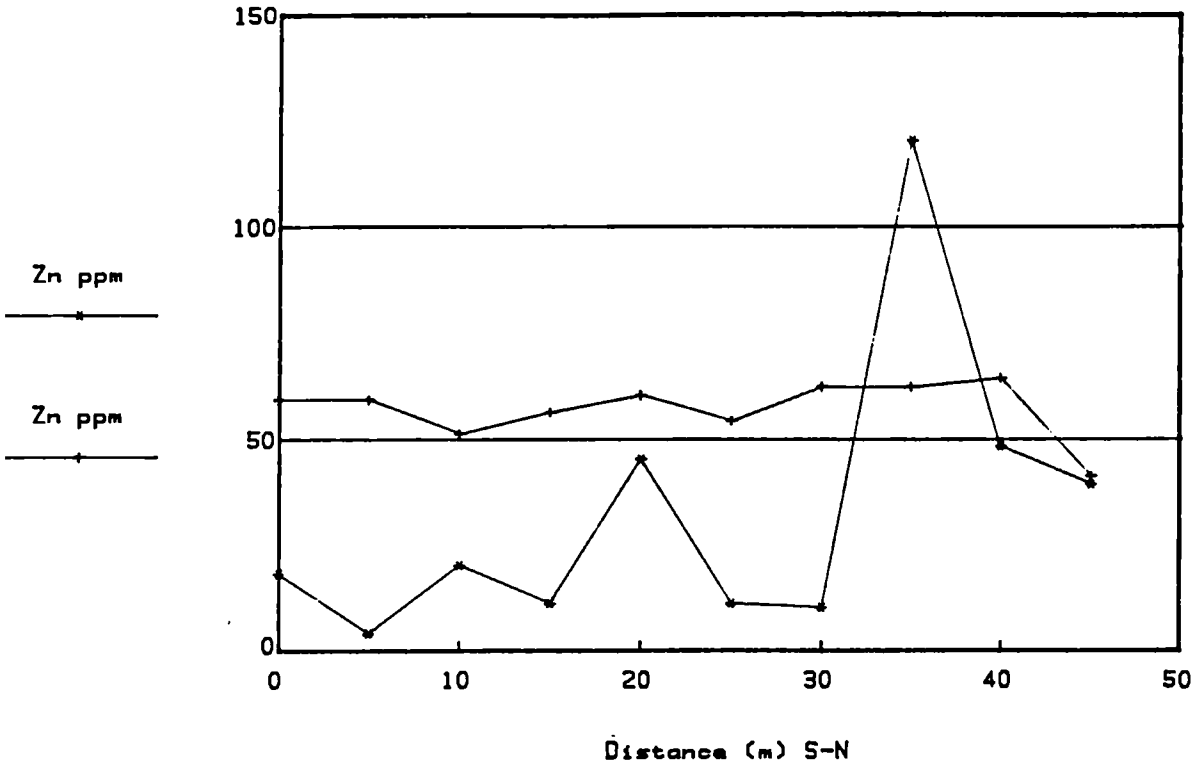

Fig.3.6.10.Broubster 1987 Traverse 1

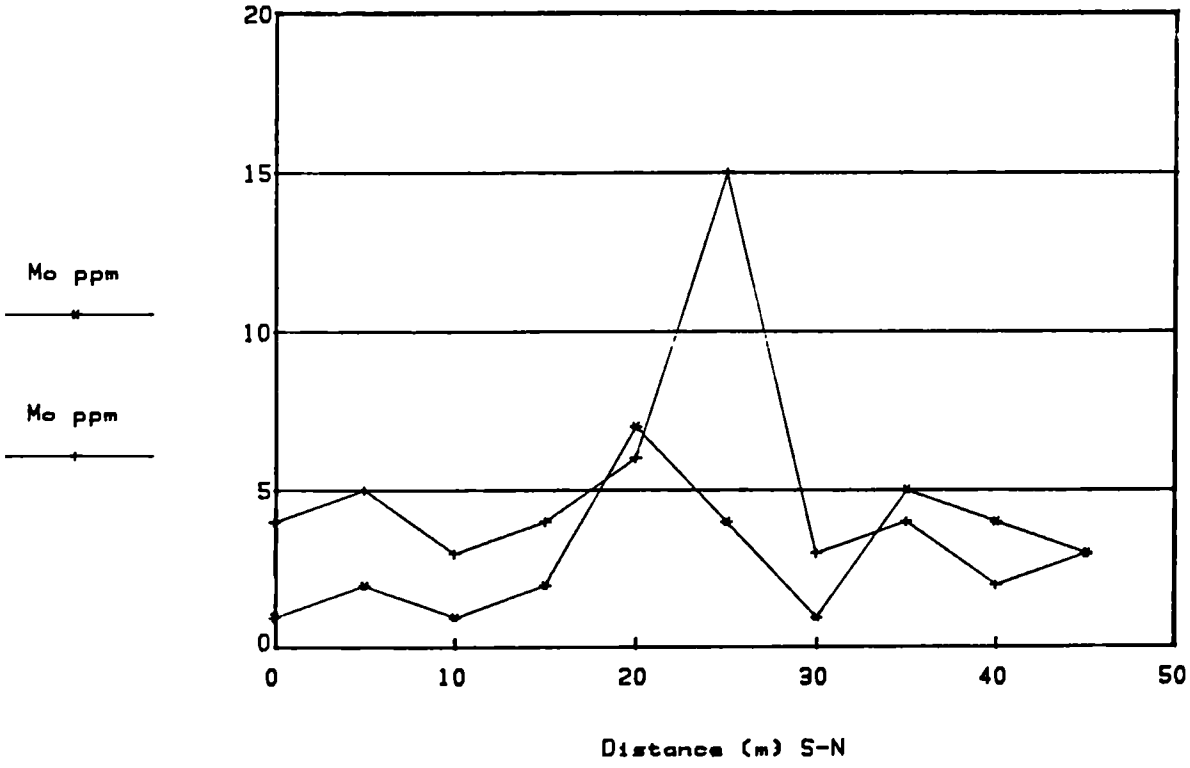

Fig.3.6.11.Broubster 1987 Traverse 1

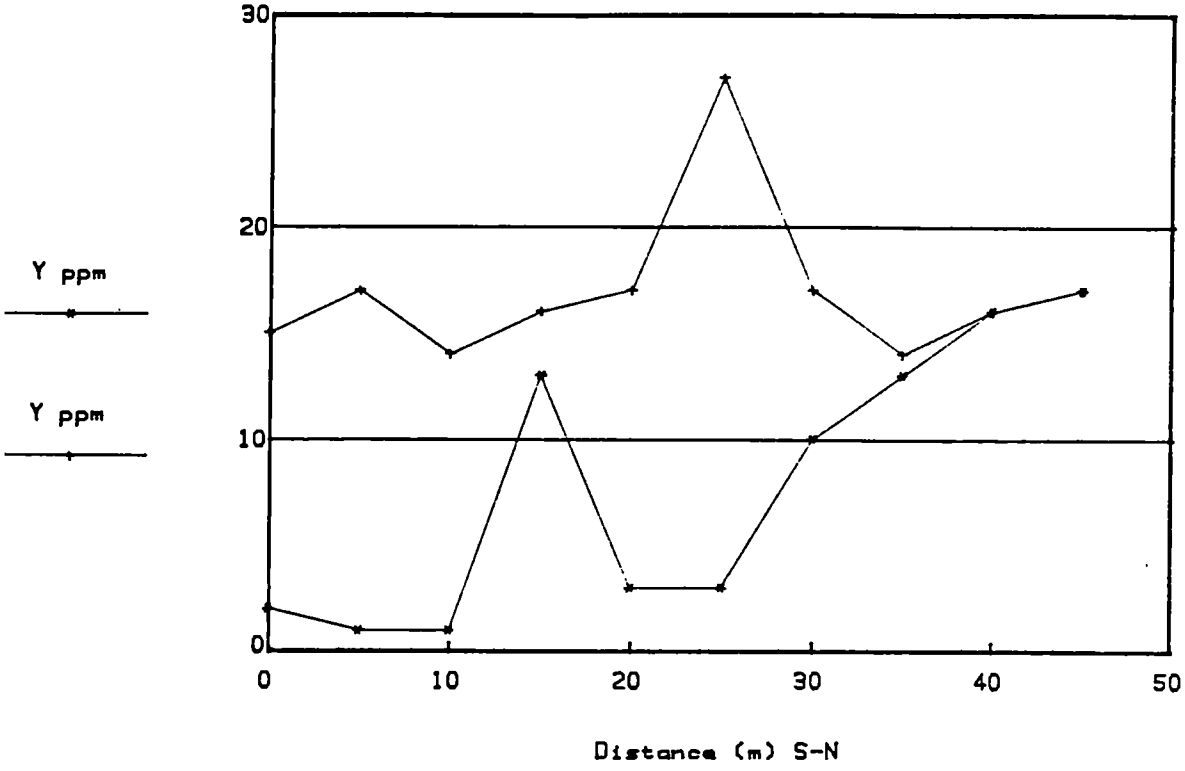

Fig.3.6.12.Broubster 1987 Traverse 1

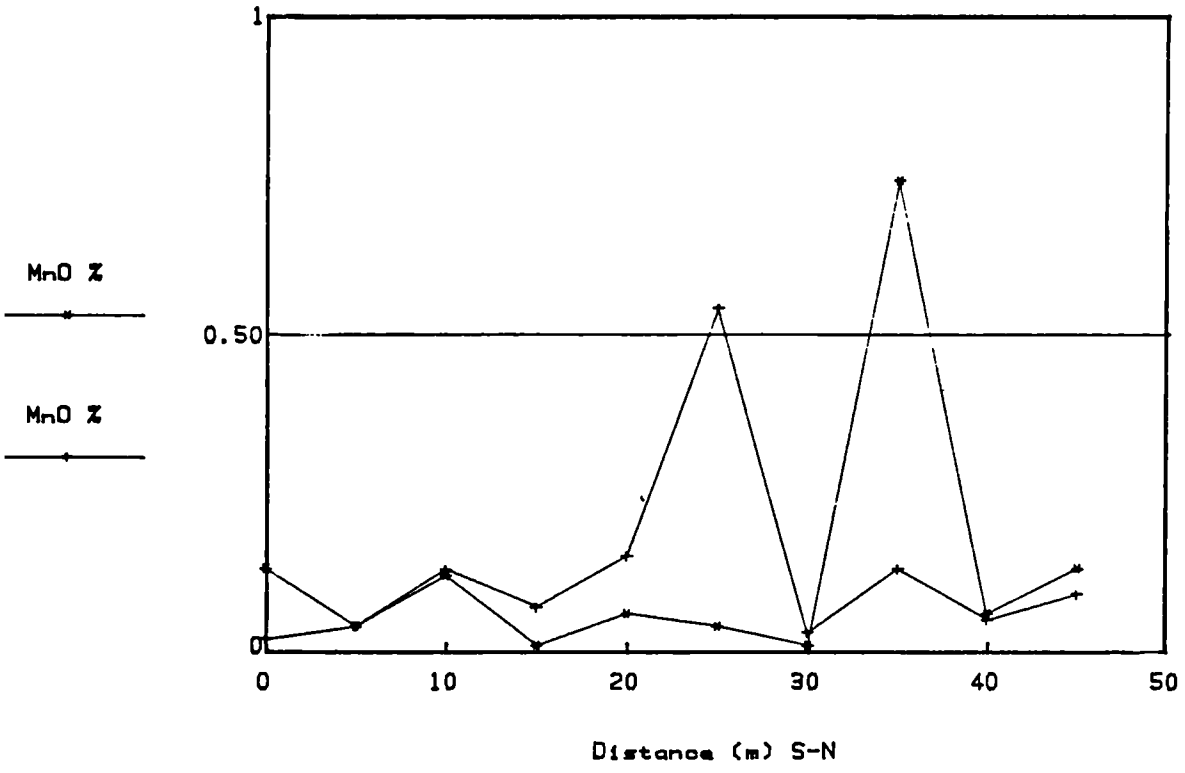

Fig.3.6.13.Broubster 1987 Traverse 1

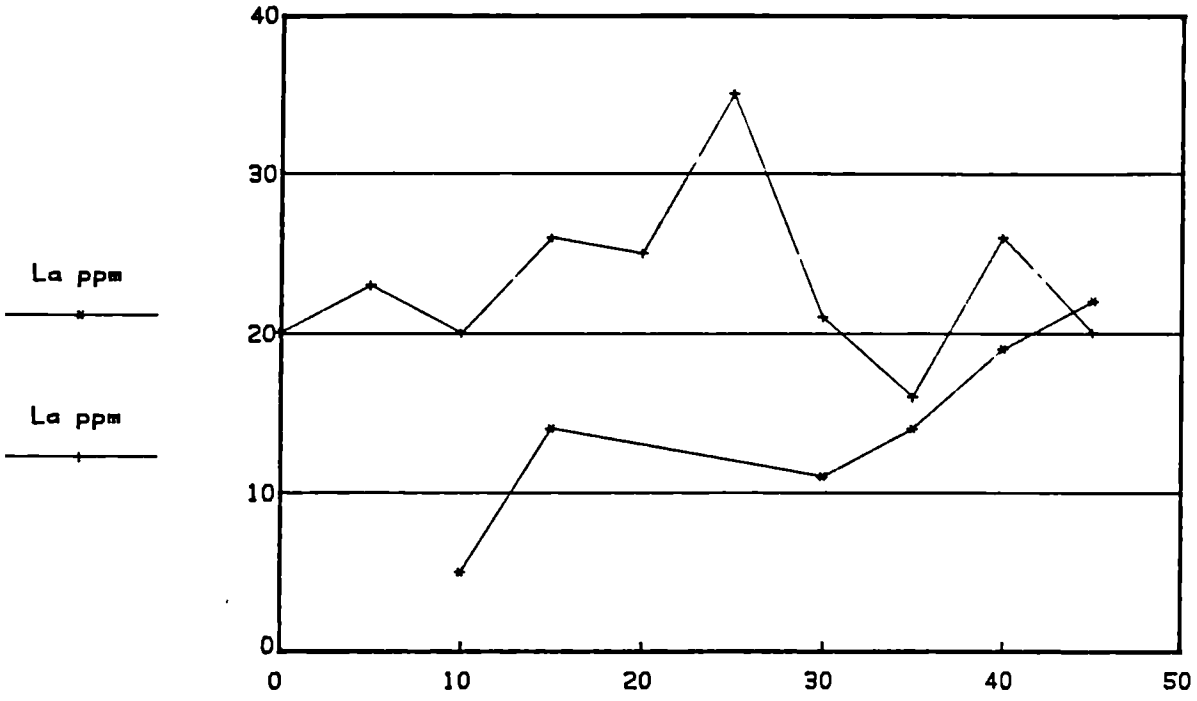

Fig.3.6.14.Broubster 1987 Traverse 1

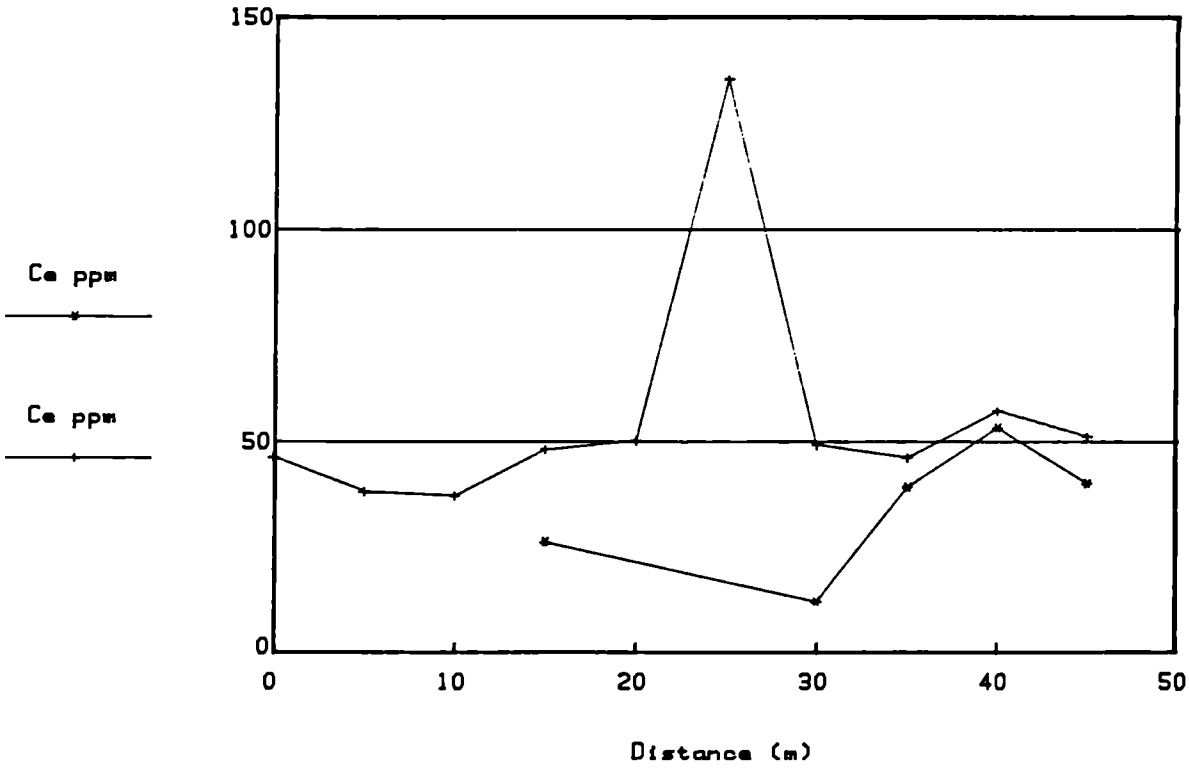

Fig.3.6.15.Broubster 1987 Traverse 1

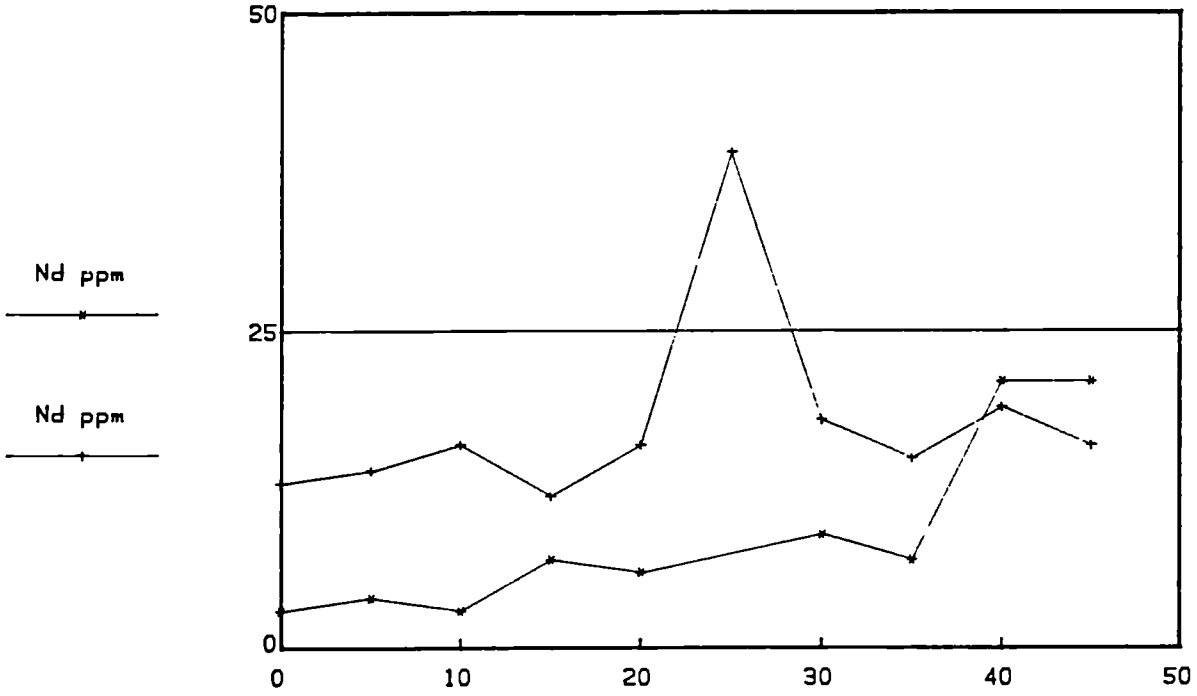

Fig.3.6.16.Broubster 1987 Traverse 1

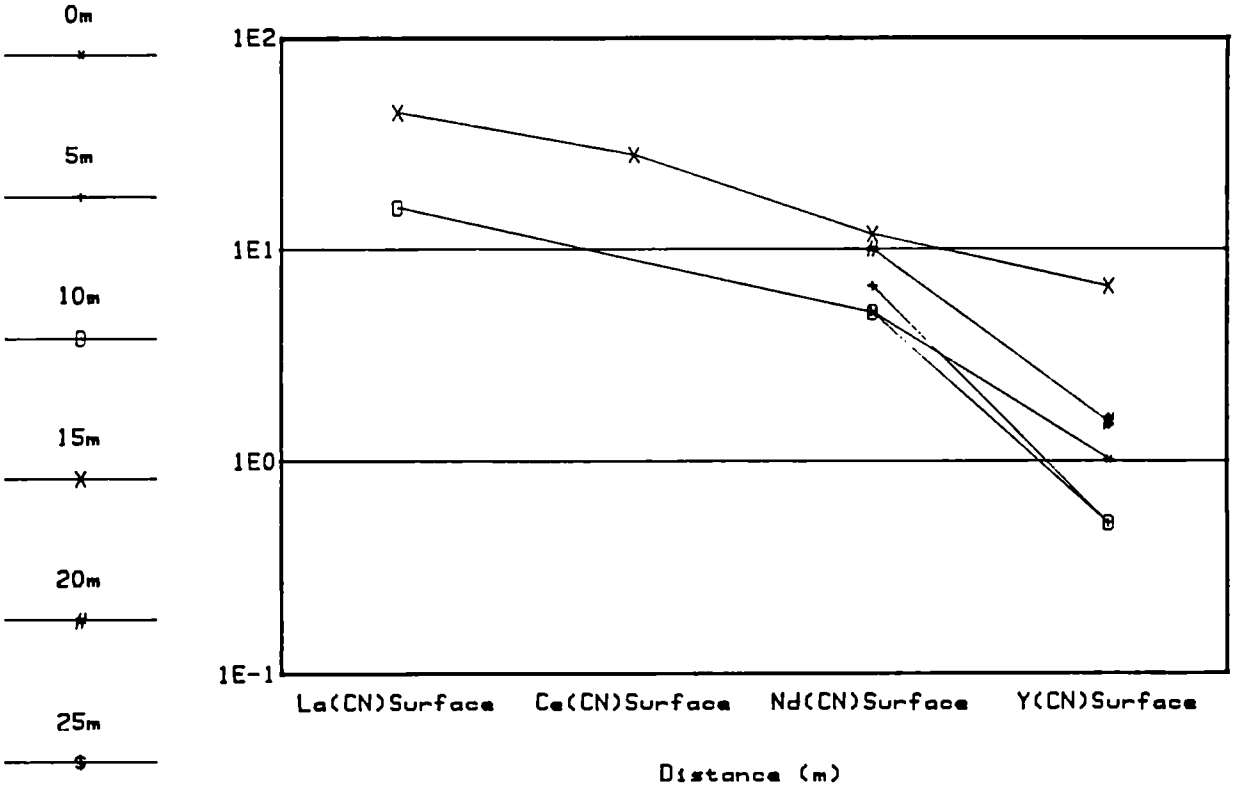

Fig.3.6.17.Broubster 1987 Traverse 1

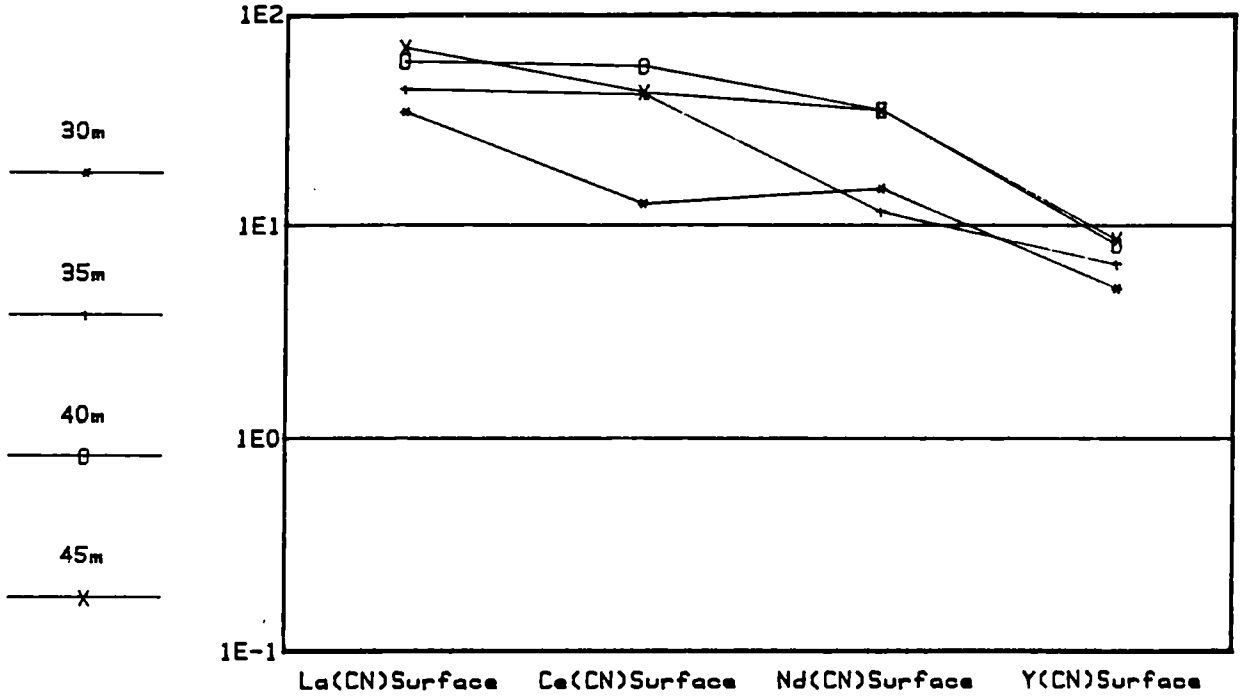

Fig.3.6.18.Broubster 1987 Traverse 1

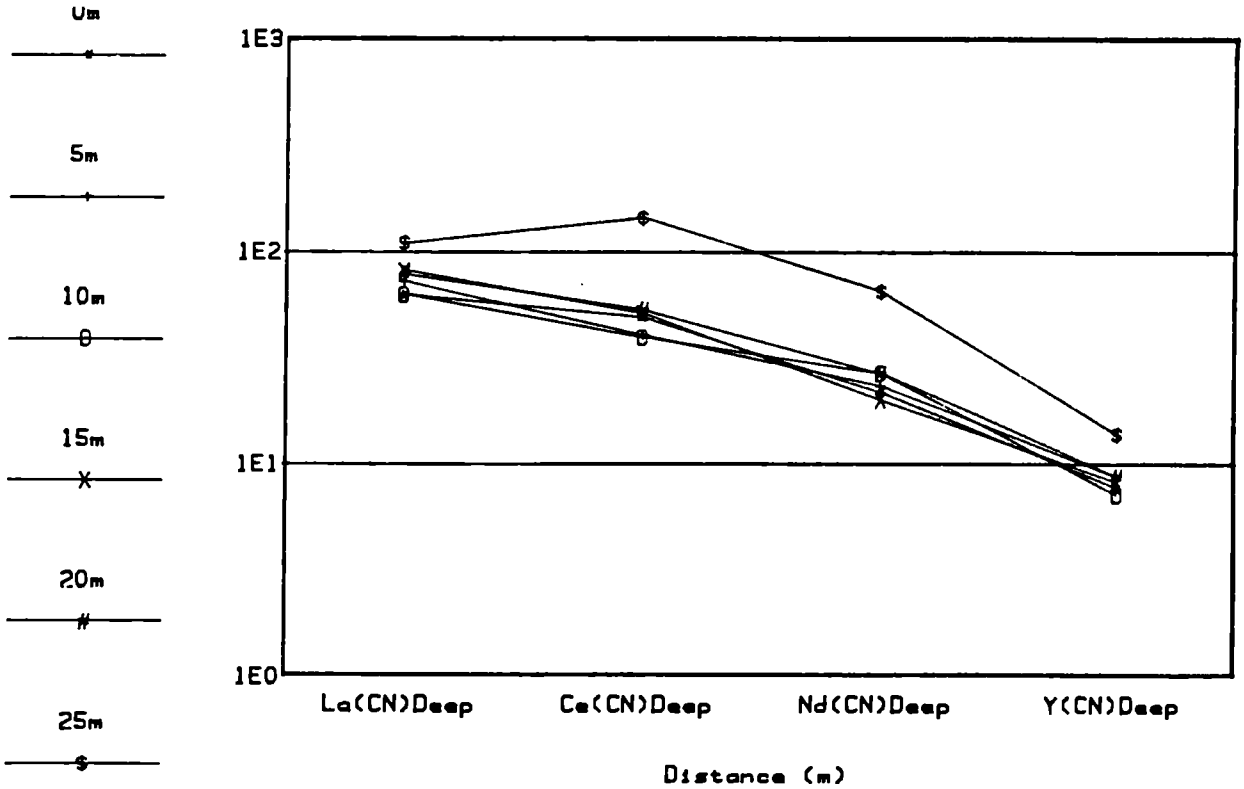

Fig.3.6.19.Broubster 1987 Traverse 1

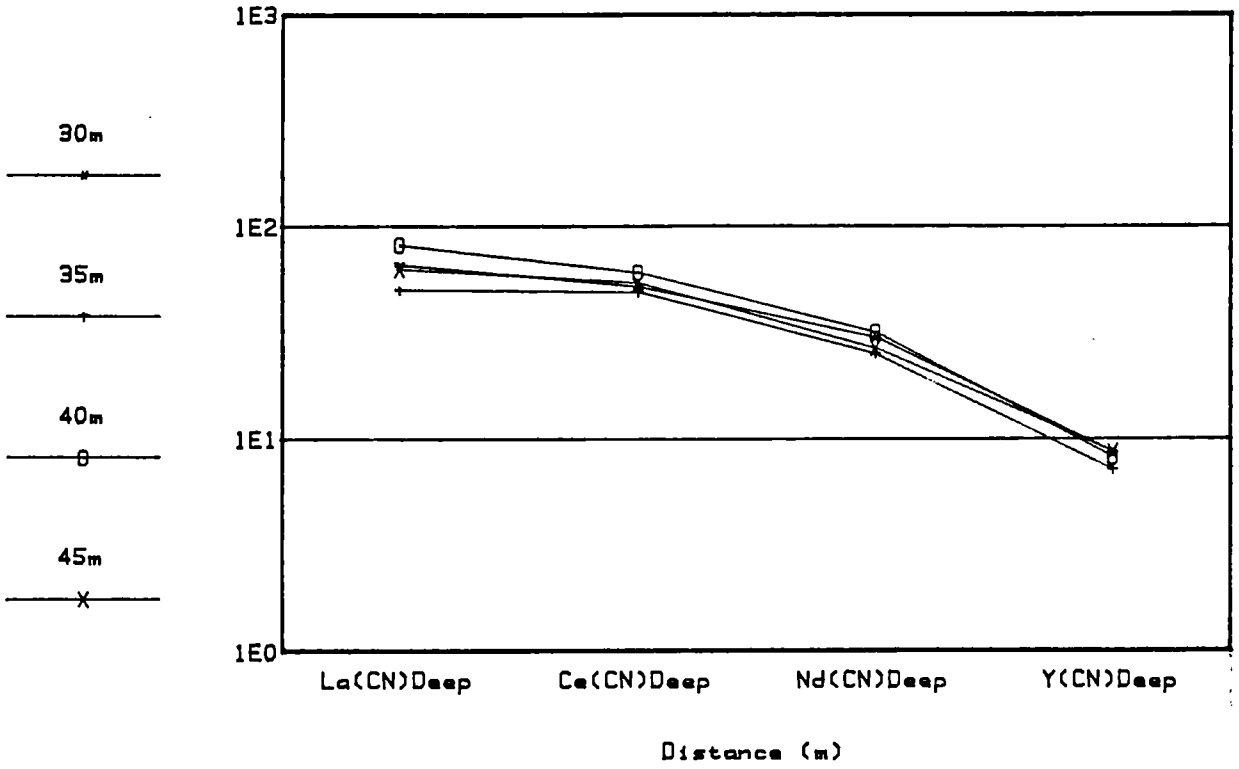

Fig.3.7.1. Broubster 1987 Traverse 2

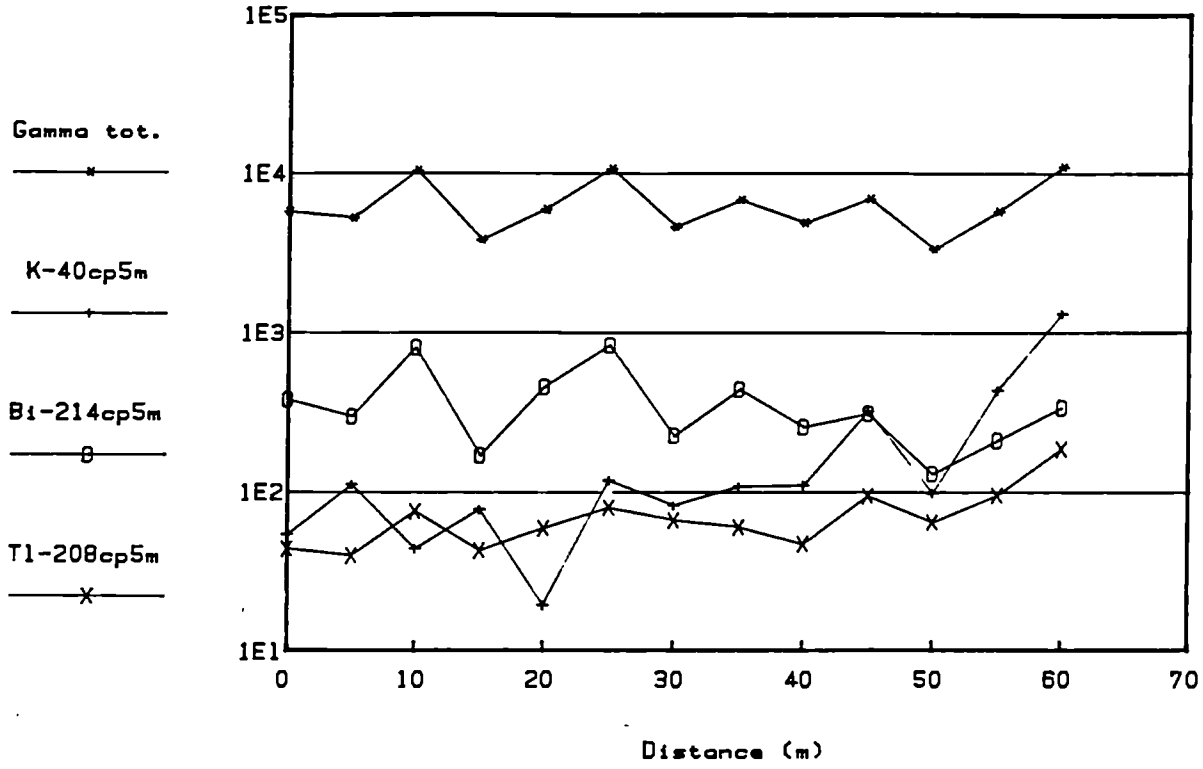

Fig.3.7.2. Broubster 1987 Traverse 2

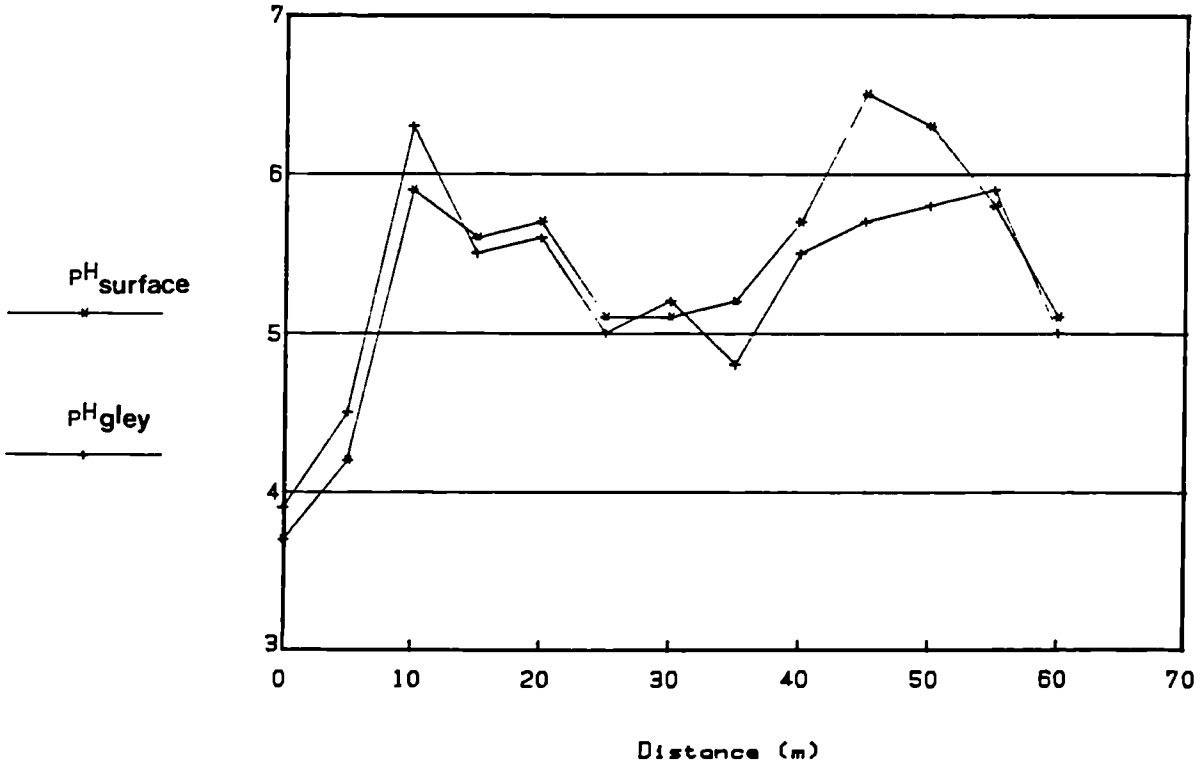

Fig.3.7.3. Broubster 1987 Traverse 2

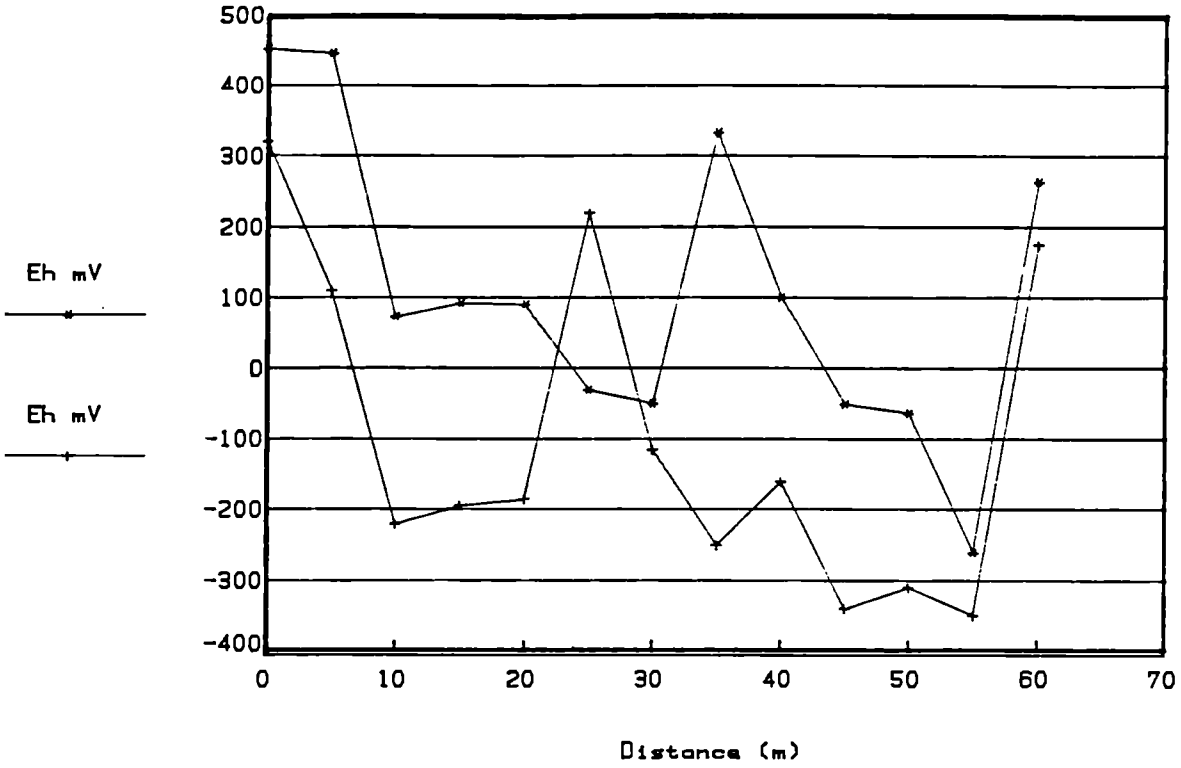

Fig.3.7.4. Broubster 1987 Traverse 2

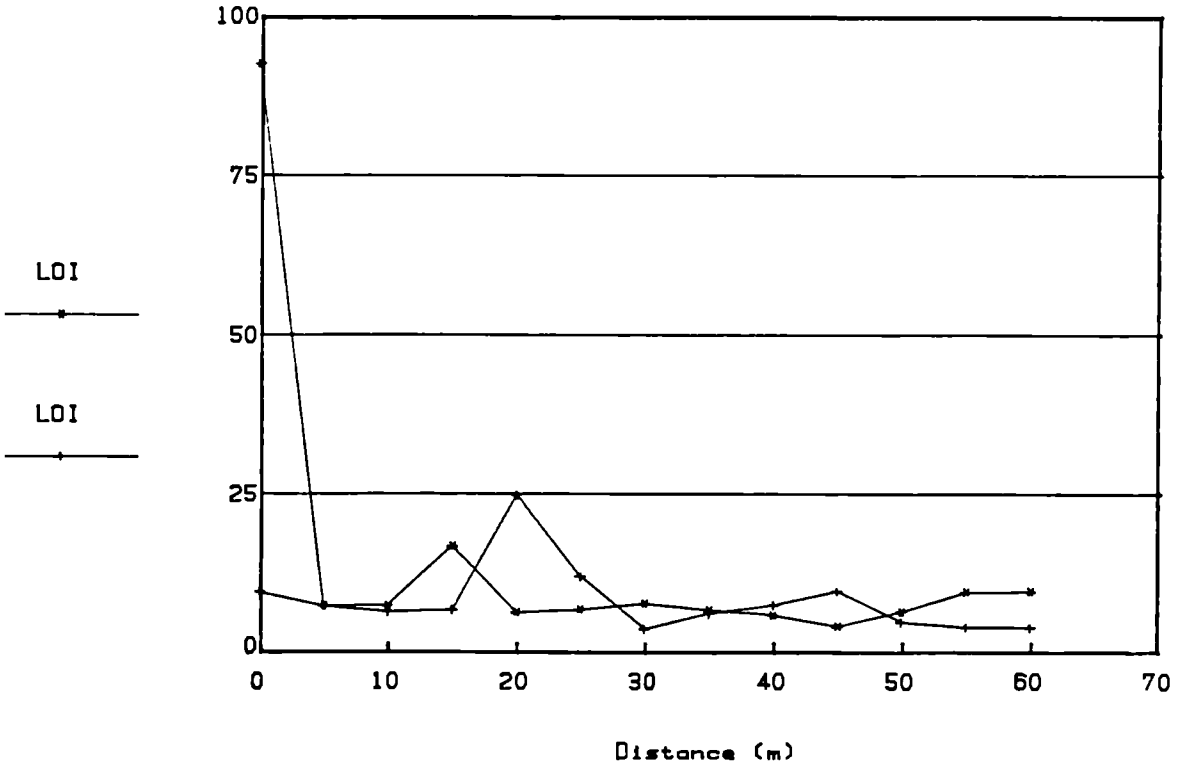

Fig.3.7.5. Broubster 1987 Traverse 2

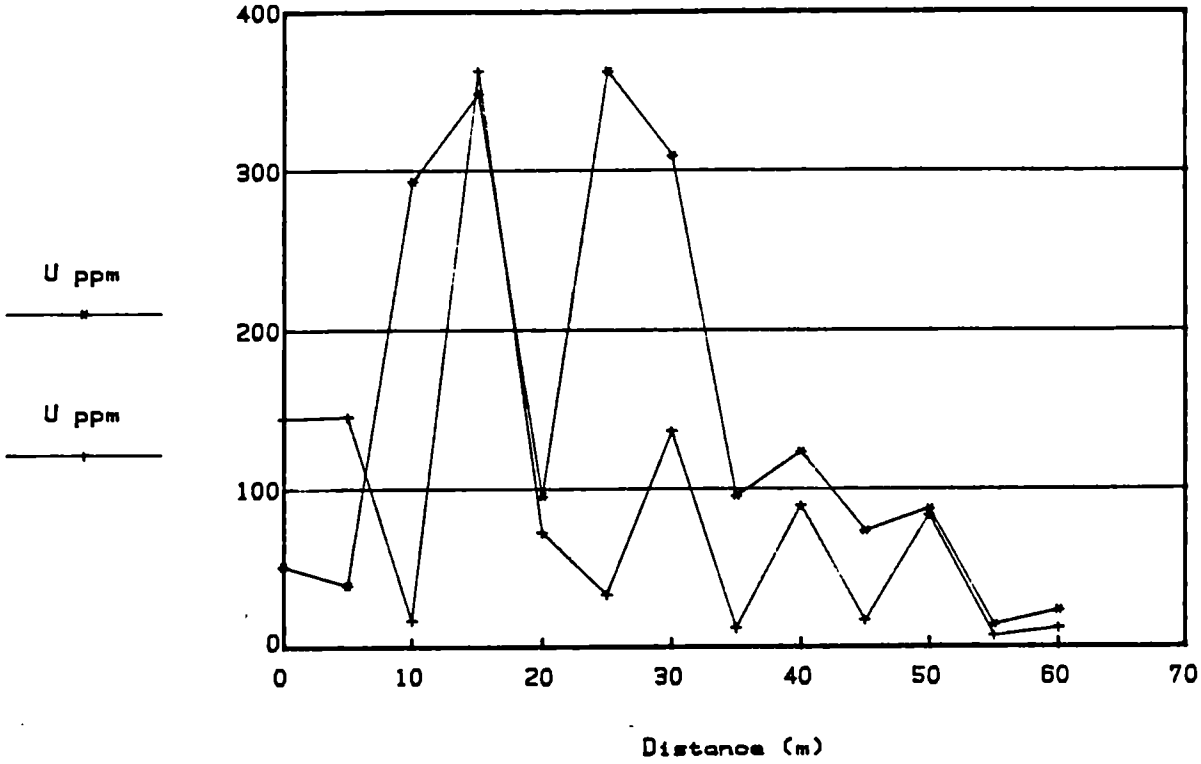

Fig.3.7.6. Broubster 1987 Traverse 2

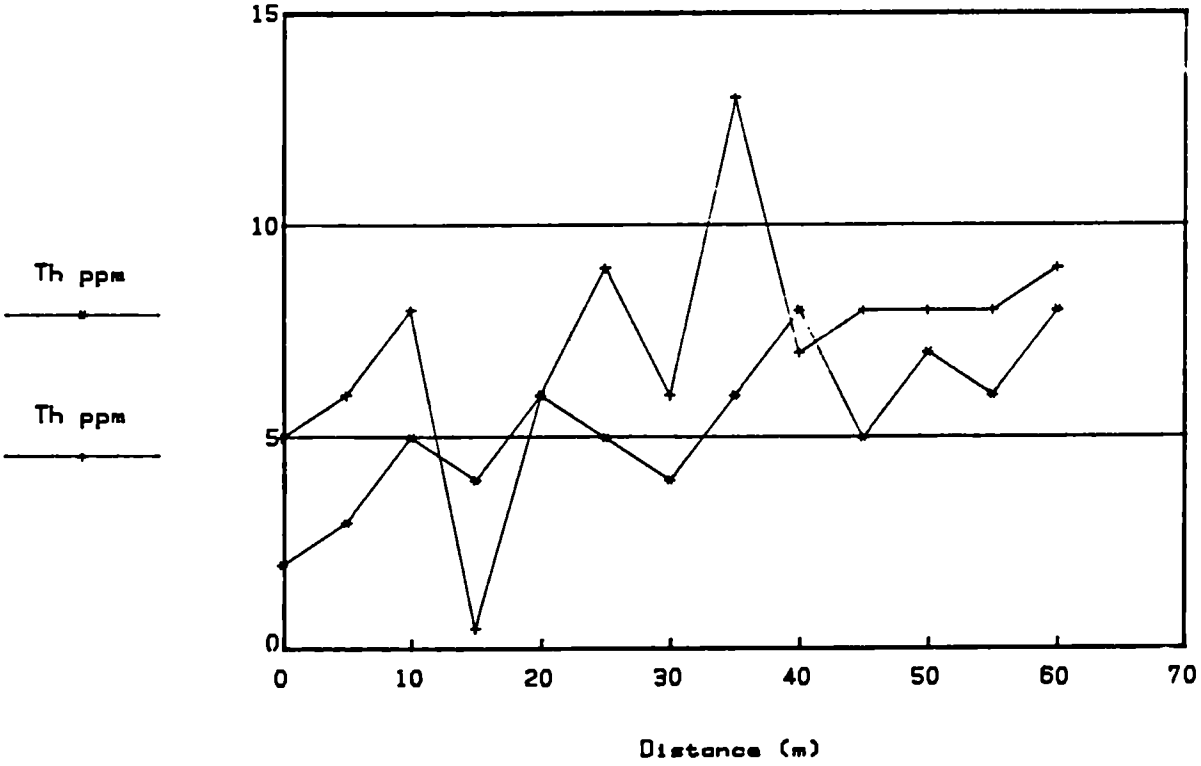

Fig.3.7.7. Broubster 1987 Traverse 2

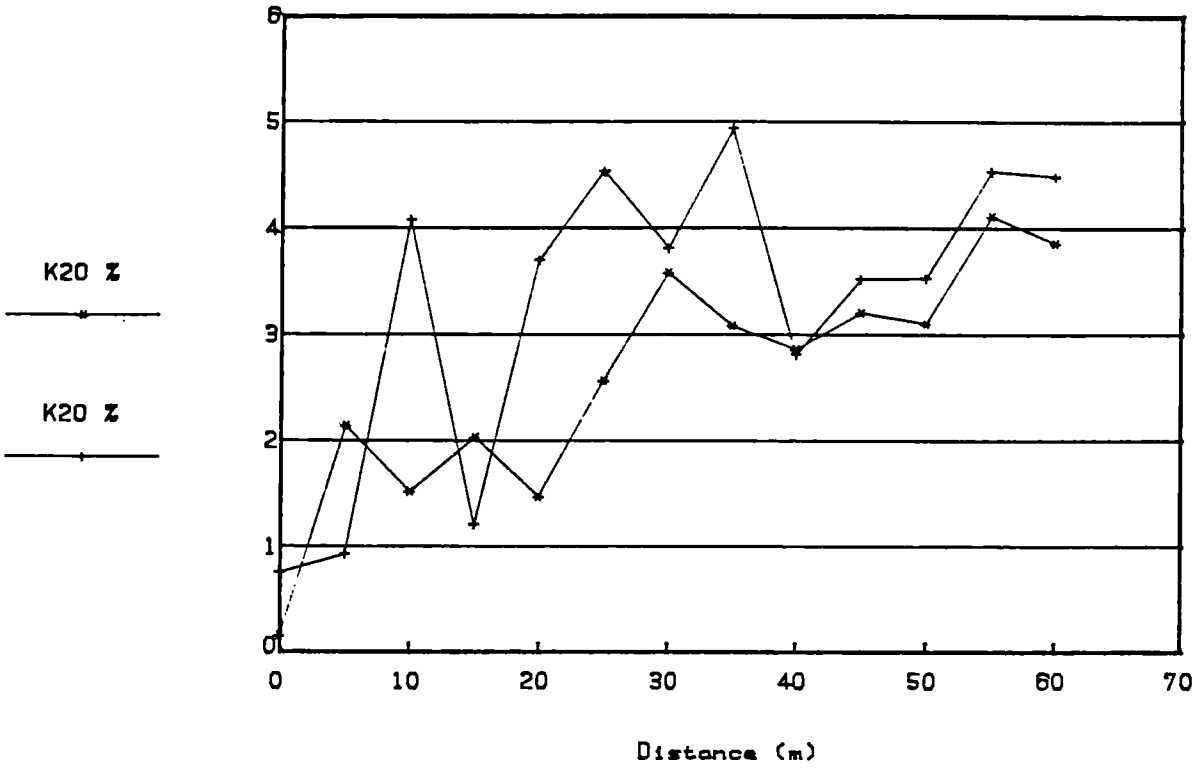

Fig.3.7.8. Broubster 1987 Traverse 2

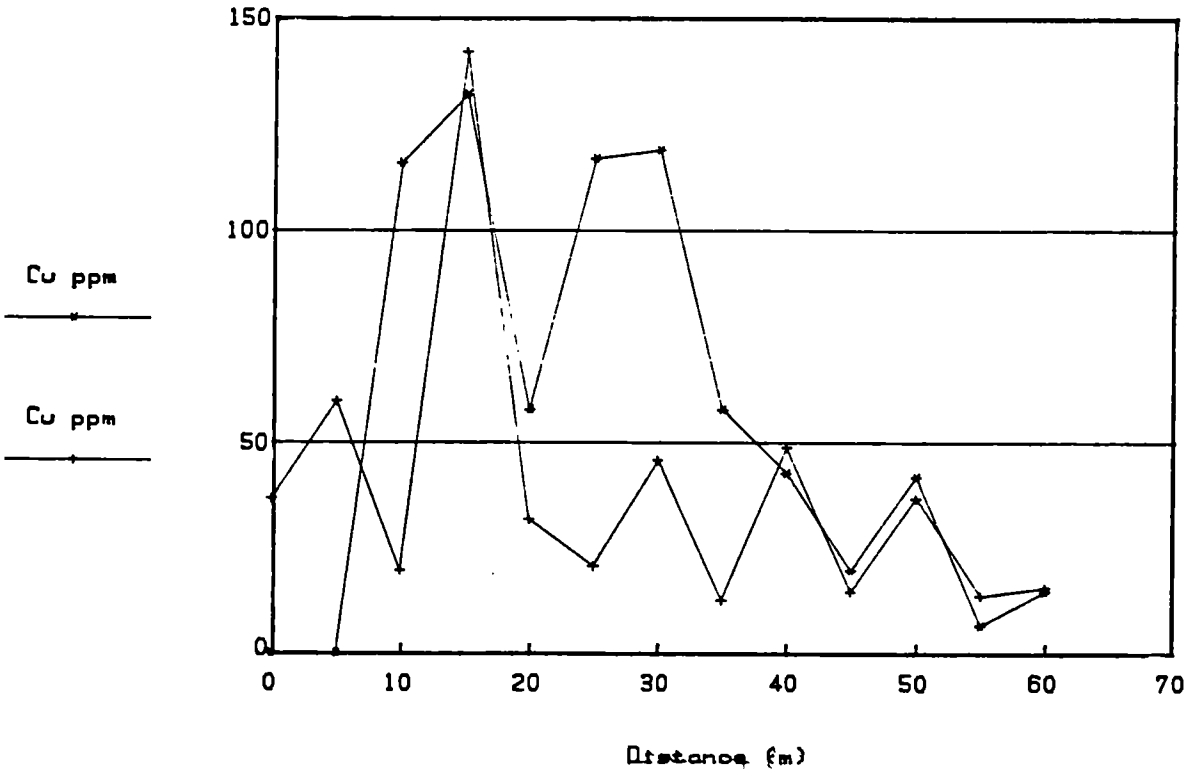

Fig.3.7.9. Broubster 1987 Traverse 2

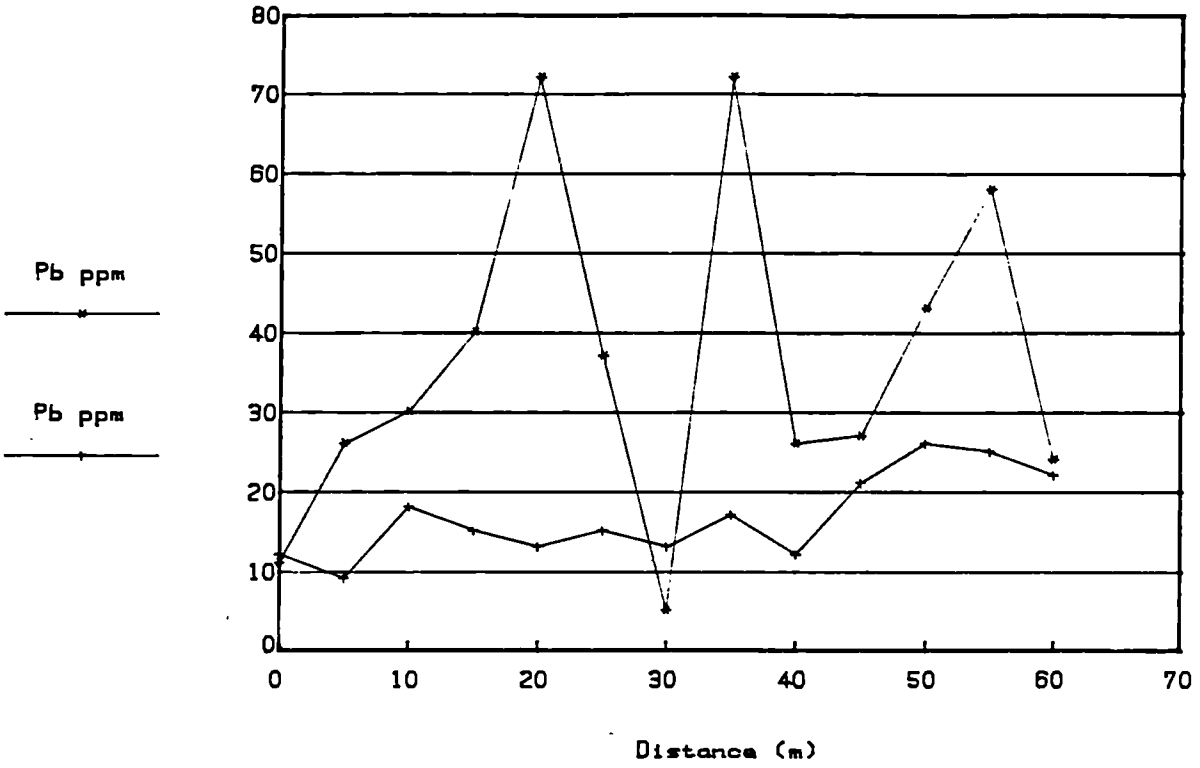

Fig.3.7.10 Broubster 1987 Traverse 2

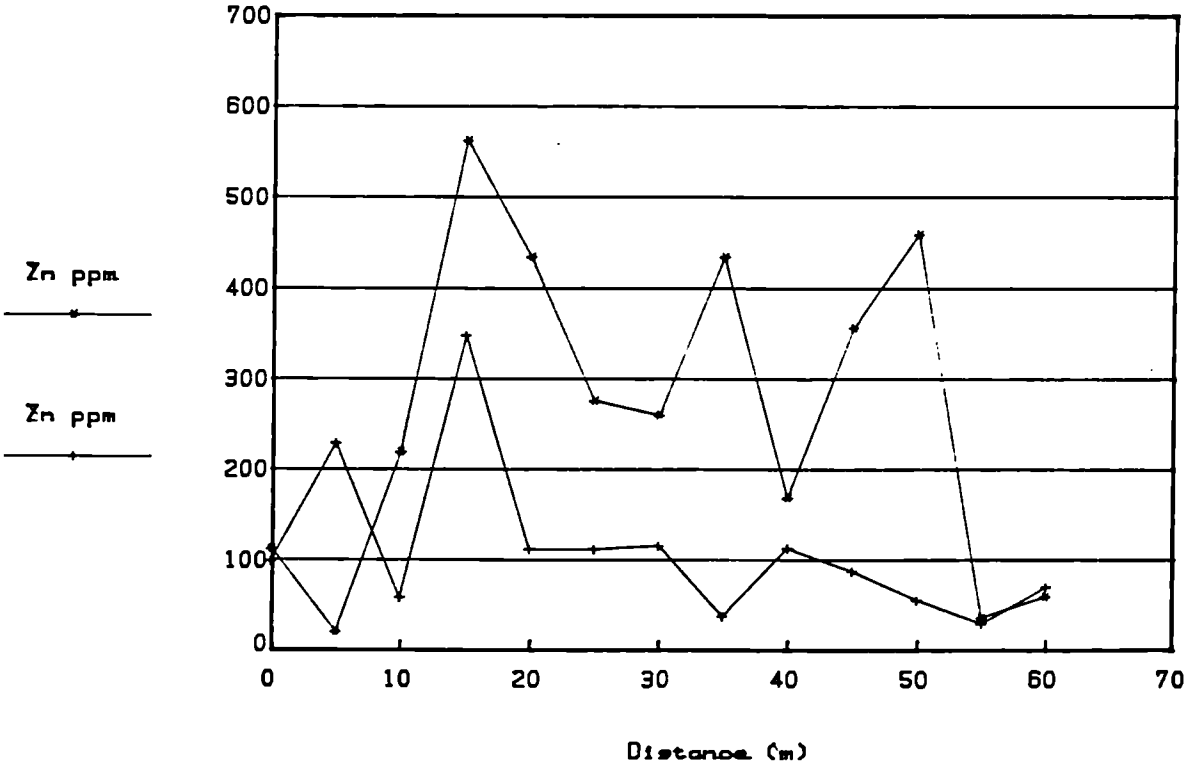

Fig.3.7.11.Broubster 1987 Traverse 2

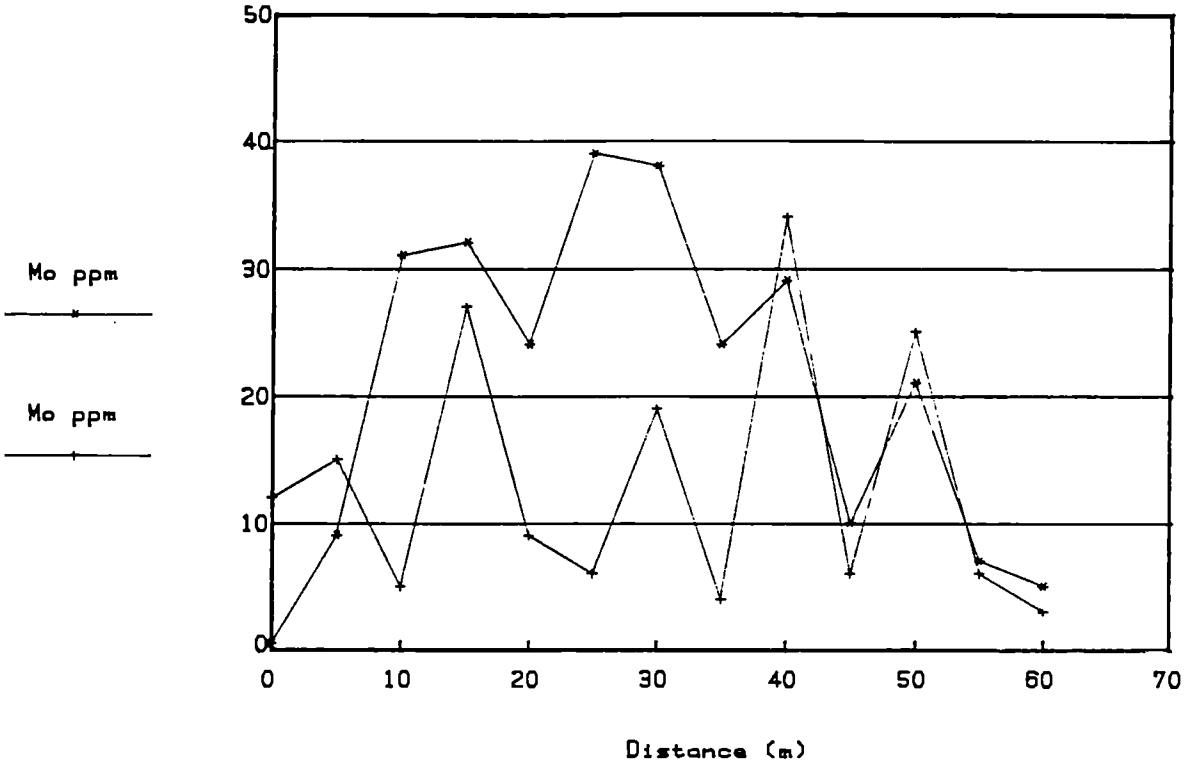

Fig.3.7.12.Broubster 1987 Traverse 2

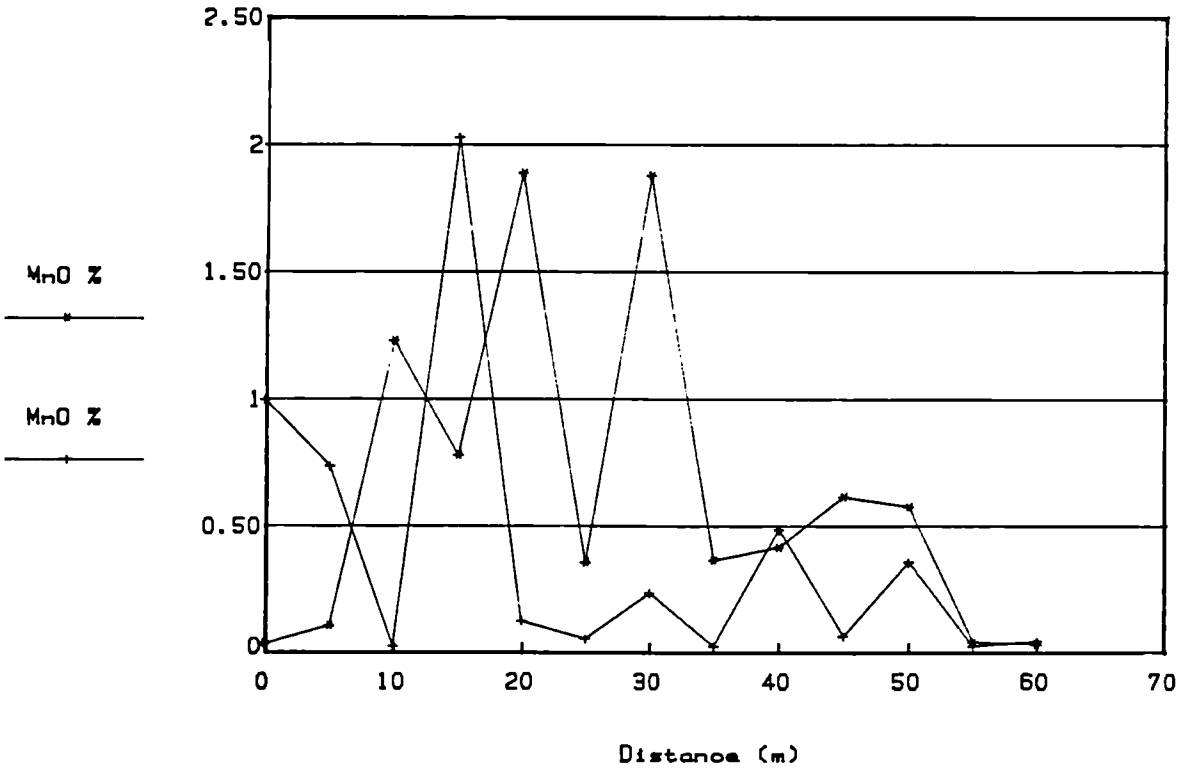

Fig.3.7.13.Broubster 1987 Traverse 2

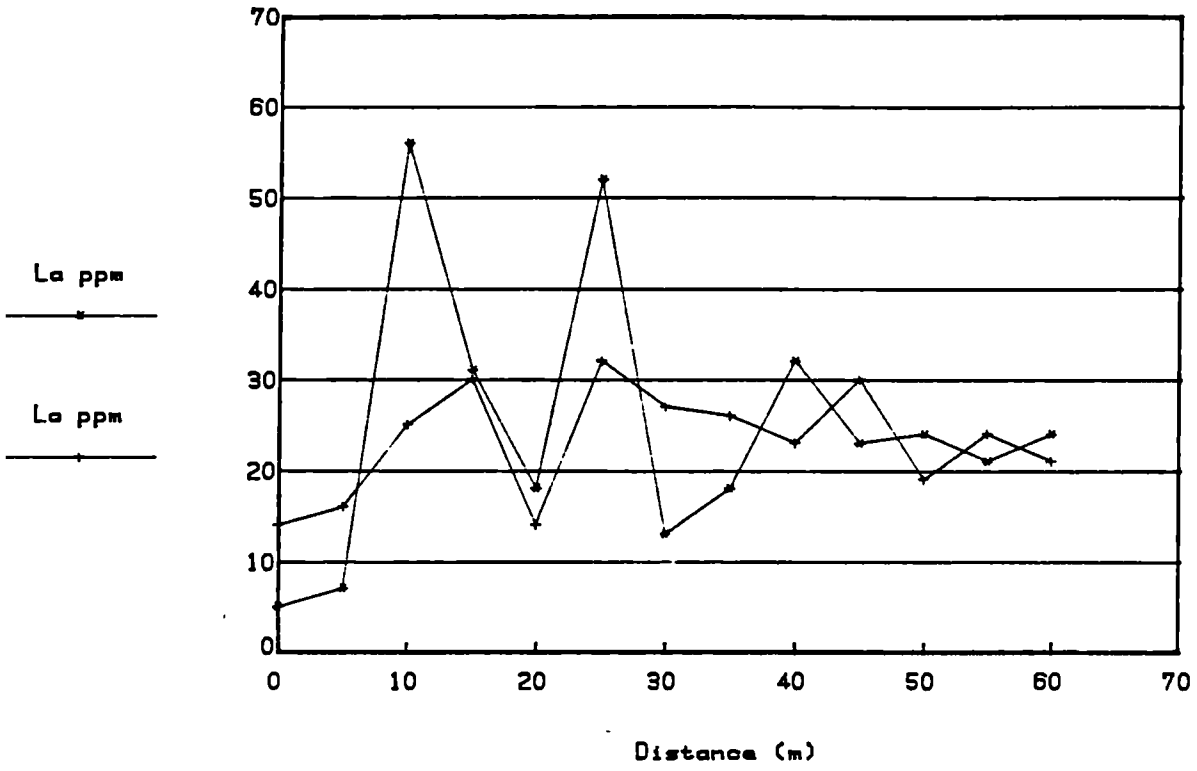

Fig.3.7.14.Broubster 1987 Traverse 2

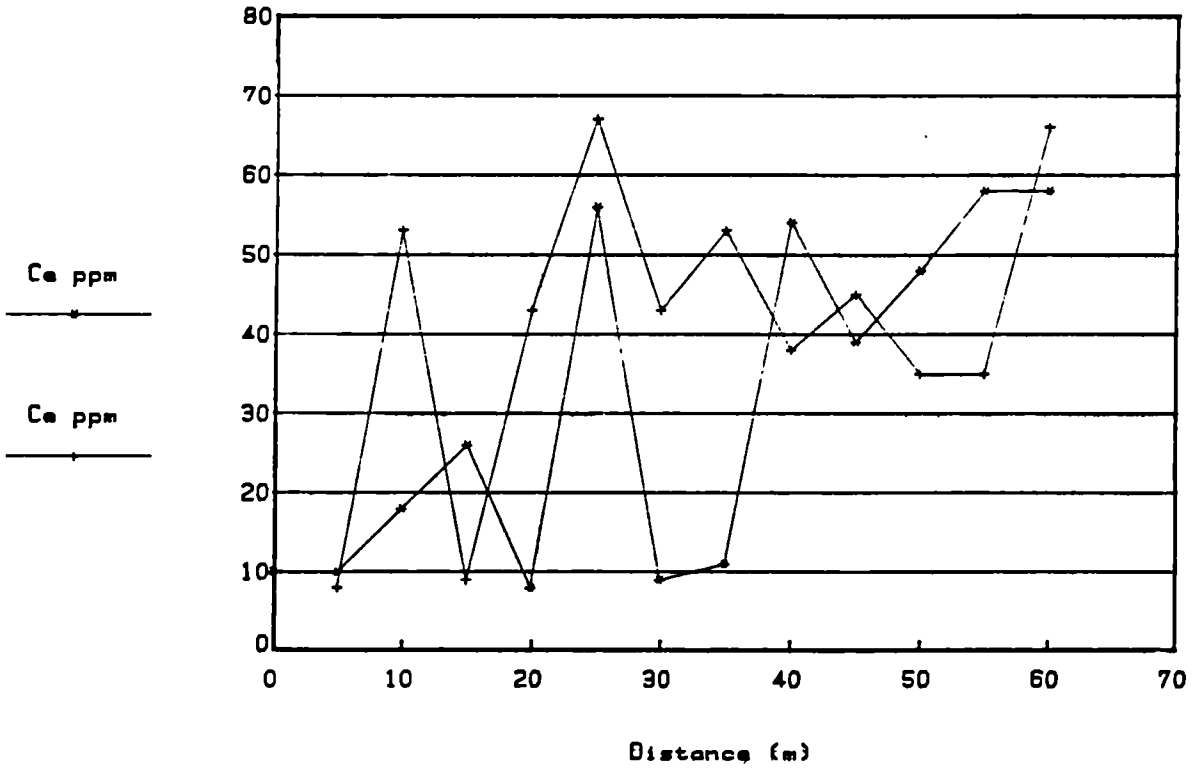

Fig.3.7.15.Broubster 1987 Traverse 2

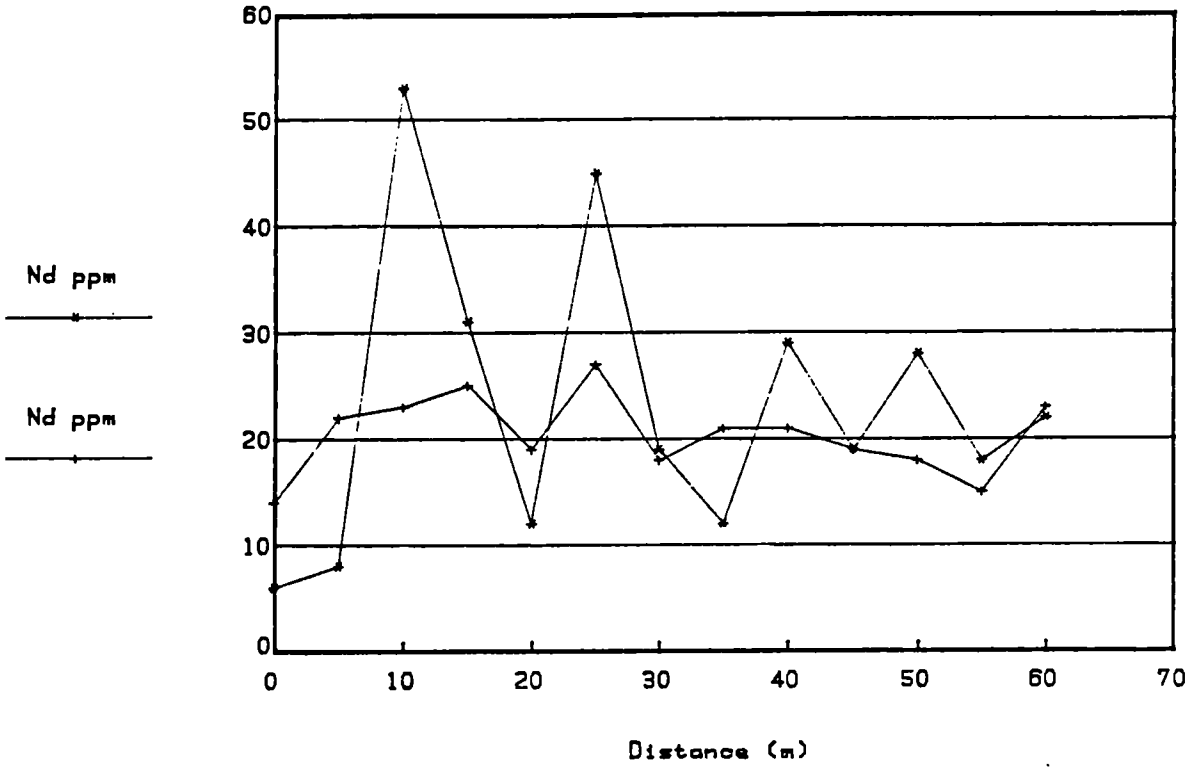

Fig.3.7.16.Broubster 1987 Traverse 2

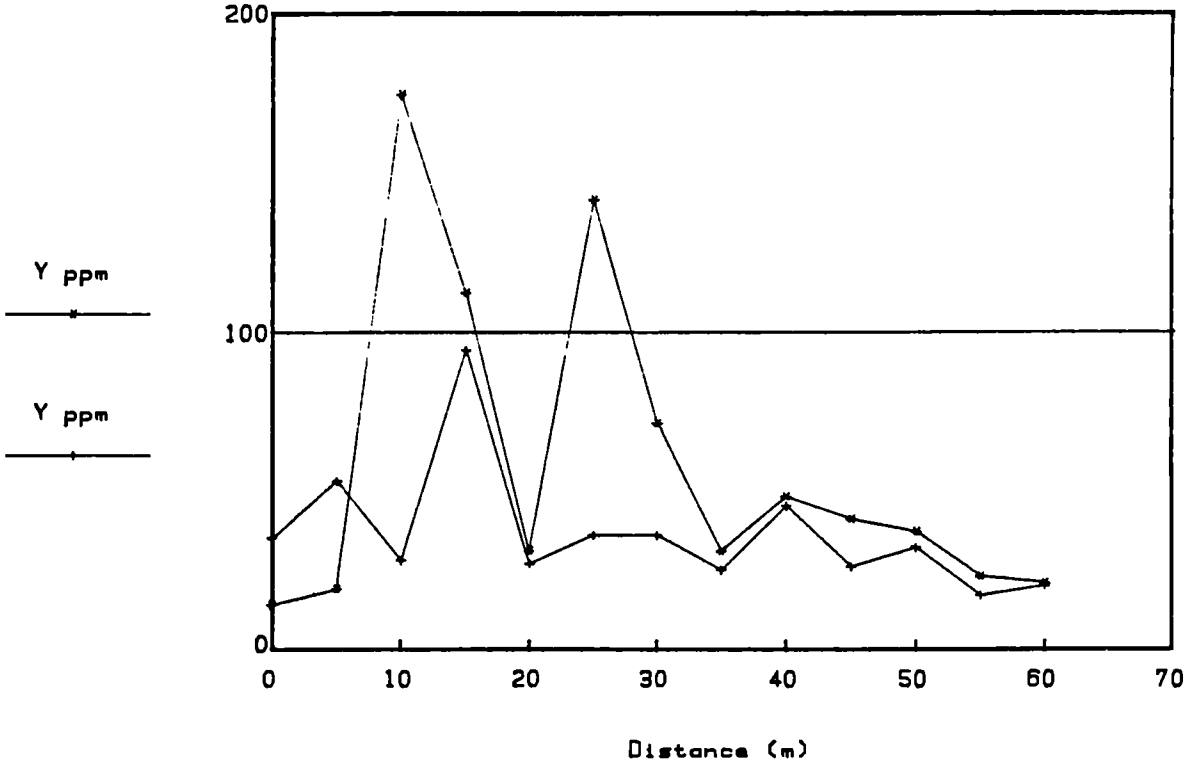

Fig.3.7.17.Broubster 1987 Traverse 2

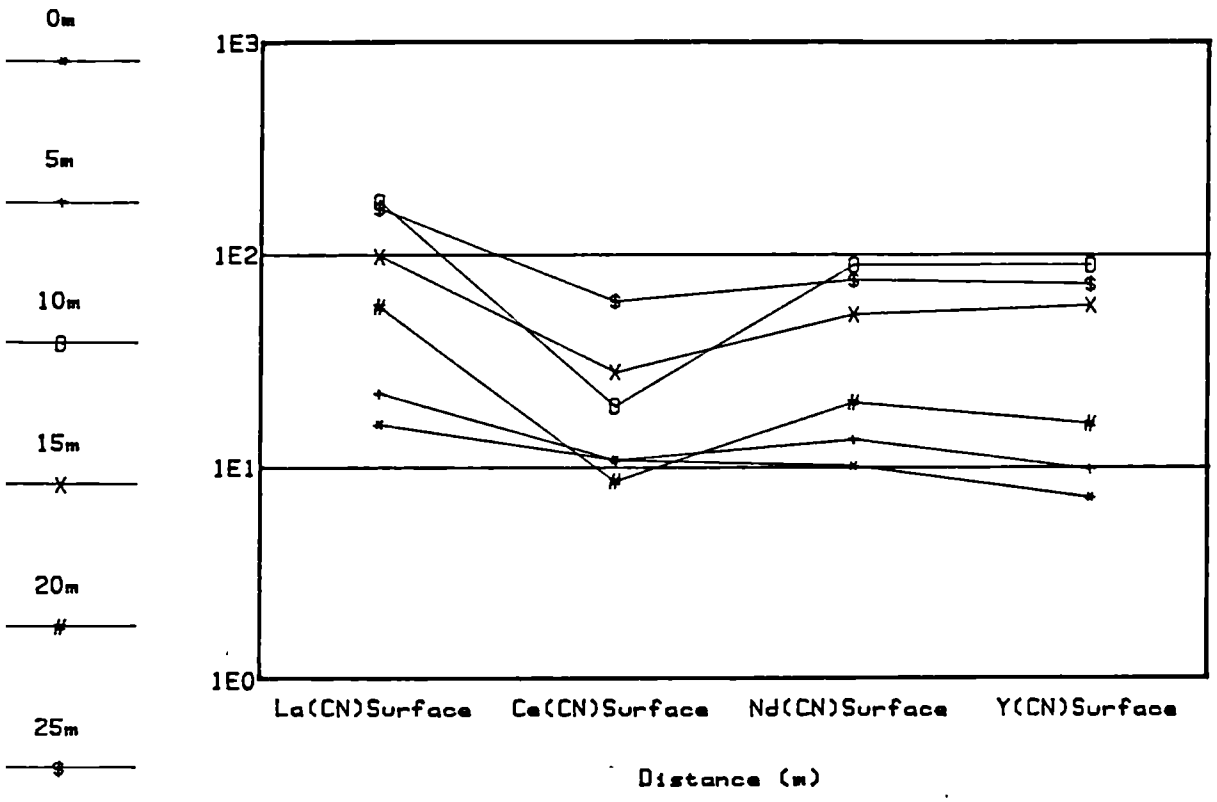

Fig.3.7.18.Broubster 1987 Traverse 2

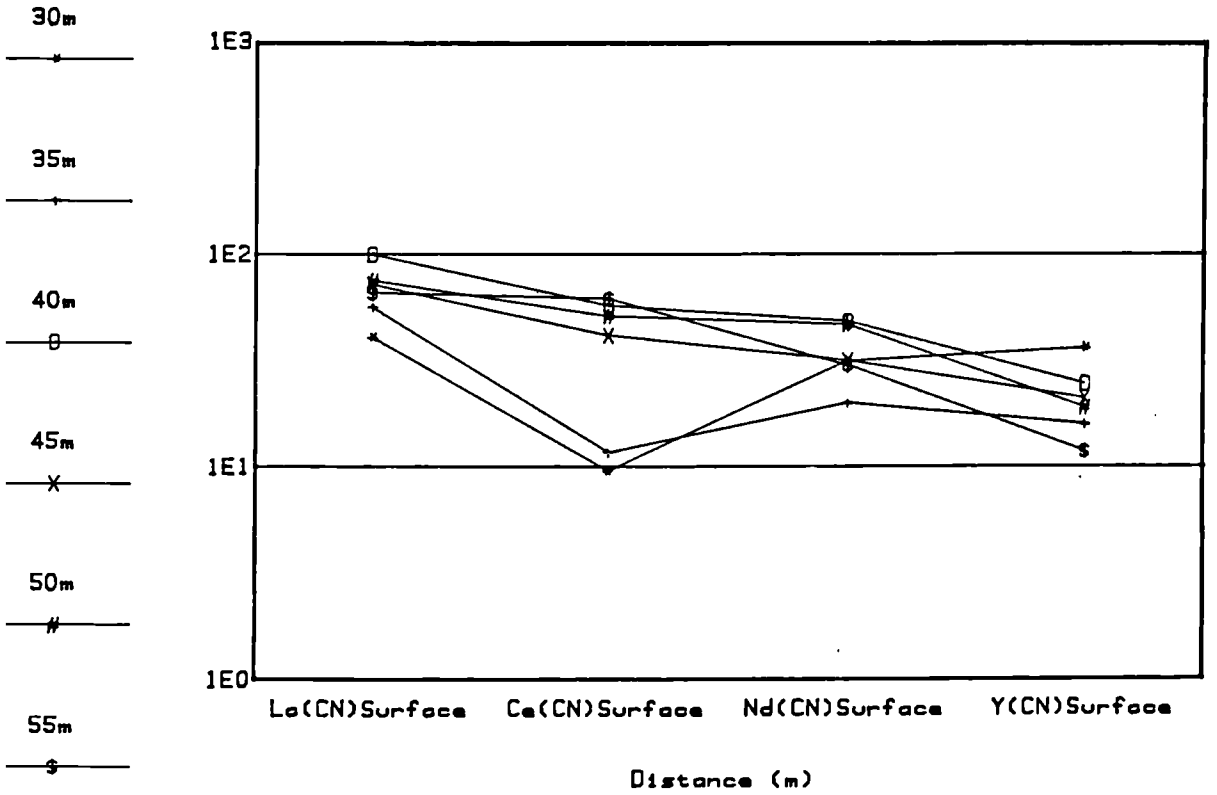

Fig.3.7.19.Broubster 1987 Traverse 2

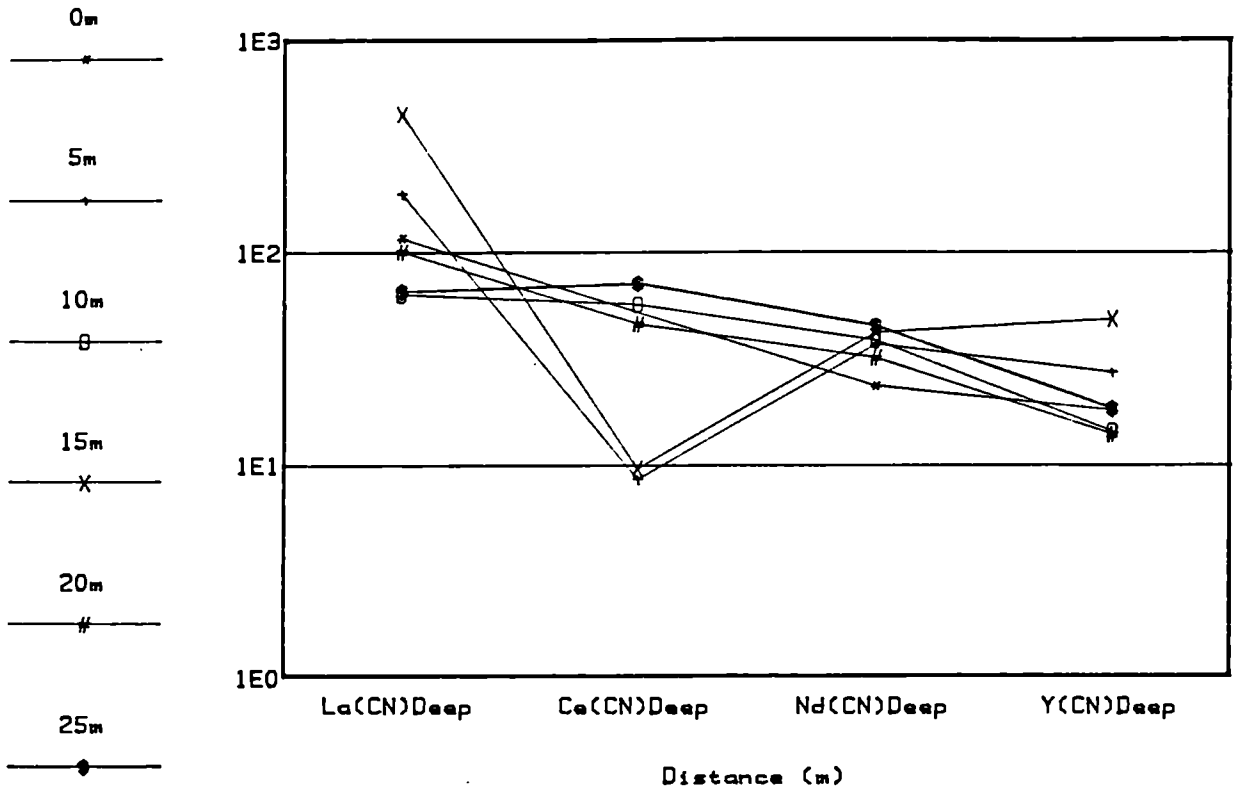

Fig.3.7.20.Broubster 1987 Traverse 2

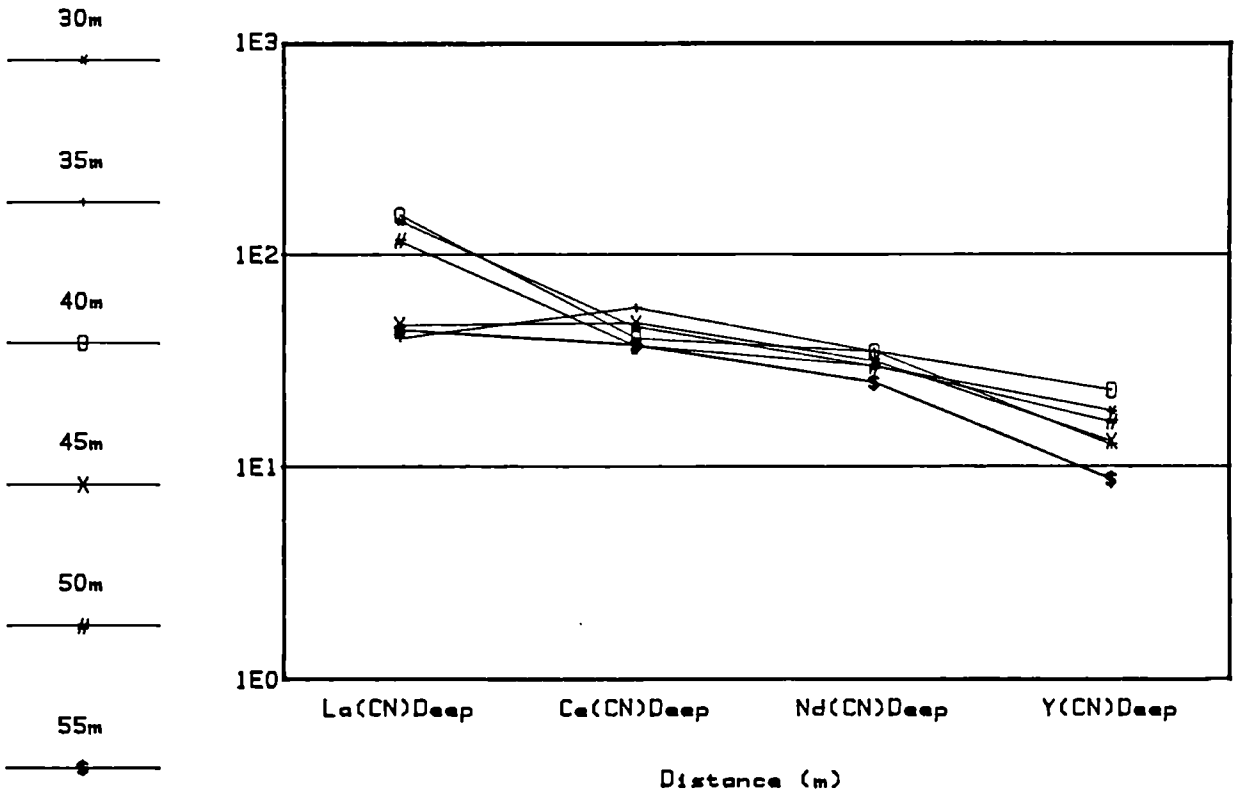

Fig.3.8.1. Broubster 1987 Traverse 3

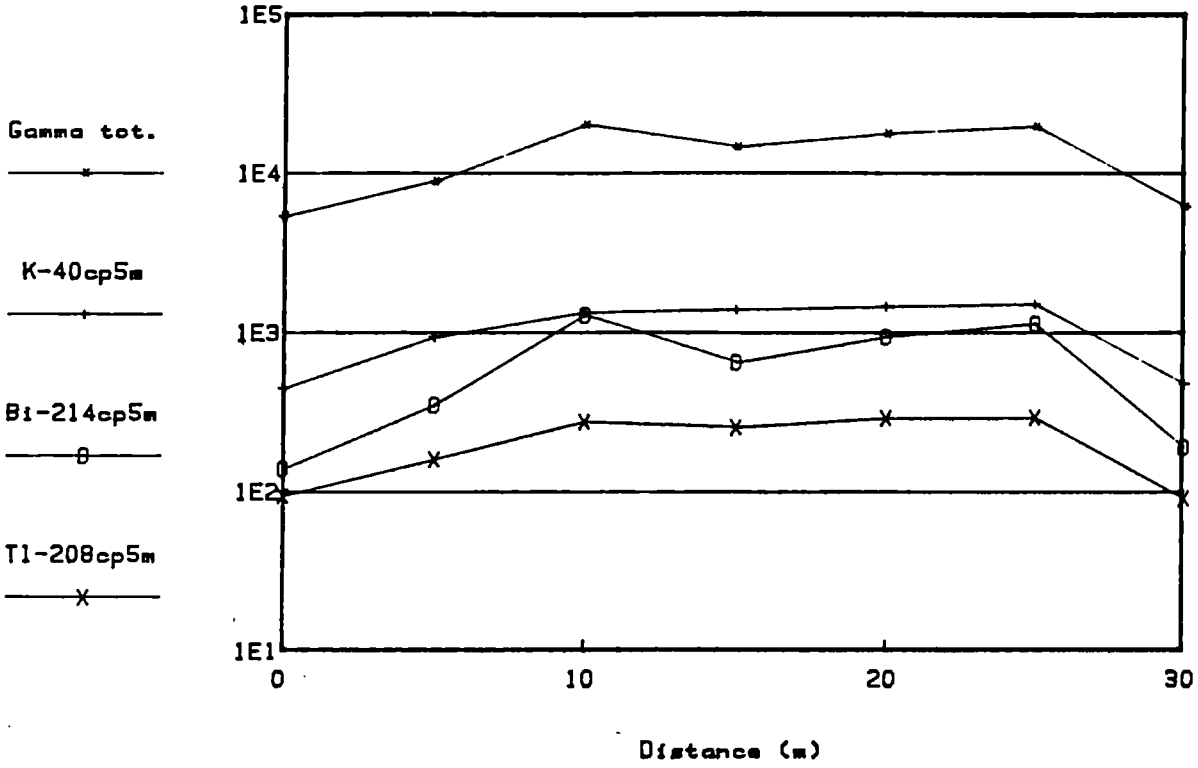

Fig.3.8.2. Broubster 1987 Traverse 3

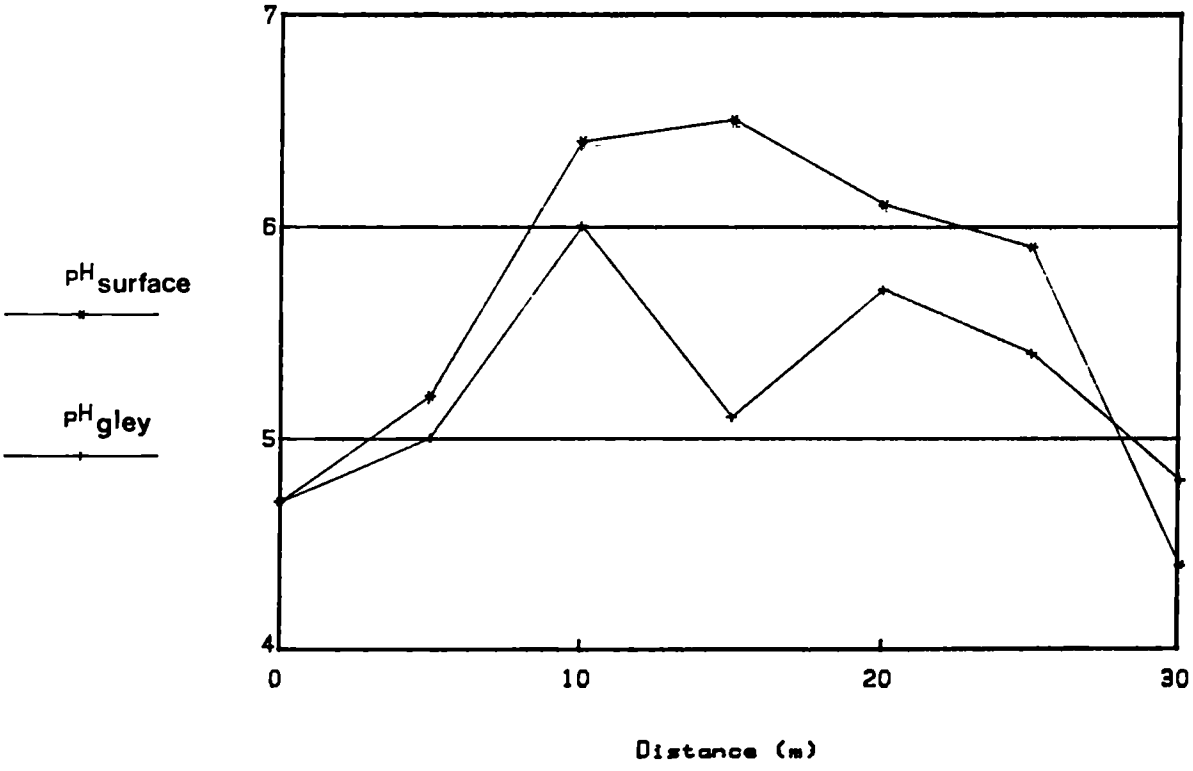

Fig.3.8.3. Broubster 1987 Traverse 3

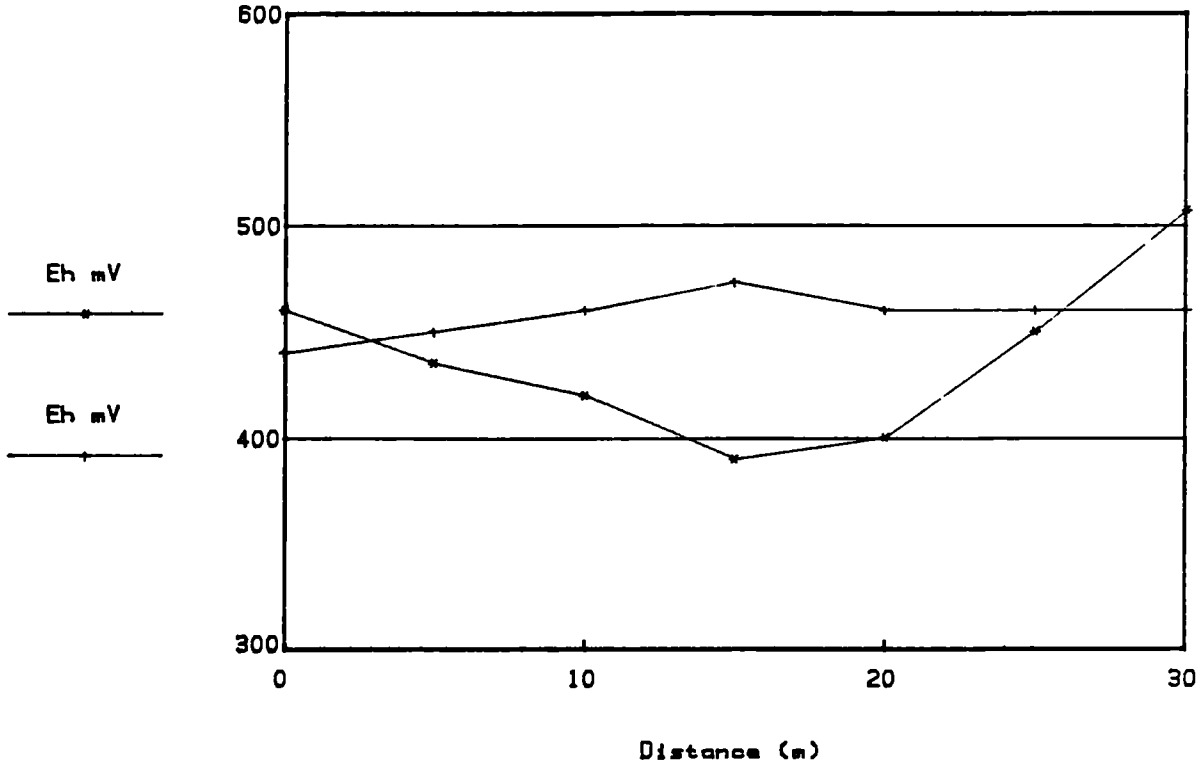

Fig.3.8.4. Broubster 1987 Traverse 3

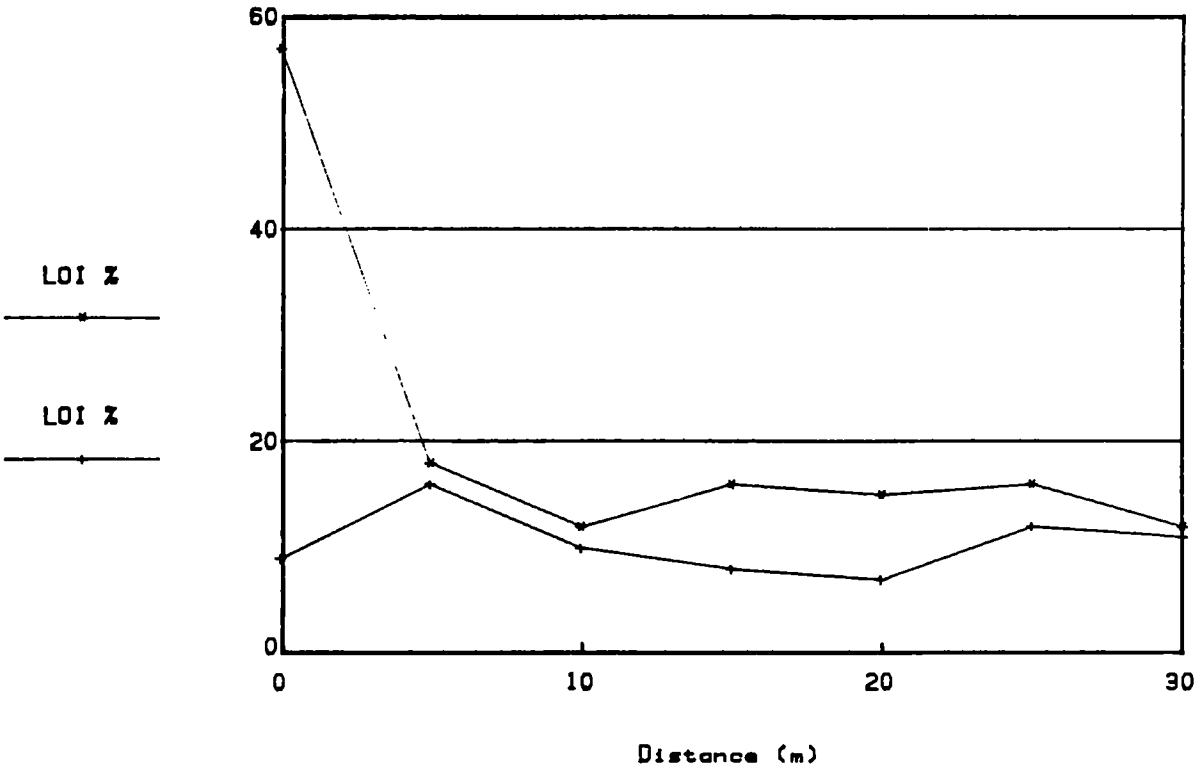

Fig.3.8.5. Broubster 1987 Traverse 3

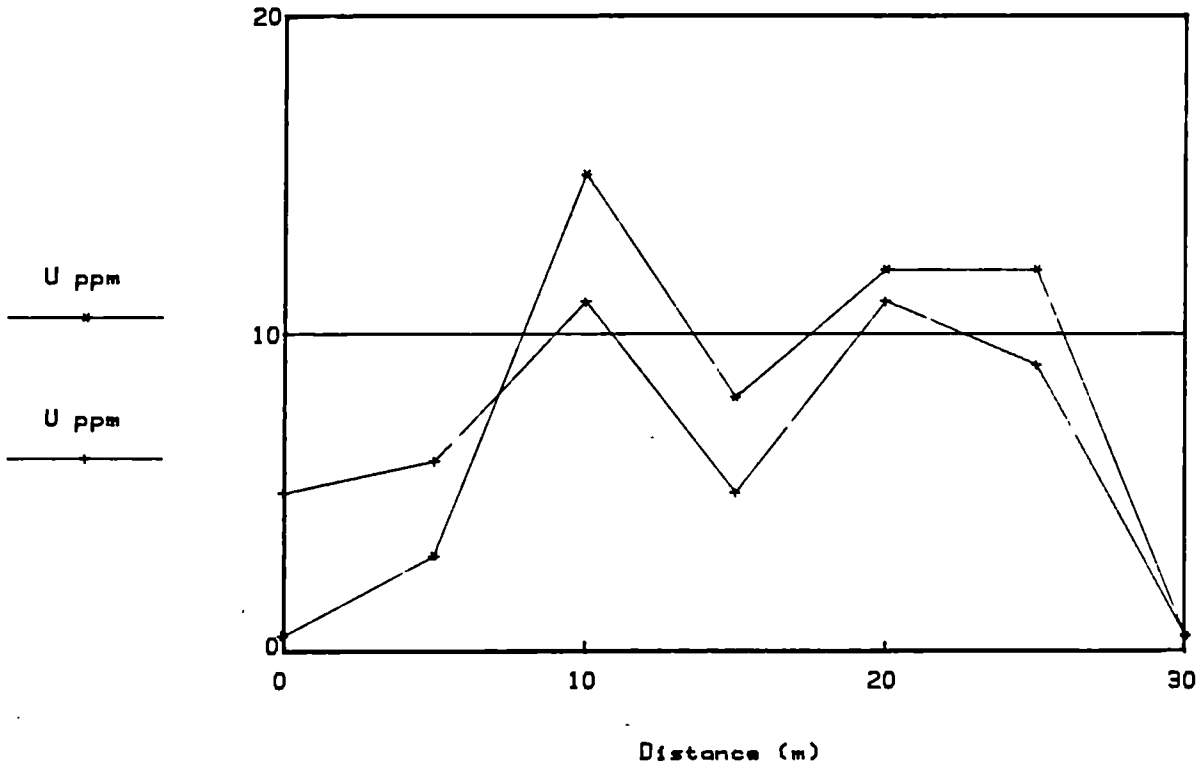

Fig.3.8.6. Broubster 1987 Traverse 3

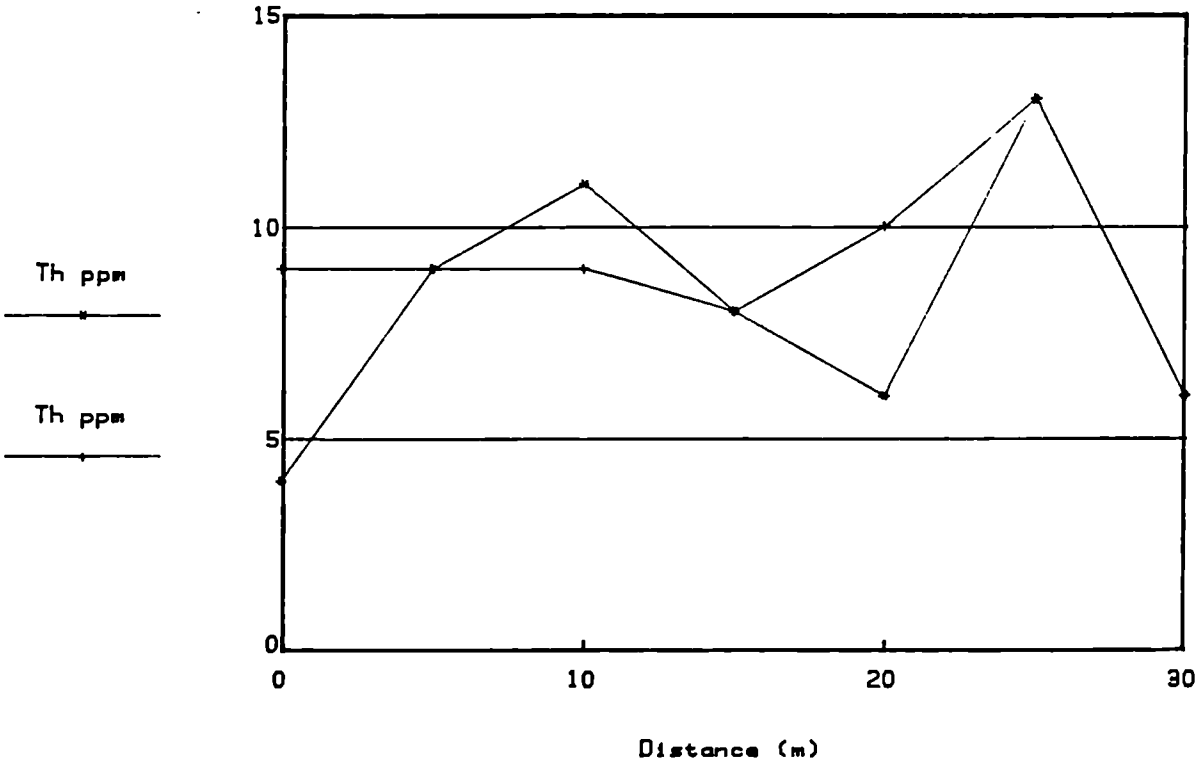

Fig.3.8.7. Broubster 1987 Traverse 3

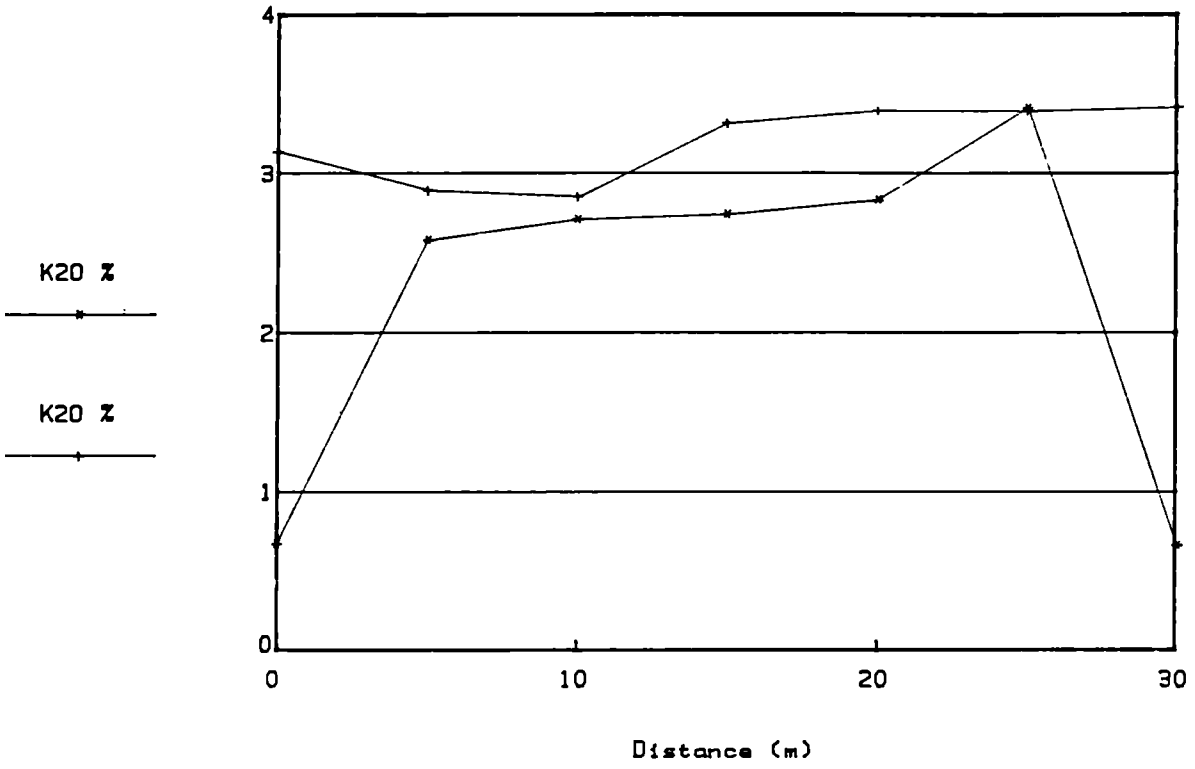

Fig.3.8.8. Broubster 1987 Traverse 3

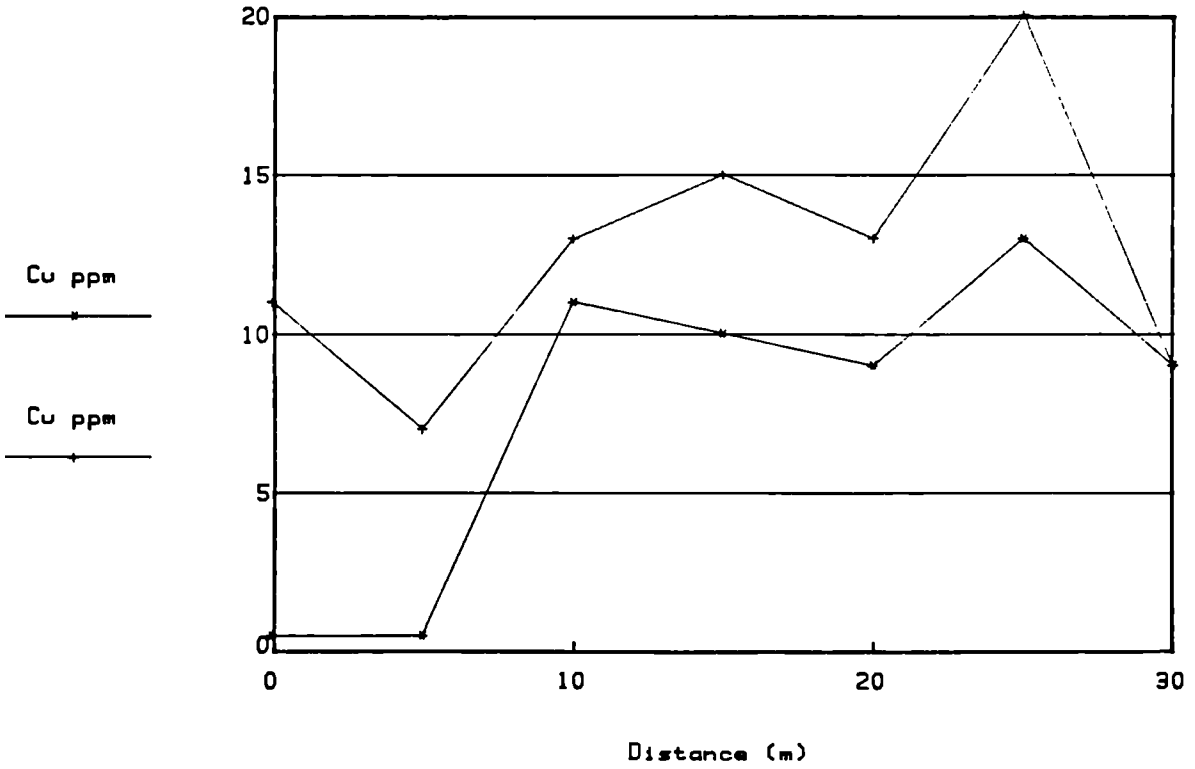

Fig.3.8.9. Broubster 1987 Traverse 3

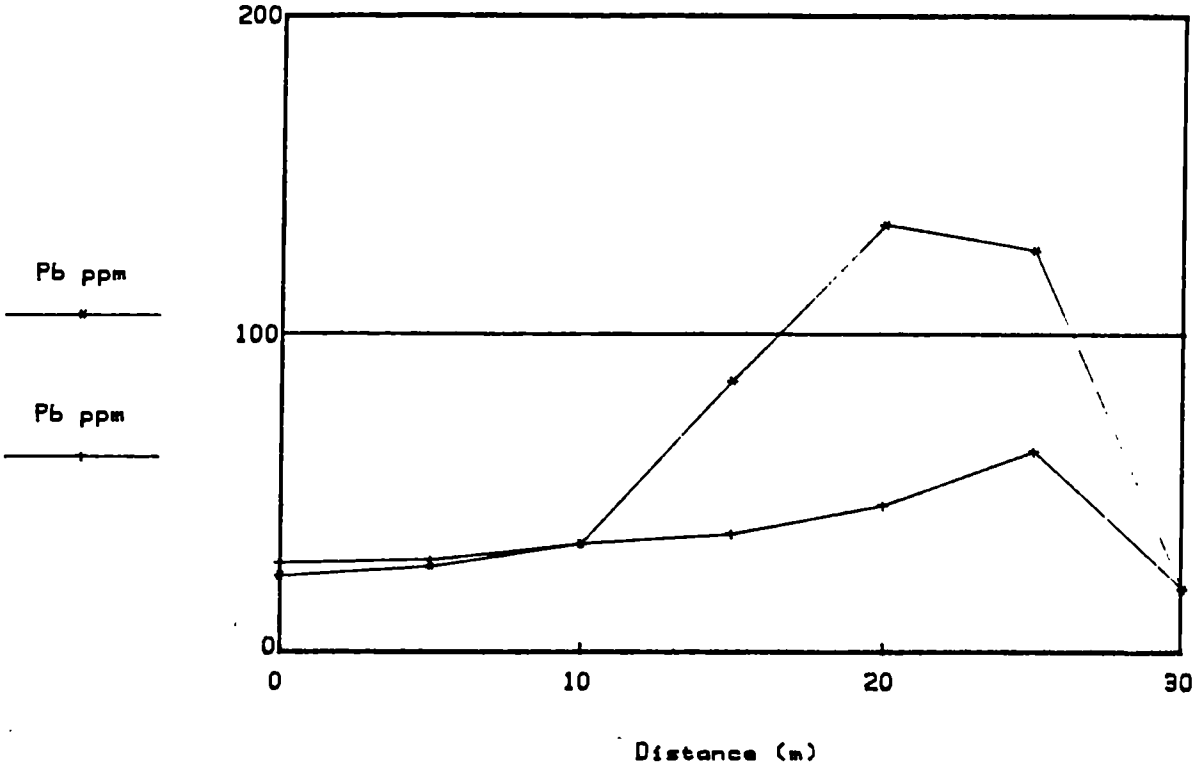

Fig.3.8.10.Broubster 1987 Traverse 3

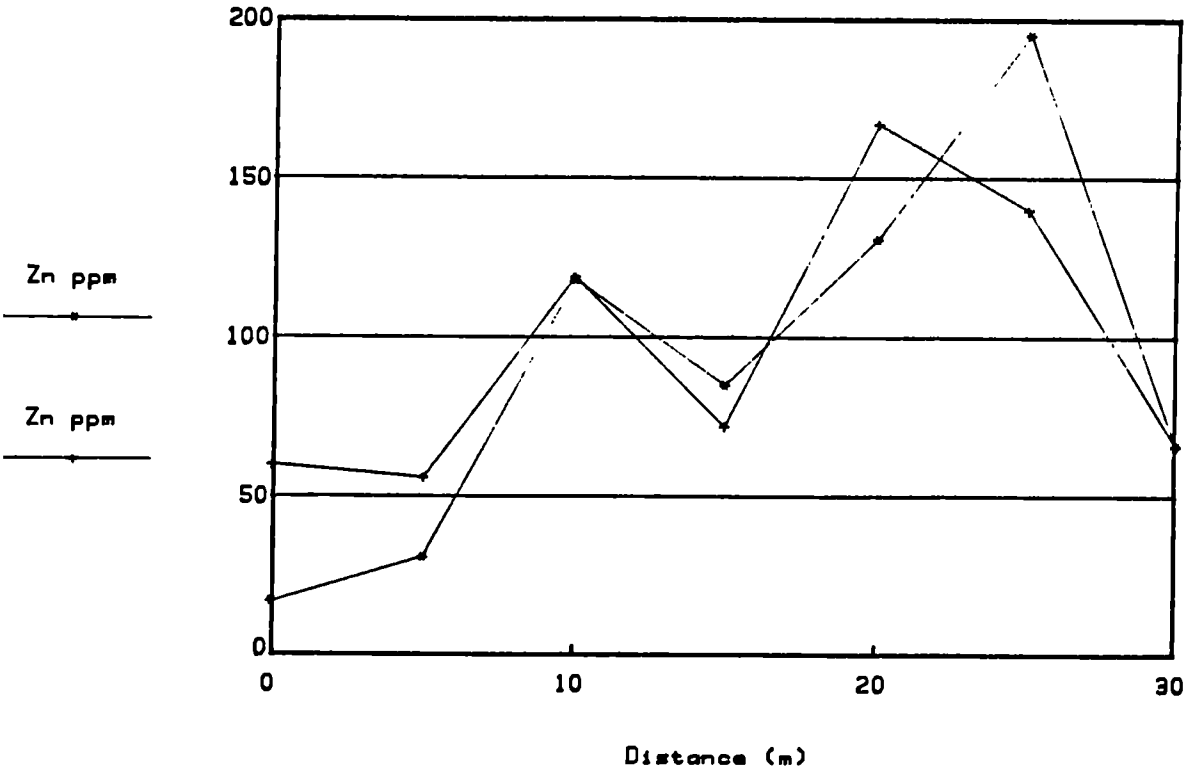

Fig.3.8.11.Broubster 1987 Traverse 3

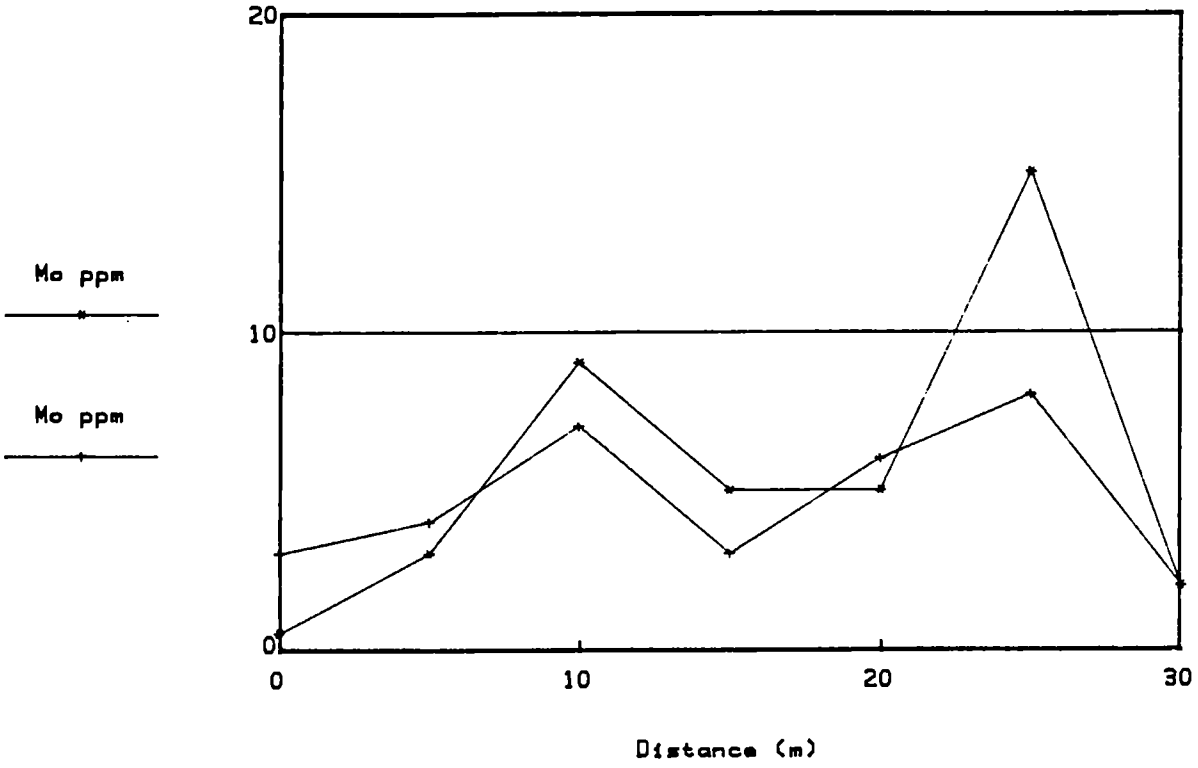

Fig.3.8.12.Broubster 1987 Traverse 3

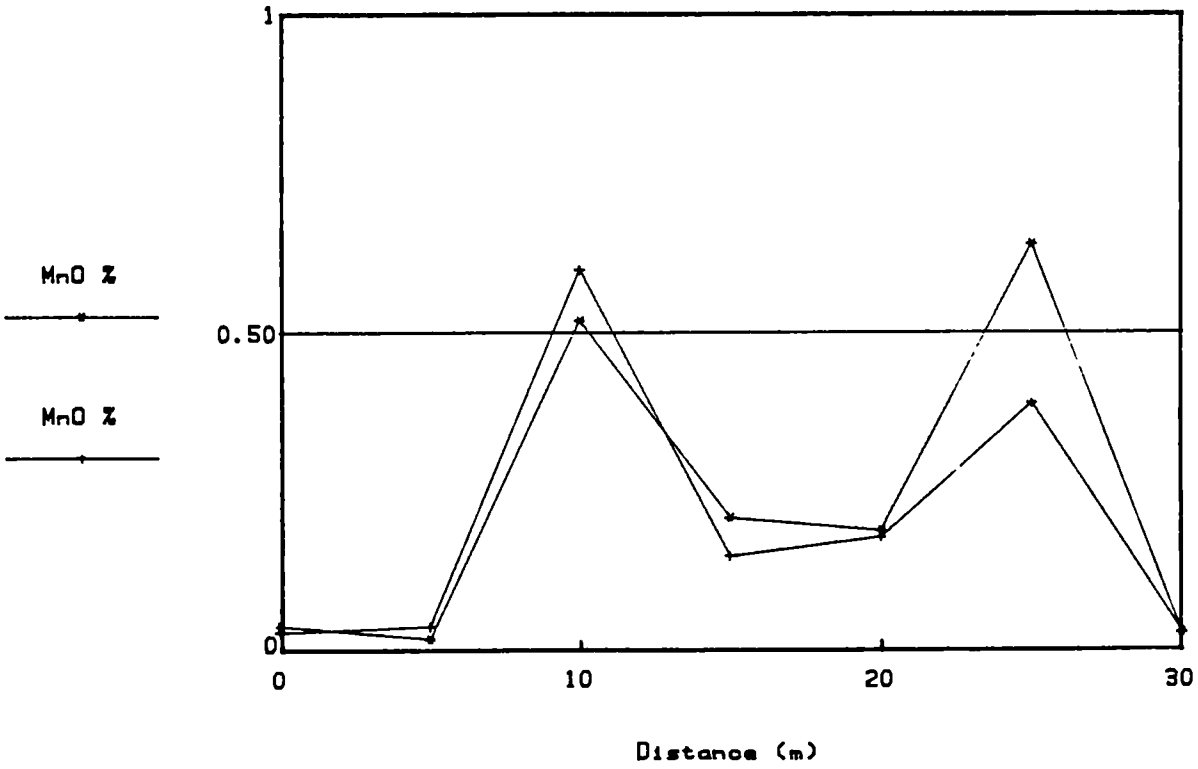

Fig.3.8.13.Broubster 1987 Traverse 3

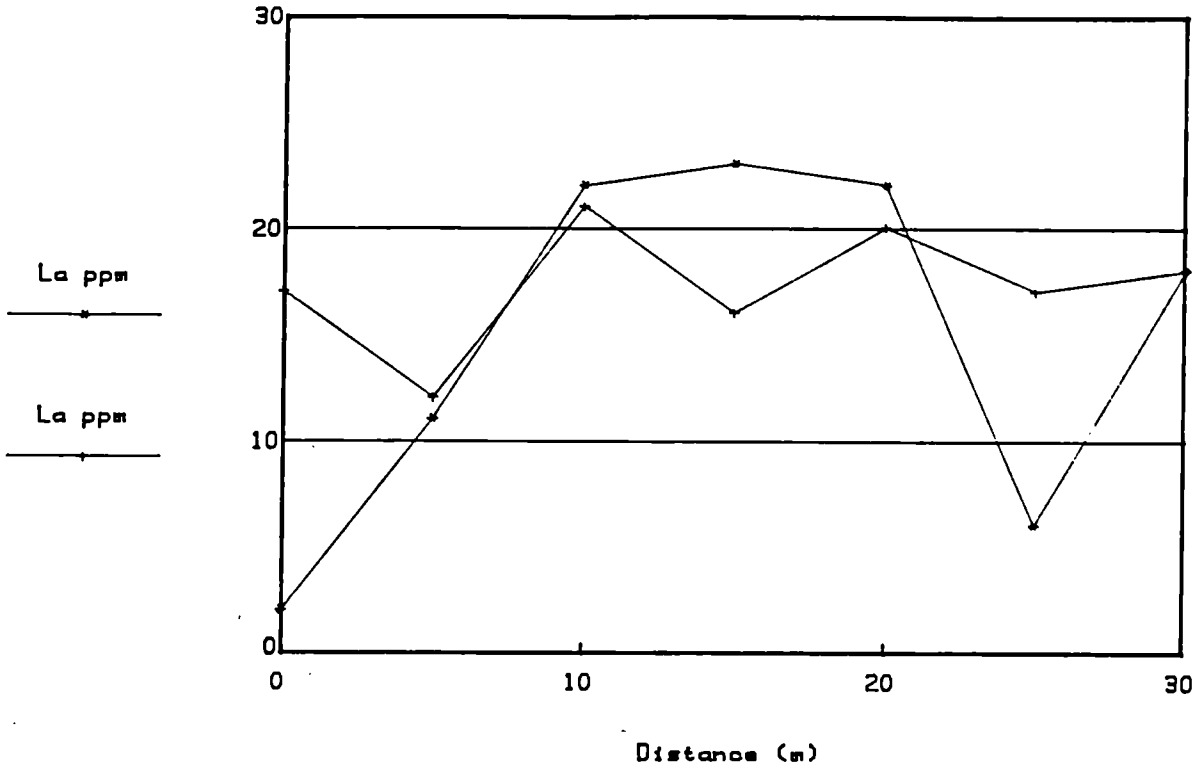

Fig.3.8.14.Broubster 1987 Traverse 3

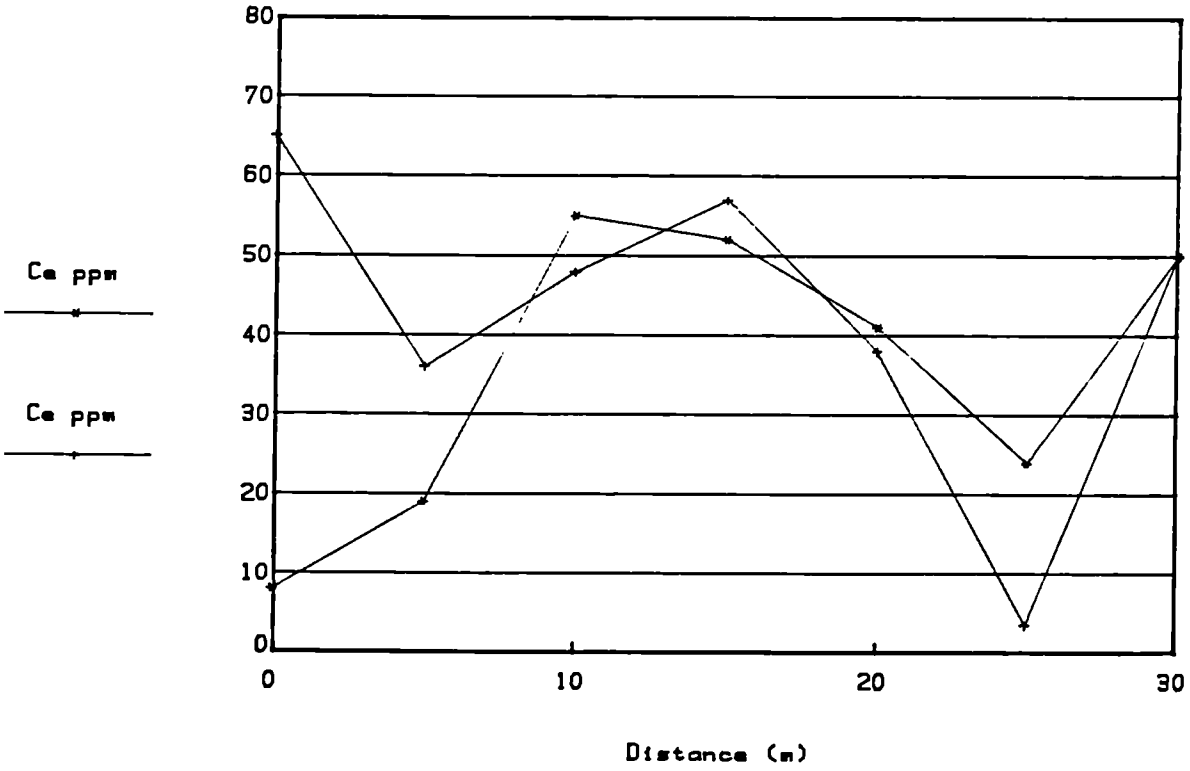

Fig.3.8.15.Broubster 1987 Traverse 3

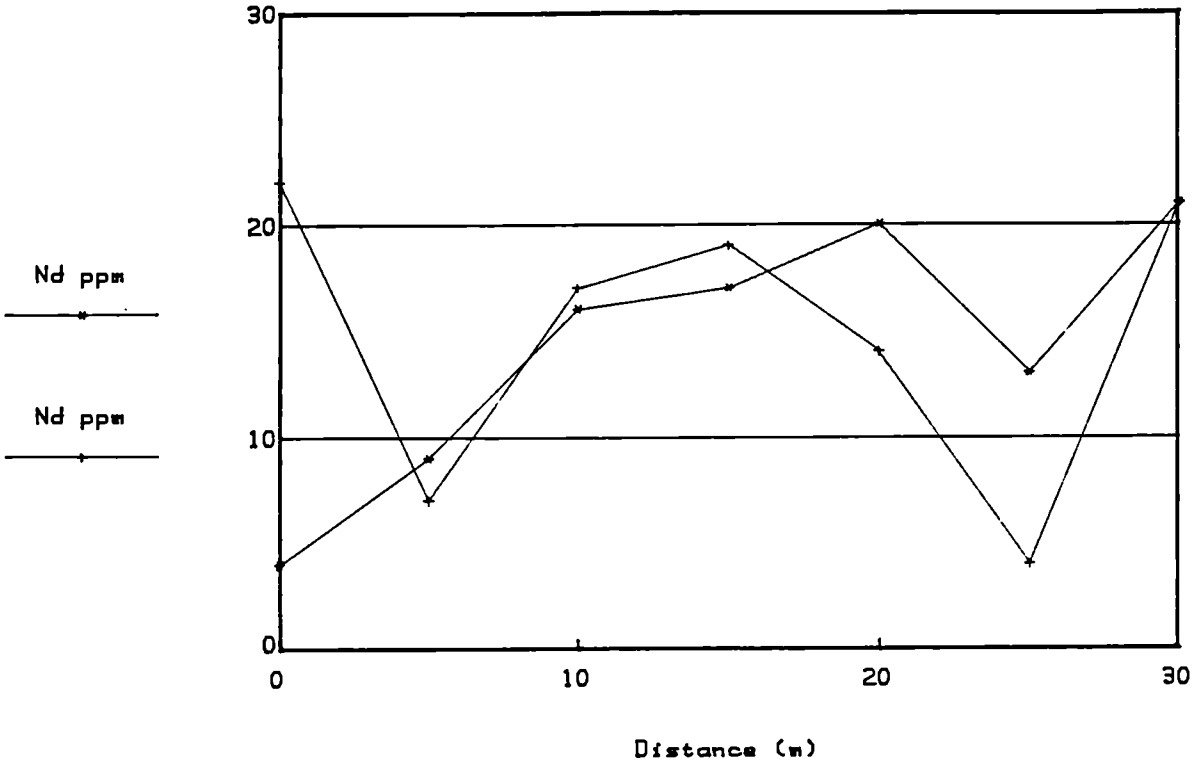

Fig.3.8.16.Broubster 1987 Traverse 3

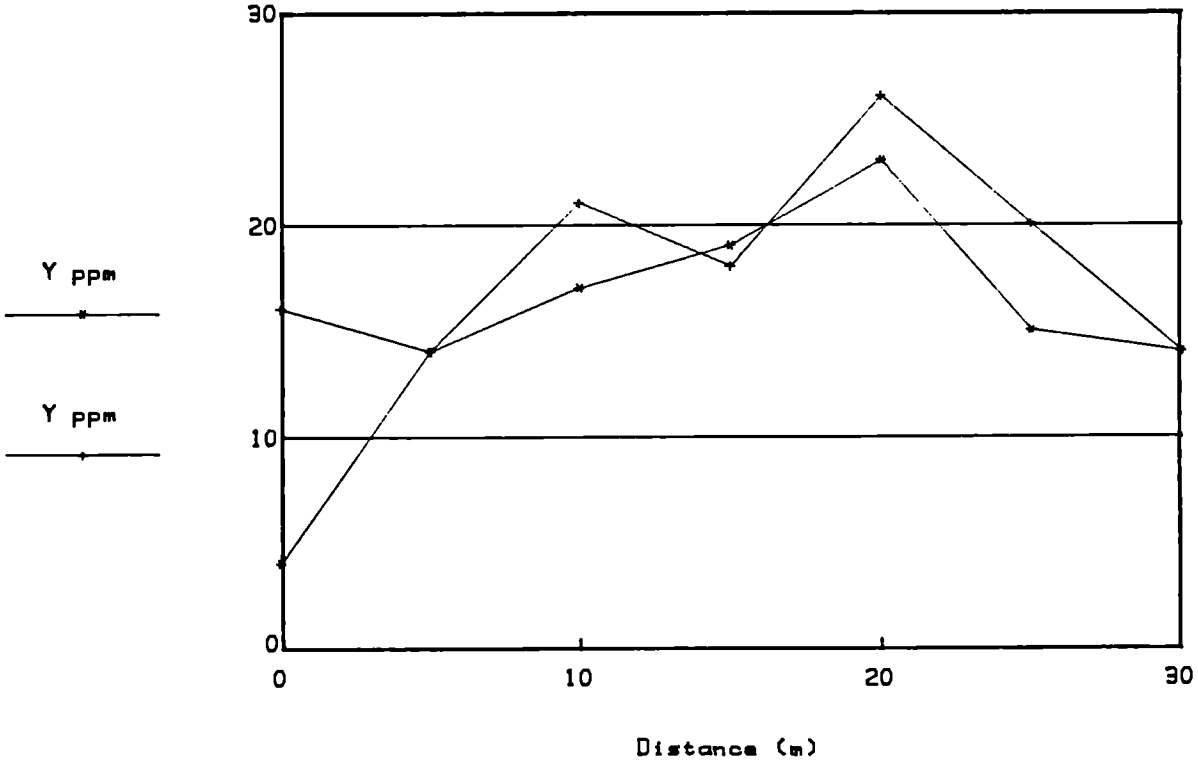

Fig.3.8.17.1987 Traverse 3 REE Surface

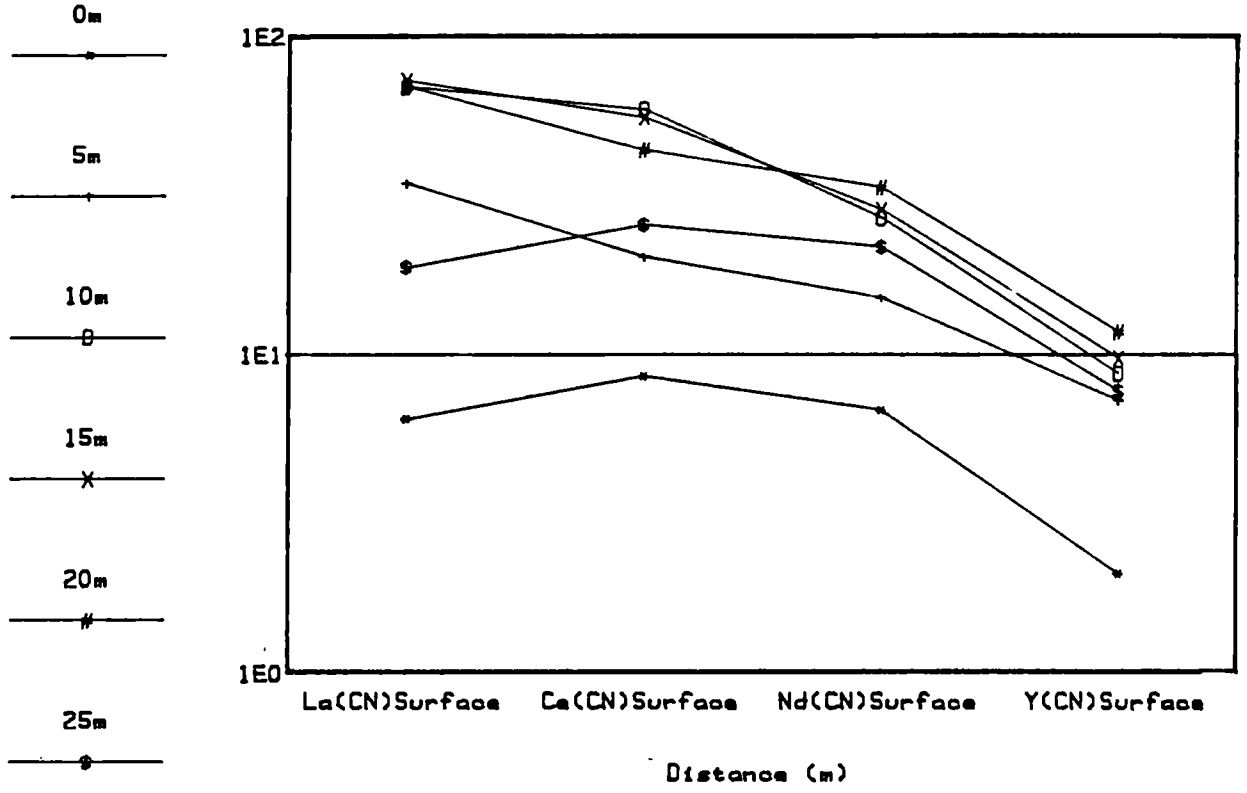

Fig.3.8.18.1987 Traverse 3 REE Surface

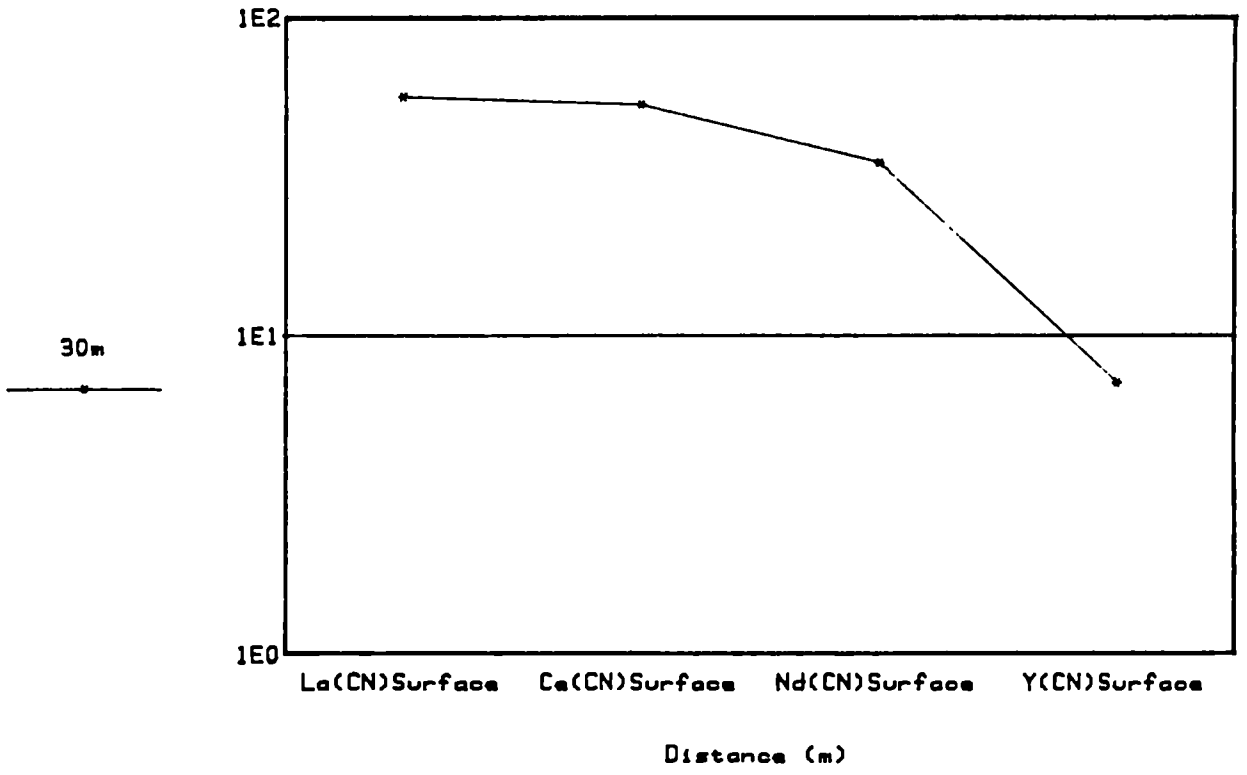

Fig.3.8.19.1987 Traverse 3 REE Deep

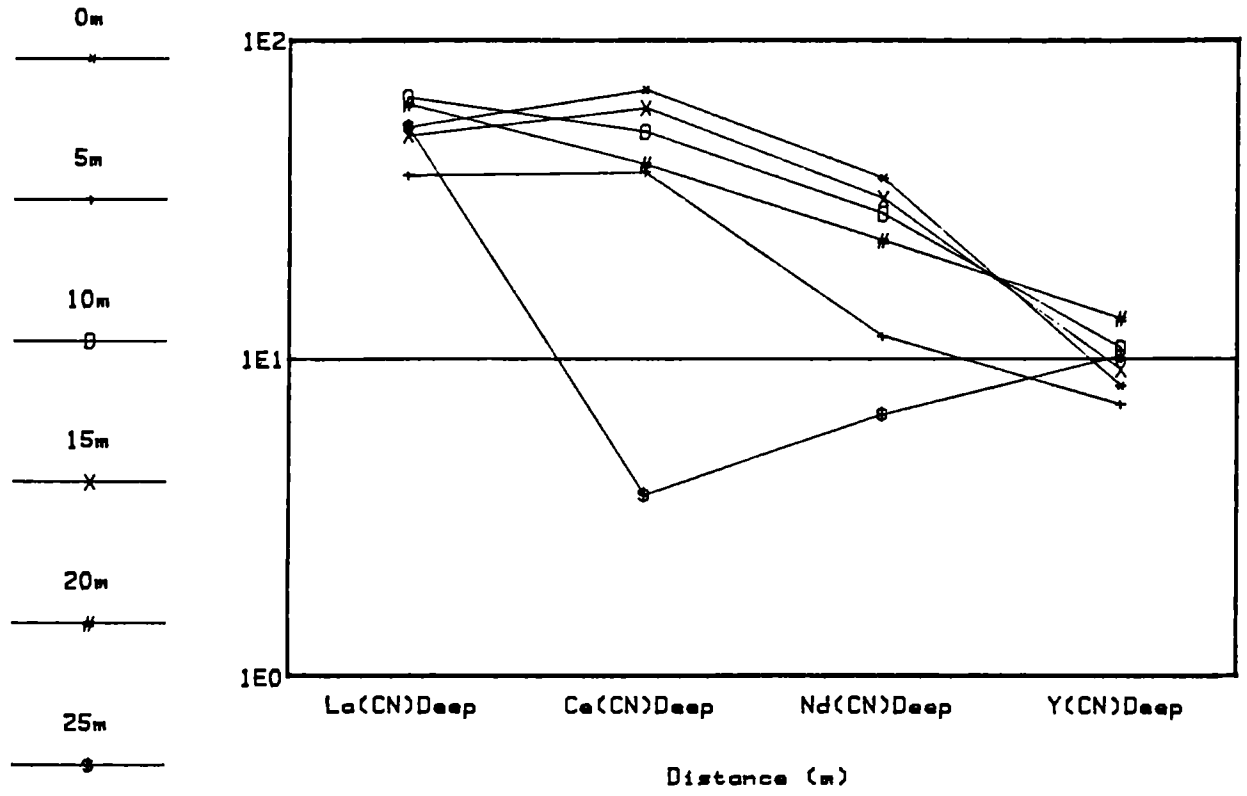

Fig.3.8.20.1987 Traverse 3 REE Deep

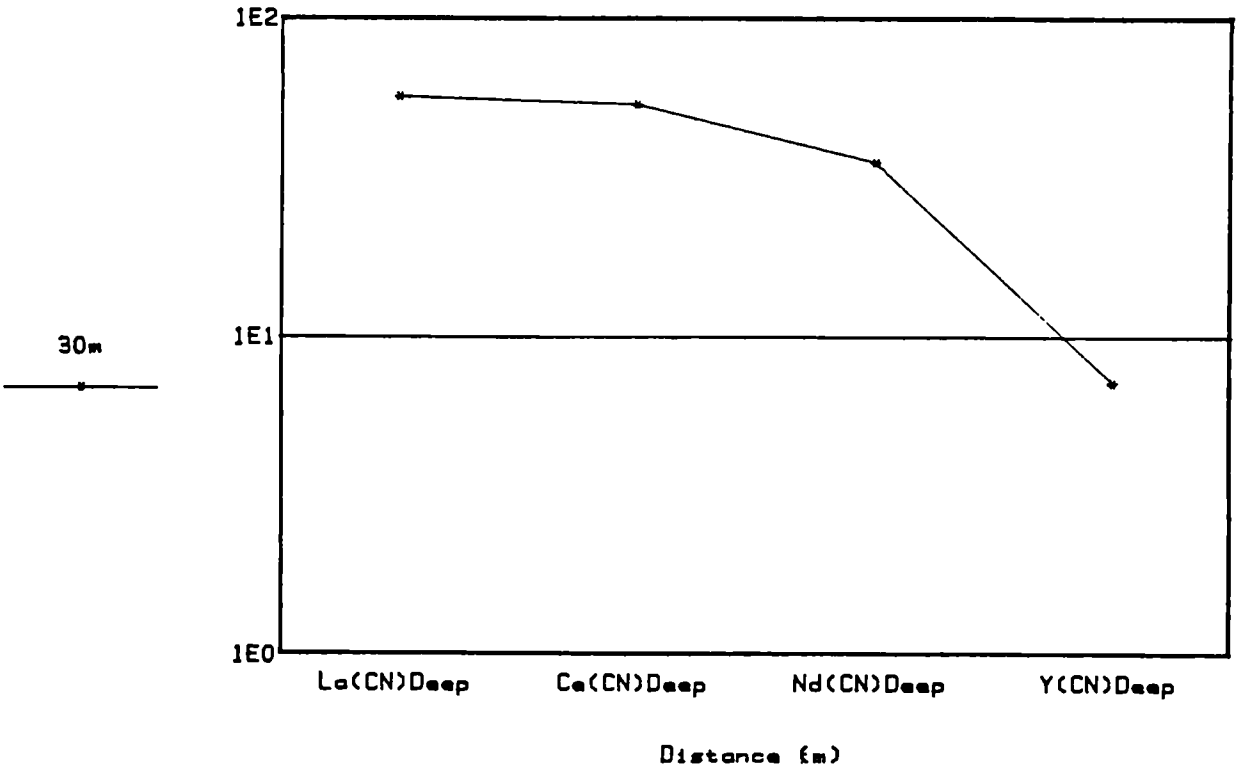

Fig.3.9.1 Broubster 1988 Traverse 4

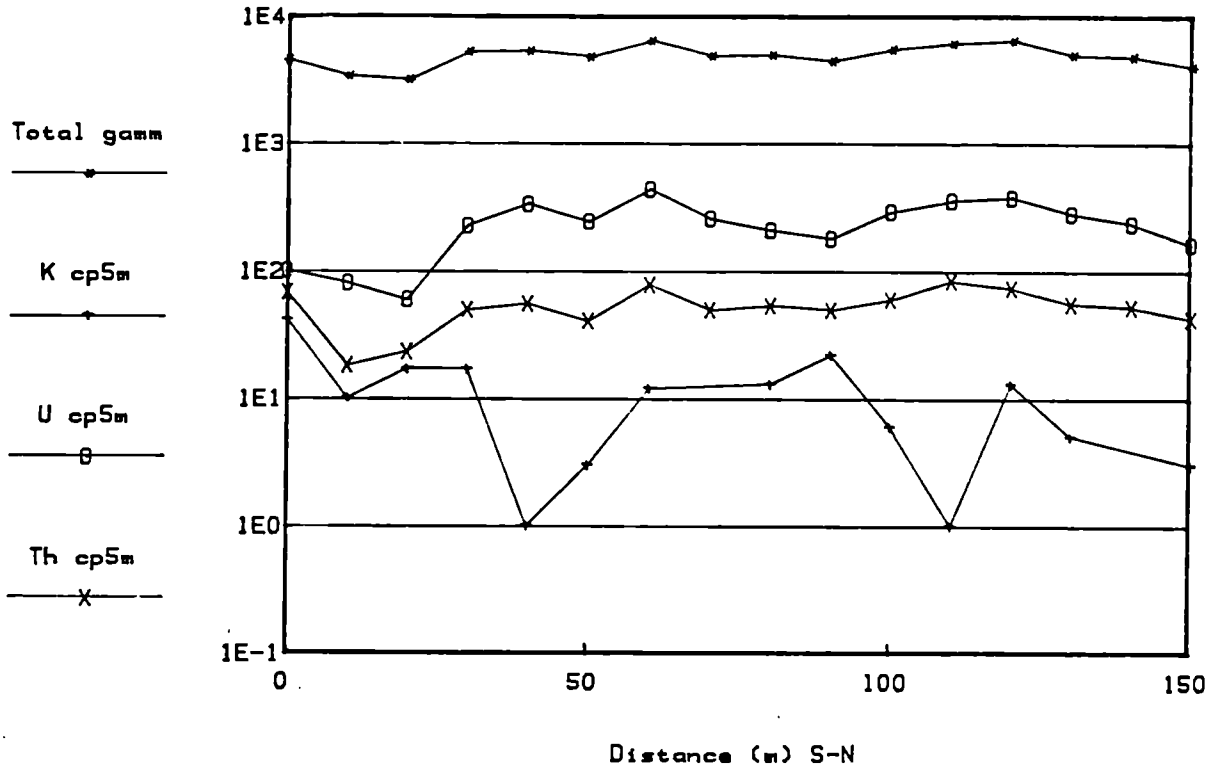

Fig.3.9.2 Broubster 1988 Traverse 4

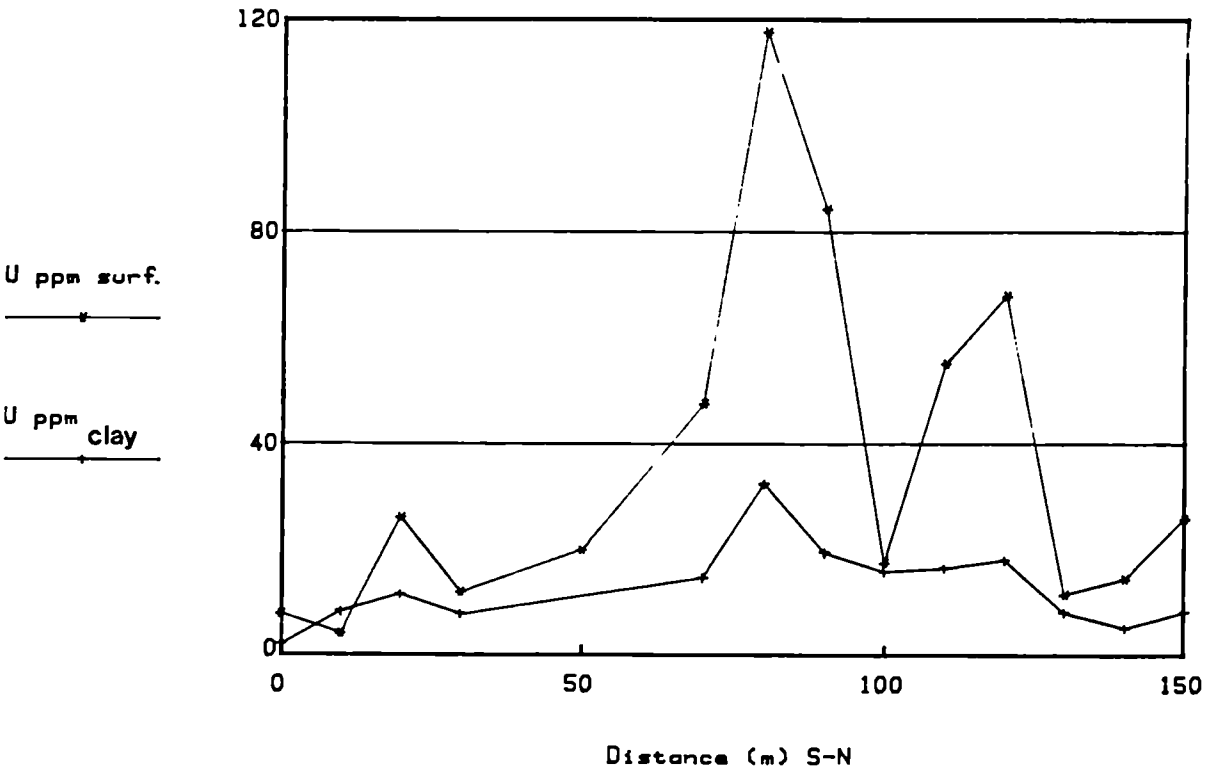

Fig.3.10.1 Broubster 1988 Traverse 5

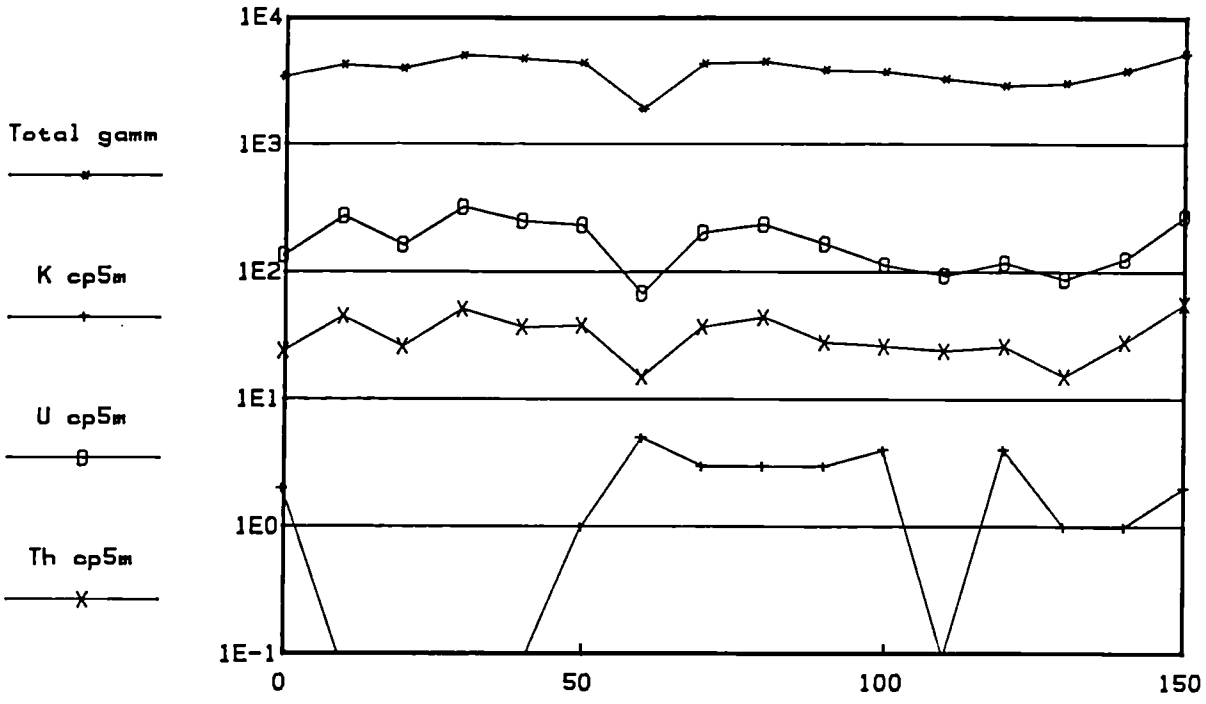

Fig.3.10.2 Broubster 1988 Traverse 5

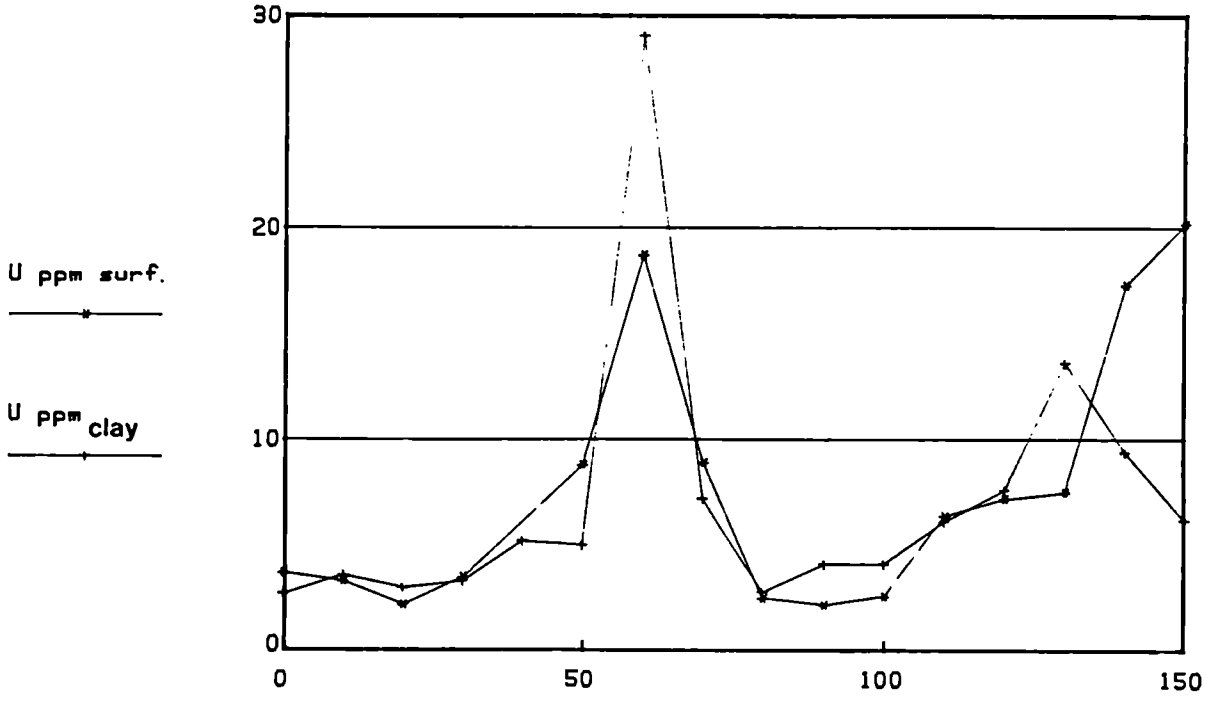

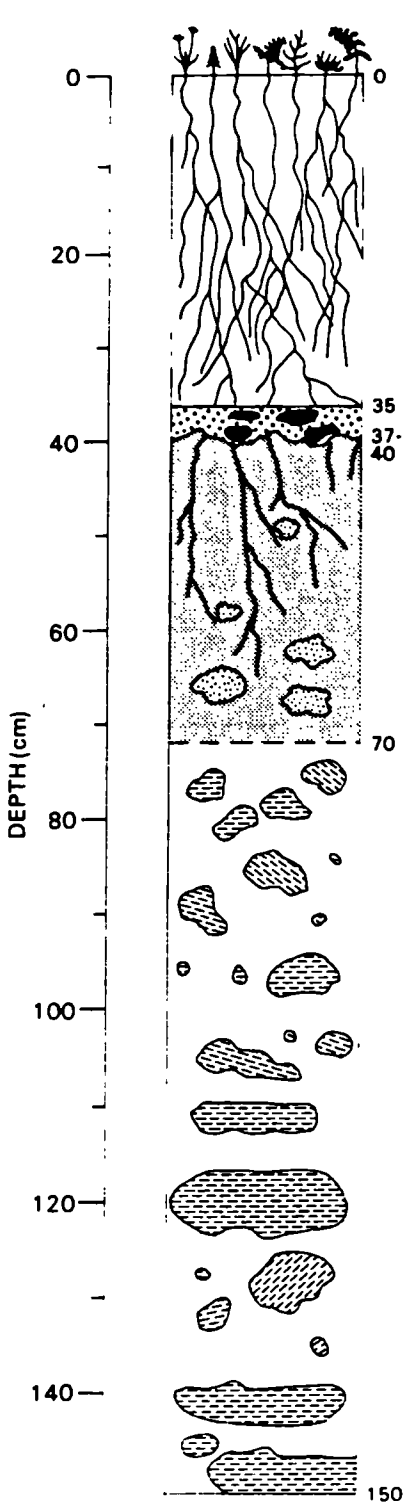

VEGETATION:
Grass, buttercup, dandylion, bog cotton, plantain, spotted orchid, northern marsh orchid, equisetum, bracken and heather.

A HORIZON:
Homogenous peaty A horizon, waterlogged, numerous roots. Coarser roots of bracken and heather from former vegetation cover. Sharp transition to underlying B/C horizon. Water seepage at junction with B/C horizon
Birch and pine bark and twigs at base.

E HORIZON:
Distinct leached horizon. Coarse sandy clay with blaeched rock fragments. Creamy colour.

B/C HORIZON:
Yellow-brown sticky, silty clay, gleyed, mottled with fine fibrous roots from surface vegetation and old vegetated roots. Stellate, hollow cross-section old roots (Equisetum).
Some root channels carrying water. Some fresh Equisetum roots seen in clay near top, yellow oxidation around root channels becoming redder with depth.
Stone fragments moderately abundant in lower part includes fragments of local flaggy sandstone and erratics of granitic (gneiss) rock, altered strong green (chloritic) friable rock; igneous fragments highly disaggregated with ? mineral alteration.
Occasional large boulders up to 0.5m.
Transitional into underlying C/D horizon.

C/D HORIZON:
Stonier, light chocolate-brown clay. Many stones, variable in size from fine gravel to commonly 5cm diameter, also frequent large blocks of ? local flags up to 0.5m (at least!)
Appear to have preferred orientation with shallow dip to E
Some blocks show strong blue-green colour

Figure 3.11.1

Fig.3.11.2. Broubster 1986 Pit 2

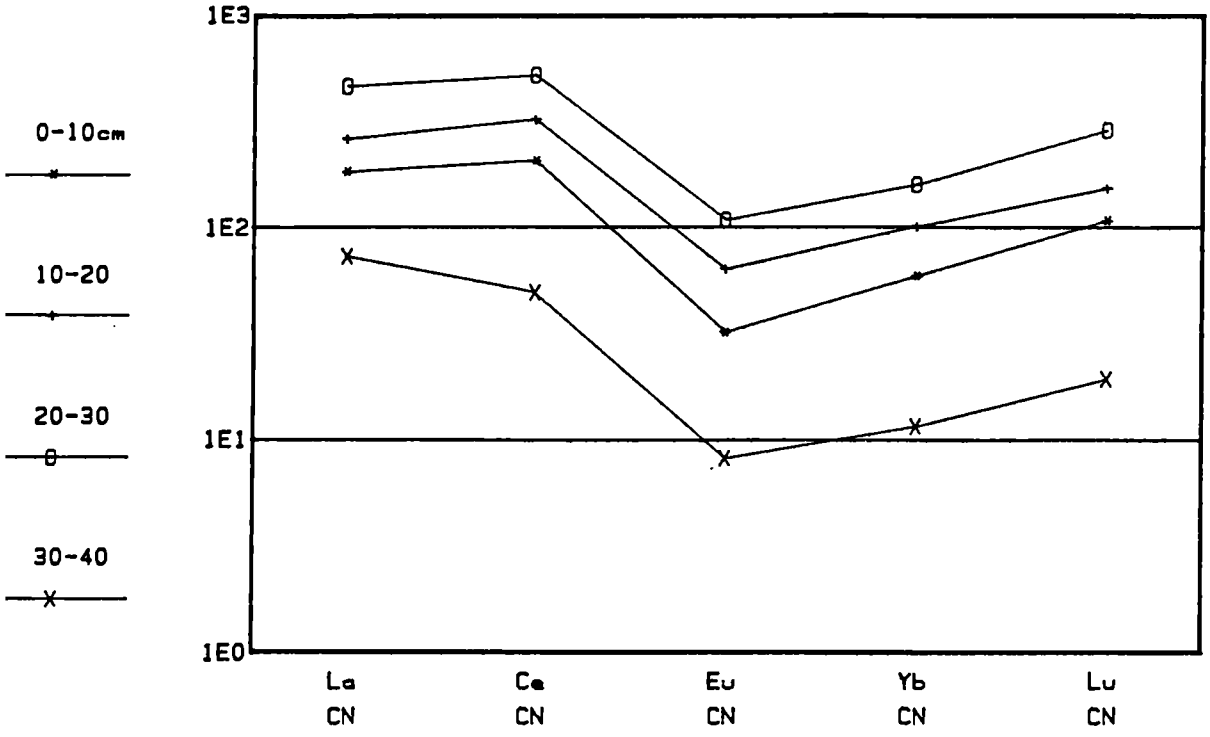

Fig.3.11.3. Broubster 1986 Pit 2

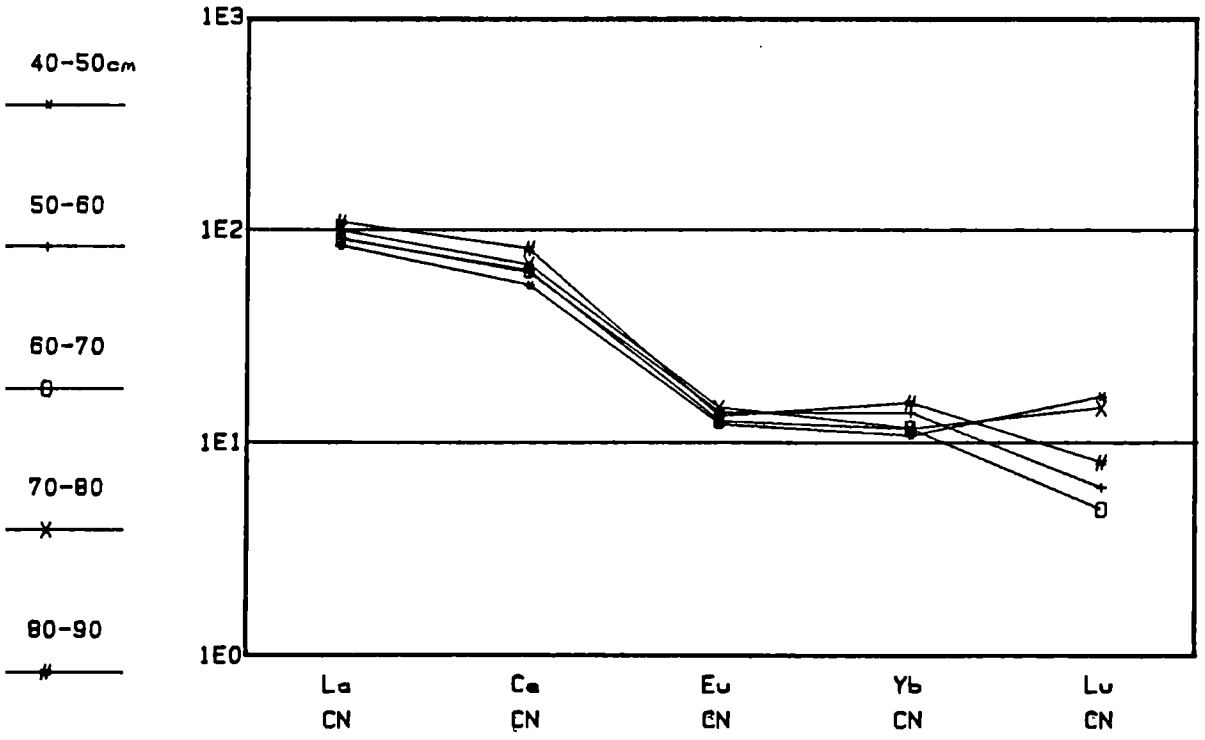

Fig.3.11.6.Broubster 1986 Pit 2

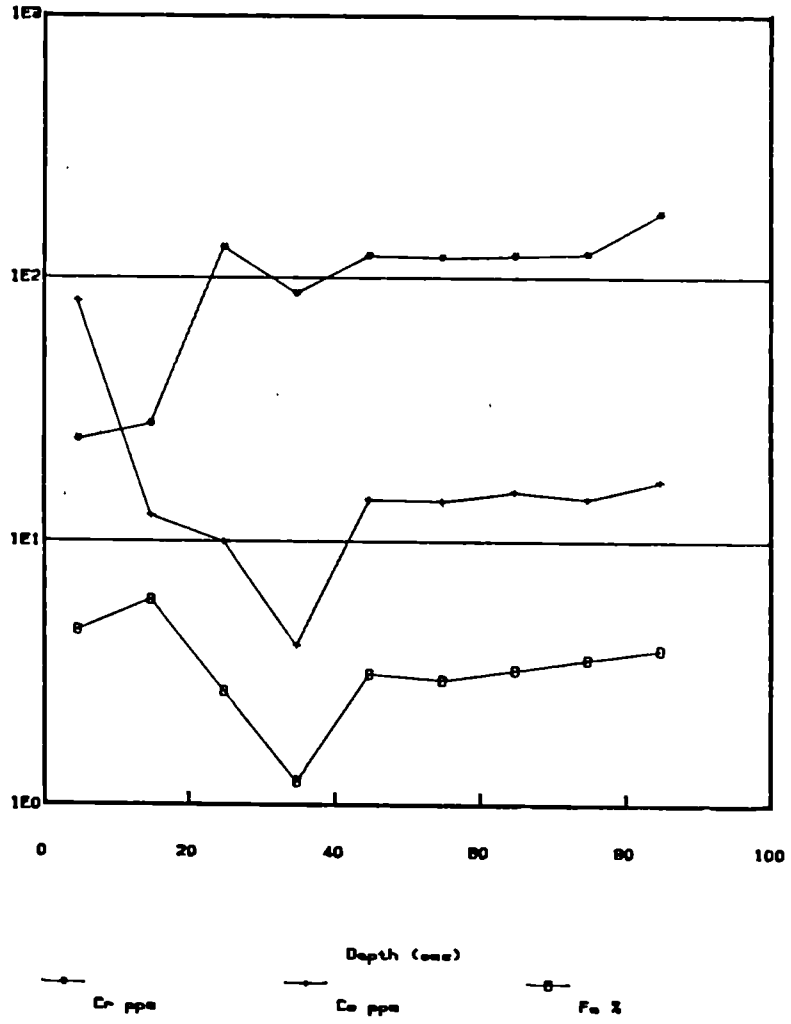

Fig.3.11.7.Broubster 1986 Pit 2

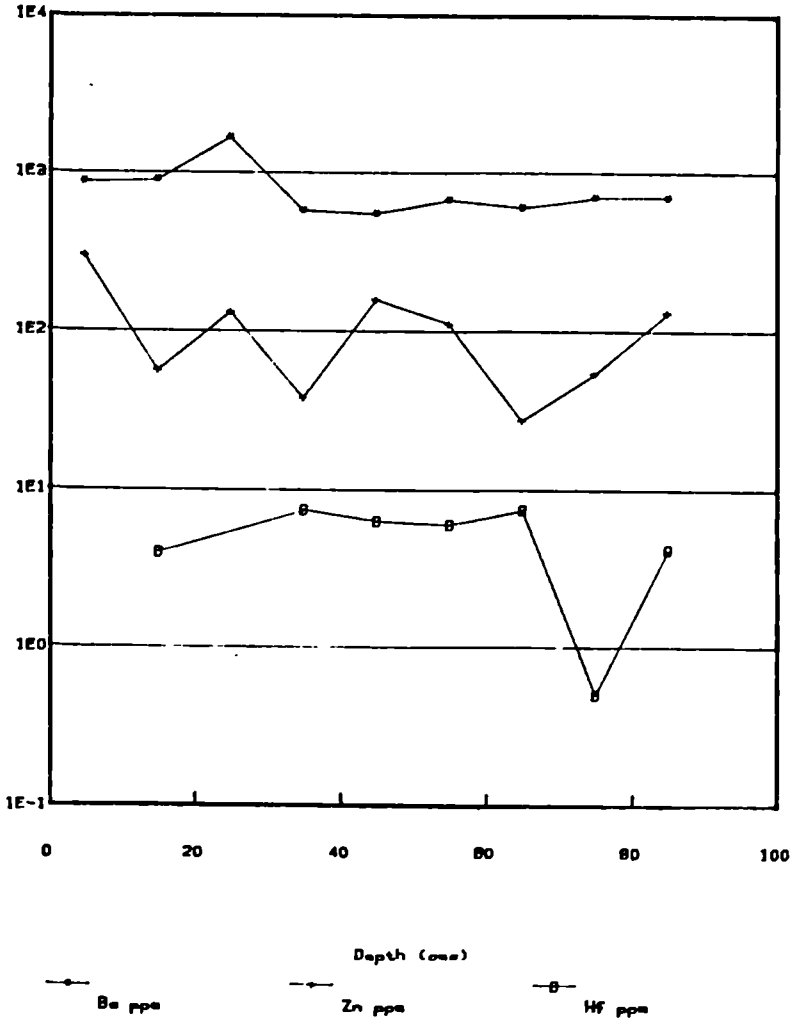

Fig.3.11.4.Broubster 1986 Pit 2

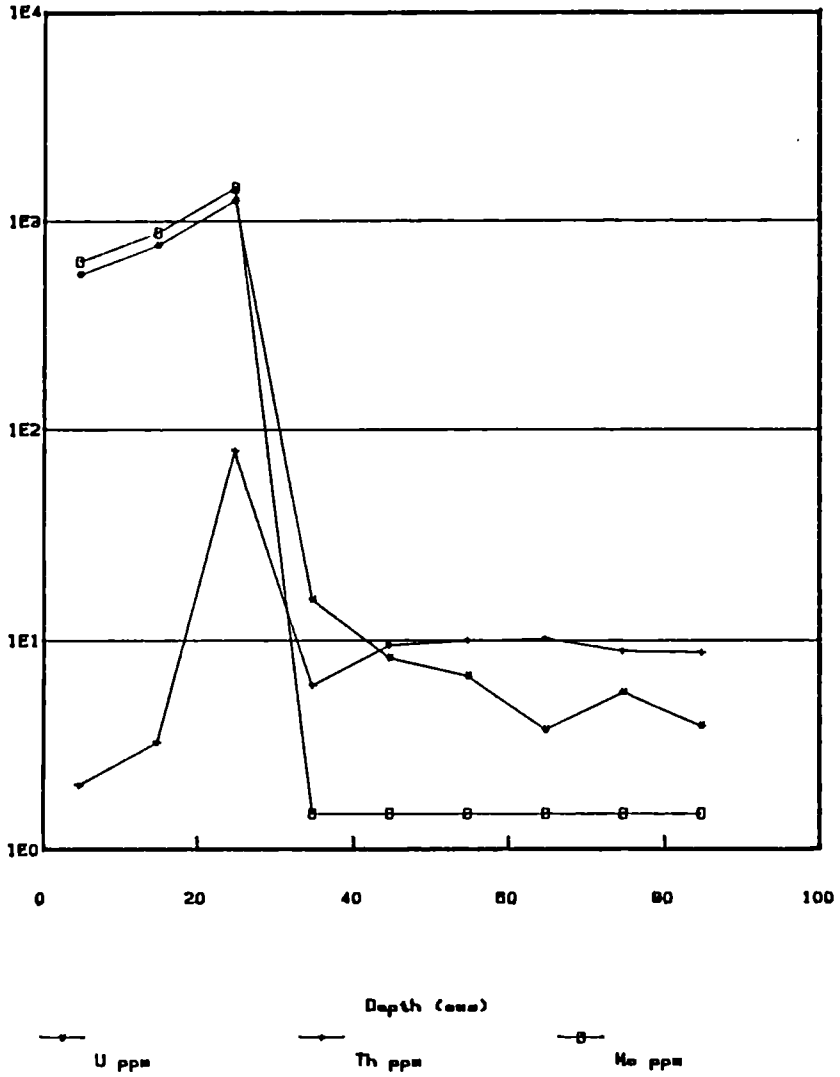

Fig.3.11.5.Broubster 1986 Pit 2

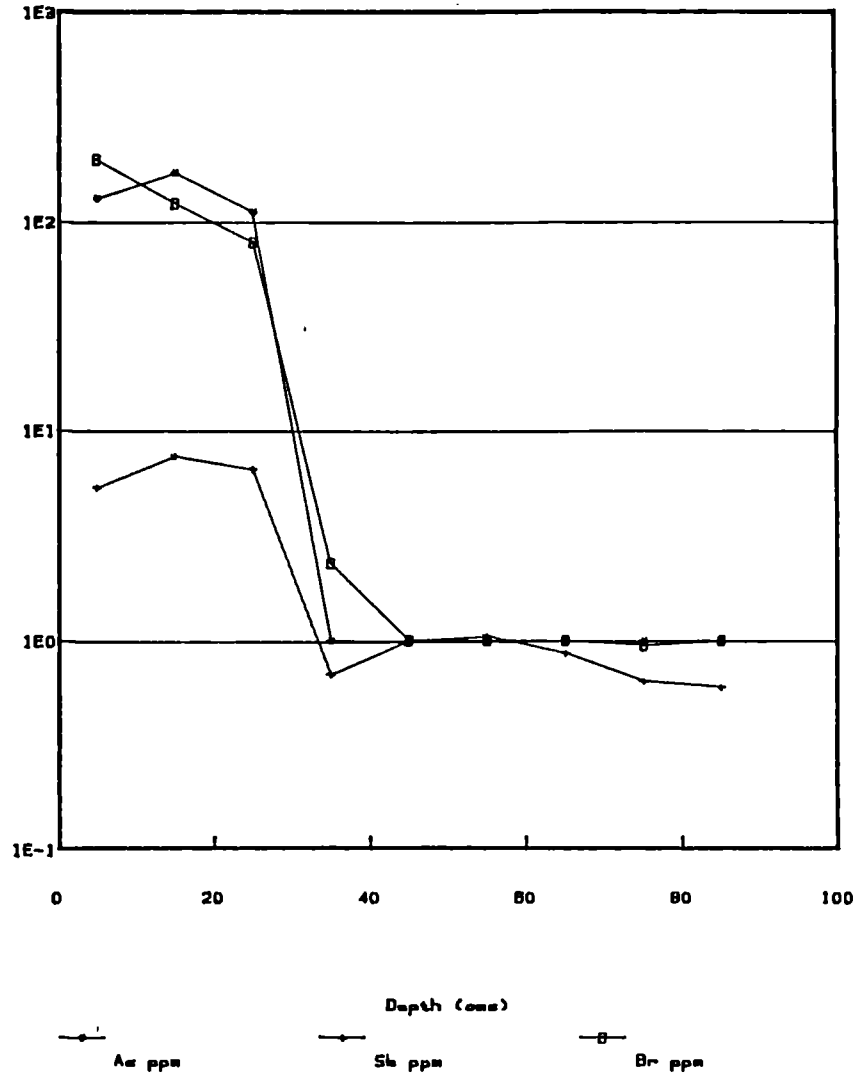

Fig 3.11.8. Broubster 1987 Pit 8 Water

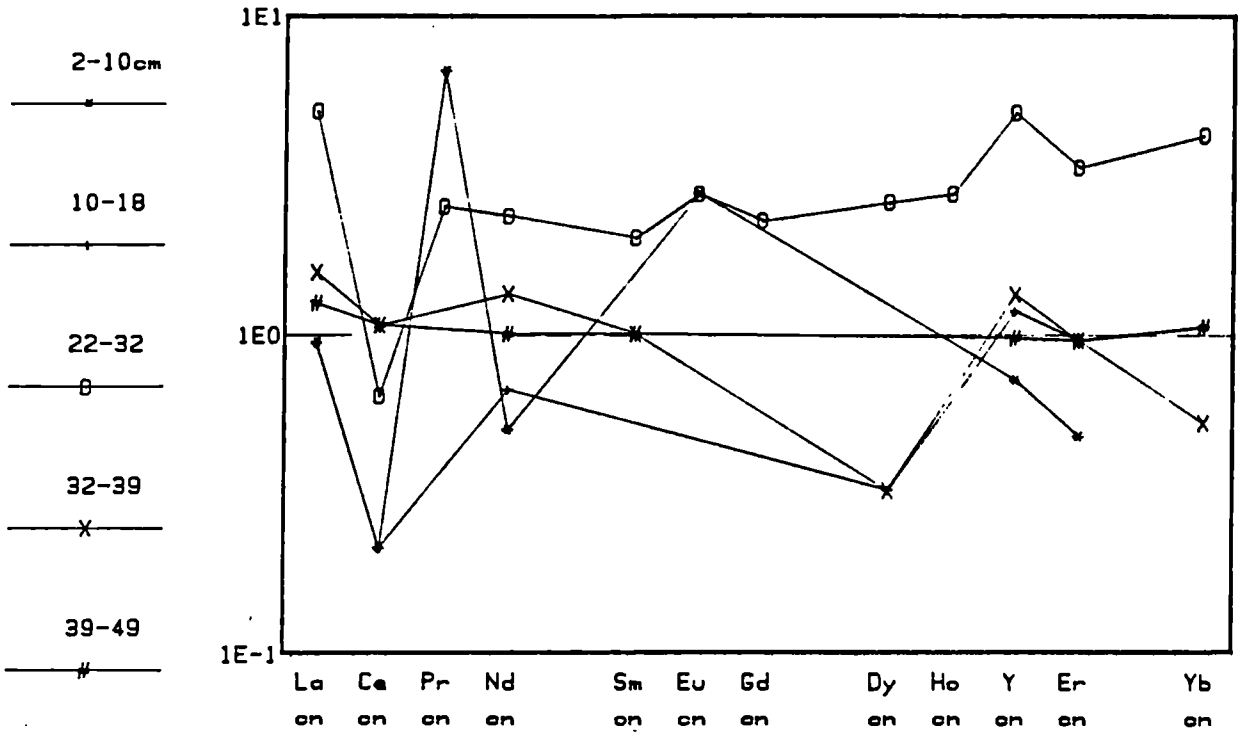

Fig 3.11.9.Broubster 1987 Pit 8 Water

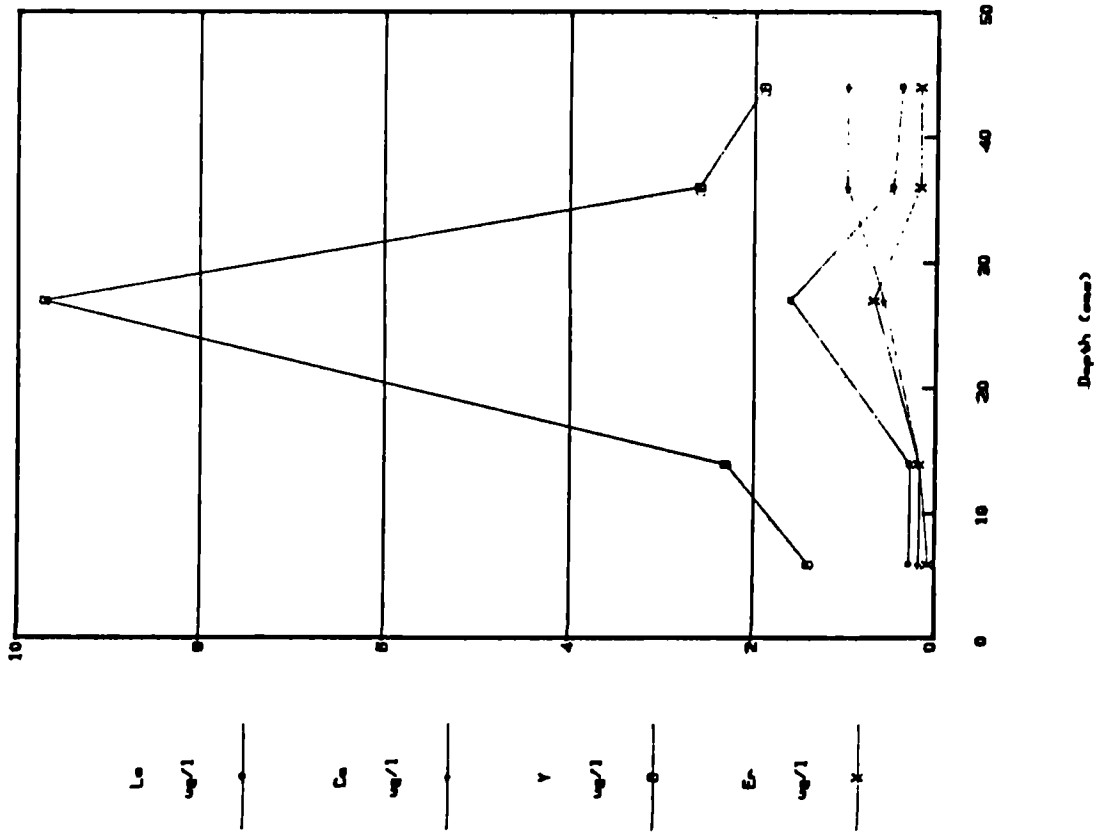

Fig 3.11.10.Broubster 1987 Pit 8 Water

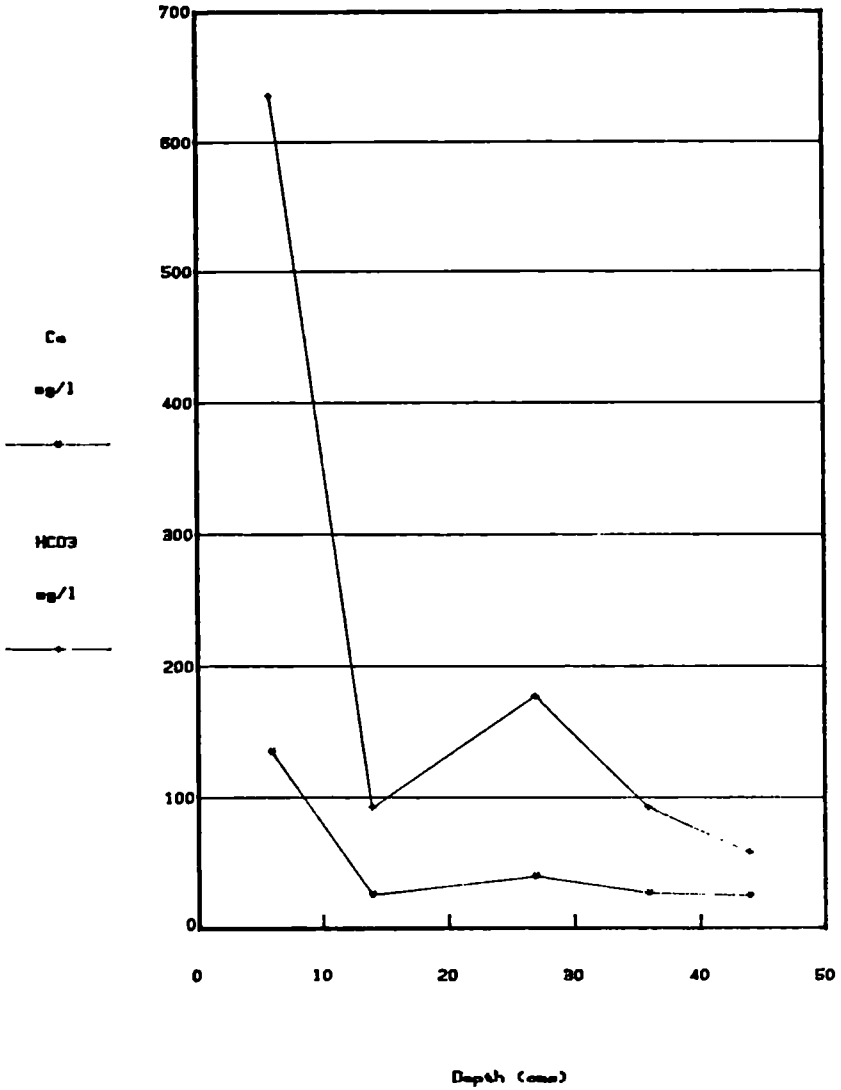

Fig.3.11.11.Broubster 1987 Pit 8 Water

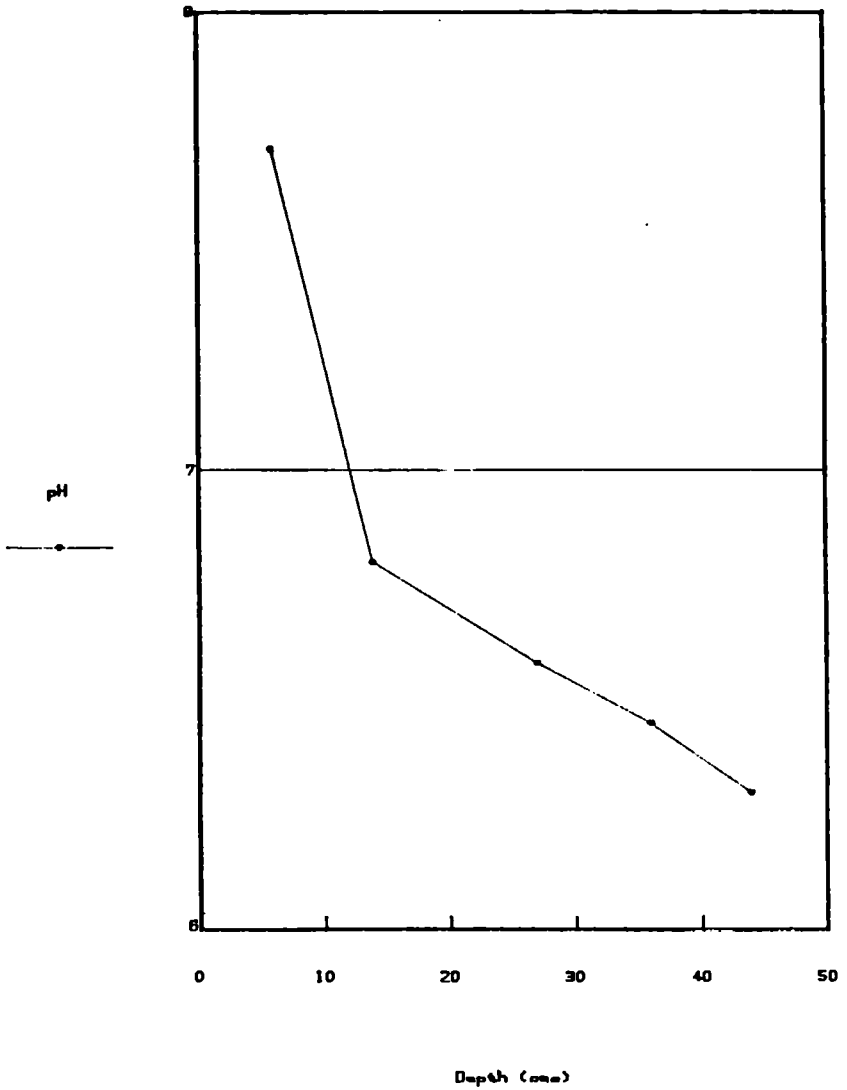

Fig.3.11.12.Broubster 1987 Pit 8 Water

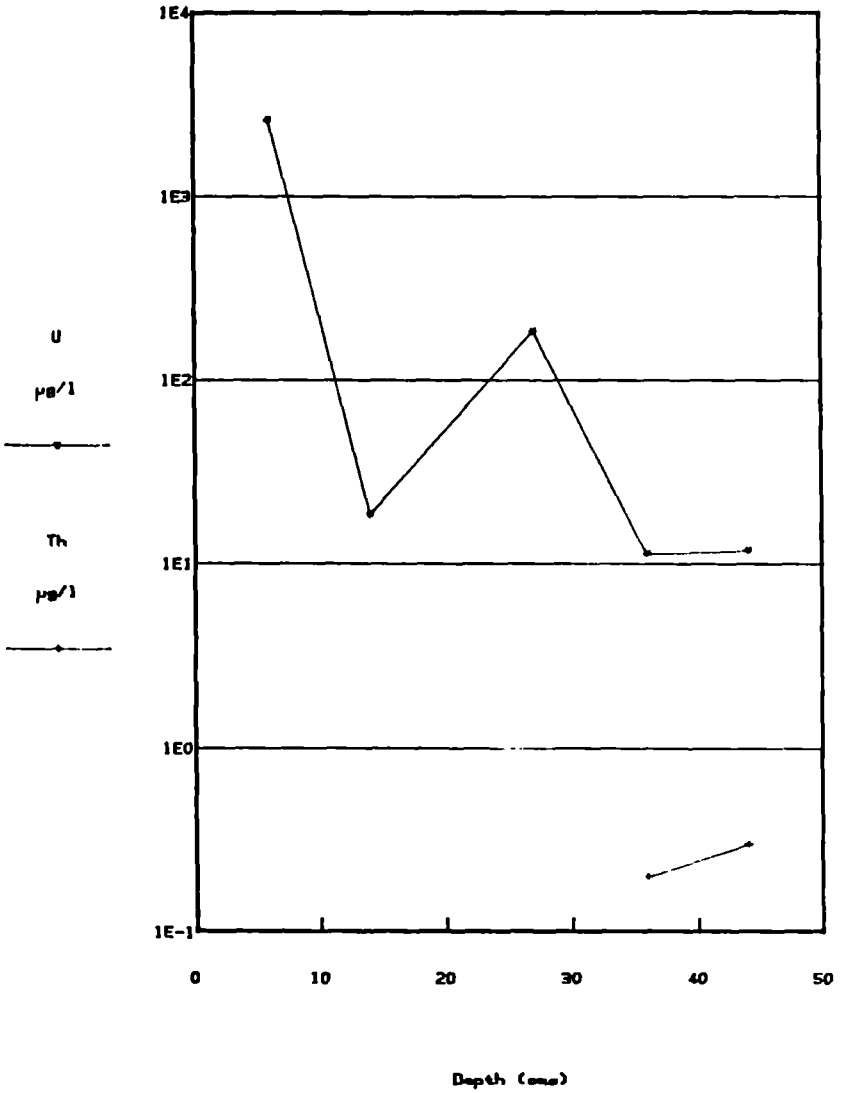

Fig.3.11.13.Broubster 1987 Pit 8 Water

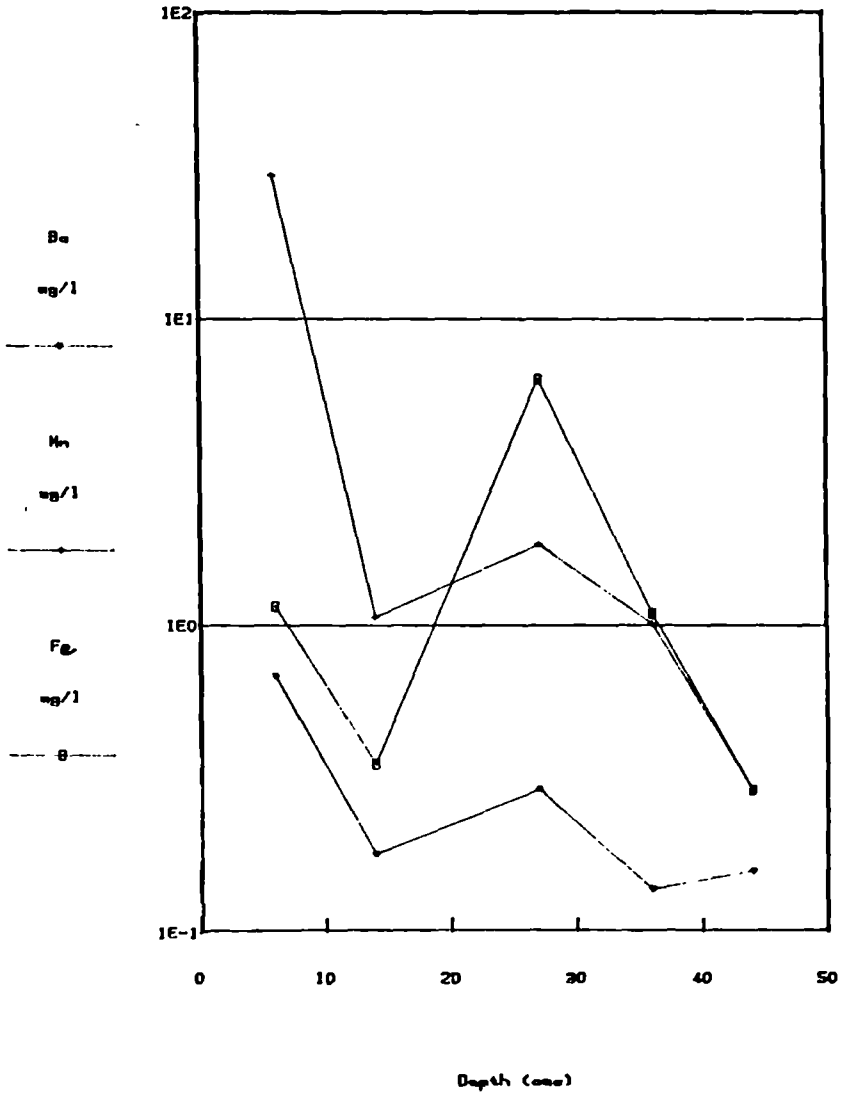

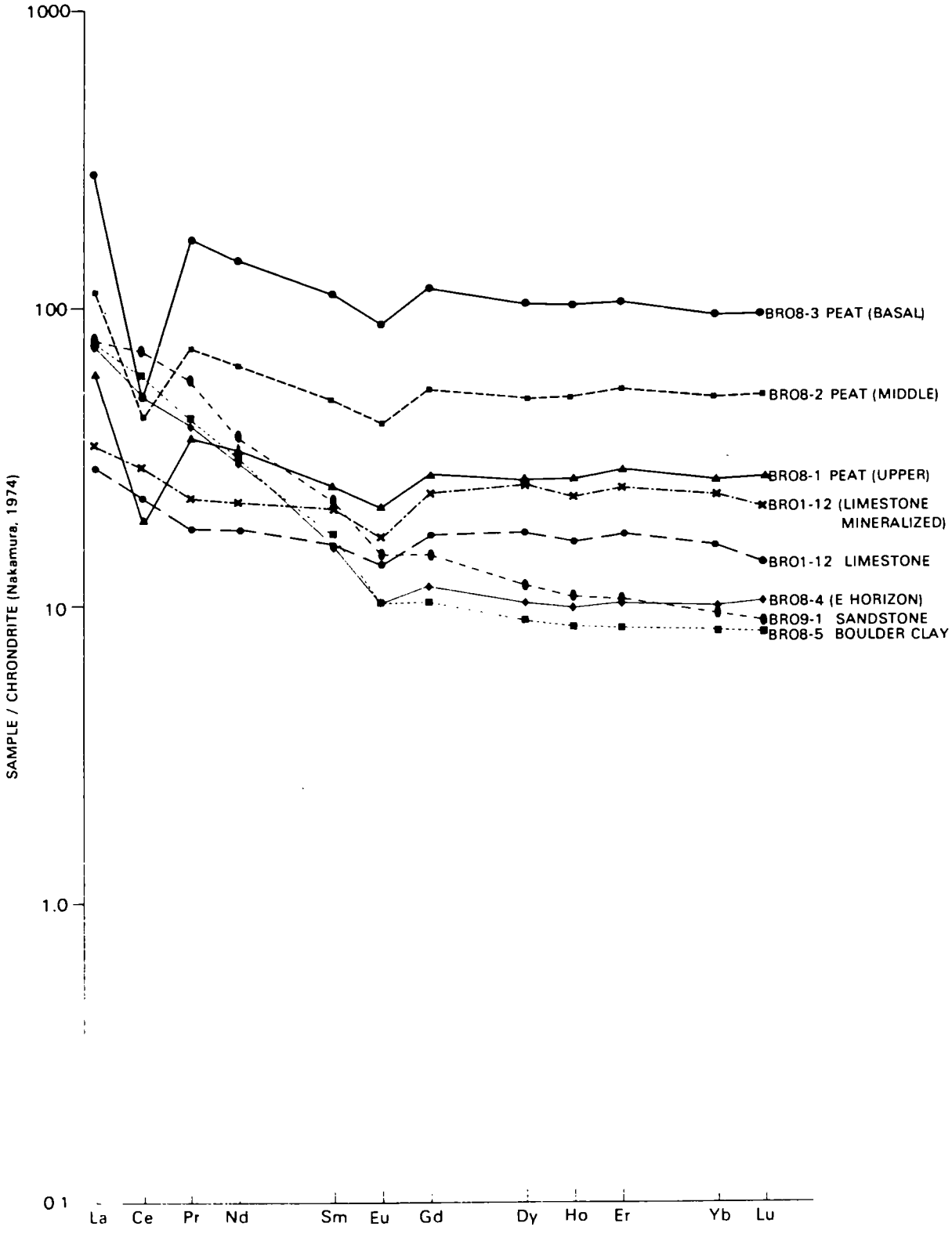

Figure 3.11.14

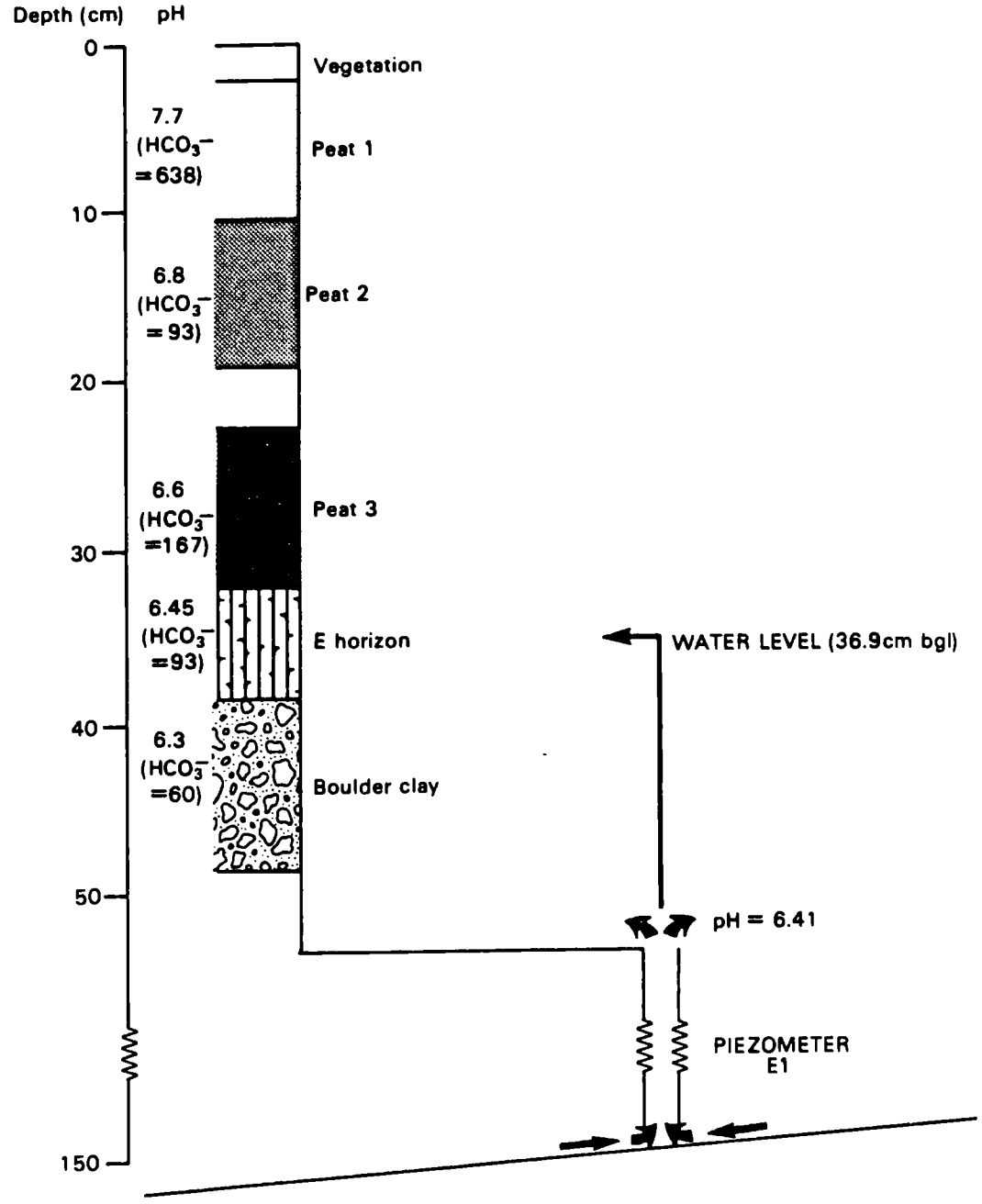

Figure 3.11.15

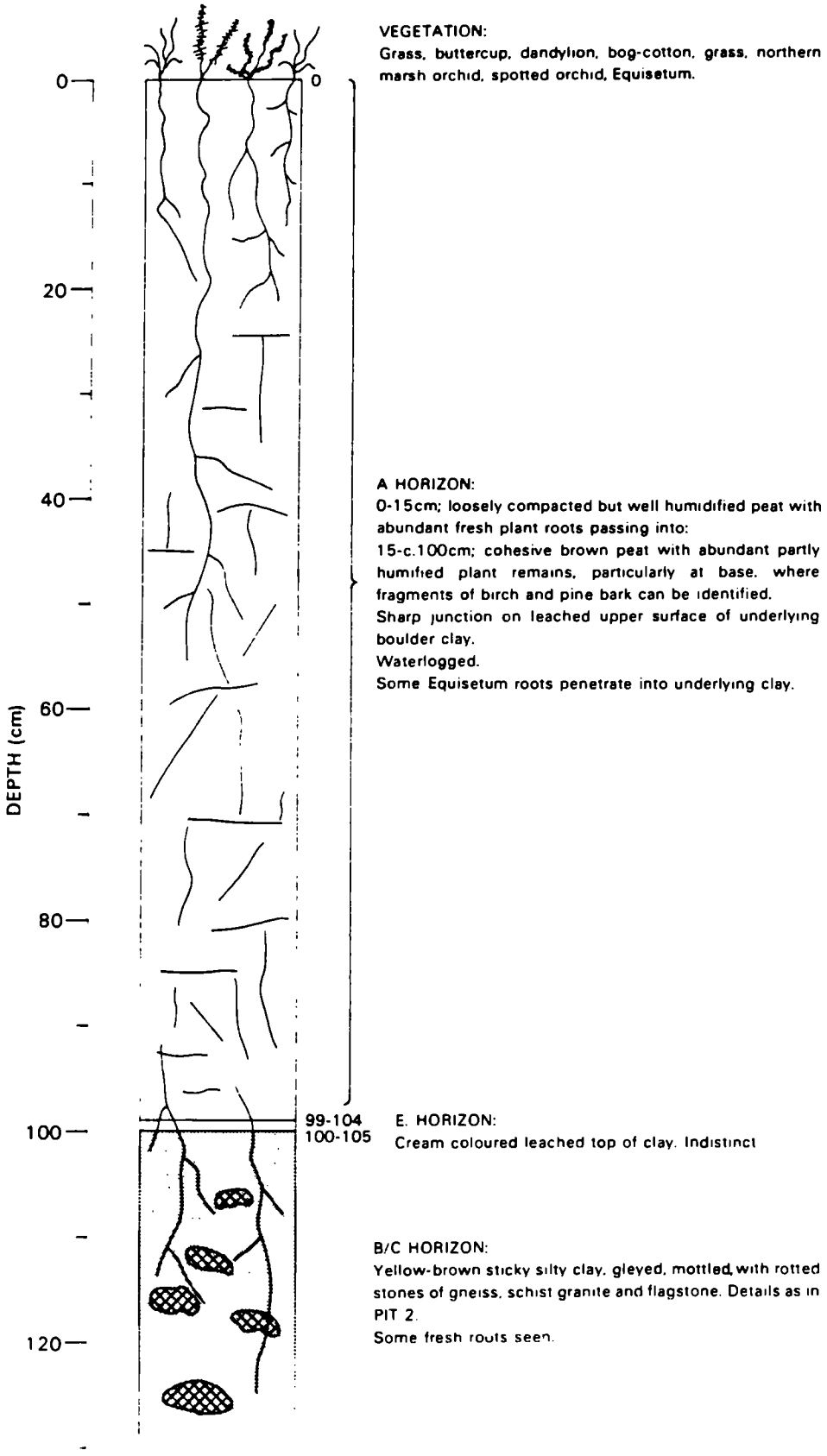

Figure 3.11.16

FIG.3.11.17 Broubster 1987 Pit 3 Soils

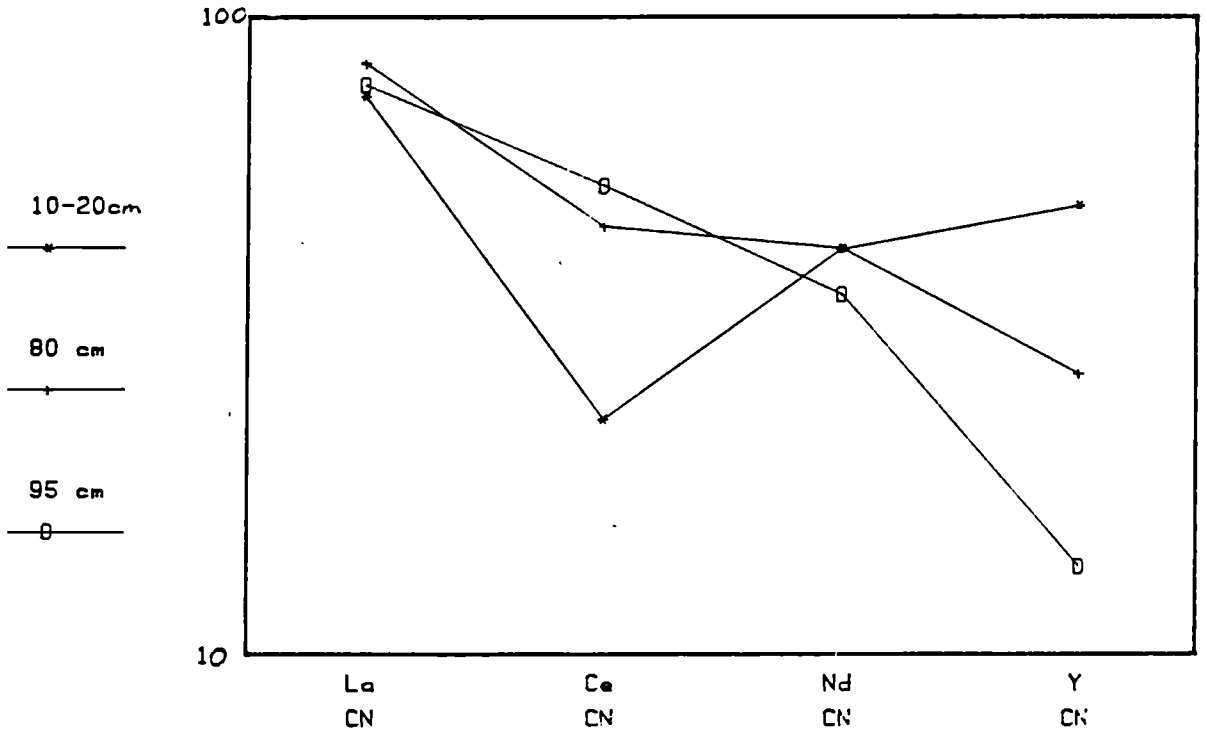

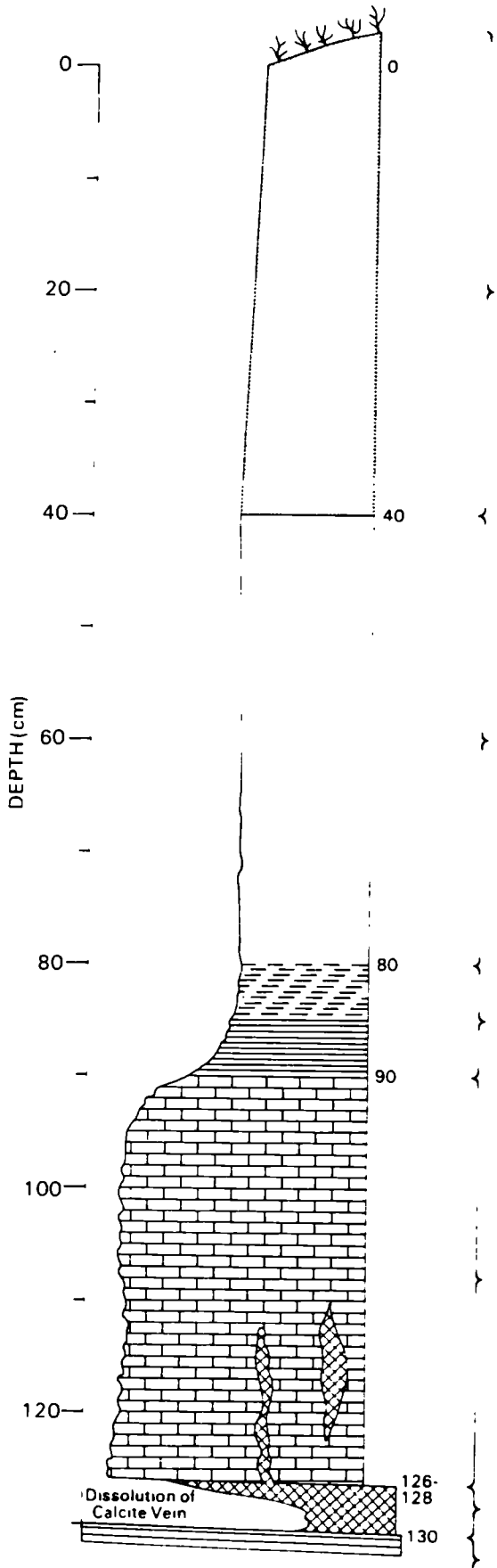

VEGETATION:
Grass, thistle, plantain, daisy

Fine to silty brown earth or loam, humic-rich and fibrous especially in upper part. Rootlets abundant in upper 10cm Becomes stonier and more clay-rich with depth

Brown, silty or sandy clay with stones. Mottled and banded with ochreous ferric oxide/hydroxide and black fine powdery manganiferous oxide/hydroxide, sometimes forming nodules and more extensively developement in lower part. Ferruginous-manganiferous soil shows strong γ-radioactivity.

Highly weathered regolith of finely laminated siltstone or very fine sandstone, soft and gleyed at top but becoming more competant with depth. Gleyed regolith is waterlogged.

Hard, finely laminated limestone with dark siltstone lamination. Occasional "Bird's-Eye" fabric, discontinuous subvertical calcite fractures, often irregular with disseminated pyrite and galena. Small vuggy fine fractures seen to contain red-brown sticky hydrocarbon. Radioactive.

Lenticular, irregular lenses of coarse calcite veining parallel to bedding with sphalerite, galena, chalcopyrite, pyrite baryte and hydrocarbon.

Light grey, hard siltstone with finely laminated calcareous bands and black silt laminations, with subvertical calcareous fractures Apparent dip 10-15 N Radioactive

Figure 3.11.18

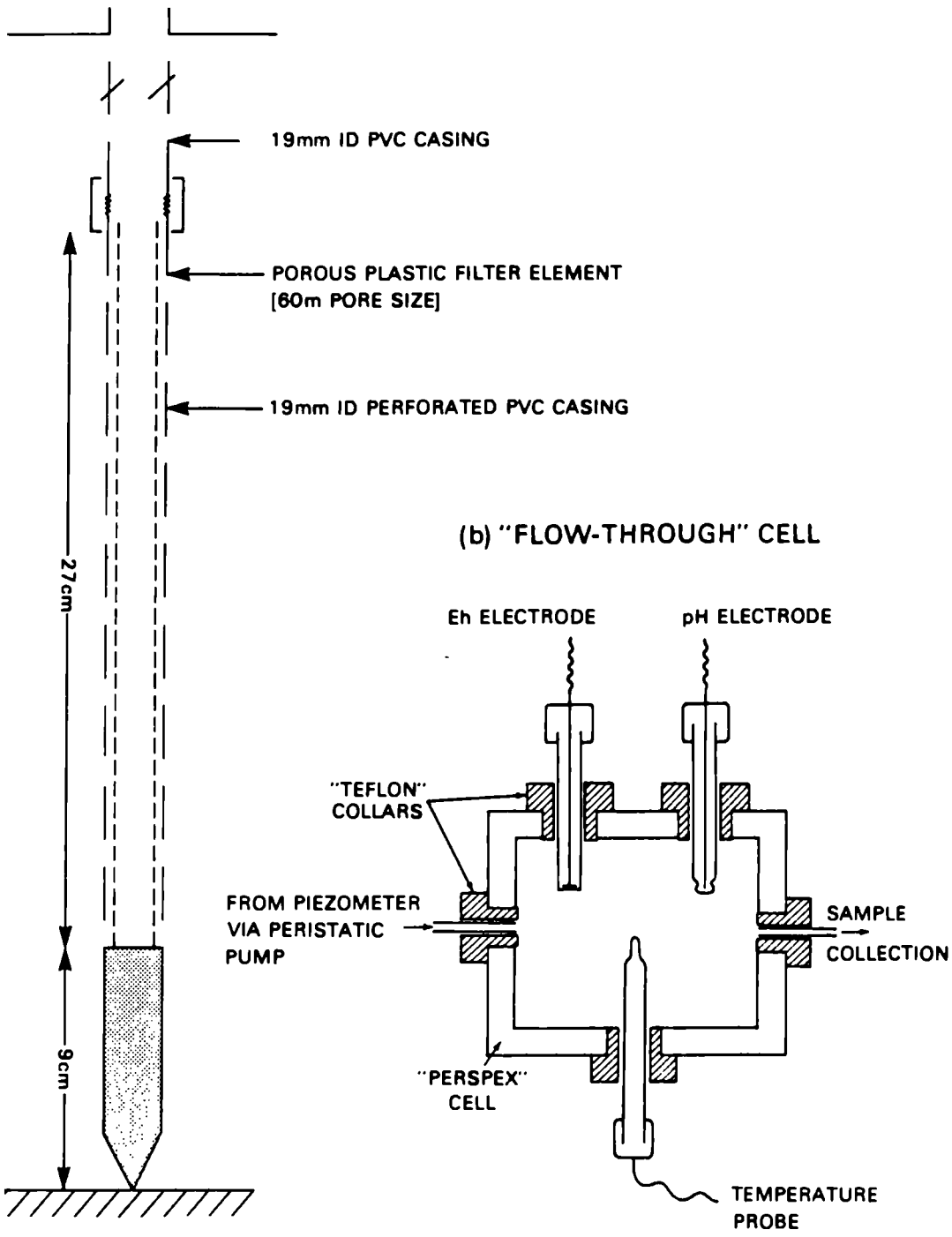
(a) "CASAGRANDE" PIEZOMETER
19mm ID PVC CASING
POROUS PLASTIC FILTER ELEMENT
[60m PORE SIZE]
19mm ID PERFORATED PVC CASING
27cm
9cm
(b) "FLOW-THROUGH" CELL
Eh ELECTRODE
pH ELECTRODE
"TEFLON"
COLLARS
FROM PIEZOMETER
VIA PERISTATIC
PUMP
SAMPLE
COLLECTION
"PERSPEX"
CELL
TEMPERATURE
PROBE

Figure 5.1

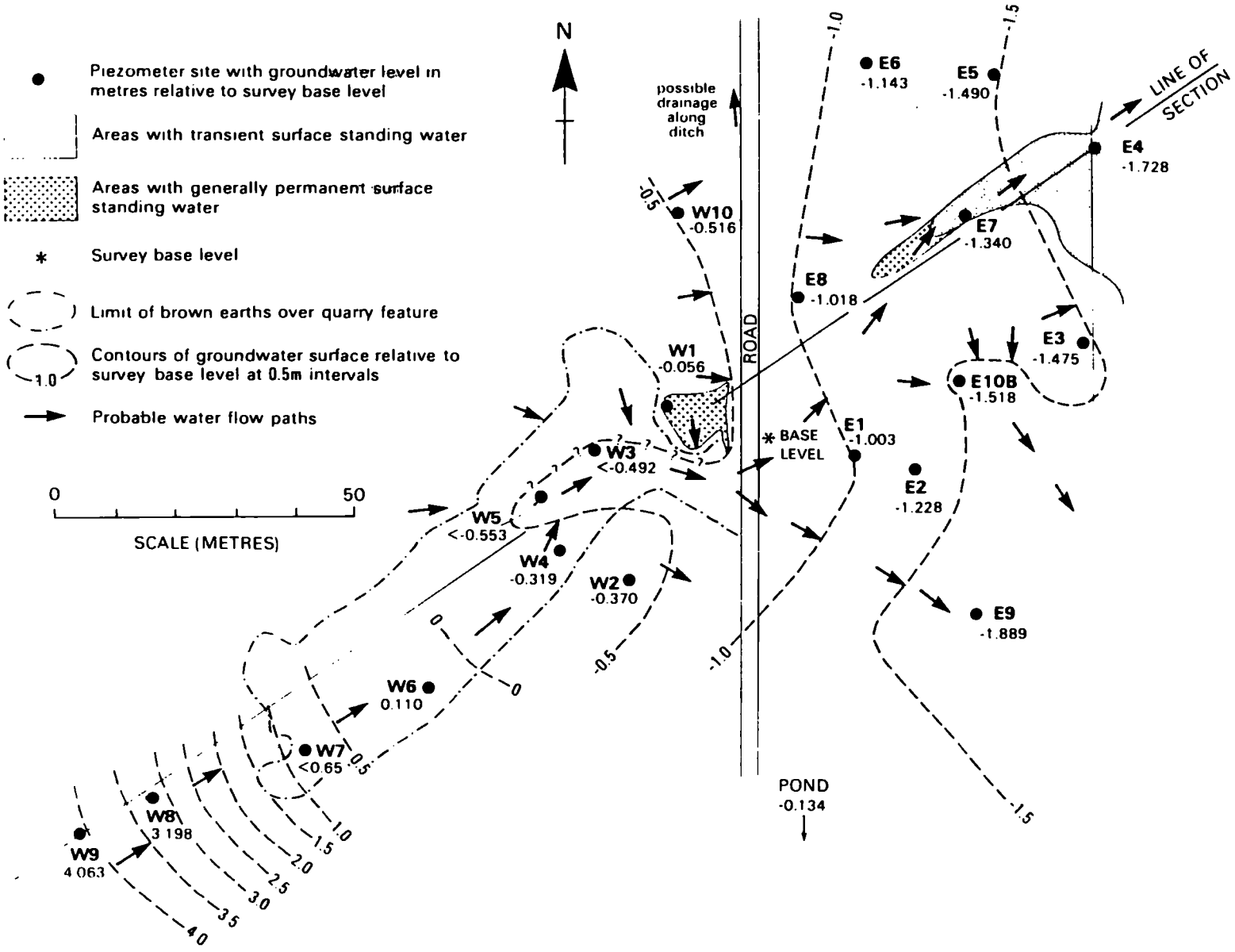
Piezometer site with groundwater level in metres relative to survey base level
Areas with transient surface standing water
Areas with generally permanent surface standing water
Survey base level
Limit of brown earths over quarry feature
Contours of groundwater surface relative to survey base level at 0.5m intervals
Probable water flow paths
0
50
SCALE (METRES)
N
possible drainage along ditch
ROAD
LINE OF SECTION
* BASE LEVEL
POND
-0.134
W1
-0.056
W2
-0.370
W3
<-0.492
W4
-0.319
W5
<-0.553
W6
0.110
W7
<0.65
W8
3.198
W9
4.063
W10
-0.516
E1
-1.003
E2
-1.228
E3
-1.475
E4
-1.728
E5
-1.490
E6
-1.143
E7
-1.340
E8
-1.018
E9
-1.889
E10B
-1.518

Figure 5.2

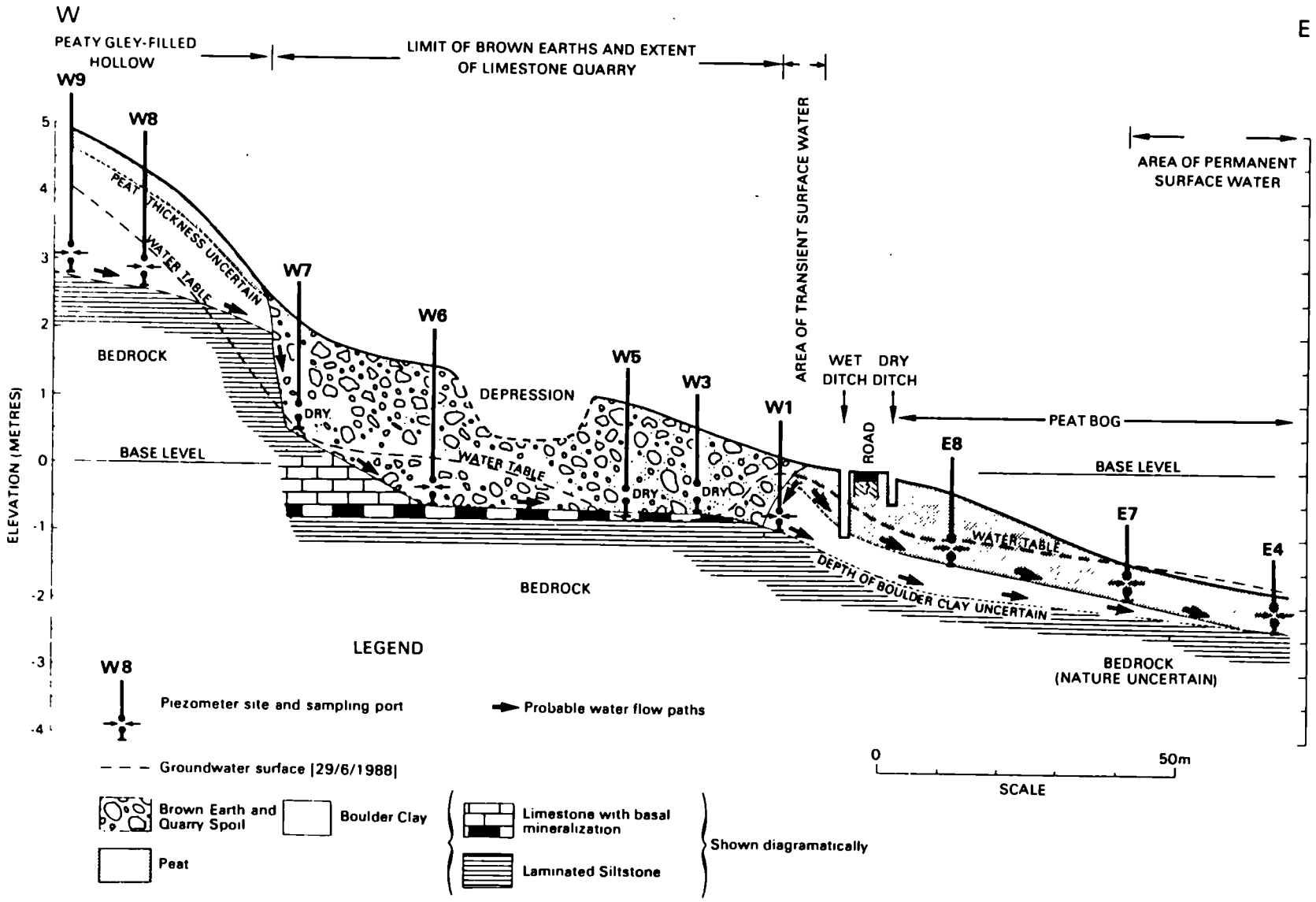
W
E
PEATY GLEY-FILLED HOLLOW
LIMIT OF BROWN EARTHS AND EXTENT OF LIMESTONE QUARRY
AREA OF PERMANENT SURFACE WATER
AREA OF TRANSIENT SURFACE WATER
W9
W8
W7
W6
W5
W3
W1
E8
E7
E4
PEAT THICKNESS UNCERTAIN
WATER TABLE
BEDROCK
DEPRESSION
DRY
WET DITCH
DRY DITCH
ROAD
PEAT BOG
BASE LEVEL
ELEVATION (METRES)
DEPTH OF BOULDER CLAY UNCERTAIN
BEDROCK (NATURE UNCERTAIN)
LEGEND
Piezometer site and sampling port
Probable water flow paths
Groundwater surface [29/6/1988]
Brown Earth and Quarry Spoil
Boulder Clay
Peat
Limestone with basal mineralization
Laminated Siltstone
Shown diagramatically
0
50m
SCALE

Figure 5.3

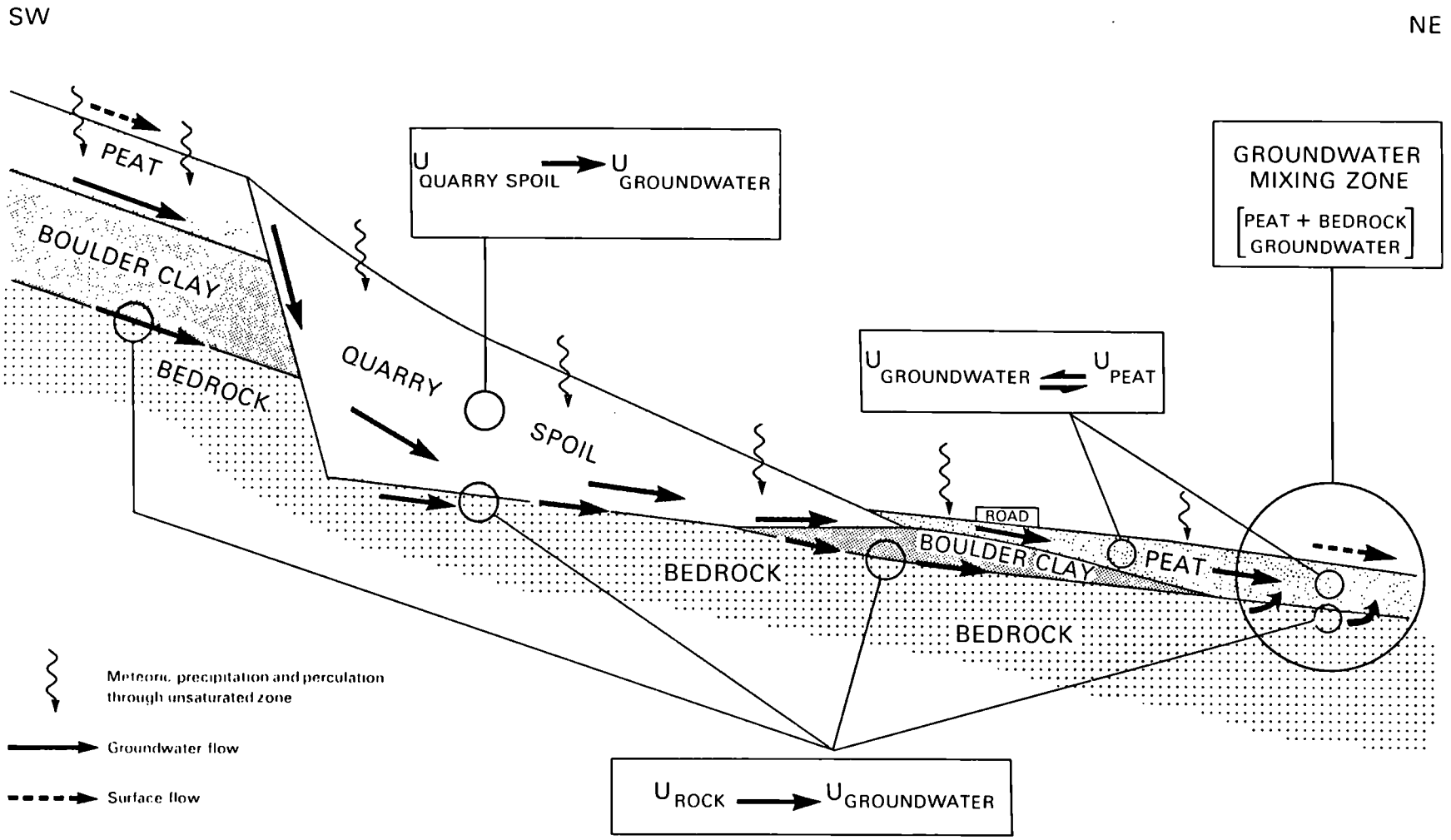
SW
NE
PEAT
BOULDER CLAY
BEDROCK
QUARRY
SPOIL
U QUARRY SPOIL → U GROUNDWATER
GROUNDWATER MIXING ZONE
[PEAT + BEDROCK GROUNDWATER]
U GROUNDWATER ⇄ U PEAT
ROAD
BOULDER CLAY
PEAT
BEDROCK
BEDROCK
Meteoric precipitation and perculation through unsaturated zone
Groundwater flow
Surface flow
U ROCK → U GROUNDWATER

Figure 5.4

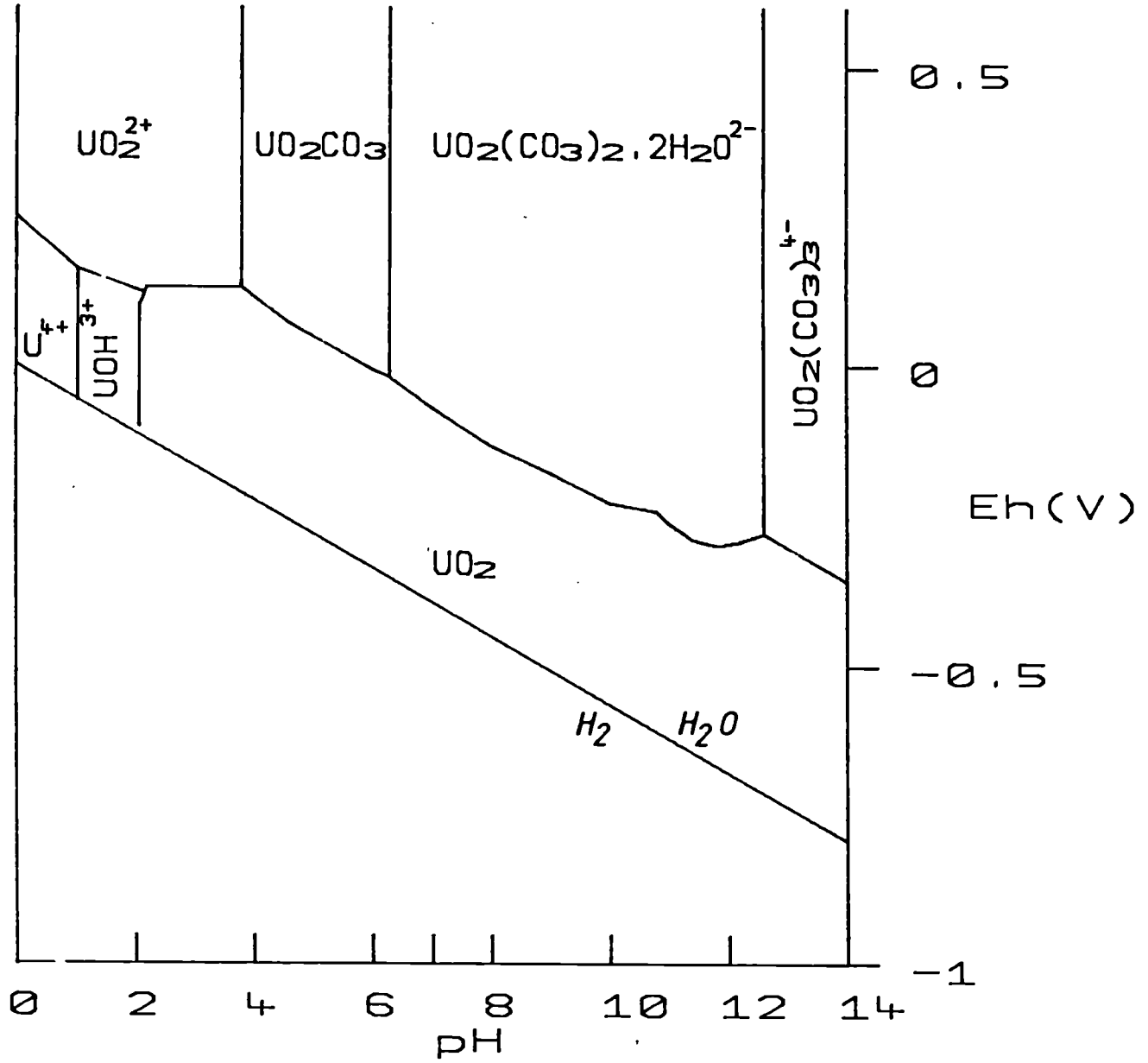
UO_2^{2+}
UO_2CO_3
$UO_2(CO_3)_2.2H_2O^{2-}$
U^{4+}
UOH^{3+}
$UO_2(CO_3)_3^{4-}$
UO_2
H_2
H_2O
0.5
0
-0.5
-1
Eh(V)
0
2
4
6
8
10
12
14
pH

Figure 6.1

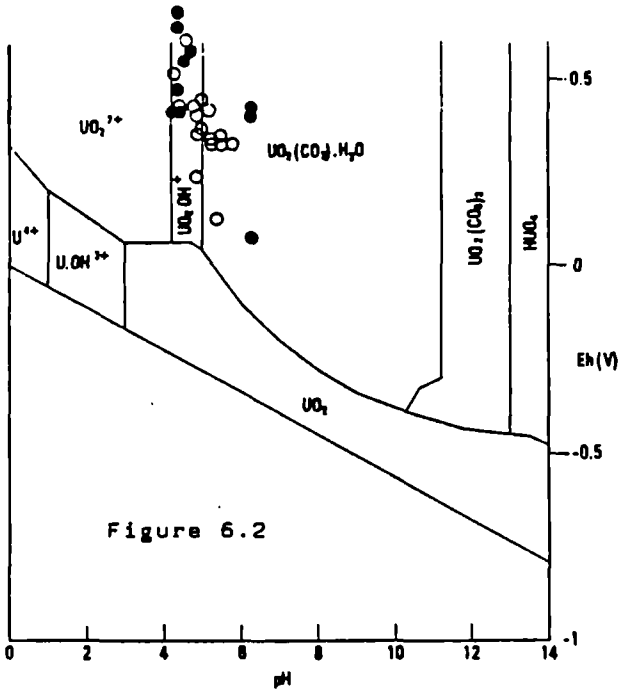

Figure 6.2

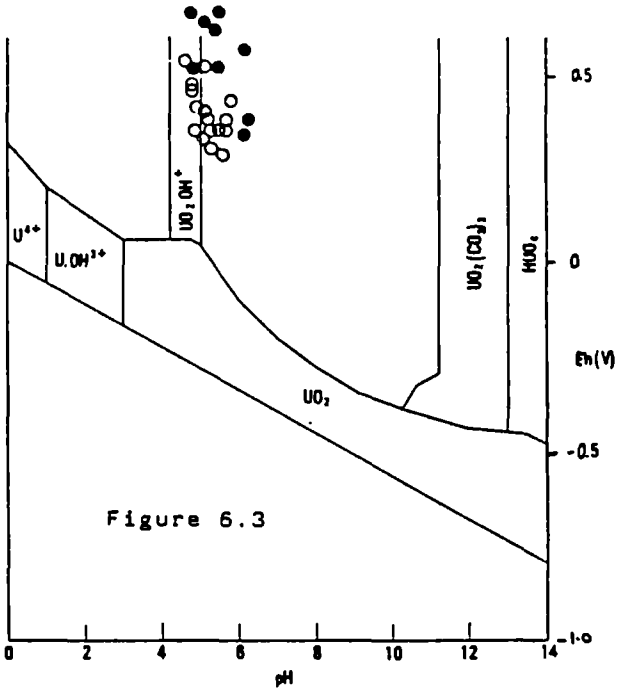

Figure 6.3

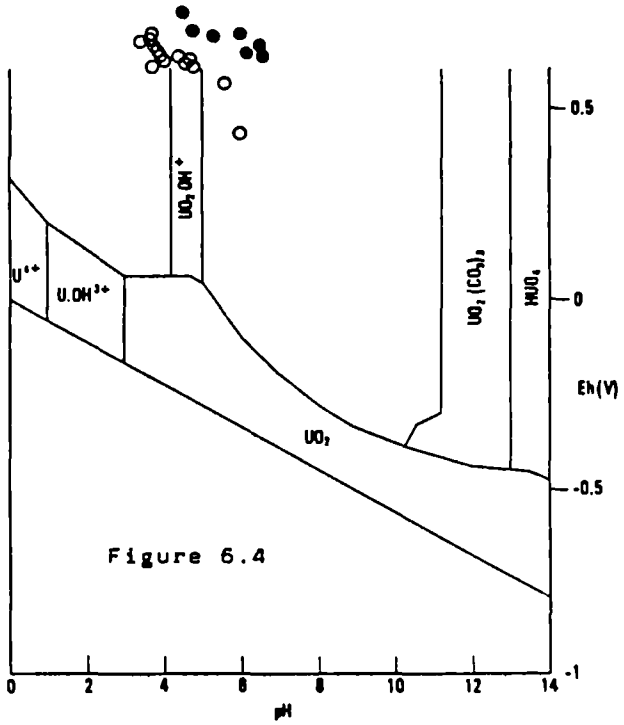

Figure 6.4

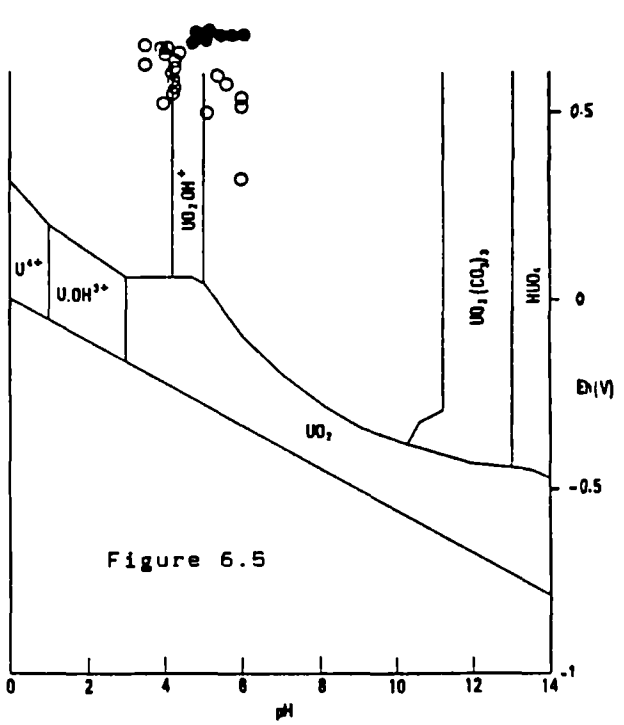

Figure 6.5

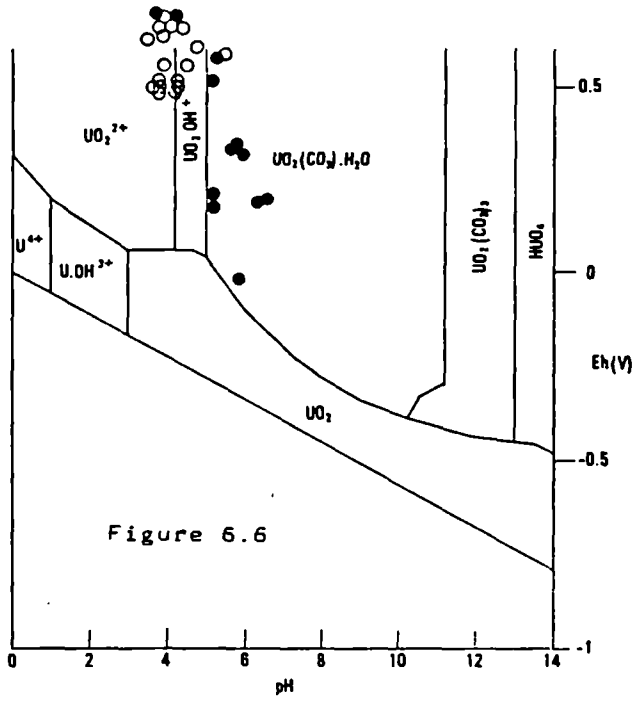

Figure 6.6

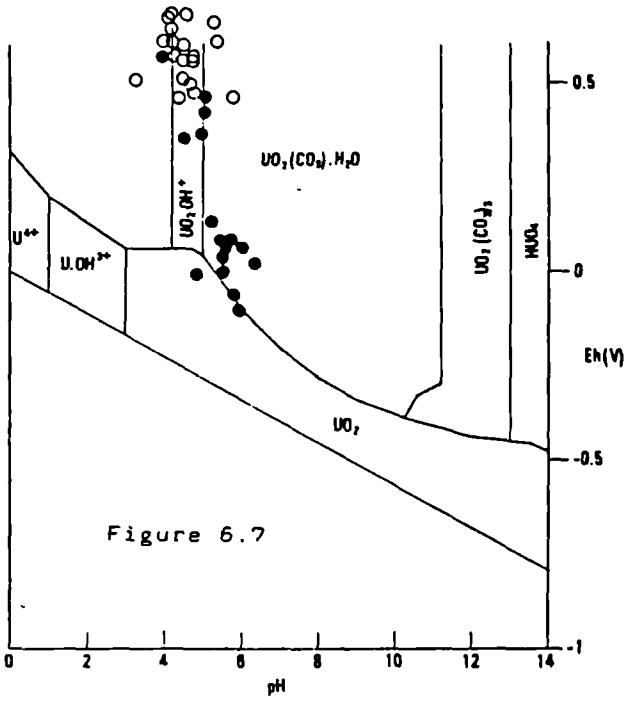

Figure 6.7

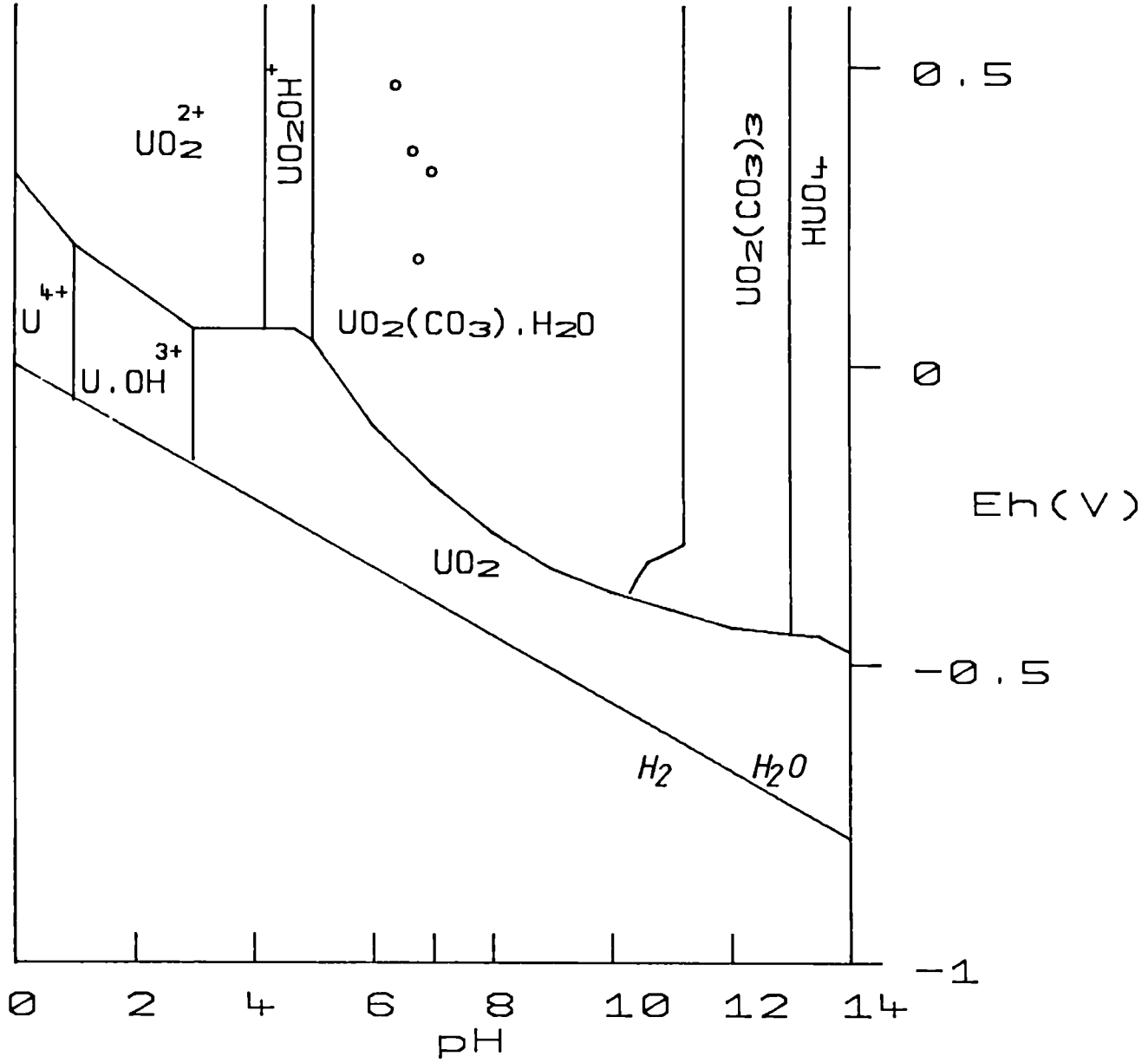
UO_2^{2+}
UO_2OH^+
U^{4+}
$U.OH^{3+}$
$UO_2(CO_3).H_2O$
$UO_2(CO_3)_3$
HUO_4^-
UO_2
H_2
H_2O
0.5
0
−0.5
−1
Eh(V)
0
2
4
6
8
10
12
14
pH

Figure 6.8

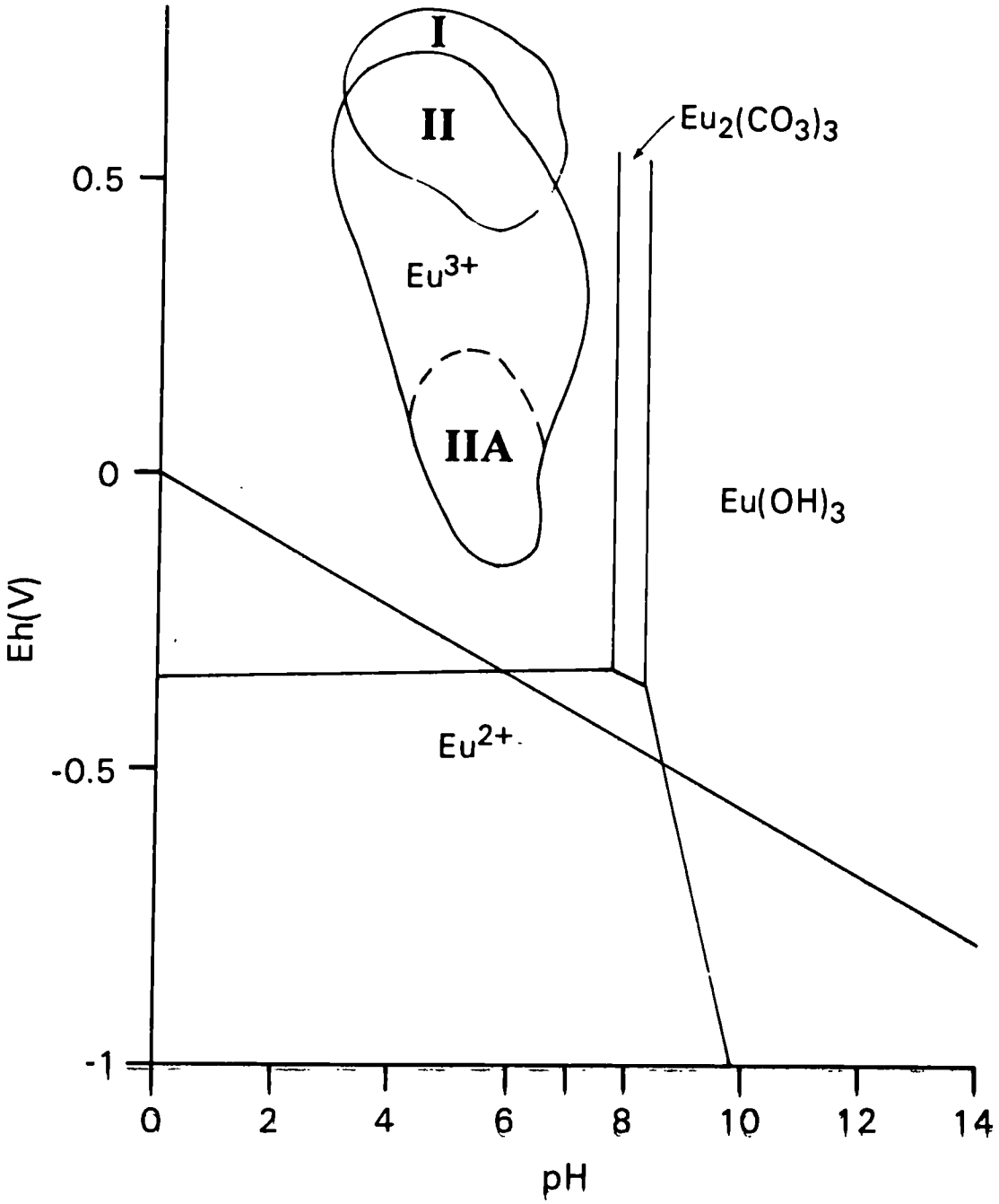

I Field of brown earths
II Field of peats and gleys
III Field of heavily gleyed soils and clays (1968)

Figure 6.9

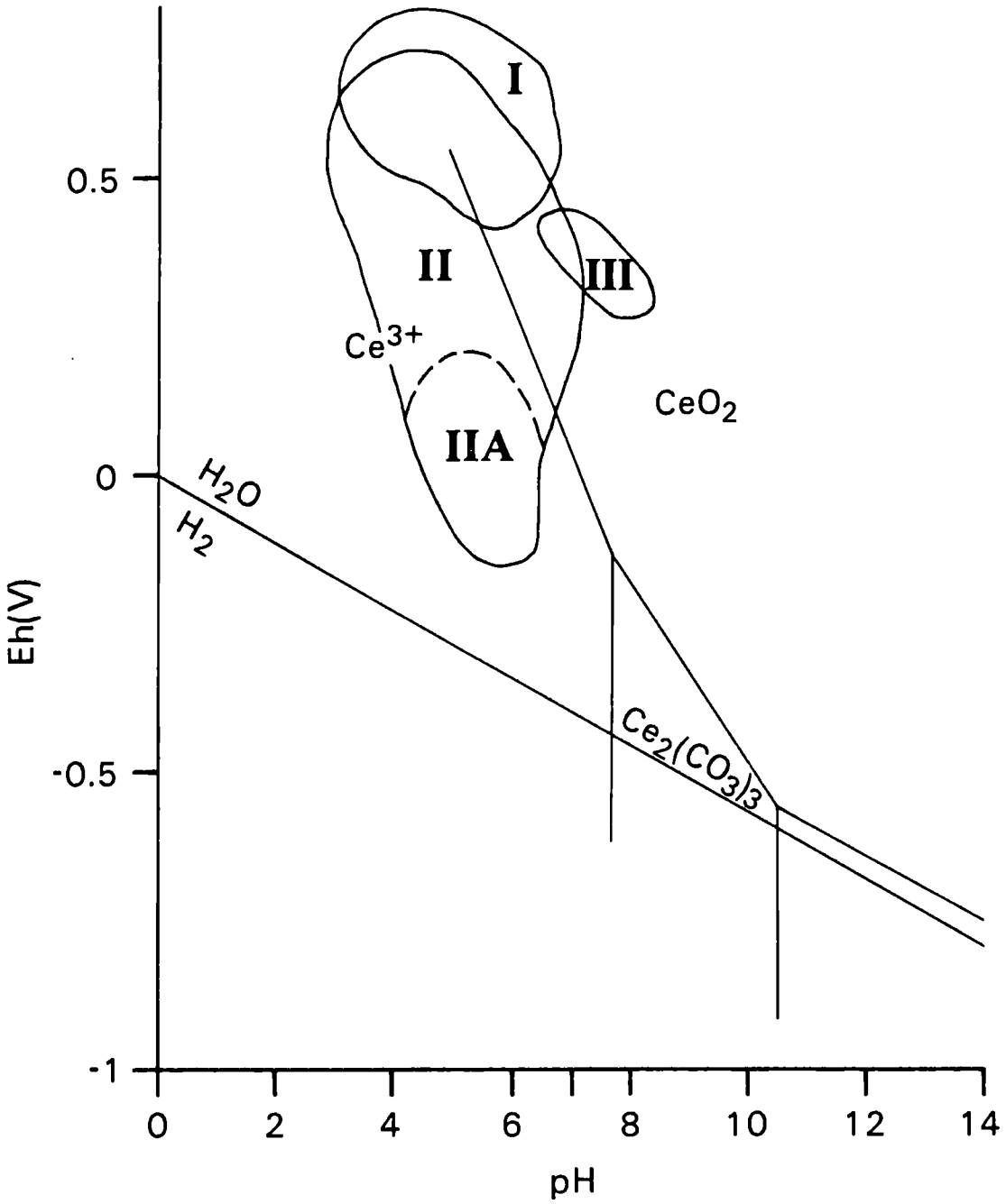

III Field of waters from Pit 8

Figure 6.10 Water Composition

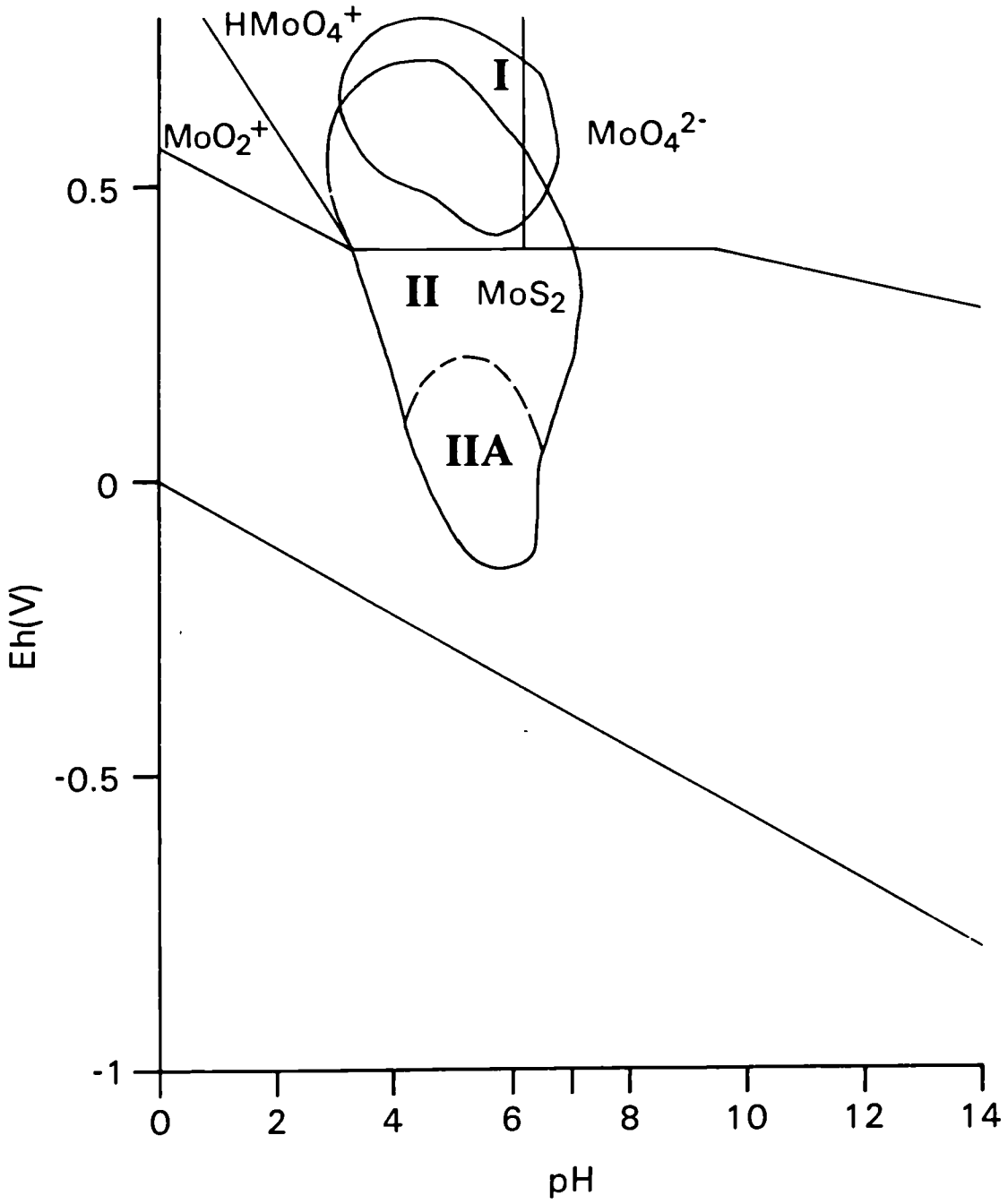

Figure 6.11

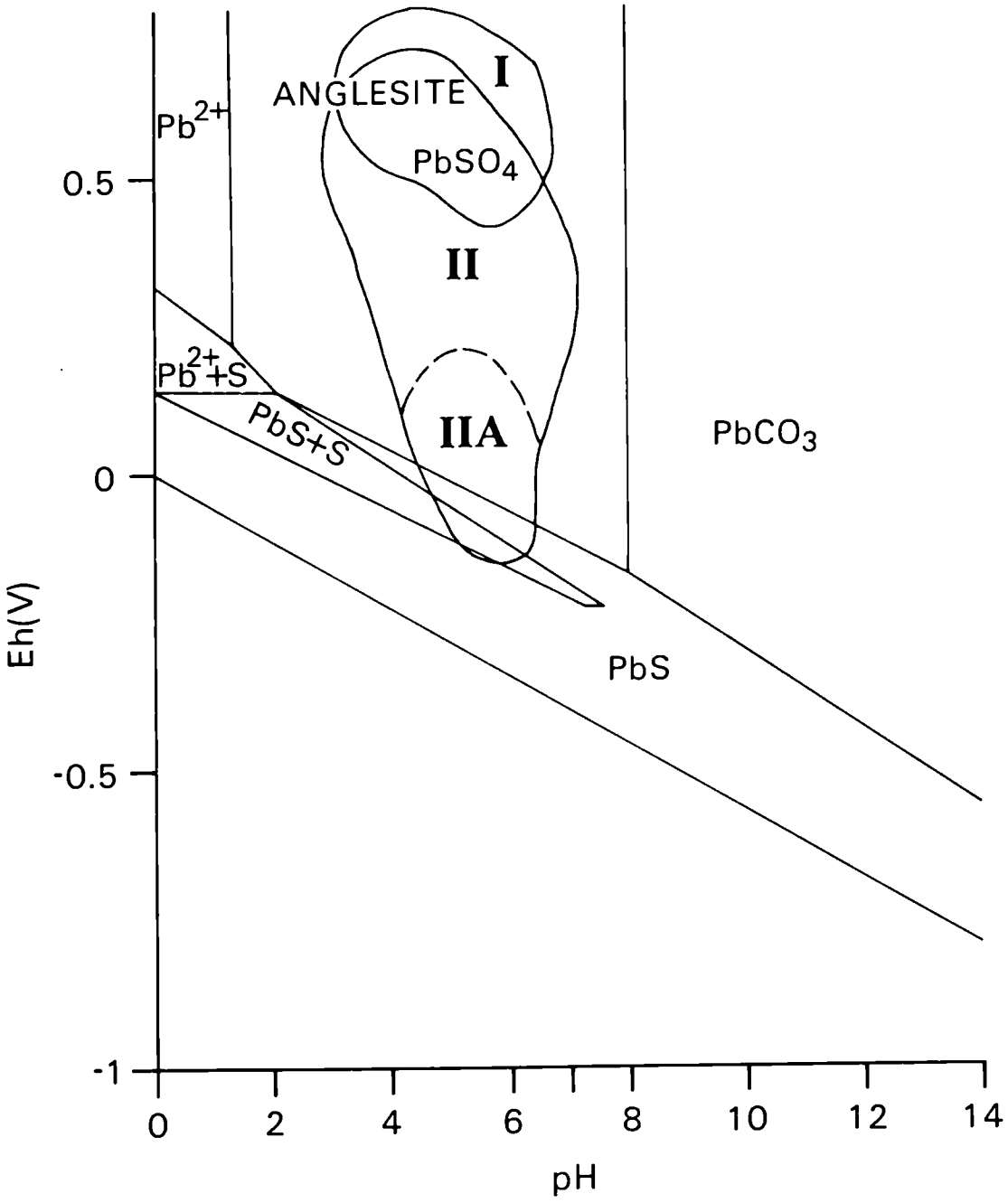
ANGLESITE
I
Pb^{2+}
$PbSO_4$
II
IIA
$Pb^{2+}+S$
PbS+S
$PbCO_3$
PbS
0.5
0
-0.5
-1
Eh(V)
0
2
4
6
8
10
12
14
pH

Figure 6.12

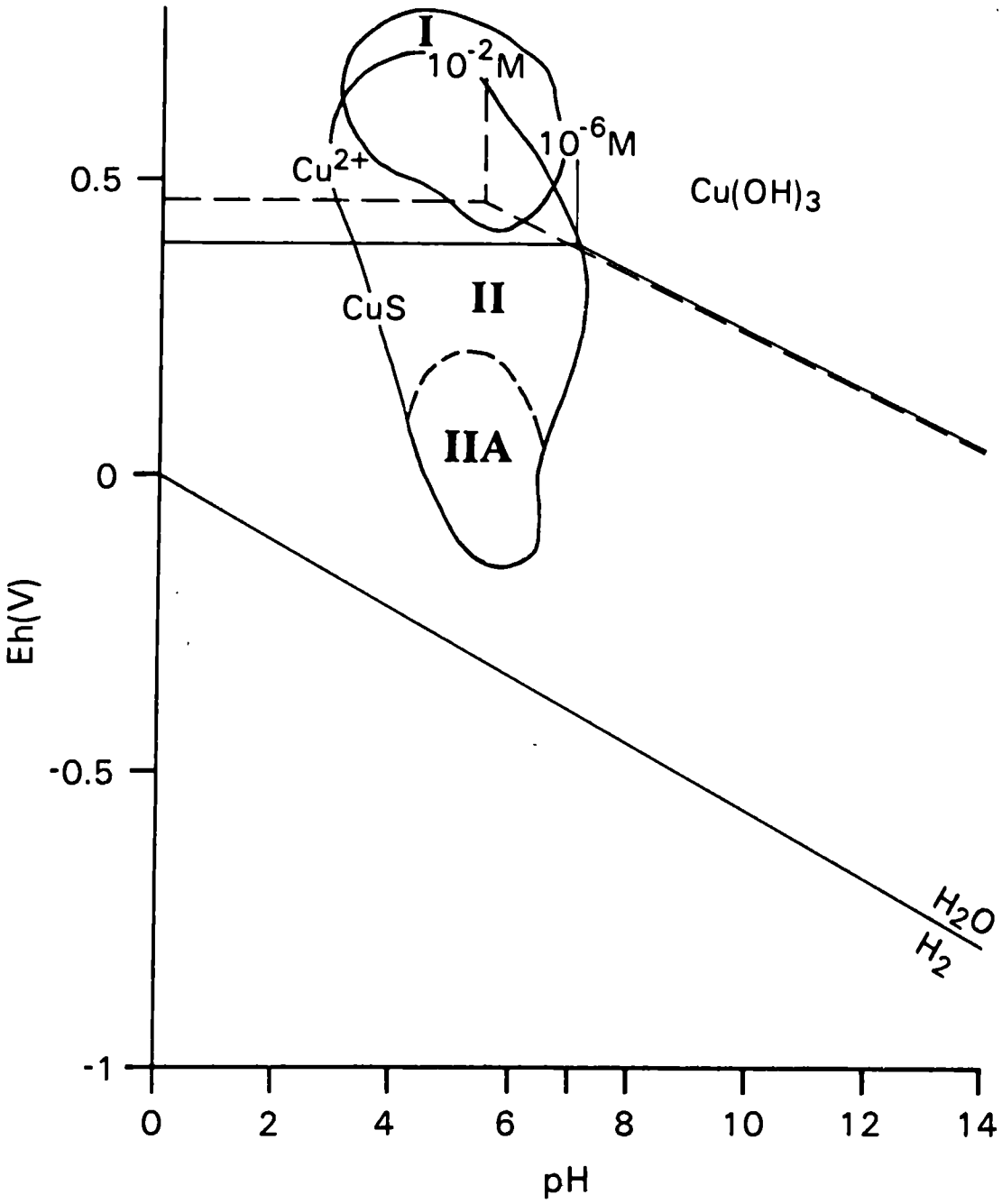
I
10^{-2}M
10^{-6}M
Cu^{2+}
$Cu(OH)_3$
CuS
II
IIA
0.5
0
-0.5
-1
Eh(V)
H_2O
H_2
0
2
4
6
8
10
12
14
pH

Figure 6.13

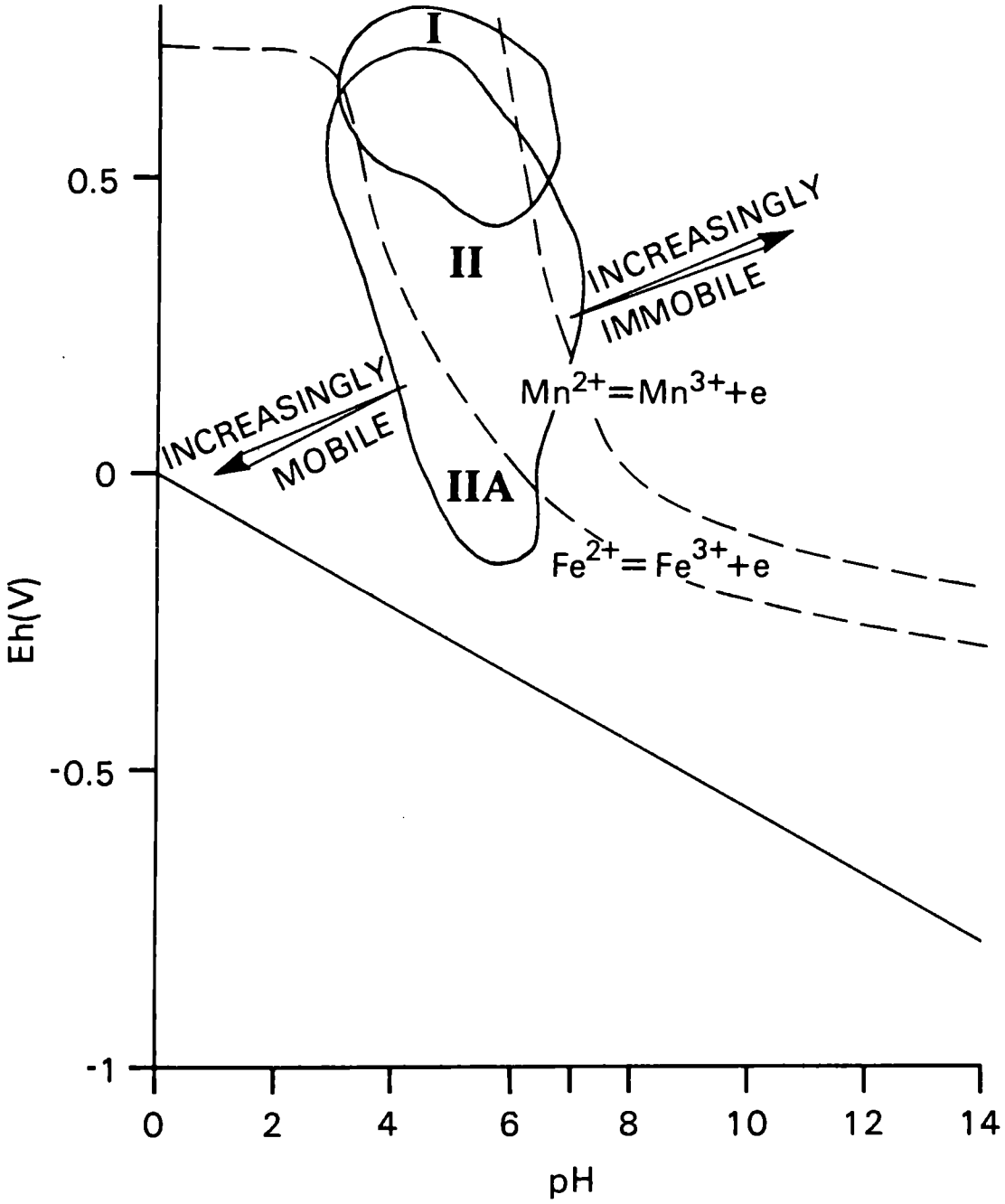
I
II
IIA
INCREASINGLY
IMMOBILE
INCREASINGLY
MOBILE
$Mn^{2+}=Mn^{3+}+e$
$Fe^{2+}=Fe^{3+}+e$
0.5
0
-0.5
-1
Eh(V)
0
2
4
6
8
10
12
14
pH

Figure 6.14

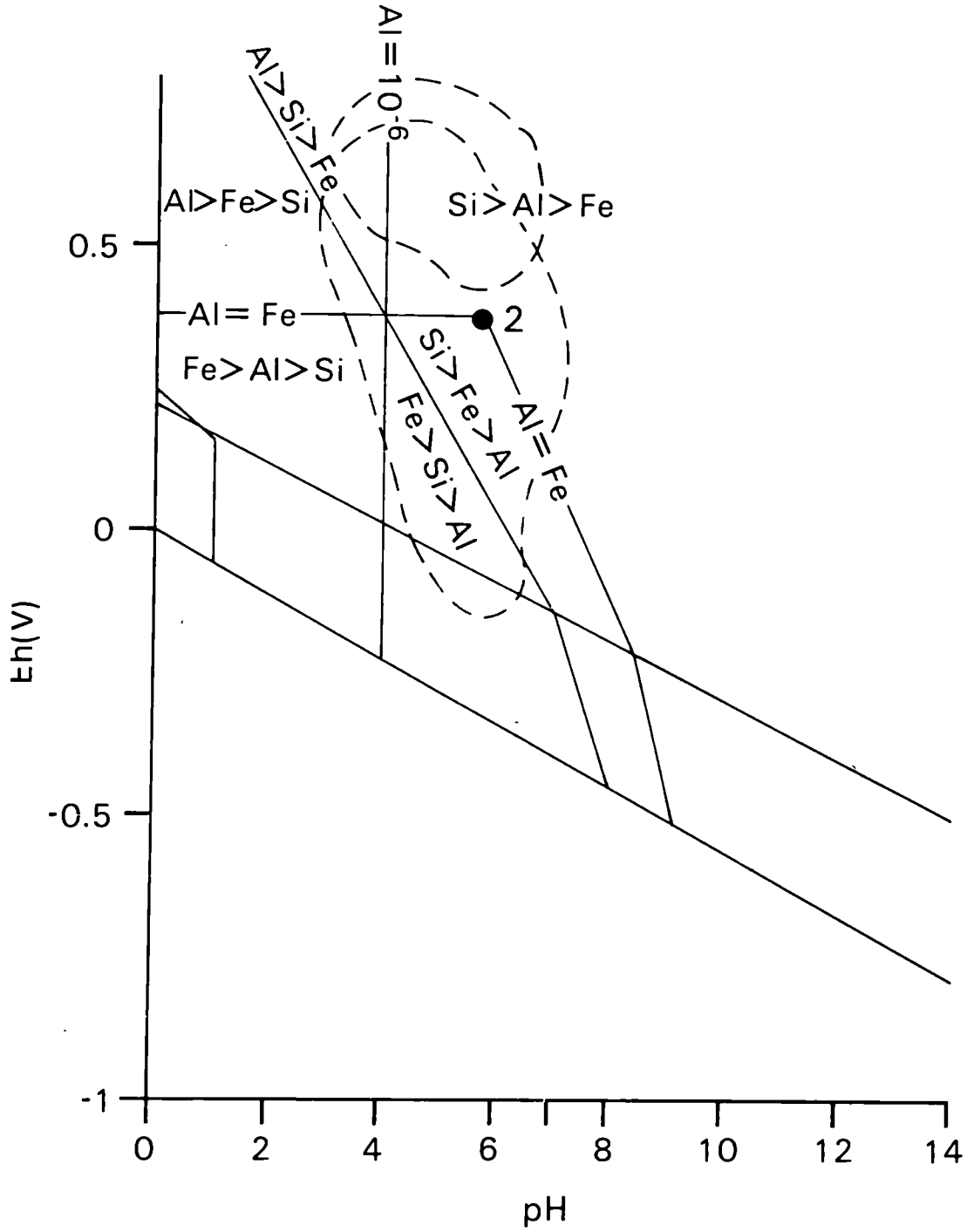

Solubility relationships for Al, Fe and Si in soil environments. Al=Fe represents conditions of equal Al and Fe solubility. Al=10^{-6} and Fe=10^{-6} are solubility levels below which quartz is more soluble than Al and Fe phases.

(From Norton, 1973)

Figure 6.15

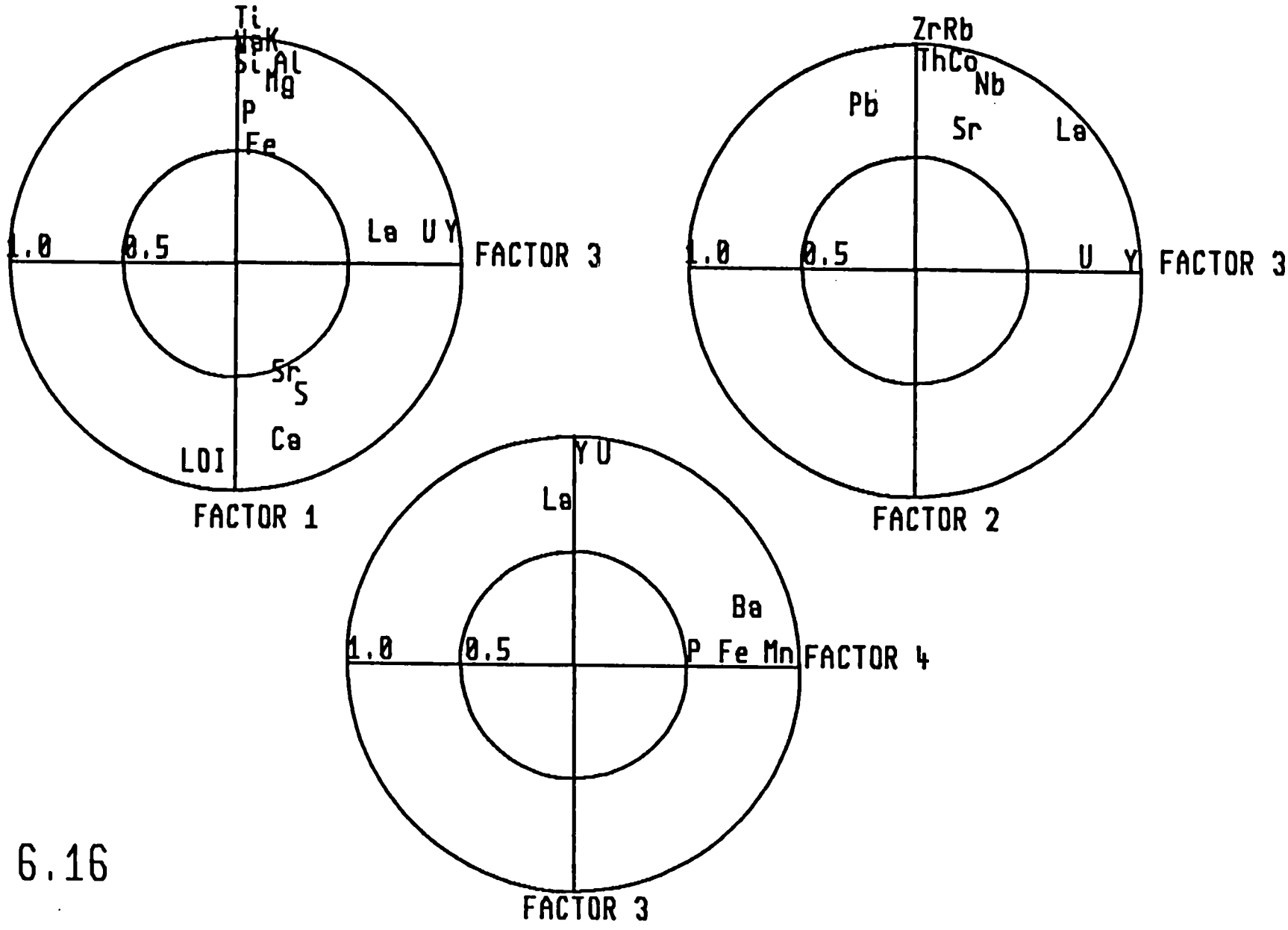
Ti
K
Al
Mg
P
Fe
1.0
0.5
La U Y
FACTOR 3
Sr
S
Ca
LOI
FACTOR 1
ZrRb
ThCo
Nb
Pb
Sr
La
1.0
0.5
U Y
FACTOR 3
FACTOR 2
Y U
La
Ba
1.0
0.5
P Fe Mn
FACTOR 4
FACTOR 3

Fig. 6.16

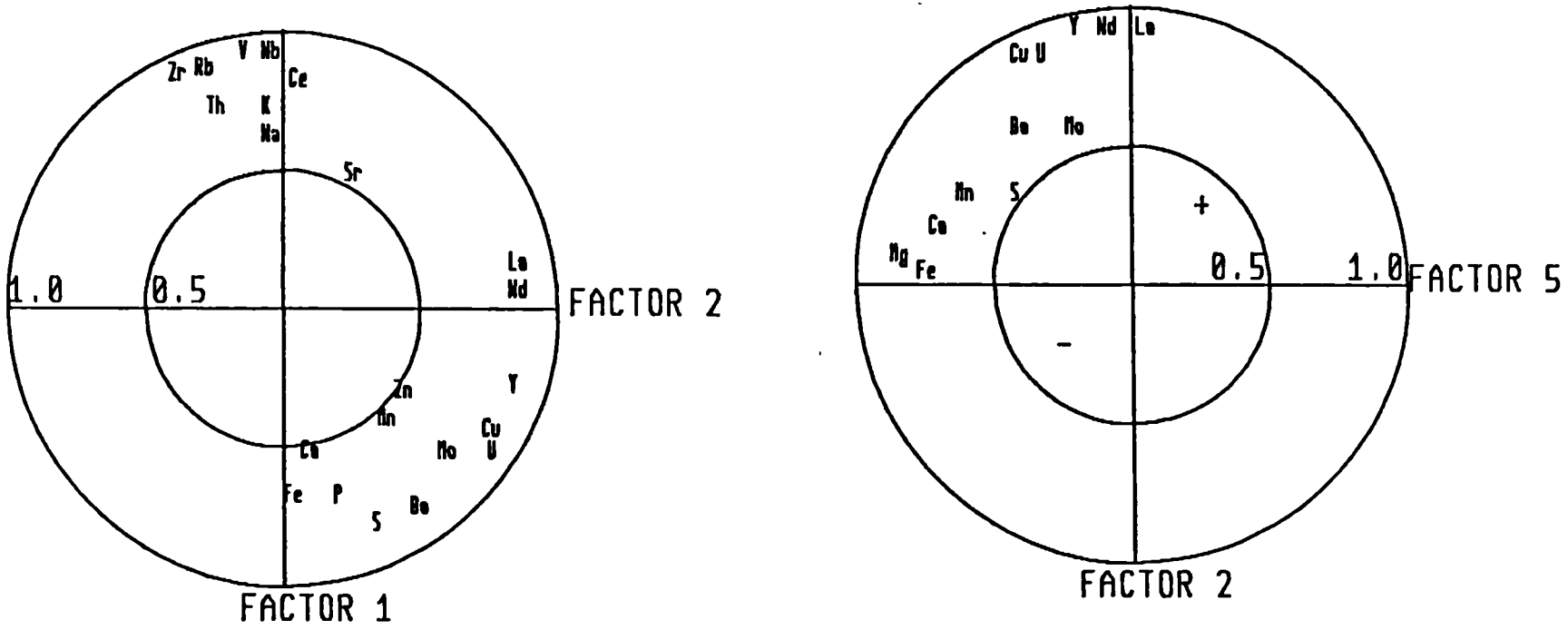
Zr Rb
V Nb
Ce
Th
K
Na
Sr
La
Nd
1.0
0.5
FACTOR 2
Zn
Mn
Y
Cu
U
Ca
Mo
Fe
P
S
Be
FACTOR 1
Y Nd La
Cu U
Be Mo
Mn
S
Ca
Mg
Fe
+
0.5
1.0
FACTOR 5
-
FACTOR 2

Fig. 6.17

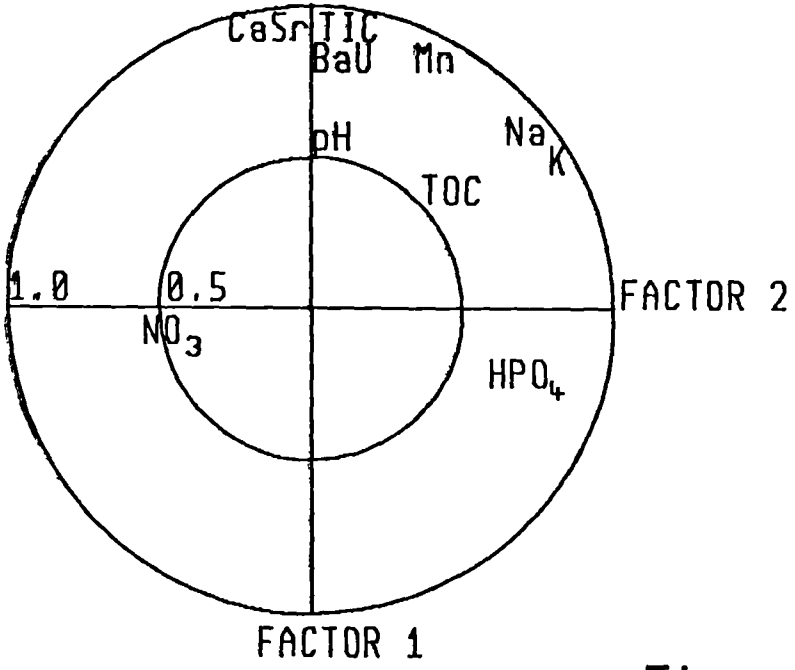
CaSr
TIC
BaU
Mn
pH
Na
K
TOC
1.0
0.5
NO3
HPO4
FACTOR 2
FACTOR 1

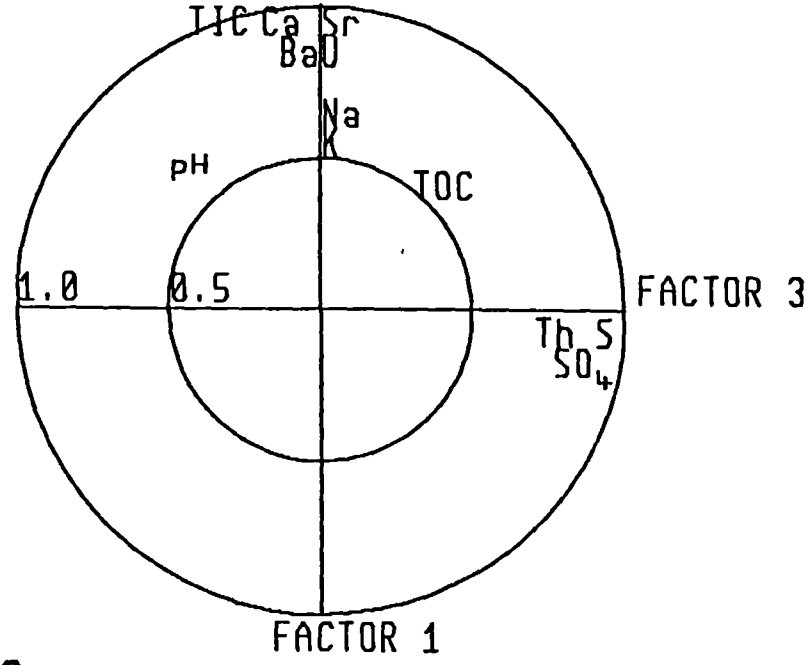
TIC
Ca
Sr
BaU
Na
K
pH
TOC
1.0
0.5
Th
S
SO4
FACTOR 3
FACTOR 1

Fig. 6.18

Table 3.1.
Broubster 1968 Data
Soil line 1

	5917	5918	5919	5920	5921	5922
Distance (m)		3.0	6.1	9.1	12.2	15.2
Peats						
pH	4.8	4.3	5.2	5.2	4.8	4.8
Eh	390.0	430.0	340.0	330.0	440.0	350.0
Gamma uR/hr	9.0	9.5	10.5	10.0	9.5	9.0
U ppm	22.0	25.0	62.0	73.0	114.0	93.0
MnO %	0.180	0.110	0.250	0.290	0.205	0.140
Cu ppm	10.0	15.0	30.0	35.0	55.0	15.0
Pb ppm	30.0	30.0	40.0	30.0	20.0	30.0
Zn ppm	60.0	70.0	100.0	70.0	80.0	50.0
Mo ppm	8.0	4.0	18.0	18.0	3.0	4.0
Clays						
pH	4.8	4.5	5.5	5.0	5.1	5.0
Eh	360.0	545.0	360.0	410.0	355.0	340.0
U ppm	8.0	8.0	9.0	10.0	9.0	12.0
MnO %	0.070	0.075	0.055	0.075	0.040	0.020
Cu ppm	10.0	20.0	20.0	20.0	10.0	30.0
Pb ppm	30.0	30.0	30.0	10.0	30.0	40.0
Zn ppm	80.0	100.0	60.0	80.0	90.0	80.0
Mo ppm	2.0	2.0	4.0	5.0	5.0	2.0

Table 3.1.
Broubster 1968 Data
Soil line 1

	5923	5924	5925	5926	5927	5928
Distance (m)	18.3	21.3	24.4	27.4	30.5	33.5
Peats						
pH	5.3	4.9	4.9	5.4	5.4	5.7
Eh	130.0	370.0	350.0	350.0	350.0	330.0
Gamma uR/hr	9.0	8.5	9.0	9.0	9.5	9.5
U ppm	26.0	16.0	15.0	31.0	57.0	28.0
MnO %	0.060	0.070	0.185	0.130	0.250	0.180
Cu ppm	20.0	15.0	10.0	15.0	25.0	20.0
Pb ppm	10.0	30.0	30.0	20.0	30.0	10.0
Zn ppm	90.0	80.0	60.0	80.0	70.0	50.0
Mo ppm	4.0	3.0	3.0	5.0	2.0	4.0
Clays						
pH	5.5	5.6	4.7	5.2	5.4	5.6
Eh	375.0	390.0	470.0	310.0	360.0	360.0
U ppm	7.0	6.0	11.0	10.0	9.0	6.0
MnO %	0.040	0.030	0.060	0.025	0.040	0.045
Cu ppm	15.0	35.0	15.0	15.0	20.0	20.0
Pb ppm	30.0	40.0	10.0	30.0	30.0	20.0
Zn ppm	80.0	90.0	90.0	80.0	60.0	90.0
Mo ppm	3.0	2.0	4.0	4.0	4.0	3.0

Table 3.1.
Broubster 1968 Data
Soil line 1

	5929	5930	5931	5932	5933	5934
Distance (m)	36.6	39.6	42.7	45.7	48.8	51.8
Peats						
pH	4.8	4.5	4.2	5.1	4.8	4.7
Eh	405.0	610.0	520.0	420.0	240.0	430.0
Gamma uR/hr	11.0	9.0	9.0	12.5	12.5	16.0
U ppm	25.0	15.0	44.0	10.0	71.0	43.0
MnO %	0.075	0.050	0.160	0.055	0.155	0.640
Cu ppm	20.0	20.0	25.0	10.0	25.0	20.0
Pb ppm	10.0	10.0	30.0	10.0	10.0	30.0
Zn ppm	60.0	80.0	230.0	80.0	100.0	160.0
Mo ppm	4.0	3.0	17.0	6.0	12.0	12.0
Clays						
pH	5.2	5.1	5.7	5.5	4.8	5.0
Eh	360.0	390.0	440.0	295.0	420.0	530.0
U ppm	14.0	19.0	31.0	51.0	10.0	8.0
MnO %	0.055	0.075	0.080	0.110	0.050	0.190
Cu ppm	15.0	20.0	20.0	20.0	20.0	15.0
Pb ppm	30.0	30.0	10.0	30.0	10.0	30.0
Zn ppm	50.0	90.0	130.0	100.0	70.0	100.0
Mo ppm	4.0	10.0	8.0	9.0	2.0	2.0

Table 3.1.
Broubster 1968 Data
Soil line 1

	5935	5936	5937
Distance (m)	54.9	57.9	61.0
Peats			
pH	4.9	5.4	4.8
Eh	450.0	330.0	360.0
Gamma uR/hr	11.5	11.0	10.5
U ppm	28.0	43.0	65.0
MnO %	0.130	0.155	0.185
Cu ppm	10.0	10.0	20.0
Pb ppm	30.0	10.0	30.0
Zn ppm	90.0	80.0	70.0
Mo ppm	6.0	8.0	9.0
Clays			
pH	4.9	4.7	5.2
Eh	385.0	480.0	360.0
U ppm	8.0	8.0	12.0
MnO %	0.130	0.130	0.070
Cu ppm	10.0	10.0	10.0
Pb ppm	20.0	0.0	20.0
Zn ppm	90.0	50.0	50.0
Mo ppm	2.0	2.0	2.0

Table 3.2
Broubster 1968 Data
Soil line 2

Distance (m)		3.0	6.1	9.1	12.2	15.2
Surface samples						
pH	4.4	3.8	3.8	3.4	3.7	3.5
Eh mv	560.0	690.0	560.0	630.0	501.0	501.0
Gamma uR/hr	5.5	5.0	5.5	5.5	6.0	6.0
U ppm	3.0	1.0	3.0	5.0	7.0	1.0
MnO %	0.0	0.0	0.1	0.0	0.1	0.1
Cu ppm	5.0	10.0	10.0	10.0	30.0	35.0
Pb ppm	10.0	20.0	10.0	10.0	70.0	20.0
Zn ppm	50.0	20.0	60.0	100.0	80.0	40.0
Mo ppm	2.0	3.0	1.0	8.0	7.0	5.0
Deep Samples						
pH	4.7	3.9	4.4	4.2	4.5	4.4
Eh mv	480.0	610.0	560.0	570.0	680.0	600.0
U ppm	4.0	5.0	4.0	1.0	9.0	4.0
MnO %	0.0	0.1	0.1	0.0	0.1	0.0
Cu ppm	10.0	20.0	15.0	10.0	30.0	10.0
Pb ppm	30.0	20.0	20.0	30.0	30.0	30.0
Zn ppm	90.0	90.0	70.0	40.0	110.0	70.0
Mo ppm	2.0	1.0	2.0	4.0	6.0	2.0

Table 3.2
Broubster 1968 Data
Soil line 2

Distance (m)	18.3	21.3	24.4	27.4	30.5	33.5
Surface samples						
pH	4.1	3.7	4.0	3.6	3.7	3.8
Eh mv	680.0	520.0	665.0	510.0	660.0	660.0
Gamma uR/hr	7.0	8.0	7.5	8.5	8.5	8.0
U ppm	1.0	1.0	1.0	1.0	1.0	1.0
MnO %	0.0	0.0	0.0	0.0	0.0	0.0
Cu ppm	10.0	10.0	15.0	20.0	50.0	40.0
Pb ppm	40.0	10.0	10.0	90.0	40.0	20.0
Zn ppm	40.0	50.0	40.0	30.0	20.0	30.0
Mo ppm	3.0	2.0	3.0	2.0	2.0	4.0
Deep Samples						
pH	4.1	4.0	3.2	4.1	4.1	4.1
Eh mv	660.0	675.0	510.0	680.0	610.0	640.0
U ppm	6.0	7.0	6.0	5.0	5.0	6.0
MnO %	0.2	0.2	0.3	0.1	0.1	0.1
Cu ppm	20.0	10.0	20.0	20.0	15.0	20.0
Pb ppm	30.0	20.0	30.0	30.0	20.0	30.0
Zn ppm	140.0	80.0	100.0	80.0	90.0	110.0
Mo ppm	4.0	4.0	4.0	4.0	4.0	5.0

Table 3.2
Broubster 1968 Data
Soil line 2

Distance (m)	36.6	39.6	42.7	45.7	48.8	51.8
Surface samples						
pH	3.8	3.7	3.7	5.4	4.2	4.7
Eh mv	640.0	530.0	490.0	590.0	520.0	610.0
Gamma uR/hr	7.5	7.5	7.0	7.0	7.0	7.0
U ppm	1.0	2.0	1.0	3.0	4.0	3.0
MnO %	0.0	0.0	0.1	1.1	1.2	0.4
Cu ppm	60.0	15.0	5.0	10.0	5.0	5.0
Pb ppm	70.0	10.0	10.0	40.0	30.0	10.0
Zn ppm	40.0	20.0	20.0	80.0	70.0	50.0
Mo ppm	1.0	2.0	4.0	6.0	0.0	2.0
Deep Samples						
pH	4.4	4.7	4.7	5.2	4.6	5.7
Eh mv	510.0	560.0	570.0	660.0	500.0	460.0
U ppm	7.0	5.0	5.0	5.0	4.0	3.0
MnO %	0.1	0.1	0.5	0.3	0.1	0.1
Cu ppm	20.0	20.0	10.0	10.0	5.0	10.0
Pb ppm	10.0	30.0	60.0	40.0	30.0	20.0
Zn ppm	90.0	100.0	120.0	100.0	70.0	80.0
Mo ppm	8.0	3.0	6.0	3.0	2.0	2.0

Table 3.2
Broubster 1968 Data
Soil line 2

Distance (m)	54.9	57.9	61.0
Surface samples			
pH	4.3	3.7	4.1
Eh mv	660.0	500.0	490.0
Gamma uR/hr	8.0	7.5	7.5
U ppm	4.0	3.0	4.0
MnO %	0.2	0.4	0.5
Cu ppm	10.0	5.0	5.0
Pb ppm	30.0	30.0	30.0
Zn ppm	80.0	60.0	40.0
Mo ppm	4.0	4.0	3.0
Deep Samples			
pH	5.3	4.3	4.5
Eh mv	610.0	460.0	495.0
U ppm	4.0	4.0	6.0
MnO %	0.4	0.1	0.6
Cu ppm	10.0	5.0	5.0
Pb ppm	30.0	20.0	30.0
Zn ppm	90.0	50.0	60.0
Mo ppm	3.0	3.0	4.0

Table 3.3
Broubster 1968 Data
Soil line 3

Distance (m)		3.0	6.1	9.1	12.2	15.2
Surface Samples						
pH	3.5	3.8	3.6	3.7	3.6	3.7
Eh(mv)	690.0	640.0	700.0	660.0	660.0	660.0
Gamma uR/hr	6.0	6.0	7.5	7.5	8.0	8.0
U ppm	2.0	1.0	3.0	3.0	3.0	2.0
MnO %	0.0	0.0	0.0	0.0	0.0	0.0
Cu ppm	5.0	10.0	5.0	5.0	5.0	45.0
Pb ppm	30.0	20.0	10.0	10.0	40.0	20.0
Zn ppm	20.0	40.0	50.0	60.0	50.0	30.0
Mo ppm	2.0	1.0	2.0	3.0	3.0	1.0
Deep samples						
pH	3.9	4.0	4.1	4.2	4.3	3.4
Eh	660.0	665.0	580.0	580.0	660.0	680.0
U ppm	4.0	4.0	4.0	4.0	4.0	4.0
MnO %	0.0	0.0	0.0	0.1	0.0	0.0
Cu ppm	15.0	5.0	10.0	20.0	10.0	15.0
Pb ppm	30.0	20.0	20.0	20.0	20.0	30.0
Zn ppm	100.0	70.0	80.0	90.0	90.0	80.0
Mo ppm	2.0	2.0	3.0	2.0	2.0	4.0

Table 3.3
Broubster 1968 Data
Soil line 3

Distance (m)	18.3	21.3	24.4	27.4	30.5	33.5
Surface Samples						
pH	3.6	3.5	4.3	4.5	4.7	5.5
Eh(mv)	615.0	680.0	640.0	625.0	615.0	570.0
Gamma uR/hr	9.5	10.0	16.0	19.0	22.0	30.0
U ppm	3.0	1.0	5.0	18.0	14.0	20.0
MnO %	0.0	0.0	0.1	0.9	1.7	0.7
Cu ppm	5.0	10.0	50.0	10.0	50.0	20.0
Pb ppm	10.0	20.0	40.0	110.0	110.0	90.0
Zn ppm	30.0	50.0	110.0	180.0	180.0	220.0
Mo ppm	3.0	3.0	3.0	10.0	13.0	13.0
Deep samples						
pH	4.1	4.2	4.2	5.9	5.9	5.5
Eh	610.0	620.0	640.0	520.0	330.0	580.0
U ppm	5.0	6.0	6.0	16.0	12.0	36.0
MnO %	0.1	0.2	0.1	0.4	0.3	0.7
Cu ppm	15.0	20.0	15.0	15.0	20.0	35.0
Pb ppm	30.0	20.0	40.0	140.0	90.0	150.0
Zn ppm	110.0	100.0	90.0	150.0	160.0	290.0
Mo ppm	4.0	4.0	4.0	8.0	7.0	17.0

Table 3.3
Broubster 1968 Data
Soil line 3

Distance (m)	36.6	39.6	42.7	45.7	48.8	51.8
Surface Samples						
pH	5.9	5.5	4.6	3.9	3.3	3.8
Eh(mv)	440.0	570.0	630.0	630.0	680.0	660.0
Gamma uR/hr	50.0	50.0	30.0	24.0	16.0	10.0
U ppm	31.0	41.0	33.0	18.0	5.0	3.0
MnO %	1.4	1.2	0.9	0.2	0.0	0.0
Cu ppm	20.0	35.0	25.0	15.0	10.0	30.0
Pb ppm	110.0	140.0	100.0	70.0	40.0	20.0
Zn ppm	420.0	550.0	610.0	180.0	40.0	30.0
Mo ppm	23.0	20.0	13.0	5.0		1.0
Deep samples						
pH	5.3	5.9	5.3	5.0	3.4	4.2
Eh	600.0	535.0	600.0	505.0	630.0	640.0
U ppm	34.0	44.0	32.0	35.0	26.0	4.0
MnO %	0.3	0.8	0.7	0.3	0.5	0.1
Cu ppm	25.0	40.0	25.0	40.0	30.0	10.0
Pb ppm	90.0	140.0	90.0	120.0	90.0	30.0
Zn ppm	510.0	600.0	550.0	540.0	250.0	70.0
Mo ppm	15.0	27.0	13.0	18.0	17.0	2.0

Table 3.3
Broubster 1968 Data
Soil line 3

Distance (m)	54.9	57.9	61.0
Surface Samples			
pH	3.7	3.5	3.6
Eh(mv)	670.0	680.0	680.0
Gamma uR/hr	9.0	7.0	7.0
U ppm	2.0	1.0	2.0
MnO %	0.0	0.0	0.0
Cu ppm	15.0	25.0	30.0
Pb ppm	40.0	20.0	10.0
Zn ppm	50.0	30.0	30.0
Mo ppm	4.0	2.0	2.0
Deep samples			
pH	3.9	4.2	3.8
Eh	530.0	570.0	670.0
U ppm	5.0	4.0	4.0
MnO %	0.3	0.2	0.1
Cu ppm	5.0	10.0	10.0
Pb ppm	50.0	20.0	20.0
Zn ppm	80.0	90.0	80.0
Mo ppm	3.0	3.0	3.0

TABLE 3.4, 1986 Traverse

sample	Depth	DISTANCE	SiO2	Al2O3	TiO2	Fe2O3	MgO
B-30M SURF.		-30.00	51.00	10.47	0.63	5.96	0.81
B-25M SURF		-25.00	53.27	10.34	0.60	3.93	0.83
B-15 SURF		-15.00	33.26	8.03	0.49	8.18	0.48
B-10M SURF		-10.00	17.94	5.65	0.34	6.84	0.45
B-5M SURF		-5.00	12.99	4.48	0.26	6.84	0.29
B 0M SURF		0.00	11.44	4.13	0.23	7.51	0.23
B+10M SURF		10.00	10.51	3.44	0.22	10.94	0.27
B+15M SURF		15.00	8.92	3.27	0.23	11.43	0.23
B+20M SURF		20.00	9.62	3.16	0.24	8.51	0.17
B+25M SURF		25.00	10.47	3.37	0.19	0.86	0.38
B+30M SURF		30.00	9.25	3.00	0.20	0.78	0.40
B+35M SURF		35.00	8.71	2.62	0.21	2.49	0.31
B+40M SURF		40.00	12.38	2.60	0.22	2.15	0.12
,-30m 30-	35.00	-30.00	70.63	13.56	0.70	3.82	1.33
,-25M 25	25.00	-25.00	69.82	13.02	0.73	5.39	1.30
,-20M 35	35.00	-20.00	68.88	14.30	0.66	4.04	1.98
,-15M 47	47.00	-15.00	69.87	14.05	0.61	3.55	2.09
,-10M 22	22.00	-10.00	30.68	8.22	0.47	6.13	0.58
,-5M 27	27.00	-5.00	14.29	5.27	0.29	7.28	0.31
,0M 40	40.00	0.00	12.72	4.75	0.26	6.84	0.33
,5M 15	15.00	5.00	10.74	4.04	0.23	9.97	0.24
,10M 40	40.00	10.00	3.92	2.55	0.14	4.05	0.17
,15M 42	42.00	15.00	3.28	1.75	0.09	2.50	0.18
,20M 48	48.00	20.00	5.01	1.85	0.10	2.74	0.17
,25M 20	20.00	25.00	53.61	10.37	0.63	6.11	0.71
,30M 52	52.00	30.00	3.98	2.18	0.13	0.76	0.22
,35M 65	65.00	35.00	0.00	0.57	0.04	1.06	0.21
,40M 65	65.00	40.00	0.45	0.73	0.05	1.43	0.11
,5m 47	47.00	5.00	9.15	3.91	0.20	4.81	0.28
,10m 80	80.00	10.00	70.56	13.61	0.59	3.63	1.98
,0m 65	65.00	0.00	71.08	13.81	0.68	2.91	1.53
,-5M 42	42.00	-5.00	73.75	13.41	0.69	1.27	0.58
,-10M 42	42.00	-10.00	69.92	14.13	0.59	3.34	1.82
,-5M 62	62.00	-5.00	70.15	13.76	0.65	3.76	2.05
,-15M 37	37.00	-15.00	75.78	12.41	0.67	1.51	0.72
,-15M 28	28.00	-15.00	47.85	9.68	0.57	4.77	0.60
,10m 75	75.00	10.00	72.00	12.76	0.77	2.91	1.50
,5m 62	62.00	5.00	76.28	11.93	0.43	2.04	0.94
,5m 52	52.00	5.00	73.32	13.06	0.70	2.16	0.99
,25m 90	90.00	25.00	9.59	3.05	0.17	0.64	0.33
,-30m 55	55.00	-30.00	70.54	13.24	0.53	4.23	2.11
,15m 85	85.00	15.00	69.86	13.81	0.64	3.74	2.01
,-15m 48	48.00	-15.00	69.87	14.05	0.61	3.55	2.09
,25m 45	45.00	25.00	1.21	0.96	0.05	4.49	0.19
,-15m 60	60.00	-15.00	68.37	14.71	0.64	3.95	2.39
,20m 90	90.00	20.00	2.78	2.01	0.09	3.45	0.20
,-20m 28	28.00	-20.00	74.54	12.56	0.59	1.80	0.72
,15m 68	68.00	15.00	76.38	10.92	0.79	1.40	0.57
,20m 110	110.00	20.00	67.66	14.03	0.65	4.33	1.99
,20m 10	10.00	20.00	47.10	9.47	0.59	5.71	0.63
,30m 80	80.00	30.00	0.00	0.62	0.02	1.89	0.13
,30m 112	112.00	30.00	71.98	13.34	0.58	3.34	1.89
,40m 125	125.00	40.00	0.00	0.75	0.05	1.24	0.19
,40m 180	180.00	40.00	79.80	10.09	0.53	1.07	0.41
,35 130	130.00	35.00	0.00	1.05	0.04	1.07	0.19
,35m 120	120.00	35.00	0.00	0.40	0.02	2.05	0.14

TABLE 3.4, 1986 Traverse

sample	CaO	Na2O	K2O	MnO	P2O5	LOI	Total
B-30M SUR	0.58	1.62	2.11	0.92	0.20	25.74	100.04
B-25M SUR	0.69	1.75	2.22	0.49	0.22	25.69	100.03
B-15 SURF	1.25	0.95	1.36	0.47	0.37	45.04	99.90
B-10M SUR	2.34	0.60	0.68	0.54	0.52	63.93	99.83
B-5M SURF	3.37	0.42	0.52	0.58	0.43	69.87	100.06
B 0M SURF	3.60	0.23	0.43	1.52	0.42	70.38	100.12
B+10M SUR	2.85	0.24	0.45	0.39	0.37	70.48	100.15
B+15M SUR	2.93	0.24	0.37	1.20	0.37	70.90	100.09
B+20M SUR	2.02	0.39	0.43	0.26	0.42	74.88	100.11
B+25M SUR	4.68	0.38	0.59	0.04	0.27	78.86	100.10
B+30M SUR	5.00	0.29	0.50	0.05	0.24	80.36	100.07
B+35M SUR	2.20	0.15	0.42	0.31	0.36	82.36	100.13
B+40M SUR	1.60	0.36	0.62	0.00	0.36	79.47	99.87
,-30m 30-	0.42	2.31	3.58	0.12	0.03	3.53	100.04
,-25M 25	0.39	2.38	3.12	0.12	0.04	3.71	100.02
,-20M 35	0.53	2.61	3.75	0.07	0.05	3.02	99.89
,-15M 47	0.54	2.57	3.57	0.04	0.07	2.84	99.81
,-10M 22	2.05	0.90	1.31	0.37	0.35	49.03	100.09
,-5M 27	3.70	0.36	0.60	0.50	0.40	67.31	100.32
,0M 40	4.03	0.29	0.48	0.81	0.34	69.04	99.99
,5M 15	3.18	0.20	0.42	2.91	0.38	67.80	100.13
,10M 40	6.00	0.06	0.18	0.17	0.21	82.81	100.26
,15M 42	5.35	0.00	0.17	0.20	0.18	86.06	99.77
,20M 48	4.23	0.28	0.27	0.23	0.16	84.64	99.70
,25M 20	0.53	1.81	2.05	0.53	0.19	23.50	100.04
,30M 52	5.91	0.18	0.21	0.00	0.13	86.13	99.84
,35M 65	7.06	0.04	0.01	0.04	0.10	90.52	99.65
,40M 65	6.56	0.00	0.03	0.03	0.12	90.32	99.82
,5m 47	4.33	0.23	0.42	0.72	0.34	75.65	100.05
,10m 80	0.51	2.14	3.65	0.04	0.06	3.11	99.89
,0m 65	0.48	2.58	3.80	0.03	0.02	2.87	99.79
,-5M 42	0.49	2.32	4.14	0.02	0.02	3.23	99.91
,-10M 42	0.49	2.59	3.91	0.03	0.05	2.84	99.73
,-5M 62	0.43	2.16	4.28	0.05	0.08	2.70	100.08
,-15M 37	0.37	2.57	3.66	0.02	0.03	2.27	100.00
,-15M 28	0.97	1.49	2.15	0.19	0.23	31.58	100.08
,10m 75	0.48	2.97	3.00	0.01	0.07	3.64	100.11
,5m 62	0.53	2.51	3.36	0.03	0.03	1.87	99.96
,5m 52	0.41	2.40	3.92	0.02	0.03	3.07	100.08
,25m 90	5.84	0.32	0.48	0.01	0.21	79.45	100.08
,-30m 55	0.55	2.63	3.48	0.04	0.10	2.65	100.08
,15m 85	0.51	2.39	3.72	0.05	0.07	3.04	99.84
,-15m 48	0.54	2.57	3.57	0.04	0.07	2.84	99.81
,25m 45	9.54	0.05	0.11	0.05	0.19	83.36	100.20
,-15m 60	0.55	2.49	4.00	0.01	0.09	2.61	99.80
,20m 90	5.82	0.05	0.17	0.12	0.19	84.99	99.87
,-20m 28	0.39	2.45	3.68	0.02	0.03	3.15	99.94
,15m 68	0.46	2.67	3.39	0.00	0.07	3.54	100.21
,20m 110	0.55	2.26	3.69	0.05	0.06	4.24	99.51
,20m 10	0.46	1.51	1.91	0.64	0.23	31.72	99.99
,30m 80	9.14	0.08	0.03	0.01	0.10	88.25	100.26
,30m 112	0.53	2.39	3.60	0.03	0.09	2.31	100.10
,40m 125	6.54	0.00	0.00	0.01	0.13	90.73	99.65
,40m 180	0.28	1.50	3.79	0.01	0.12	2.28	99.87
,35 130	7.04	0.04	0.01	0.02	0.08	90.85	100.39
,35m 120	7.42	0.00	0.00	0.00	0.08	90.12	100.23

TABLE 3.4, 1986 Traverse

sample	Ba	Ce	Co	Cs	La	Nb	Pb
B-30M SUR	3082.00	137.00	41.00	1.00	74.00	26.00	69.00
B-25M SUR	929.00	30.00	5.00	0.50	19.00	7.00	16.00
B-15 SURF	1195.00	22.00	7.00	1.00	23.00	8.00	16.00
B-10M SUR	1107.00	26.00	6.00	0.50	31.00	8.00	36.00
B-5M SURF	1246.00	14.00	4.00	0.50	31.00	8.00	18.00
B 0M SURF	1678.00	12.00	7.00	1.00	21.00	6.00	11.00
B+10M SUR	1773.00	8.00	9.00	0.50	14.00	5.00	15.00
B+15M SUR	2113.00	0.01	12.00	0.50	16.00	6.00	19.00
B+20M SUR	992.00	0.01	6.00	2.00	10.00	5.00	33.00
B+25M SUR	755.00	23.00	3.00	0.50	38.00	4.00	22.00
B+30M SUR	819.00	17.00	3.00	1.00	31.00	4.00	18.00
B+35M SUR	763.00	26.00	8.00	0.50	24.00	5.00	30.00
B+40M SUR	480.00	11.00	0.01	0.50	19.00	5.00	26.00
,-30m 30-	1554.00	117.00	7.00	0.05	77.00	31.00	33.00
,-25M 25	1784.00	132.00	28.00	1.00	75.00	28.00	42.00
,-20M 35	1904.00	120.00	38.00	1.00	72.00	29.00	50.00
,-15M 47	1758.00	95.00	33.00	2.00	64.00	25.00	48.00
,-10M 22	1667.00	23.00	5.00	0.50	46.00	9.00	15.00
,-5M 27	1671.00	17.00	7.00	0.50	57.00	9.00	15.00
,0M 40	1166.00	15.00	4.00	1.00	27.00	7.00	10.00
,5M 15	3935.00	0.01	9.00	0.50	24.00	6.00	13.00
,10M 40	2184.00	0.01	5.00	2.00	34.00	6.00	7.00
,15M 42	1015.00	0.01	3.00	0.50	18.00	5.00	7.00
,20M 48	1115.00	0.01	4.00	1.00	17.00	3.00	5.00
,25M 20	844.00	29.00	11.00	0.50	20.00	8.00	15.00
,30M 52	592.00	0.01	3.00	0.50	15.00	4.00	7.00
,35M 65	688.00	0.01	1.00	0.50	7.00	2.00	1.00
,40M 65	1044.00	0.01	0.01	0.50	10.00	3.00	3.00
,5m 47	2488.00	11.00	5.00	0.50	43.00	8.00	11.00
,10m 80	1653.00	111.00	33.00	2.00	60.00	26.00	54.00
,0m 65	1860.00	74.00	24.00	2.00	57.00	28.00	47.00
,-5M 42	2139.00	85.00	5.00	2.00	59.00	30.00	38.00
,-10M 42	1772.00	107.00	32.00	0.50	55.00	25.00	47.00
,-5M 62	1641.00	110.00	27.00	1.00	75.00	28.00	49.00
,-15M 37	1868.00	90.00	13.00	1.00	49.00	31.00	33.00
,-15M 28	950.00	28.00	3.00	0.50	19.00	9.00	14.00
,10m 75	1593.00	82.00	20.00	1.00	62.00	30.00	38.00
,5m 62	1619.00	62.00	13.00	0.50	42.00	19.00	41.00
,5m 52	1928.00	94.00	16.00	1.00	50.00	29.00	43.00
,25m 90	2866.00	149.00	34.00	1.00	79.00	28.00	48.00
,-30m 55	1589.00	152.00	36.00	1.00	63.00	25.00	42.00
,15m 85	1612.00	118.00	28.00	2.00	71.00	25.00	49.00
,-15m 48	1758.00	95.00	33.00	2.00	64.00	25.00	48.00
,25m 45	491.00	10.00	4.00	0.50	39.00	3.00	6.00
,-15m 60	1718.00	120.00	38.00	1.00	63.00	28.00	47.00
,20m 90	709.00	11.00	3.00	1.00	46.00	5.00	6.00
,-20m 28	1632.00	117.00	32.00	2.00	77.00	25.00	49.00
,15m 68	1830.00	111.00	40.00	0.50	75.00	28.00	43.00
,20m 110	2413.00	108.00	19.00	0.50	62.00	28.00	45.00
,20m 10	960.00	34.00	7.00	0.50	25.00	7.00	17.00
,30m 80	486.00	0.01	3.00	1.00	29.00	3.00	5.00
,30m 112	486.00	23.00	8.00	0.50	17.00	7.00	13.00
,40m 125	693.00	0.01	0.01	0.50	9.00	2.00	0.50
,40m 180	1347.00	159.00	12.00	1.00	97.00	22.00	47.00
,35 130	1.00	0.01	0.01	0.50	4.00	0.50	0.50
,35m 120	550.00	0.01	0.01	0.50	6.00	2.00	3.00

TABLE 3.4, 1986 Traverse

sample	Rb	S	Sr	Th	U	Y	Zr
B-30M SUR	129.00	11959.00	238.00	17.00	88.00	71.00	430.00
B-25M SUR	35.00	3993.00	73.00	6.00	25.00	19.00	106.00
B-15 SURF	20.00	8849.00	63.00	7.00	125.00	43.00	86.00
B-10M SUR	14.00	13439.00	68.00	4.00	224.00	90.00	63.00
B-5M SURF	13.00	14344.00	84.00	5.00	320.00	106.00	62.00
B 0M SURF	10.00	11476.00	84.00	2.00	240.00	83.00	51.00
B+10M SUR	8.00	14095.00	67.00	3.00	168.00	45.00	45.00
B+15M SUR	8.00	16514.00	71.00	4.00	184.00	59.00	47.00
B+20M SUR	7.00	6023.00	57.00	4.00	153.00	51.00	56.00
B+25M SUR	16.00	30049.00	116.00	6.00	147.00	105.00	43.00
B+30M SUR	12.00	29202.00	122.00	5.00	111.00	85.00	46.00
B+35M SUR	10.00	16472.00	87.00	3.00	92.00	22.00	49.00
B+40M SUR	8.00	15608.00	59.00	6.00	65.00	22.00	47.00
,-30m 30-	173.00	10955.00	315.00	13.00	41.00	63.00	425.00
,-25M 25	206.00	824.00	305.00	18.00	6.00	55.00	490.00
,-20M 35	238.00	518.00	439.00	16.00	6.00	52.00	464.00
,-15M 47	226.00	934.00	437.00	16.00	10.00	40.00	440.00
,-10M 22	24.00	11198.00	79.00	7.00	270.00	133.00	87.00
,-5M 27	15.00	17538.00	92.00	5.00	495.00	176.00	66.00
,0M 40	13.00	7302.00	87.00	5.00	350.00	114.00	54.00
,5M 15	9.00	14577.00	74.00	3.00	205.00	73.00	47.00
,10M 40	9.00	30128.00	129.00	3.00	376.00	135.00	38.00
,15M 42	8.00	15530.00	122.00	4.00	259.00	76.00	18.00
,20M 48	6.00	17980.00	105.00	5.00	146.00	70.00	24.00
,25M 20	32.00	2901.00	68.00	8.00	26.00	23.00	120.00
,30M 52	7.00	45147.00	132.00	5.00	74.00	37.00	22.00
,35M 65	1.00	48032.00	149.00	3.00	27.00	14.00	14.00
,40M 65	0.50	42461.00	144.00	1.00	25.00	13.00	19.00
,5m 47	16.00	21251.00	108.00	3.00	491.00	154.00	52.00
,10m 80	213.00	1957.00	396.00	17.00	11.00	39.00	443.00
,0m 65	241.00	723.00	415.00	10.00	17.00	38.00	481.00
,-5M 42	249.00	1386.00	446.00	12.00	50.00	53.00	486.00
,-10M 42	231.00	563.00	451.00	11.00	17.00	43.00	424.00
,-5M 62	233.00	559.00	324.00	17.00	14.00	39.00	506.00
,-15M 37	219.00	900.00	386.00	13.00	19.00	38.00	532.00
,-15M 28	30.00	4465.00	78.00	5.00	119.00	39.00	110.00
,10m 75	188.00	3105.00	273.00	19.00	23.00	64.00	511.00
,5m 62	181.00	1389.00	543.00	10.00	8.00	32.00	465.00
,5m 52	261.00	1899.00	354.00	13.00	24.00	46.00	492.00
,25m 90	121.00	11736.00	249.00	18.00	103.00	86.00	429.00
,-30m 55	210.00	680.00	419.00	17.00	2.00	46.00	431.00
,15m 85	225.00	4738.00	400.00	17.00	21.00	36.00	447.00
,-15m 48	226.00	934.00	437.00	16.00	10.00	40.00	440.00
,25m 45	5.00	85032.00	129.00	3.00	240.00	114.00	6.00
,-15m 60	245.00	428.00	401.00	16.00	10.00	43.00	433.00
,20m 90	8.00	56670.00	111.00	5.00	246.00	126.00	17.00
,-20m 28	218.00	4891.00	355.00	16.00	14.00	66.00	408.00
,15m 68	231.00	911.00	366.00	16.00	8.00	42.00	468.00
,20m 110	217.00	1784.00	461.00	16.00	9.00	43.00	469.00
,20m 10	31.00	4491.00	62.00	6.00	26.00	21.00	111.00
,30m 80	4.00	63676.00	134.00	5.00	188.00	100.00	1.00
,30m 112	53.00	792.00	113.00	4.00	3.00	13.00	113.00
,40m 125	0.50	55335.00	132.00	3.00	26.00	12.00	13.00
,40m 180	191.00	5136.00	255.00	8.00	11.00	54.00	496.00
,35 130	0.50	332.00	7.00	4.00	2.00	1.00	10.00
,35m 120	1.00	62314.00	142.00	3.00	44.00	19.00	7.00
sample	Rb	S	Sr	Th	U	Y	Zr
B-30M SUR	129.00	11959.00	238.00	17.00	88.00	71.00	430.00
B-25M SUR	35.00	3993.00	73.00	6.00	25.00	19.00	106.00
B-15 SURF	20.00	8849.00	63.00	7.00	125.00	43.00	86.00

Table 3.5
INAA for 1986 Traverse
Soils

	La ppm	Ce ppm	Eu ppm	Y ppm	Yb ppm	Lu ppm
10m 5cms	28.60	125.00	1.49	45.00	7.03	1.96
10m 40cms	69.70	26.20	3.42	135.00	16.90	4.69
0m 65cms	29.80	60.60	1.42	38.00	2.45	0.57
10m 75cms	30.80	58.20	1.59	64.00	2.55	0.94
5m 65cms	27.30	54.80	0.99	32.00	2.41	0.49
10m 80cms	29.50	60.20	1.33	39.00	2.03	0.47
15m 85cms	35.30	74.10	1.47	36.00	2.74	0.52
20m 110cms	31.80	54.50	1.51	43.00	2.38	0.46

Table 3.5
INAA for 1986 Traverse
Soils

	U ppm	Th ppm	Br ppm
10m 5cms	382.00	2.83	178.00
10m 40cms	749.00	2.64	84.50
0m 65cms	10.20	9.13	3.33
10m 75cms	15.00	9.45	5.53
5m 65cms	7.68	8.61	0.70
10m 80cms	7.00	15.70	0.40
15m 85cms	15.80	11.10	0.60
20m 110cms	8.62	8.10	0.01

Table 3.6 1987 Traverse 1

sample	Tot.cp5m	K cp5m	U cp5m	Th cp5m	pH	Eh
st1-0m surf	3300	192	61	50	4.3	230
st1-5m surf	3500	177	56	50	4.5	310
st1-10m su	3800	177	101	56	4.2	170
st1-15m sur	12400	404	780	119	4.3	170
st1-20m sur	4800	221	154	67	4.3	400
st1-25m sur	6750	324	275	84	4.3	440
st1-30m sur	5900	515	156	98	4.6	330
st1-35m sur	4375	274	165	78	6.2	-170
st1-40m sur	6600	684	164	111	6.2	173
st1-45m sur	8000	1020	152	157	6.2	160
st1-0m 55					4.7	280
st1-5m 60					5.2	300
st1-10m 60					5.1	400
st1-15m 30					5.2	440
st1-20m 60					4.5	440
st1-25m 80					5.2	447
st1-30m 30					4.9	420
st1-35m 60					6	160
st1-40m 30					5.9	110
st1-45m 40					5.9	330

Table 3.6 1987 Traverse 1

sample	SiO2	Al2O3	TiO2	Fe2O3	MgO	CaO
st1-0m surf	59.81	8.03	0.67	12.97	1.86	3.01
st1-5m surf	60.26	12.21	0.62	3.38	1.05	0.36
st1-10m su	61.19	9.06	0.65	9.38	2.44	4.38
st1-15m sur	51.97	7.95	0.55	0.61	0.39	0.31
st1-20m sur	66.32	8.92	0.68	4.77	2.13	3.05
st1-25m sur	62.6	10.93	0.77	8.33	1.99	2.93
st1-30m sur	44.92	6.89	0.49	1.64	0.37	0.35
st1-35m sur	51.22	8.56	0.52	6.65	0.53	0.93
st1-40m sur	63.49	11.12	0.61	2.6	0.86	0.44
st1-45m sur	64.32	11.52	0.55	3.84	0.84	0.41
st1-0m 55	64.36	12.5	0.61	4.29	1.57	0.35
st1-5m 60	66.65	12.21	0.62	3.38	1.05	0.36
st1-10m 60	61.99	11.16	0.55	4.7	1.14	0.34
st1-15m 30	65.55	11.92	0.59	4.28	1.07	0.34
st1-20m 60	57.75	11.24	0.59	6.04	1.46	0.29
st1-25m 80	56.11	10.34	0.37	9.95	0.8	0.26
st1-30m 30	65.63	13.29	0.6	3.66	1.76	0.35
st1-35m 60	67.59	11.66	0.6	2.36	0.99	0.48
st1-40m 30	68.29	12.43	0.62	3.17	1.3	0.4
st1-45m 40	68.21	12.17	0.56	3.18	1	0.42

Table 3.6 1987 Traverse 1

sample	Na2O	K2O	MnO	P2O5	LOI	Total
st1-0m surf	1.48	1.89	0.13	3.4	6.97	100.23
st1-5m surf	2.38	2.95	0.04	0.2	10.47	100.32
st1-10m su	1.39	1.79	0.12	2.9	6.96	100.28
st1-15m sur	1.44	1.9	0.01	0.18	34.86	100.16
st1-20m sur	2.97	2.72	0.06	1.84	6.58	100.04
st1-25m sur	1.91	2.37	0.04	2.63	5.71	100.21
st1-30m sur	1.39	1.7	0.01	0.14	42.47	100.39
st1-35m sur	1.55	2.02	0.74	0.32	27.33	100.35
st1-40m sur	2.16	2.84	0.06	0.17	15.74	100.09
st1-45m sur	2.23	2.88	0.13	0.12	13.24	100.08
st1-0m 55	2.41	2.94	0.02	0.17	10.87	100.09
st1-5m 60	2.38	2.95	0.04	0.2	10.47	100.32
st1-10m 60	2.02	2.84	0.13	0.21	15.13	100.21
st1-15m 30	2.19	2.8	0.07	0.23	11.18	100.22
st1-20m 60	1.82	2.69	0.15	0.2	18	100.22
st1-25m 80	1.38	2.92	0.54	0.23	17.42	100.32
st1-30m 30	2.33	3.19	0.03	0.09	9.01	99.93
st1-35m 60	2.35	2.83	0.13	0.15	10.78	99.92
st1-40m 30	2.59	3.22	0.05	0.09	8.06	100.23
st1-45m 40	2.76	3.12	0.09	0.1	8.65	100.25

Table 3.6 1987 Traverse 1

sample	Ba	Ce	Co	Cs	Cu	La
st1-0m surf	148		3			0
st1-5m surf	184		3			
st1-10m su	174		5			5
st1-15m sur	529	26	3	3		14
st1-20m sur	316		3			
st1-25m sur	229		4			
st1-30m sur	538	12		10		11
st1-35m sur	965	39	17			14
st1-40m sur	678	53	7		1	19
st1-45m sur	673	40	11	14	4	22
st1-0m 55	749	46	9	11	9	20
st1-5m 60	700	38	7		9	23
st1-10m 60	646	37	9	5	5	20
st1-15m 30	604	48	8	5	7	26
st1-20m 60	637	50	13		10	25
st1-25m 80	578	135	38	7	67	35
st1-30m 30	706	49	12		17	21
st1-35m 60	947	46	9	1	7	16
st1-40m 30	707	57	10	18	4	26
st1-45m 40	703	51	11	21	4	20

Table 3.6 1987 Traverse 1

sample	Mo	Nb	Nd	Pb	Rb	S
st1-0m surf	1	2	3	33	3	17034
st1-5m surf	2	3	4	18	3	16953
st1-10m su		2	3	21	2	17399
st1-15m sur	2	12	7	28	68	7093
st1-20m sur	7	3	6	43	8	16498
st1-25m sur	4	3		15	3	14950
st1-30m sur	1	10	9	16	51	6217
st1-35m sur	5	10	7	40	56	5869
st1-40m sur	4	13	21	31	88	3660
st1-45m sur	3	12	21	27	94	3004
st1-0m 55	4	13	13	21	93	1612
st1-5m 60	5	15	14	22	95	1405
st1-10m 60	3	13	16	21	90	2663
st1-15m 30	4	14	12	23	87	2200
st1-20m 60	6	12	16	35	82	2146
st1-25m 80	15	7	39	132	72	3522
st1-30m 30	3	12	18	25	96	1690
st1-35m 60	4	12	15	25	79	2627
st1-40m 30	2	12	19	26	98	2122
st1-45m 40	3	11	16	28	101	1846

Table 3.6 1987 Traverse 1

sample	Se	Sr	Th	U	V	Y
st1-0m surf	3	21	3		11	2
st1-5m surf	3	33	5		16	1
st1-10m su	2	31	4	2	15	1
st1-15m sur		120	4	4	51	13
st1-20m sur	2	49			11	3
st1-25m sur	3	32	4	3	14	3
st1-30m sur		114	6	2	45	10
st1-35m sur	2	125	4		63	13
st1-40m sur		152	5	5	69	16
st1-45m sur		174	7	4	72	17
st1-0m 55		174	4	4	76	15
st1-5m 60		185	9	4	75	17
st1-10m 60		155	8	5	80	14
st1-15m 30		160	6	3	76	16
st1-20m 60		136	7	4	78	17
st1-25m 80	3	127	15	13	72	27
st1-30m 30		168	13	4	77	17
st1-35m 60		167	9	4	73	14
st1-40m 30		174	8	1	78	16
st1-45m 40		199	6	2	71	17

Table 3.6 1987 Traverse 1

sample	Zn	Zr
st1-0m surf	18	18
st1-5m surf	4	20
st1-10m su	20	19
st1-15m sur	11	174
st1-20m sur	45	31
st1-25m sur	11	22
st1-30m sur	10	170
st1-35m sur	120	160
st1-40m sur	48	208
st1-45m sur	39	214
st1-0m 55	59	207
st1-5m 60	59	219
st1-10m 60	51	197
st1-15m 30	56	218
st1-20m 60	60	185
st1-25m 80	54	137
st1-30m 30	62	213
st1-35m 60	62	199
st1-40m 30	64	198
st1-45m 40	41	209

Table 3.7 1987 Traverse 2

POSITION	DEPTH	TOTAL COUK COUNT	U COUNT	Th COUNT	pH
0	0	5650	53	371	43	3.7
5	0	5150	109	291	39	4.2
10	0	10200	43	788	74	5.9
15	0	3750	76	166	42	5.6
20	0	5850	19	446	58	5.7
25	0	10550	116	813	78	5.1
30	0	4550	81	221	65	5.1
35	0	6700	106	432	59	5.2
40	0	4800	108	251	46	5.7
45	0	6770	315	304	92	6.5
50	0	3282	96	127	63	6.3
55	0	5700	425	206	93	5.8
60	0	10870	1286	331	182	5.1
0	150					3.9
5	100					4.5
10	110					6
10	130					6.3
15	130					5.5
20	130					5.6
25	130					4.9
25	150					5
30	140					5.2
35	100					4.8
40	70					5.5
45	60					5.7
50	80					5.8
55	80					5.9
60	80					5

Table 3.7 1987 Traverse 2

POSITION	DEPTH	Eh	SiO2	Al2O3	TiO2	Fe2O3
0	0	452	3.79	0.96	0.15	1.26
5	0	446	56.63	11.79	1.01	14.2
10	0	73	35.25	12.17	0.65	7.91
15	0	92	45.91	13.24	0.87	10.27
20	0	90	29.34	10.23	0.5	15.32
25	0	-30	55.06	18.35	1.12	8.73
30	0	-49	12.2	11.14	0.36	21.46
35	0	334	60.49	12.66	0.8	8.51
40	0	100	62.66	13.46	0.75	6.94
45	0	-50	68.08	12.58	0.6	5.23
50	0	-63	58.3	14.56	0.86	8.41
55	0	-260	66.87	12.66	0.7	2.48
60	0	265	66.31	11.86	0.62	4.44
0	150	321	14.74	13.33	1.12	16.53
5	100	110	20.75	11.19	0.7	19.43
10	110	-180	60.18	10.79	0.51	4.71
10	130	-220	70.33	12.31	0.57	2.45
15	130	-194	27.54	9.85	0.54	15.8
20	130	-185	52.65	10.06	0.57	4.21
25	130	120	55.11	13.46	0.7	9.25
25	150	220	62.6	12.51	0.73	3.75
30	140	-115	67.9	11.98	0.71	4.39
35	100	-250	70.71	12.85	0.7	1.84
40	70	-160	57.59	12.36	0.65	9.88
45	60	-340	66.83	12.02	0.58	3.2
50	80	-310	61.16	15.18	0.8	7.23
55	80	-350	72.45	12.62	0.56	2.35
60	80	175	69.06	13.56	0.6	3.73

Table 3.7 1987 Traverse 2

POSITION	DEPTH	MgO	CaO	Na2O	K2O	MnO
0	0	0.14	0.66	0.04	0.15	0.04
5	0	0.69	2.82	1.85	2.13	0.11
10	0	1.2	17.26	1.26	1.51	1.23
15	0	1.13	6.09	1.94	2.02	0.78
20	0	1.27	16.31	1.2	1.46	1.89
25	0	1.52	2.92	1.66	2.55	0.36
30	0	2.54	16.14	0.77	3.57	1.88
35	0	1.18	3.19	2.13	3.07	0.37
40	0	1.09	3.21	2.3	2.85	0.42
45	0	1.23	1.95	2.21	3.19	0.62
50	0	1.61	3.36	1.91	3.09	0.58
55	0	1.27	0.32	2.16	4.1	0.05
60	0	0.97	0.35	2.08	3.85	0.04
0	150	2.75	22.06	1.23	0.75	1
5	100	2.23	25.11	1.41	0.92	0.74
10	110	0.87	7.61	1.69	3.45	0.29
10	130	1.14	0.66	2.4	4.07	0.03
15	130	1.32	16.07	1.04	1.2	2.03
20	130	1.73	1.34	1.24	3.69	0.13
25	130	1.71	5.28	1.65	3.63	0.51
25	150	1.78	0.64	1.85	4.53	0.06
30	140	1.02	3.62	1.84	3.8	0.24
35	100	0.73	0.38	1.83	4.93	0.03
40	70	1.08	4.8	2.07	2.8	0.49
45	60	1.21	0.54	2.54	3.51	0.07
50	80	1.46	3.1	1.91	3.52	0.36
55	80	1.01	0.35	2.4	4.53	0.03
60	80	1.4	0.5	2.51	4.48	0.05

Table 3.7 1987 Traverse 2

POSITION	DEPTH	P2O5	LOI	Total	Ba	Ce
0	0	0.13	92.35	99.67	1191	10
5	0	1.31	7.24	99.77	1619	10
10	0	1.3	7.25	87	2348	18
15	0	1.27	16.58	100.11	2235	26
20	0	0.75	6.16	84.45	2213	8
25	0	0.91	6.62	99.79	2571	56
30	0	0.98	7.55	78.59	2086	9
35	0	1.03	6.51	99.93	1422	11
40	0	0.47	5.73	99.9	1763	54
45	0	0.26	3.99	99.94	1269	39
50	0	0.79	6.28	99.76	1202	48
55	0	0.04	9.28	99.94	909	58
60	0	0.09	9.41	100.03	799	58
0	150	1.53	9.3	84.34	1735	
5	100	1.38	7.14	91	1800	8
10	110	0.2	4.92	95.23	1036	27
10	130	0.08	6.22	100.03	799	53
15	130	0.84	6.57	82.81	2192	9
20	130	0.12	24.6	100.35	873	43
25	130	0.43	7.24	98.97	1759	28
25	150	0.14	11.79	100.39	782	67
30	140	0.24	3.6	99.35	1153	43
35	100	0.1	5.99	100.09	703	53
40	70	0.38	7.32	99.42	1770	38
45	60	0.1	9.53	100.12	907	45
50	80	0.36	4.66	99.74	1333	35
55	80	0.05	3.89	100.22	814	35
60	80	0.07	3.82	99.77	815	66

Table 3.7 1987 Traverse 2

POSITION	DEPTH	Co	Cs	Cu	La	Mo
0	0	3	0.5	0.5	5	0.5
5	0	1	4	0.5	7	9
10	0	8	0.5	116	56	31
15	0	10	0.5	132	31	32
20	0	12	0.5	58	18	24
25	0	9	0.5	117	52	39
30	0	10	0.5	119	13	38
35	0	8	0.5	58	18	24
40	0	11	0.5	43	32	29
45	0	14	0.5	20	23	10
50	0	9	0.5	42	24	21
55	0	9	3	7	21	7
60	0	6	8	15	24	5
0	150	5	0.5	37	14	12
5	100	4	0.5	60	16	15
10	110	10	0.5	69	32	16
10	130	15	9	20	25	5
15	130	10	0.5	142	30	27
20	130	13	0.5	32	14	9
25	130	10	0.5	107	33	28
25	150	15	0.5	21	32	6
30	140	8	0.5	46	27	19
35	100	11	1	13	26	4
40	70	12	0.5	49	23	34
45	60	15	0.5	15	30	6
50	80	9	0.5	37	19	25
55	80	9	5	14	24	6
60	80	16	1	16	21	3

Table 3.7 1987 Traverse 2

POSITION	DEPTH	Nb	Nd	Pb	Rb	S
0	0	5	6	11	2	29032
5	0	4	8	26	5	28599
10	0	7	53	30	9	52182
15	0	8	31	40	14	38730
20	0	7	12	72	21	33728
25	0	11	45	37	29	36332
30	0	5	19	5	5	65515
35	0	7	12	72	21	33728
40	0	8	29	26	29	36602
45	0	9	19	27	55	17589
50	0	9	28	43	39	27492
55	0	16	18	58	128	2603
60	0	12	22	24	98	2437
0	150	7	14	12	0.5	58328
5	100	4	22	9	1	61359
10	110	7	27	8	39	44777
10	130	12	23	18	104	4573
15	130	6	25	15	10	57813
20	130	11	19	13	80	12917
25	130	8	37	14	33	40717
25	150	14	27	15	107	7620
30	140	8	18	13	43	39071
35	100	13	21	17	122	3948
40	70	7	21	12	24	40566
45	60	13	19	21	92	5482
50	80	9	18	26	46	29183
55	80	13	15	25	113	1179
60	80	12	23	22	108	829

Table 3.7 1987 Traverse 2

POSITION	DEPTH	Se	Sr	Th	U	V
0	0	8	58	2	51	13
5	0	7	41	3	39	18
10	0	16	164	5	293	28
15	0	17	109	4	348	35
20	0	8	77	6	95	31
25	0	16	96	5	362	55
30	0	15	136	4	309	19
35	0	8	77	6	95	31
40	0	11	121	8	123	41
45	0	4	145	5	73	44
50	0	8	86	7	87	51
55	0	1	129	6	14	92
60	0	1	129	8	23	75
0	150	9	118	5	144	13
5	100	10	117	6	145	14
10	110	6	165	2	161	37
10	130	1	185	8	17	71
15	130	13	166	0.5	362	25
20	130	3	100	6	72	63
25	130	11	116	4	296	42
25	150	1	85	9	33	84
30	140	5	127	6	136	41
35	100	1	113	13	12	84
40	70	11	123	7	89	32
45	60	1	161	8	17	80
50	80	8	137	8	83	51
55	80	1	147	8	7	85
60	80	1	191	9	12	90

Table 3.7 1987 Traverse 2

POSITION	DEPTH	Y	Zn	Zr
0	0	14	113	45
5	0	19	22	33
10	0	174	220	27
15	0	112	563	50
20	0	31	435	54
25	0	141	277	63
30	0	71	261	12
35	0	31	435	54
40	0	48	170	95
45	0	41	357	128
50	0	37	460	85
55	0	23	38	229
60	0	21	61	234
0	150	35	100	50
5	100	53	230	17
10	110	59	164	76
10	130	28	60	244
15	130	94	348	28
20	130	27	113	169
25	130	106	308	60
25	150	36	113	251
30	140	36	117	117
35	100	25	39	300
40	70	45	114	77
45	60	26	89	207
50	80	32	57	110
55	80	17	31	239
60	80	20	71	229

Table 3.8 1987 Traverse 3

POSITION	DEPTH	Tot.cp5m	K cp5m	U cp5m	Th cp5m	pH
0	0	5370	440	138	93	4.7
5	0	8900	930	347	158	5.2
10	0	20200	1321	1269	272	6.4
15	0	14550	1386	644	252	6.5
20	0	17700	1442	927	287	6.1
25	0	19650	1492	1122	289	5.9
30	0	6200	473	188	90	4.4
0	50					4.7
5	100					5
10	80					6
15	30					5.1
20	40					5.7
25	90					5.4
30	60					4.8

Table 3.8 1987 Traverse 3

POSITION	DEPTH	eh	SiO2	Al2O3	TiO2	Fe2O3
0	0	460	27.87	1.8	0.39	9.52
5	0	435	59.86	12.85	0.95	2.74
10	0	420	57.78	13.73	0.87	6.77
15	0	390	56.78	12.7	0.81	5.52
20	0	400	57.4	12.86	0.82	5.23
25	0	450	57.86	11.08	0.76	6.12
30	0	507	27.26	1.76	0.32	5.26
0	50	440	61.83	15.51	0.84	4.08
5	100	450	57.4	13.74	0.86	4.72
10	80	460	59.58	14.34	0.82	6.25
15	30	473	60.1	15.26	0.82	5.96
20	40	460	60.67	14.82	0.75	6.37
25	90	460	57.79	14	0.83	5.5
30	60	460	58.1	14.95	0.82	4.81

Table 3.8 1987 Traverse 3

POSITION	DEPTH	MgO	CaO	Na2O	K2O	MnO
0	0	0.42	1.69	0.17	0.67	0.04
5	0	1.32	0.41	1.55	2.58	0.02
10	0	2.86	0.79	1.6	2.71	0.52
15	0	2.66	0.75	1.53	2.74	0.21
20	0	2.71	0.8	1.59	2.83	0.19
25	0	1.7	0.52	1.18	3.41	0.64
30	0	0.29	0.86	0.12	0.66	0.03
0	50	2.87	0.36	1.76	3.13	0.03
5	100	2.25	0.38	1.5	2.89	0.04
10	80	3.17	0.61	1.74	2.85	0.6
15	30	3.98	0.46	1.77	3.31	0.15
20	40	4.09	0.47	1.69	3.39	0.18
25	90	2.98	0.47	1.53	3.39	0.39
30	60	3.98	0.37	1.62	3.41	0.03

Table 3.8 1987 Traverse 3

POSITION	DEPTH	P2O5	LOI	Total	Ba	Ce
0	0	0.58		43.13	560	8
5	0	0.24		82.54	589	19
10	0	0.27		87.9	1102	55
15	0	0.28		83.98	875	52
20	0	0.26		84.71	930	41
25	0	0.29		83.57	2928	24
30	0	0.56		88.23	657	50
0	50	0.19		90.6	712	65
5	100	0.22		84.02	638	36
10	80	0.2	0	90.15	1394	48
15	30	0.18		91.99	851	57
20	40	0.16		92.59	967	38
25	90	0.19		88.07	6367	3.5
30	60	0.14		88.23	657	50

Table 3.8 1987 Traverse 3

POSITION	DEPTH	Co	Cs	Cu	La	Mo
0	0	0.5	2	0.5	2	0.5
5	0	5	3	0.5	11	3
10	0	11	6	11	22	9
15	0	8	7	10	23	5
20	0	10	11	9	22	5
25	0	15	3	13	6	15
30	0	11	9	9	18	2
0	50	10	9	11	17	3
5	100	6	2	7	12	4
10	80	16	12	13	21	7
15	30	13	13	15	16	3
20	40	19	0.5	13	20	6
25	90	13	11	20	17	8
30	60	11	9	9	18	2

Table 3.8 1987 Traverse 3

POSITION	DEPTH	Nb	Nd	Pb	Rb	S
0	0	3	4	24	11	9928
5	0	15	9	27	84	2640
10	0	12	16	34	83	1894
15	0	12	17	85	82	2449
20	0	11	20	134	85	2279
25	0	12	13	126	101	2656
30	0	12	21	20	104	1294
0	50	14	22	28	98	1217
5	100	14	7	29	87	2183
10	80	12	17	34	88	1340
15	30	13	19	37	98	1485
20	40	10	14	46	96	977
25	90	13	4	63	110	2766
30	60	12	21	20	104	1294

Table 3.8 1987 Traverse 3

POSITION	DEPTH	Se	Sr	Th	U	Y
0	0		50	4	0.5	4
5	0		154	9	3	14
10	0		167	11	15	17
15	0		168	8	8	19
20	0		171	6	12	23
25	0		216	13	12	15
30	0		185	6	0.5	14
0	50		186	9	5	16
5	100		172	9	6	14
10	80		169	9	11	21
15	30		184	8	5	18
20	40		196	10	11	26
25	90		393	13	9	20
30	60		185	6	0.5	14

Table 3.8 1987 Traverse 3

POSITION	DEPTH	Zn	Zr
0	0	17	33
5	0	31	196
10	0	118	198
15	0	85	184
20	0	131	199
25	0	195	187
30	0	66	196
0	50	60	221
5	100	56	201
10	80	119	204
15	30	72	197
20	40	167	193
25	90	140	199
30	60	66	196

TABLE 3.9
1988 Traverse 4

Distance (m)	0.0	10.0	20.0	30.0	40.0	50.0
Total gamma	4470.0	3340.0	3110.0	5149.0	5260.0	4771.0
K cp5m	41.0	10.0	17.0	17.0	1.0	3.0
U cp5m	100.0	80.0	59.0	225.0	333.0	242.0
Th cp5m	67.0	18.0	23.0	49.0	55.0	40.0
U ppm surf.	7.8	4.2	26.1	12.1		20.0
U ppm deep	3.4		14.8			
U ppm drift	2.1	8.4	11.6	7.9		

TABLE 3.9
1988 Traverse 4

Distance (m)	60.0	70.0	80.0	90.0	100.0	110.0
Total gamma	6335.0	4831.0	4925.0	4416.0	5453.0	6052.0
K cp5m	12.0		13.0	22.0	6.0	1.0
U cp5m	437.0	257.0	207.0	178.0	291.0	355.0
Th cp5m	77.0	49.0	53.0	49.0	59.0	83.0
U ppm surf.		47.5	117.5	84.2	17.5	55.1
U ppm deep						
U ppm drift		14.7	32.5	19.5	15.9	16.5

TABLE 3.9
1988 Traverse 4

Distance (m)	120.0	130.0	140.0	150.0
Total gamma	6340.0	4908.0	4761.0	4022.0
K cp5m	13.0	5.0		3.0
U cp5m	376.0	281.0	236.0	162.0
Th cp5m	73.0	55.0	52.0	42.0
U ppm surf.	67.9	11.6	14.5	25.9
U ppm deep				
U ppm drift	18.0	8.2	5.3	8.3

TABLE 3.10
1988 Traverse 5

Distance (m)	0.0	10.0	20.0	30.0	40.0	50.0
Total gamma	3428.0	4236.0	3973.0	4979.0	4729.0	4361.0
K cp5m	2.0	0.0	0.0	0.0	0.0	1.0
U cp5m	136.0	277.0	163.0	323.0	251.0	233.0
Th cp5m	24.0	45.0	26.0	51.0	37.0	38.0
U ppm surf.	3.7	3.3	2.2	3.5		8.8
U ppm deep						
U ppm drift	2.7	3.6	3.0	3.3	5.2	5.0

TABLE 3.10
1988 Traverse 5

Distance (m)	60.0	70.0	80.0	90.0	100.0	110.0
Total gamma	1914.0	4289.0	4445.0	3823.0	3715.0	3272.0
K cp5m	5.0	3.0	3.0	3.0	4.0	0.0
U cp5m	68.0	203.0	236.0	166.0	113.0	94.0
Th cp5m	15.0	37.0	44.0	28.0	26.0	24.0
U ppm surf.	18.7	8.9	2.5	2.2	2.6	6.4
U ppm deep						
U ppm drift	29.0	7.2	2.8	4.1	4.1	6.1

TABLE 3.10
1988 Traverse 5

Distance (m)	120.0	130.0	140.0	150.0
Total gamma	2906.0	3010.0	3781.0	5162.0
K cp5m	4.0	1.0	1.0	2.0
U cp5m	118.0	87.0	126.0	272.0
Th cp5m	26.0	15.0	28.0	56.0
U ppm surf.	7.2	7.5	17.3	20.2
U ppm deep		13.6		
U ppm drift	7.6	13.6	9.4	6.2

Table 3.11
Analytical data for Pit 2
Broubster

	La ppm	Ce ppm	Eu ppm	Yb ppm	Lu ppm	La CN
Pit 0-10cms	58.50	194.00	2.35	11.20	3.35	182.81
Pit 10-20cms	83.60	303.00	4.64	19.20	4.74	261.25
Pit 20-30cms	148.00	490.00	7.91	30.30	8.89	462.50
Pit 30-40cms	23.40	46.40	0.60	2.20	0.60	73.13
Pit 40-50cms	26.70	51.50	0.89	2.05	0.51	83.44
Pit 50-60cms	28.80	58.90	1.01	2.61	0.19	90.00
Pit 60-70cms	28.60	60.10	0.92	2.20	0.15	89.38
Pit 70-80cms	31.40	64.20	1.06	2.21	0.45	98.13
Pit 80-90cms	34.60	76.00	0.97	2.92	0.25	108.13
Detection Limit	1.00	1.00	0.01	0.10	0.10	3.13

Table 3.11
Analytical data for Pit 2
Broubster

	Ce CN	Eu CN	Yb CN	Lu CN	U ppm	Th ppm
Pit 0-10cms	206.38	32.19	58.95	108.06	553.00	2.05
Pit 10-20cms	322.34	63.56	101.05	152.90	766.00	3.27
Pit 20-30cms	521.28	108.36	159.47	286.77	1,252.00	79.70
Pit 30-40cms	49.36	8.22	11.58	19.35	15.60	6.11
Pit 40-50cms	54.79	12.19	10.79	16.45	8.24	9.50
Pit 50-60cms	62.66	13.84	13.74	6.13	6.75	10.00
Pit 60-70cms	63.94	12.60	11.58	4.84	3.78	10.20
Pit 70-80cms	68.30	14.52	11.63	14.52	5.66	8.90
Pit 80-90cms	80.85	13.29	15.37	8.06	3.91	8.75
Detection Limit	1.06	0.14	0.53	3.23	0.10	0.10

Table 3.11
Analytical data for Pit 2
Broubster

	Br ppm	Mo ppm	As ppm	Sb ppm	Cr ppm	Ba ppm
Pit 0-10cms	195.00	642.00	128.00	5.32	24.20	877.00
Pit 10-20cms	121.00	887.00	169.00	7.51	27.70	901.00
Pit 20-30cms	78.50	1,446.00	110.00	6.51	130.00	1,670.00
Pit 30-40cms	2.33	1.50	1.00	0.69	87.00	583.00
Pit 40-50cms	1.00	1.50	1.00	1.00	121.00	558.00
Pit 50-60cms	1.00	1.50	1.00	1.05	119.00	682.00
Pit 60-70cms	1.00	1.50	1.00	0.87	121.00	617.00
Pit 70-80cms	0.95	1.50	1.00	0.64	123.00	713.00
Pit 80-90cms	1.00	1.50	1.00	0.60	175.00	710.00
Detection Limit	2.00	3.00	2.00	0.10	1.00	2.00

Table 3.11
Analytical data for Pit 2
Broubster

	Sc ppm	Co ppm	Zn ppm	Fe %	Hf ppm	Ir ppm
Pit 0-10cms	9.83	81.00	299.00	4.57	0.00	1.11
Pit 10-20cms	12.50	12.50	56.40	5.99	4.04	0.12
Pit 20-30cms	19.80	9.95	132.00	2.68	0.00	0.07
Pit 30-40cms	10.60	4.00	38.00	1.23	7.44	0.03
Pit 40-50cms	14.20	14.40	158.00	3.13	6.33	0.02
Pit 50-60cms	41.00	14.20	112.00	2.96	6.07	0.02
Pit 60-70cms	15.50	15.40	27.80	3.23	7.60	0.05
Pit 70-80cms	16.60	14.50	55.00	3.55	0.51	0.01
Pit 80-90cms	16.70	16.90	133.00	3.87	4.25	0.01
Detection Limit	1.00	0.10	1.00	0.01	3.00	0.00

Table 3.12
REE data for PIT 8

	La CN	Ce CN	Pr CN	Nd CN	Sm CN
Pit 2-10cm	58.70	19.30	36.10	33.00	25.40
Pit 10-18cm	112.30	33.80	72.10	64.00	48.70
Pit 22-32cms	277.20	49.80	171.10	143.00	110.40
Pit 32-39cms	74.60	51.60	40.20	30.00	16.90
Pit 39-49cms	74.80	57.90	42.20	31.30	16.80

Table 3.12
REE data for PIT 8

	Eu CN	Gd CN	Dy CN	Ho CN	Y CN
Pit 2-10cm	20.90	27.40	25.70	26.10	46.00
Pit 10-18cm	39.90	52.20	48.40	48.70	85.00
Pit 22-32cms	87.80	113.90	100.10	98.70	162.00
Pit 32-39cms	10.40	11.50	10.00	9.60	12.00
Pit 39-49cms	9.90	10.10	8.70	8.40	8.50

Table 3.12
REE data for PIT 8

	Er CN	Yb CN	Lu CN		
Pit 2-10cm	28.10	25.90	26.50	0.00	0.00
Pit 10-18cm	52.30	48.00	48.70	0.00	0.00
Pit 22-32cms	101.70	92.30	93.20	0.00	0.00
Pit 32-39cms	9.90	9.70	10.10	0.00	0.00
Pit 39-49cms	8.40	8.10	7.90	0.00	0.00

Table 3.12
Analytical data for Pit 8
Other Elements

	Ba ppm	Co ppm	Cu ppm	Nb ppm	Ni ppm
Pit 2-10cm	2093.00	17.00	10.00	8.00	76.00
Pit 10-18cm	5959.00	34.00	20.00	9.00	100.00
Pit 22-32cms	2524.00	32.00	7.00	13.00	132.00
Pit 32-39cms	932.00	31.00	6.00	11.00	39.00
Pit 39-49cms	884.00	13.00	12.00	12.00	60.00

Table 3.12
Analytical data for Pit 8
Other Elements

	P ppm	Pb ppm	Rb ppm	S ppm	Sr ppm
Pit 2-10cm	2789.00	26.00	18.00	21220.00	133.00
Pit 10-18cm	2274.00	24.00	17.00	21007.00	137.00
Pit 22-32cms	3047.00	25.00	41.00	27936.00	185.00
Pit 32-39cms	214.00	21.00	108.00	1484.00	201.00
Pit 39-49cms	300.00	17.00	109.00	444.00	223.00

Table 3.12
Analytical data for Pit 8
Other Elements

	Th ppm	U ppm	Y ppm	Zn ppm	Zr ppm
Pit 2-10cm	-	430.00	148.00	264.00	66.00
Pit 10-18cm	-	498.00	195.00	365.00	77.00
Pit 22-32cms	7.00	949.00	392.00	168.00	97.00
Pit 32-39cms	6.00	29.00	28.00	58.00	217.00
Pit 39-49cms	2.00	7.00	21.00	57.00	205.00

Table 3.13
Analyses for Pit 3

	La ppm	Ce ppm	Nd ppm	Y ppm	La CN	Ce CN
Pit 10-20cms	24.00	22.00	26.00	99.00	75.00	23.40
Pit 80 cms	27.00	44.00	26.00	54.00	84.38	46.81
Pit 95 cms	25.00	51.00	22.00	27.00	78.13	54.26
Detection Limit	1.00	1.00	0.01	0.10	3.13	1.06

Table 3.13
Analyses for Pit 3

	Nd CN	Y CN	U ppm	Th ppm	Mo ppm	Ba ppm
Pit 10-20cms	43.33	50.51	318.00	6.00	33.00	3,168.00
Pit 80 cms	43.33	27.55	353.00	9.00	16.00	849.00
Pit 95 cms	36.67	13.78	8.00	7.00	3.00	758.00
Detection Limit	0.02	0.05	0.10	0.10	3.00	2.00

Table 3.13
Analyses for Pit 3

	Co ppm	Zn ppm	Fe %
Pit 10-20cms	5.00	205.00	13.88
Pit 80 cms	8.00	33.00	8.42
Pit 95 cms	11.00	118.00	5.04
Detection Limit	0.10	1.00	0.01

Table 3.14

	Pit 9	Pit 9	Pit 9	Pit 3	Pit 3	Pit3
Depth (cms)	10	30-35	40	10-20	80	95
SiO_2	69.18	62.42	56.25	24.52	21.39	61.74
Al_2O_3	11.22	10.61	9.39	2.96	2.14	16.16
TiO_2	0.55	0.54	0.57	0.58	0.18	0.84
Fe_2O_3	6.37	5.59	2.17	13.88	8.42	5.04
MgO	0.55	0.58	0.59	0.20	0.20	4.60
CaO	0.38	0.63	0.94	4.18	11.72	0.66
Na_2O	2.01	1.99	1.82	0.15	0.02	1.86
K_2O	3.29	2.46	2.05	0.59	0.42	3.74
MnO	0.70	2.72	0.31	0.79	0.28	0.05
P_2O_5	0.09	0.12	0.20	0.53	0.26	0.12
LOI	5.28	12.48	25.86			6.40
S	2151	2493	6202	30193	77765	2564
V	73	81	61			
Co	39	31	8	5	8	11
Cu	<1	<1	<1	53	338	18
Zn	68	47	64	205	33	118
Rb	99	70	58	14	15	103
Sr	156	172	146	104	160	167
Y	20	17	12	99	54	27
Zr	208	189	175	88	8	222
Nb	12	12	12	11	6	12
Mo	17	7	4	33	16	3
Ba	1759	3034	773	3168	849	758
La	28	16	17	24	27	25
Ce	66	31	25	22	44	51
Nd	14	10	11	26	26	22
Pb	25	28	34	39	11	25
Th	10	3	4	6	9	7
U	15	7	5	318	353	8

TABLE 4.1
Summary of bedrock analyses

	BR01 12	BR01 14	Mean	BR09 1	BR09 2	BR09 3	BR09 4	Mean
SiO2	16.30	17.64	16.97	69.05	75.09	75.27	76.38	73.95
Al203	2.34	2.73	2.54	14.69	11.43	11.36	10.94	12.11
TiO2	0.12	0.13	0.13	0.72	0.44	0.47	0.47	0.53
Fe203	1.22	1.06	1.14	4.42	3.76	3.84	3.62	3.91
MgO	1.04	0.79	0.92	0.68	0.41	0.35	0.35	0.45
CaO	41.57	40.79	41.18	0.16	0.17	0.19	0.19	0.18
Na20	0.44	0.45	0.45	1.92	1.96	1.91	2.04	1.96
K20	1.13	1.39	1.26	5.71	4.49	4.37	4.23	4.70
MnO	0.17	0.19	0.18	-	0.01	0.02	0.02	0.01
P205	0.21	0.22	0.22	0.11	0.14	0.11	0.09	0.11
LOI	35.36	34.56	34.96	2.63	2.11	2.31	1.81	2.22
Total	99.89	99.95	99.92	100.10	100.01	100.19	100.13	100.11
Ba	266.00	176.00	221.00	584.00	523.00	543.00	723.00	593.25
Ce	48.00	27.00	37.50	40.00	27.00	37.00	18.00	30.50
Co	4.00	-	2.00	14.00	13.00	13.00	10.00	12.50
Cs	1.00	2.00	1.50	1.00	1.00	2.00	1.00	1.25
Cu	6.00	8.00	7.00	19.00	15.00	15.00	8.00	14.00
La	-	23.00	11.50	35.00	9.00	27.00	24.00	23.75
Ni	25.00	21.00	23.00	72.00	49.00	43.00	38.00	50.50
Nb	4.00	-	2.00	13.00	9.00	8.00	9.00	9.75
Nd	31.00	25.00	28.00	21.00	23.00	24.00	25.00	23.25
Pb	31.00	80.00	55.50	16.00	18.00	14.00	16.00	16.00
Rb	32.00	35.00	33.50	149.00	103.00	100.00	104.00	114.00
S	3679.00	4313.00	3996.00	598.00	341.00	762.00	493.00	548.50
Sr	1812.00	1306.00	1559.00	104.00	112.00	164.00	123.00	125.75
Th	13.00	12.00	12.50	9.00	16.00	5.00	-	7.50
U	39.00	35.00	37.00	2.00	7.00	6.00	3.00	4.50
Y	36.00	51.00	43.50	17.00	18.00	18.00	23.00	19.00
Zn	58.00	96.00	77.00	50.00	65.00	30.00	39.00	46.00
Zr	52.00	63.00	57.50	225.00	173.00	212.00	180.00	197.50

Table 5.1 Summary of water analyses.(mg/l)

SAMPLE	Ca	Mg	Na	K	Eh Field	pH Lab
E1	66.1	4.09	21.6	0.5	-168	6.68
E2	22.5	2.18	24.5	8.85	363	6.64
E3	50.3	3.7	24.1	2.12	361	7.29
E4	43.5	7.43	22.3	2.86	320	7.09
E5	29.1	5.76	23.2	4.92	348	
E6	49.9	6.98	23.4	1.59	387	7.56
E7	50.8	3.5	23	3.99	387	6.9
E8	39.8	3.05	19.1	1.41	362	7.12
E9	25	3.36	25.4	5.16	357	6.88
E10A	24.3	2.44	24.4	4.42	336	
E10B	32.7	2.86	21	25.6	341	
PIT4	43.9	7.7	18.5	2.05	175	6.99
PIT5	38.3	3.97	22	0.5	233	6.95
PIT6	30.9	6.38	16.6	1.04	335	6.8
PIT7	11.2	3.63	22.2	1.42		5.93
W1	72.6	7.77	19.5	6.2	-124	
W2	44.8	7.87	20.9	85	423	
W6	31.7	7.09	20	5.89	136	7.88
W9	36.6	6.2	22.4	8.14	154	7
W10	14.5	4.65	21.8	2.48	306	
CHAL	12.1	5.02	24.4	1.96	350	6.81
BR8/4	28.1	2.47	18	0.5		6.45
BR8/5	26.3	2.68	23	2.66		6.3
BR8/3	40.8	4.63	19.8	0.5		6.58
BR8/2	27.1	3.19	18.9	0.5		6.8
BR1/5	35.5	4.04	13	1.37		7.5
BR8/1	136	15.7	33.4	10.7		7.7

Table 5.1 Summary of water analyses.(mg/l)

SAMPLE	pH Field	HCO3	Cl	SO4	NO3	Br
E1	6.41	195	27.7	3.46	0.57	0.11
E2	5.89	95	32.9	4.09	0.48	0.22
E3	6.12	182	38.1	3.18	0.49	0.14
E4	6.77	171	31.3	8.19	0.66	0.14
E5	6.42					
E6	6.29	201	35	4.69	0.53	0.15
E7	6.39	199	28.8	5.3	1.74	0.14
E8	6.66	150	25.9	4.86	0.42	0.11
E9	5.57	79	43.2	3.32	0.53	0.16
E10A	5.92		24.3	6.94	2.48	0.2
E10B	6.23		27	10.6	2.18	0.21
PIT4	6.76	217	31.7	5.25	0.58	0.2
PIT5	6.76	94	33.9	2.65	0.55	0.2
PIT6	6.54	122	27.8	8.46	0.99	0.12
PIT7		54	34.9	9.04	3.43	0.11
W1	7.01		40.3	14.3	1	0.29
W2	6.88					
W6	6.79	146	33.5	6.83	0.91	0.13
W9	6.23	140	42.7	7.64	1.04	0.18
W10	5.98		16.7	4.55	1.99	0.26
CHAL	6.5	60	43.3	3.39	0.23	0.11
BR8/4		93	30.7	3.23	0.05	0.09
BR8/5		59	33.9	27.1	0.05	0.02
BR8/3		178	24.5	1.7	0.14	0.23
BR8/2		93	25.8	14	0.37	0.1
BR1/5		101	22.2	5.87	12.6	0.11
BR8/1		636	35.3	1	0.13	1.21

Table 5.1 Summary of water analyses.(mg/l)

SAMPLE	NO2	HPO4	F	TOC	TIC	S
E1	0	0	0.06	13.5	43.5	1.52
E2		1.58	0.04	52.5	17.4	1.46
E3		0.37	0.03	37.3	33.2	1.24
E4		0.29	0.07	13.1	33.6	3.29
E5						17.4
E6		0.31	0.03	14.6	33.2	1.48
E7	2.66	0.33	0.06	9.5	33.8	0.73
E8		0.31	0.04	10.7	26.2	1.33
E9		0.41	0.05	68.3	10.6	2.12
E10A		0.33				2.64
E10B		0.38				2.65
PIT4		0.29	0.07	28.5	33.5	1.99
PIT5		0	0.08	30.5	25.5	1.39
PIT6		0.32	0.03	10	23	2.52
PIT7		0.31	0.02	34.5	0	2.6
W1		0.24				3.61
W2						3.2
W6		0	0.1	16.5	27.5	2.34
W9		0.32	0.06	12.6	25.3	2.64
W10		0.23				1.27
CHAL		0.32	0.05	18.5	11.5	0.75
BR8/4		0	0.03	68.8	8.9	1.25
BR8/5		0	0.03	73.9	12	8.9
BR8/3		0	0.02	45.4	28.5	1.11
BR8/2		0	0.02	16.9	17.1	4.92
BR1/5		0	0.05	7.3	18.9	1.9
BR8/1		0	0.07	102	102	1.63

Table 5.1 Summary of water analyses.(mg/l)

SAMPLE	Si	Ba	Sr	Mn	Fe	Al
E1	2.84	0.259	0.326	2.103	23.3	
E2	1.09	0.222	0.115	1.082	0.38	
E3	1.59	0.296	0.262	2.286	2.06	
E4	2.09	0.25	0.267	2.174	1.14	
E5	0.88	0.183	0.155	1.151	0.57	
E6	2.74	0.291	0.19	1.142	0.08	
E7	1.74	0.273	0.27	0.342	0.09	
E8	1.45	0.185	0.221	0.133	0.04	
E9	1.48	0.196	0.127	1.153	3.26	0.27
E10A	1.15	0.242	0.132	2.581	0.52	
E10B	1.11	0.327	0.165	1.656	0.44	0.19
PIT4	1.45	0.33	0.251	9.9	11.66	
PIT5	1.1	0.221	0.222	1.549	3.08	
PIT6	2.07	0.158	0.161	0.045	0.05	
PIT7	1.01	0.132	0.069	0.873	15.5	0.15
W1	2.28	0.316	0.412	0.272	0.08	
W2	1.96	0.363	0.224	0.123	0.03	
W6	1.4	0.322	0.148	6.69	0.04	
W9	2.12	0.201	0.192	11.07	0.08	
W10	0.89	0.39	0.085	1.495	3.08	
CHAL	0	0.045	0.077	0.068	0.1	
BR8/4	1.21	0.14	0.196	1.02	1.11	
BR8/5	1.77	0.161	0.205	0.11	0.294	
BR8/3	0.74	0.296	0.24	1.85	6.41	0.13
BR8/2	0.75	0.183	0.15	1.07	0.356	
BR1/5	1.17	0.187	0.203	0.02	0.01	
BR8/1	0.89	0.689	0.705	29.6	1.16	

Table 5.1 Summary of water analyses.(mg/l)

SAMPLE	Cu	Zn	Pb	U ppb	Th ppb
E1	0	0.04	0	1	0.12
E2	0.03	0.14	0	5.4	0.02
E3	0.023	0.09	0.25	4.2	0.03
E4	0	0.04	0	4	0
E5	0	0.06	0	1.3	0.03
E6	0	0.07	0	2	0
E7	0	0.05	0	2.6	0
E8	0	0.07	0	8.3	0
E9	0	0.22	0.4	5	0.05
E10A	0.022	0.39	0.06	8.1	0.04
E10B	0.015	0.11	0	13	0.36
PIT4	0	0	0	3.1	0.03
PIT5	0	0	0	2.1	0
PIT6	0	0	0	1.2	0
PIT7	0	0.06	0	0.4	0
W1	0	0.15	0	22.4	0
W2	0.043	0.14	0	7.8	0
W6	0	0.17	0	3.9	0
W9	0	0.39	0	1.8	0.03
W10	0	0.1	0.08	0.6	0
CHAL	0	0	0	0.3	0
BR8/4	0.026	0.105	0	11.2	0.2
BR8/5	0.045	0.091	0	11.7	0.3
BR8/3	0.023	0.055	0	182	0
BR8/2	0	0	0	18.5	0
BR1/5	0	0	0	4.5	0
BR8/1	0	0.06	0	2580	0

TABLE 6.1a

CORRELATION MATRIX FOR SELECTED ELEMENTS IN THE 1986 TRAVERSE

	SiO_2	Al_2O_3	TiO_2	Fe_2O_3	MgO	CaO
Th	0.79	0.80	0.77	-0.21	0.76	-0.63
U	-0.61	-0.53	-0.50	0.44	-0.53	0.44
Y	-0.34	-0.27	-0.26	0.26	-0.30	0.31
La	0.71	0.70	0.67	-0.19	0.59	-0.53
Ce	0.82	0.79	0.75	-0.23	0.71	-0.65

	Na_2O	K_2O	MnO	P_2O_5	LOI	Ba
Th	0.82	0.79	-0.32	-0.59	-0.79	0.46
U	-0.62	-0.61	0.42	0.70	0.57	0.10
Y	-0.35	-0.34	0.25	0.45	0.31	0.245
La	0.67	0.72	-0.24	-0.45	-0.71	0.52
Ce	0.79	0.83	-0.30	-0.56	-0.81	0.47

	Ce	Co	Cs	La	Nb	Pb
Th	0.91	0.87	0.43	0.88	0.92	0.86
U	-0.53	-0.46	-0.14	-0.24	-0.48	-0.47
Y	-0.17	-0.15	0.02	0.18	-0.15	-0.17
La	0.91	0.76	0.38	1.00	0.87	0.82
Ce	1.00	0.85	0.35	0.91	0.93	0.90

	Rb	S	Sr	Th	U	Y
Th	0.89	-0.54	0.81	1.00	-0.53	-0.17
U	-0.58	0.31	-0.54	-0.53	1.00	0.87
Y	-0.26	0.25	-0.23	-0.17	0.87	1.00
La	0.82	-0.41	0.73	0.83	-0.24	0.18
Ce	0.90	-0.55	0.81	0.91	-0.53	0.25

	Zr
Th	0.91
U	-0.57
Y	-0.24
La	0.85
Ce	0.93

TABLE 6.1b

RESULTS OF FACTOR ANALYSIS FOR 1986 TRAVERSE DATA

FACTOR 1 : +ve SiO_2, Al_2O_3, TiO_2, Na_2O, K_2O
-ve CaO, LOI, S

FACTOR 2 : +ve La, Co, Ce, Ba, Nb, Pb, Th, Zr, (Rb, Sr)

FACTOR 3 : +ve Fe_2O_3, MnO

FACTOR 4 : +ve Y, U

FACTOR 5 : +ve Cs

TABLE 6.2a

SPEARMAN RANK CORRELATION MATRIX FOR PEAT SAMPLES 1986 TRAVERSE

Element	SiO_2	Al_2O_3	TiO_2	Fe_2O_3	MgO	CaO	Na_2O	K_2O	MnO	P_2O_5
U	.459	.561	.478	.583	.303	-.24	.320	.366	.661	.498
Th	.446	.351	.333	-.164	.400	-.29	.651	.585	-.15	.111
Ce	.678	.661	.589	.051	.803	-.46	.659	.774	.268	.515
La	.446	.490	.365	.089	.521	-.13	.445	.519	.269	.345
Y	.403	.488	.360	.292	.382	-.08	.383	.407	.426	.350

	Ba	Ce	Co	Cs	La	Nb	Pb	Rb	S
U	.522	.264	.452	.180	.679	.664	.215	.548	-.14
Th	-.50	.470	.040	.235	.433	.358	.414	.501	-.26
La	.386	.679	.396	.192	1.00	.657	.428	.749	.015
Ce	.249	1.00	.401	.038	.679	.625	.675	.832	-.36
Y	.437	.431	.358	.258	.886	.615	.258	.630	.015

	Th	U	Y	Zr
U	.092	1.00	.901	.387
Th	1.00	.092	.293	.401
Ce	.470	.264	.431	.691
La	.433	.679	.886	.460
Y	.292	.901	1.00	.363

TABLE 6.2b

RESULTS OF FACTOR ANALYSIS FOR PEAT SAMPLES 1986 TRAVERSE

FACTOR 1 : +ve SiO_2, Al_2O_3, TiO_2, MgO, Na_2O, K_2O, P_2O_5
-ve LOI, CaO, S

FACTOR 2 : +ve Ce, Co, Nb, Zr, Th, La, Rb, Sr

FACTOR 3 : +ve MnO, Fe_2O_3, Ba
-ve S,CaO

FACTOR 4 : +ve U, Y, La, Ba

TABLE 6.3

SPEARMAN RANK CORRELATION MATRIX FOR SURFACE SAMPLES 1987 TRAVERSE 2

Element	SiO_2	Al_2O_3	TiO_2	Fe_2O_3	MgO	CaO	Na_2O	K_2O	MnO	P_2O_5
U	-.47	.354	.248	.580	.379	.729	-.26	-.34	.62	.558
Th	.596	.427	.084	-.25	.176	-.05	.585	.468	-.46	-.43
Ce	.725	.677	.377	-.58	.029	-.53	.653	.57	-.49	-.48
La	.256	.705	.427	-.105	.189	.281	.339	.036	.197	.10
Nd	.091	.652	.380	.052	.31	.402	.179	.069	.317	.220
Y	-.14	.505	.253	.358	.508	.652	.003	-.07	.647	.434

	Ba	Ce	Co	Cu	La	Mo	Nd	Pb	S
U	.886	-.20	.395	.92	.483	.956	.62	.069	.879
Th	-.28	.569	.247	-.31	.434	-.08	.281	.351	-.326
Ce	-.32	1.00	-.003	-.16	.609	-.13	.497	.076	-.452
La	.432	.609	.257	.481	1.00	.505	.950	.191	.248
Nd	.518	.497	.278	.627	.95	.646	1.00	.039	.411
Y	.781	.099	.492	.855	.742	.895	.852	.105	.714

	Th	U	V	Y	Zn	Zr
U	-.17	1.00	-.17	.862	.587	-.455
Th	1.00	-.17	.686	.008	.089	.734
Ce	.569	-.20	.888	.099	-.19	.800
La	.434	.483	.532	.742	.254	.290
Nd	.281	.621	.422	.852	.306	.102
Y	.008	.862	.118	1.00	.493	-.22

TABLE 6.4

SPEARMAN RANK CORRELATION MATRIX FOR DEEP SAMPLES 1987 TRAVERSE 2

Element	SiO_2	Al_2O_3	TiO_2	Fe_2O_3	MgO	CaO	Na_2O	K_2O	MnO	P_2O_5
U	-.82	-.47	-.006	.886	.260	.956	-.71	-.75	.914	.902
Th	.724	.657	.39	-.73	-.10	-.85	.667	.727	-.77	-.67
Ce	.639	.375	.262	-.72	-.07	-.75	.574	.745	-.76	-.68
La	.070	-.044	-.73	-.04	-.24	.104	-.62	.067	.060	.100
Nd	-.36	-.086	-.13	.292	.261	.400	-.33	-.15	.269	.296
Y	-.76	-.37	.051	.838	.268	.917	-.64	-.67	.844	.881

	Ba	Ce	Co	Cu	La	Mo	Nd	Pb	S
U	.821	-.71	-.47	.978	.306	.827	.445	-.66	.956
Th	-.76	.801	.487	-.87	-.20	-.74	-.25	.635	-.84
Ce	-.80	1.00	.762	-.73	.013	-.69	-.05	.407	-.79
La	-.53	.013	.093	.234	1.00	.155	.573	-.13	.170
Nd	.088	-.05	.309	.477	.573	.084	1.00	-.37	.34
Y	.722	-.62	-.37	.946	.431	.782	.604	.671	.920

	Th	U	V	Y	Zn	Zr
U	-.87	1.00	-.89	.957	.915	-.88
Th	1.00	-.87	.813	-.77	-.83	.854
Ce	.801	-.72	.767	-.62	-.57	.875
La	-.20	.305	-.01	.431	.358	.002
Nd	-.25	.445	-.19	.604	.562	-.22
Y	-.77	.957	-.84	1.00	.893	-.78

SUMMARY OF FACTOR ANALYSIS FOR THE 1987 TRAVERSE TWO

FACTOR 1 +ve V, Zr, Rb, Nb, Ce, (K_2O, Th)

-ve S,(P, Fe, Ba, Mo)

FACTOR 2 Y, Nd, La, Cu, U, (Mo, Ba)

FACTOR 3 +ve Al_2O_3, Na_2O, (SiO_2)

-ve LOI

FACTOR 4 Pb, (Zn)

FACTOR 5 -ve MgO, CaO, (MnO, Fe_2O_3

TABLE 6.5

CORRELATION MATRIX FOR WATER SAMPLES

Component	Ca	Mg	Na	K	pH	HCO_3	Cl	SO_4	NO_3
U	0.86	0.81	0.66	0.57	0.35	0.91	0.08	-.23	-.10
Th	-.11	-.31	-.02	-.13	-.44	-.21	0.05	0.57	-.19

Component	HPO_4	TOC	TIC	S	Si	Ba	Sr	Mn	Fe
U	-.18	0.61	0.85	-.08	-.21	-.21	0.83	0.87	-.08
Th	-.20	0.46	-.21	0.59	0.21	-.21	-.00	-.14	0.11

Component	Zn	U	Th
U	-.05	1.00	-.11
Th	0.14	-.11	1.00

SUMMARY OF FACTOR ANALYSIS FOR THE WATER ANALYSES DATA

FACTOR 1: Ca, HCO_3, TIC, Ba, Sr, U, Mn, Mg, (K, Na)

FACTOR 2: Cl, Zn, (K, Na).

FACTOR 3: SO_4, S, Th

FACTOR 4: (pH)

FACTOR 5: Si

European Communities — Commission

EUR 13275 – The geological, geochemical, topographical and hydrogeological characteristics of the Broubster natural analogue site, Caithness

T. K. Ball, A. E. Milodowski

Luxembourg: Office for Official Publications of the European Communities

1991 — XV, 185 pp., num. tab., fig. — 21.0 × 29.7 cm

Nuclear science and technology series

ISBN 92-826-2358-0

Catalogue number: CD-NA-13275-EN-C

Price (excluding VAT) in Luxembourg: ECU 15

One of the four analogue sites chosen for investigation by the British Geological Survey is the uranium mineralization at Broubster, Caithness, Scotland. Naturally occurring uranium has been leached from a thin mineralized limestone horizon and has been carried by groundwater flow into a peat bog about 100 m away. This process has probably been going on for at least 5 000 years. Standard surveying, hydrogeological and geochemical methods have been applied in the investigation and analysis of the area. Selected samples of the mineralization, peat soils and associated groundwaters have been examined in detail. This report summarizes the main findings accumulated since 1968 when the site was first discovered, and provides a useful information base for further modelling work.

Venta y suscripciones • Salg og abonnement • Verkauf und Abonnement • Πωλήσεις και συνδρομές
Sales and subscriptions • Vente et abonnements • Vendita e abbonamenti
Verkoop en abonnementen • Venda e assinaturas

BELGIQUE / BELGIË

Moniteur belge / Belgisch Staatsblad
Rue de Louvain 42 / Leuvenseweg 42
1000 Bruxelles / 1000 Brussel
Tél. (02) 512 00 26
Fax 511 01 84
CCP / Postrekening 000-2005502-27

Autres distributeurs /
Overige verkooppunten

Librairie européenne/ Europese Boekhandel
Avenue Albert Jonnart 50 /
Albert Jonnartlaan 50
1200 Bruxelles / 1200 Brussel
Tél. (02) 734 02 81
Fax 735 08 60

Jean De Lannoy
Avenue du Roi 202 /Koningslaan 202
1060 Bruxelles / 1060 Brussel
Tél. (02) 538 51 69
Télex 63220 UNBOOK B
Fax (02) 538 08 41

CREDOC
Rue de la Montagne 34 / Bergstraat 34
Bte 11 / Bus 11
1000 Bruxelles / 1000 Brussel

DANMARK

J. H. Schultz Information A/S
EF-Publikationer
Ottiliavej 18
2500 Valby
Tlf. 36 44 22 66
Fax 38 44 01 41
Girokonto 6 00 08 86

BR DEUTSCHLAND

Bundesanzeiger Verlag
Breite Straße
Postfach 10 80 06
5000 Köln 1
Tel. (02 21) 20 29-0
Fernschreiber:
ANZEIGER BONN 8 882 595
Fax 20 29 278

GREECE

G.C. Eleftheroudakis SA
International Bookstore
Nikis Street 4
10563 Athens
Tel. (01) 322 63 23
Telex 219410 ELEF
Fax 323 98 21

ESPAÑA

Boletín Oficial del Estado
Trafalgar, 27
28010 Madrid
Tel. (91) 44 82 135

Mundi-Prensa Libros, S.A.
Castelló, 37
28001 Madrid
Tel. (91) 431 33 99 (Libros)
431 32 22 (Suscripciones)
435 36 37 (Dirección)
Télex 49370-MPLI-E
Fax (91) 575 39 98

Sucursal:

Librería Internacional AEDOS
Consejo de Ciento, 391
08009 Barcelona
Tel. (93) 301 86 15
Fax (93) 317 01 41

Llibreria de la Generalitat de Catalunya
Rambla dels Estudis , 118 (Palau Moja)
08002 Barcelona
Tel. (93) 302 68 35
302 64 62
Fax 302 12 99

FRANCE

Journal officiel
Service des publications des Communautés européennes
26, rue Desaix
75727 Paris Cedex 15
Tél. (1) 40 58 75 00
Fax (1) 40 58 75 74

IRELAND

Government Publications Sales Office
Sun Alliance House
Molesworth Street
Dublin 2
Tel. 71 03 09

or by post

Government Stationery Office
EEC Section
6th floor
Bishop Street
Dublin 8
Tel. 78 16 66
Fax 78 06 45

ITALIA

Licosa Spa
Via Benedetto Fortini, 120/10
Casella postale 552
50125 Firenze
Tel. (055) 64 54 15
Fax 64 12 57
Telex 570466 LICOSA I
CCP 343 509

Subagenti:

Libreria scientifica Lucio de Biasio - AEIOU
Via Meravigli, 16
20123 Milano
Tel. (02) 80 76 79

Herder Editrice e Libreria
Piazza Montecitorio, 117-120
00186 Roma
Tel. (06) 679 46 28/679 53 04

Libreria giuridica
Via XII Ottobre, 172/R
16121 Genova
Tel. (010) 59 56 93

GRAND-DUCHÉ DE LUXEMBOURG

Abonnements seulement
Subscriptions only
Nur für Abonnements

Messageries Paul Kraus
11, rue Christophe Plantin
2339 Luxembourg
Tél. 499 88 88
Télex 2515
Fax 499 88 84 44
CCP 49242-63

NEDERLAND

SDU Overheidsinformatie
Externe Fondsen
Postbus 20014
2500 EA 's-Gravenhage
Tel. (070) 37 89 911
Fax (070) 34 75 778

PORTUGAL

Imprensa Nacional
Casa da Moeda, EP
Rua D. Francisco Manuel de Melo, 5
P-1092 Lisboa Codex
Tel. (01) 69 34 14

Distribuidora de Livros Bertrand, Ld.ª
Grupo Bertrand, SA
Rua das Terras dos Vales, 4-A
Apartado 37
P-2700 Amadora Codex
Tel. (01) 49 59 050
Telex 15798 BERDIS
Fax 49 60 255

UNITED KINGDOM

HMSO Books (PC 16)
HMSO Publications Centre
51 Nine Elms Lane
London SW8 5DR
Tel. (071) 873 9090
Fax GP3 873 8463
Telex 29 71 138

Sub-agent:

Alan Armstrong Ltd
2 Arkwright Road
Reading, Berks RG2 0SQ
Tel. (0734) 75 18 55
Telex 849937 AAALTD G
Fax (0734) 75 51 64

ÖSTERREICH

Manz'sche Verlags- und Universitätsbuchhandlung
Kohlmarkt 16
1014 Wien
Tel. (0222) 531 61-0
Telex 11 25 00 BOX A
Fax (0222) 531 61-81

SVERIGE

BTJ
Box 200
22100 Lund
Tel. (046) 18 00 00
Fax (046) 18 01 25

SCHWEIZ / SUISSE / SVIZZERA

OSEC
Stampfenbachstraße 85
8035 Zürich
Tel. (01) 365 51 51
Fax (01) 365 54 11

MAGYARORSZÁG

Agroinform
Központ:
Budapest I., Attila út 93. H-1012

Levélcím:
Budapest, Pf.: 15 H-1253
Tel. 36 (1) 56 82 11
Telex (22) 4717 AGINF H-61

POLAND

Business Foundation
ul. Wspólna 1/3
PL-00-529 Warszawa
Tel. 48 (22) 21 99 93/21 84 20
Fax 48 (22) 28 05 49

YUGOSLAVIA

Privredni Vjesnik
Bulevar Lenjina 171/XIV
11070 - Beograd
Tel. 123 23 40

TÜRKIYE

Pres Dagitim Ticaret ve sanayi A.Ş.
Narlibahçe Sokak No. 15
Cağaloğlu
Istanbul
Tel. 512 01 90
Telex 23822 DSVO-TR

AUTRES PAYS
OTHER COUNTRIES
ANDERE LÄNDER

Office des publications officielles des Communautés européennes
2, rue Mercier
L-2985 Luxembourg
Tél. 49 92 81
Télex PUBOF LU 1324 b
Fax 48 85 73
CC bancaire BIL 8-109/6003/700

CANADA

Renouf Publishing Co. Ltd
Mail orders — Head Office:
1294 Algoma Road
Ottawa, Ontario K1B 3W8
Tel. (613) 741 43 33
Fax (613) 741 54 39
Telex 0534783

Ottawa Store:
61 Sparks Street
Tel. (613) 238 89 85

Toronto Store:
211 Yonge Street
Tel. (416) 363 31 71

UNITED STATES OF AMERICA

UNIPUB
4611-F Assembly Drive
Lanham, MD 20706-4391
Tel. Toll Free (800) 274 4888
Fax (301) 459 0056

AUSTRALIA

Hunter Publications
58A Gipps Street
Collingwood
Victoria 3066

JAPAN

Kinokuniya Company Ltd
17-7 Shinjuku 3-Chome
Shinjuku-ku
Tokyo 160-91
Tel. (03) 3439-0121

Journal Department
PO Box 55 Chitose
Tokyo 156
Tel. (03) 3439-0124

15

CD-NA-13275-EN-C

NOTICE TO THE READER

All scientific and technical reports published by the Commission of the European Communities are announced in the monthly periodical **'euro abstracts'**. For subscription (1 year: ECU 92) please write to the address below.

Price (excluding VAT) in Luxembourg: ECU 15

OFFICE FOR OFFICIAL PUBLICATIONS
OF THE EUROPEAN COMMUNITIES

L-2985 Luxembourg

ISBN 92-826-2358-0

9 789282 623589